Advances in High Energy Physics

Supersymmetry beyond the NMSSM

Guest Editors: Florian Staub, Mark D. Goodsell, Michal Malinský, and Kai Schmidt-Hoberg

Supersymmetry beyond the NMSSM

Advances in High Energy Physics

Supersymmetry beyond the NMSSM

Guest Editors: Florian Staub, Mark D. Goodsell,
Michal Malinský, and Kai Schmidt-Hoberg

Editorial Board

Contents

Hindawi Publishing Corporation
Advances in High Energy Physics
Volume 2015, Article ID 121508, 2 pages
http://dx.doi.org/10.1155/2015/121508

Editorial

Supersymmetry beyond the NMSSM

Florian Staub,[1] Mark D. Goodsell,[2,3] Michal Malinský,[4] and Kai Schmidt-Hoberg[5]

[1] *Theory Division, CERN, 1211 Geneva 23, Switzerland*
[2] *Sorbonne Universités, UPMC Univ. Paris 06, UMR 7589, LPTHE, 75005 Paris, France*
[3] *CNRS, UMR 7589, LPTHE, 75005 Paris, France*
[4] *Institute of Particle and Nuclear Physics, Faculty of Mathematics and Physics, Charles University in Prague, V Holešovičkách 2, 180 00 Praha 8, Czech Republic*
[5] *Deutsches Elektronen-Synchrotron (DESY), Notkestraße 85, 22607 Hamburg, Germany*

Correspondence should be addressed to Florian Staub; florian.staub@cern.ch

Received 13 August 2015; Accepted 16 August 2015

With the start of run II of the Large Hadron Collider (LHC) a new milestone of high energy particle physics has been reached. Run I was on the one side a great success because of the discovery of a fundamental scalar with all expected properties of the so long-expected standard model (SM) Higgs boson [1, 2]. On the other side, no clear sign of any physics beyond the SM has shown up. This has placed severe constraints on the simplest scenarios for new physics. In particular the minimal realization of supersymmetry (SUSY), the minimal supersymmetric standard model (MSSM), has lost some of its appeal since it is no longer clear that it can address the question of naturalness. In general, there are two possibilities to explain the measured mass of 125 GeV within the MSSM: either heavy SUSY masses are needed, or the stop mixing has to be very large. In the first case, a new hierarchy problem is introduced, while the second can be dangerous because of charge and colour breaking minima [3–7].

These observations together with the other null results from SUSY searches have created a much stronger interest in nonminimal SUSY models in recent years. Extensions of the MSSM not only might provide a natural explanation for the size of the Higgs mass, but also can explain other (non)observations such as neutrino masses (e.g., in seesaw models) and the missing signals for supersymmetry (e.g., due to broken R-parity). More theoretical issues of the MSSM can also be addressed, such as the μ-problem in singlet extensions and the origin of R-parity in models with gauged $B - L$.

This special issue discusses several theoretical and experimental aspects of nonminimal SUSY models. To set the scene, the first article reconsiders the beginnings of supersymmetry and reveals its secret history: "Supersymmetry: Early Roots That Did Not Grow" by C. Jarlskog points out that the fundamental concepts of SUSY were already known in the 1940s.

Our first research article is inspired by top-down approaches: "Phenomenological Hints from a Class of String Motivated Model Constructions" by H. P. Nilles connects string theoretical considerations with LHC phenomenology. Generic predictions of a specific class of string motivated models are presented.

The next two articles consider singlet extensions of the MSSM. In "Two Higgs Bosons near 125 GeV in the Complex NMSSM and the LHC Run-I Data" by S. Moretti and S. Munir the properties of the Higgs fields in the Z_3 invariant singlet extensions with complex parameters are discussed. In particular, they consider the case where two Higgs bosons have such close masses that they are not separately resolved by the LHC experiments and find that for some parameter points this can provide a better fit to the data than a single Higgs.

The authors M. Ratz and P. K. S. Vaudrevange, in "Singlet Extensions of the MSSM with Z_4^R Symmetry," consider a different discrete symmetry which allows for more parameters in the superpotential. It is shown that the potentially

dangerous linear term can be avoided in this class of models.

As mentioned, one of the best possibilities to hide SUSY at the LHC is to assume that R-parity is not conserved. In this case the limits on SUSY masses are significantly reduced. The two articles "Status of LHC searches for SUSY without R-parity" by R. Franceschini and "Searches for Prompt R-Parity-Violating Supersymmetry at the LHC" by A. Redelbach discuss the current status of SUSY searches at the LHC in the context of R-parity violation. Together these provide an excellent and up-to-date reference for this class of searches.

SUSY models which include an explanation for the neutrino masses and mixing angles also predict nonvanishing rates for lepton-flavour violating (LFV) observables like $\mu \to e\gamma$ or $\mu \to 3e$. The article "Lepton Flavor Violation beyond the MSSM" by A. Vicente discusses the constraints on different SUSY models derived by the strong experimental bounds for LFV observables.

A possible origin of R-parity in SUSY models is the presence of an Abelian $B - L$ gauge group which is broken in a specific way to retain an unbroken Z_2 subgroup. These models are always accompanied by an extended Higgs sector. The article "The Higgs Sector of the Minimal SUSY $B - L$ Model" by L. Basso discusses the Higgs properties in the minimal SUSY model with a gauged $U(1)_{B-L}$ and unbroken R-parity.

Dirac gaugino models have recently attracted much attention in the literature due to their many attractive properties over their Majorana counterparts (as in the MSSM). However when in addition an unbroken R-symmetry is imposed, such models are expected to have difficulties to explain the observed Higgs mass: since the left- and right-handed stops cannot mix, the stop radiative corrections to the Higgs are suppressed. The article "Two-Loop Correction to the Higgs Boson Mass in the MRSSM" by P. Diessner et al. discusses the minimal R-symmetric SUSY model and shows that the observed Higgs mass can be generated via large radiative corrections involving other states. It includes all of the latest corrections which have recently become available, equivalent to the precision available for the MSSM: an illustration of the rapid recent developments in beyond-the-MSSM phenomenology.

The above articles give a cross section of current thinking in this rapidly expanding area. We hope that this special issue will therefore prove to be a useful resource for those entering the field and experts alike, as we eagerly wait for the data with, we hope, the first signs of what may lie beyond the (minimal supersymmetric) standard model.

Acknowledgment

We sincerely thank all authors for their contribution to this special issue.

Florian Staub
Mark D. Goodsell
Michal Malinský
Kai Schmidt-Hoberg

References

[1] S. Chatrchyan, V. Khachatryan, A. M. Sirunyan et al., "Observation of a new boson at a mass of 125 GeV with the CMS experiment at the LHC," *Physics Letters B*, vol. 716, no. 1, pp. 30–61, 2012.

[2] G. Aad, T. Abajya, B. Abbott et al., "Observation of a new particle in the search for the standard model Higgs boson with the ATLAS detector at the LHC," *Physics Letters B*, vol. 716, no. 1, pp. 1–29, 2012.

[3] J. E. Camargo-Molina, B. O'Leary, W. Porod, and F. Staub, "Stability of the CMSSM against sfermion VEVs," *Journal of High Energy Physics*, vol. 2013, no. 12, article 103, 2013.

[4] N. Blinov and D. E. Morrissey, "Vacuum stability and the MSSM Higgs mass," *Journal of High Energy Physics*, vol. 2014, no. 3, article 106, 2014.

[5] D. Chowdhury, R. M. Godbole, K. A. Mohan, and S. K. Vempati, "Charge and color breaking constraints in MSSM after the Higgs discovery at LHC," *Journal of High Energy Physics*, vol. 2014, article 110, 2014.

[6] J. E. Camargo-Molina, B. Garbrecht, B. O'Leary, W. Porod, and F. Staub, "Constraining the Natural MSSM through tunneling to color-breaking vacua at zero and non-zero temperature," *Physics Letters B*, vol. 737, pp. 156–161, 2014.

[7] U. Chattopadhyay and A. Dey, "Exploring MSSM for charge and color breaking and other constraints in the context of Higgs@125 GeV," *Journal of High Energy Physics*, vol. 2014, no. 11, article 161, 2014.

Hindawi Publishing Corporation
Advances in High Energy Physics
Volume 2015, Article ID 785217, 6 pages
http://dx.doi.org/10.1155/2015/785217

Research Article

Singlet Extensions of the MSSM with $\mathbb{Z}_4^R$ Symmetry

Michael Ratz[1] and Patrick K. S. Vaudrevange[2,3]

[1]*Physik-Department T30, Technische Universität München, James-Franck-Straße 1, 85748 Garching, Germany*
[2]*Excellence Cluster Universe, Boltzmannstraße 2, 85748 Garching, Germany*
[3]*Arnold Sommerfeld Center for Theoretical Physics, Ludwig-Maximilians-Universität München, Theresienstraße 37, 80333 München, Germany*

Correspondence should be addressed to Patrick K. S. Vaudrevange; patrick.vaudrevange@tum.de

Received 3 March 2015; Accepted 9 June 2015

Academic Editor: Kai Schmidt-Hoberg

We discuss singlet extensions of the MSSM with $\mathbb{Z}_4^R$ symmetry. We show that holomorphic zeros can avoid a potentially large coefficient of the term linear in the singlet. The emerging model has both an effective μ term and a supersymmetric mass term for the singlet μ_N which are controlled by the gravitino mass. The μ term turns out to be suppressed against μ_N by about one or two orders of magnitude. We argue that this class of models might provide us with a solution to the little hierarchy problem of the MSSM.

1. Purpose of This Paper

The $\mathbb{Z}_4^R$ symmetry [1, 2] provides us with compelling solutions of the μ and proton decay problems of the minimal supersymmetric extension of the standard model (MSSM). This symmetry appears anomalous, but the anomaly is cancelled by the (discrete) Green-Schwarz (GS) mechanism [3] in such a way that it does not spoil gauge coupling unification (see, e.g., [4] for a discussion). More precisely, if one extends the MSSM by a symmetry (continuous or discrete) that solves the μ problem and (i) demands anomaly freedom (while allowing GS anomaly cancellation), (ii) demands that the usual Yukawa couplings and the Weinberg operator be allowed, (iii) demands consistency with $SO(10)$ grand unification, and (iv) demands precision gauge coupling unification, then this $\mathbb{Z}_4^R$ is the unique solution [2] (see also [5] for an alternative proof). By relaxing (iii) to consistency with $SU(5)$, one obtains four additional symmetries [6]. Further, $\mathbb{Z}_4^R$ can be thought of as a discrete remnant of the Lorentz symmetry of compact extra dimensions; that is, it has a simple geometric interpretation and can arise in explicit string-derived models with the precise MSSM matter content [7]. The charge assignment is very simple: MSSM matter superfields have $\mathbb{Z}_4^R$ charge 1 while the Higgs superfields have 0, and the superpotential $\mathcal{W}$ carries R charge 2.

However, if one attempts to construct singlet extensions of the $\mathbb{Z}_4^R$ MSSM, one faces the problem that the presence of superpotential coupling of the singlet N to the Higgs bilinear H_uH_d implies that also a linear term in the singlet is allowed by all symmetries. In more detail, since the Higgs bilinear has $\mathbb{Z}_4^R$ charge 0, the singlet N needs to carry charge 2 in order to match the $\mathbb{Z}_4^R$ charge 2 of the superpotential. Then the desired term $\mathcal{W} \supset NH_uH_d$ is allowed. However, in this case one might expect to have a problematic, unsuppressed linear term in N in the (effective) superpotential,

$$\mathcal{W}_{\text{eff}} \supset \Lambda^2 N, \tag{1}$$

with Λ of the order of the fundamental scale. In order to forbid this linear term, one may try to add a new symmetry. It is quite straightforward to see that an ordinary symmetry cannot forbid this linear term and be, at the same time, consistent with criteria (i)–(iv) above: in order to forbid the linear term, the singlet N needs to carry a nontrivial charge under the new symmetry. But, as we want the term NH_uH_d, this implies that also H_uH_d carries a nontrivial charge.

Consequently, the new symmetry would yield a solution to the μ problem. However, this is not possible: as stated above, one can prove that (under our assumptions) the unique solution to the μ problem is $\mathbb{Z}_4^R$, and this symmetry does not forbid the linear term.

In this paper, we take an alternative route and describe how one can get rid of the linear term (1) by employing holomorphic zeros [8] associated with an additional pseudoanomalous $U(1)$ gauge symmetry.

2. Forbidding the Linear Term in the $\mathbb{Z}_4^R$ (G)NMSSM

2.1. Setup. Consider a singlet extension of the MSSM with a singlet N and an additional $\mathbb{Z}_4^R \times U(1)_{\text{anom}}$ symmetry. $U(1)_{\text{anom}}$ is pseudoanomalous $U(1)$ symmetry, whose anomaly is cancelled by the GS mechanism. Such $U(1)$ factors often arise in string compactifications and are accompanied by nontrivial Fayet-Iliopoulos (FI) term [9] ξ, which arises at 1-loop [10]. The FI term of the $U(1)_{\text{anom}}$ is assumed to be cancelled by a nontrivial vacuum expectation value (VEV) of a "flavon" ϕ, which carries negative $U(1)_{\text{anom}}$ charge and $\mathbb{Z}_4^R$ charge 0. Without loss of generality, we can normalize $U(1)_{\text{anom}}$ such that ϕ has charge -1 and $\xi > 0$. (Of course, in true string-derived models the situation is usually more complicated: in approximately 500 out of a total of 11940 MSSM-like models from [11] the FI term can be cancelled with one field only. In all other models, one would have to identify ϕ with an appropriate monomial of MSSM singlet fields (see Appendix A for details).) For the sake of definiteness, we assume that

$$\varepsilon := \frac{\langle \phi \rangle}{M_P} \sim \sin \vartheta_{\text{Cabibbo}} \sim 0.2, \tag{2}$$

where the Planck scale M_P is identified with the "fundamental scale." In this case, $U(1)_{\text{anom}}$ can be used as Froggatt-Nielsen symmetry [12] to explain the flavor structure of quarks and leptons. However, this assumption is not crucial for the subsequent discussion, yet this is what one gets in explicit orbifold compactifications of the heterotic string which exhibit the exact MSSM spectrum at energies below the compactification scale.

Further, also the anomaly of $\mathbb{Z}_4^R$ is assumed to be cancelled by the GS mechanism with the GS axion being contained in the dilaton or another superfield, which we will denote by S. Since the mixed $U(1)_{\text{anom}} - G_{\text{SM}}^2$ and $\mathbb{Z}_4^R - G_{\text{SM}}^2$ anomalies are universal, the GS mechanism does not interfere with the beautiful picture of MSSM gauge coupling unification (see, e.g., [4]). The "nonperturbative" term e^{-bS} carries the same $\mathbb{Z}_4^R$ charge as the superpotential, namely, 2. It might be thought of as some nonperturbative hidden sector (see, e.g., [13]). Further, e^{-bS} will also carry positive $U(1)_{\text{anom}}$ charge $s > 0$ such that holomorphic zeros get lifted by "nonperturbative" terms. More details on the charge of e^{-bS} can be found in Appendix B (see, e.g., [6, 14]). In more detail, we demand that

$$\mathscr{W}_{\text{hid}} \sim M_P^3 \left(\frac{\phi}{M_P}\right)^s e^{-bS} \tag{3}$$

Table 1: Charge assignment.

	ϕ	$H_u H_d$	N	e^{-bS}
$U(1)_{\text{anom}}$	-1	$h > 0$	$n < 0$	$s > 0$
$\mathbb{Z}_4^R$	0	0	2	2

be allowed, which is equivalent to the statement that e^{-bS} carries $U(1)_{\text{anom}}$ charge $s > 0$. (Note that s may also be fractional even if the charges of all "fundamental" fields are integer, for instance, if one assumes that $\mathscr{W}_{\text{hid}}$ is given by the Affleck-Dine-Seiberg superpotential [15]. Examples for such terms can be found, e.g., in [13].) $\mathscr{W}_{\text{hid}}$ may be thought of as gaugino condensate [16] or some other nonperturbative physics, such as the one discussed in [17], which is involved in spontaneous supersymmetry breaking. We discuss this in more detail in Appendix B. Inserting the ϕ VEV we obtain

$$\mathscr{W}_{\text{hid}} \xrightarrow{\phi \to \phi} M_P^2 m_{3/2} \tag{4}$$

in Planck units. (Note that (3) is not the "full" hidden sector superpotential. One must, of course, make sure that ϕ does not attain an F-term VEV, and one needs to cancel the vacuum energy. A detailed discussion of these issues is, however, beyond the scope of the present paper.) This implies, in particular, that

$$\left\langle e^{-bS} \right\rangle \sim \frac{m_{3/2}}{M_P} \varepsilon^{-s}. \tag{5}$$

That is, R symmetry breaking is controlled by the gravitino mass, as it should be, and due to the presence of $U(1)_{\text{anom}}$ we obtain a Froggatt-Nielsen-like [12] modification of the terms. However, in contrast to the usual Froggatt-Nielsen mechanism, it yields in our setup an enhancement rather than a suppression factor for the lifting of the holomorphic zeros by nonperturbative effects.

2.2. Charges and Allowed Terms in the Superpotential. We summarize the $U(1)_{\text{anom}}$ and $\mathbb{Z}_4^R$ charges in Table 1.

Below the $U(1)_{\text{anom}}$ breaking scale set by the ϕ VEV, we wish to have a nontrivial μ term at the nonperturbative level; that is,

$$\mathscr{W}_{\text{eff}} \supset M_P e^{-bS} \left(\frac{\phi}{M_P}\right)^{s+h} H_u H_d. \tag{6}$$

This implies

$$s + h \geq 0. \tag{7}$$

We will then get effectively

$$\mathscr{W}_{\text{eff}} \supset M_P e^{-bS} \left(\frac{\langle \phi \rangle}{M_P}\right)^{s+h} H_u H_d =: \mu H_u H_d \quad \text{with } \mu \sim m_{3/2} \varepsilon^h. \tag{8}$$

Next, we wish to couple the singlet N to the Higgs bilinear. We hence demand that

$$n + h \geq 0 \tag{9}$$

such that

$$\begin{aligned}\mathscr{W}_{\text{eff}} &\supset \left(\frac{\langle\phi\rangle}{M_P}\right)^{n+h} NH_uH_d \sim \varepsilon^{n+h} NH_uH_d \\ &=: \lambda NH_uH_d \quad \text{with } \lambda \sim \varepsilon^{n+h}.\end{aligned} \tag{10}$$

Now we wish to forbid the linear term in N at the perturbative level. This can be achieved with holomorphic zeros [8], which amounts in our setup to demanding that

$$n \overset{!}{<} 0. \tag{11}$$

This implies, in particular, that the cubic term in N is also forbidden.

Of course, this all works only if we make sure that ϕ rather than N cancels the FI term. This might be achieved by postulating that the soft mass squared of N is positive while the one of ϕ is negative; that is,

$$\begin{aligned}\widetilde{m}_\phi^2 &< 0, \\ \widetilde{m}_N^2 &> 0.\end{aligned} \tag{12}$$

Full justification of such an assumption would require deriving the setting from some UV complete construction such as a string model. This is, however, beyond the scope of this paper.

We further obtain nonperturbative terms which are linear or quadratic in N if $n + 2s \geq 0$ or $2n + s \geq 0$, respectively. Altogether we have

$$n + h \geq 0 \tag{13a}$$

$$\Longleftrightarrow \text{coupling } \lambda \text{ between } N \text{ and } H_uH_d \text{ with } \lambda \sim \varepsilon^{n+h},$$

$$n < 0 \quad \Longleftrightarrow \text{suppress linear term in } N, \tag{13b}$$

$$s + h \geq 0 \tag{13c}$$

$$\Longleftrightarrow \mu \text{ term with } \mu \sim M_P \varepsilon^{s+h} e^{-bS} \sim \varepsilon^h m_{3/2},$$

$$n + 2s \geq 0 \tag{13d}$$

$$\Longleftrightarrow f^2 N \text{ term with } f \sim M_P \varepsilon^{(n+2s)/2} e^{-bS} \sim \varepsilon^{n/2} m_{3/2},$$

$$2n + s \geq 0 \tag{13e}$$

$$\Longleftrightarrow \mu_N N^2 \text{ term with } \mu_N \sim M_P \varepsilon^{2n+s} e^{-bS} \sim \varepsilon^{2n} m_{3/2},$$

$$3n + 2s \geq 0 \tag{13f}$$

$$\Longleftrightarrow \kappa N^3 \text{ term with } \kappa \sim \varepsilon^{3n+2s} \left(e^{-bS}\right)^2 \sim \varepsilon^{3n} \frac{m_{3/2}^2}{M_P^2},$$

where the coefficient κ of the cubic term is generically highly suppressed. Not all conditions on $\{n, h, s\}$ are independent; for example, if the quadratic term is allowed also, since $s > 0$, the linear term will be present.

There are many possible values that satisfy all the constraints; for instance, $\{n, h, s\} = \{-1, 1, 2\}$, which gives us

$$\begin{aligned}\lambda &\sim \mathcal{O}(1), \\ \mu &\sim \varepsilon m_{3/2}, \\ \mu_N &\sim \frac{1}{\varepsilon^2} m_{3/2}, \\ f &\sim \frac{1}{\sqrt{\varepsilon}} m_{3/2}.\end{aligned} \tag{14}$$

That is, the (holomorphic) μ term is roughly two orders of magnitude smaller than μ_N, which might be favorable in view of the so-called "little hierarchy problem."

Note also that the effective superpotential

$$\mathscr{W}_{\text{eff}} = f^2 N + \mu H_d H_u + \lambda N H_d H_u + \mu_N N^2 \tag{15}$$

admits two solutions to the F- and D-term equations, the first one being (recall that $n < 0$)

$$\langle N \rangle = -\frac{\mu}{\lambda} \sim -\varepsilon^{|n|} m_{3/2}, \tag{16a}$$

$$\langle H_u \rangle = \langle H_d \rangle = \frac{\sqrt{2\mu\mu_N - \lambda f^2}}{\lambda} \sim \varepsilon^{-h/2} m_{3/2}. \tag{16b}$$

Here one has electroweak symmetry breaking prior to supersymmetry breaking, and the Higgs VEV may be subject to cancellations since both $\mu\mu_N$ and λf^2 are of the order ε^{2n+h}, for example, ε^{-1} in our example. The second solution is

$$\langle N \rangle = -\frac{f^2}{2\mu_N} \sim -\frac{1}{2}\varepsilon^{|n|} m_{3/2}, \tag{17a}$$

$$\langle H_u \rangle = \langle H_d \rangle = 0 \tag{17b}$$

with unbroken electroweak symmetry for unbroken supersymmetry.

2.3. Discussion. In summary, we find that the $\mathbb{Z}_4^R \times U(1)_{\text{anom}}$ charge assignment of Table 1 yields an effective superpotential,

$$\mathscr{W}_{\text{eff}} = f^2 N + \mu H_d H_u + \lambda N H_d H_u + \mu_N N^2, \tag{18}$$

with all the dimensionful parameters μ, μ_N, and f of the order of the gravitino mass $m_{3/2}$. This description is valid below the $U(1)_{\text{anom}}$ breaking scale, which is set by the flavon VEV $\langle\phi\rangle$. In particular, the linear term in the singlet is sufficiently suppressed. In contrast to the original (G)NMSSM [18], here,

(i) there is (essentially) no cubic term in N;

(ii) there is a suppressed linear term in N. (Note that, unlike in [18], we cannot shift the singlet in order to eliminate the linear term because the point $N = 0$ is special as it denotes the point of unbroken $\mathbb{Z}_4^R$.)

The scheme leads to certain predictions and expectations:

(1) Forbidding the linear term by holomorphic zeros implies the absence of a perturbative cubic term in N.

(2) Further, we obtain the "little hierarchies" (recall that $n < 0$)

$$\mu \sim \varepsilon^{h+2|n|}\mu_N, \qquad f \sim \frac{\mu}{\varepsilon^{h+|n|/2}}. \tag{19}$$

2.4. Further Applications. Clearly, this method of avoiding a linear term in a gauge singlet may find further applications. For instance, in model building one sometimes introduces so-called "driving fields" in order to "explain" a certain structure of flavon VEVs. Here, one may forbid too large tadpole terms in the same way as we have discussed above.

3. Discussion

We have discussed how to build singlet extensions of the MSSM with $\mathbb{Z}_4^R$ symmetry. We have shown that a potentially large linear term in the singlet can be avoided by using holomorphic zeros. The resulting model has a μ term, a supersymmetric mass of the order of the gravitino mass $m_{3/2}$, as well as a coefficient of an effective linear term in the singlet of the order $m_{3/2}^2$. μ is expected to be one or two orders of magnitude smaller than μ_N. This might be viewed as the first step towards a solution to the little hierarchy problem; that is, explain why the electroweak scale is at least one order of magnitude smaller than the soft supersymmetric terms. Obtaining a complete solution requires the derivation of our setting from a UV complete model, which allows us to compute various terms precisely. This, however, is beyond the scope of this paper.

Appendices

A. Cancellation of the FI Term

In this appendix, we discuss how the FI term gets cancelled by a single monomial $\mathscr{M}$. The generalization to the case of several monomials is straightforward. We consider a monomial of chiral superfields ϕ_i, which are assumed to be standard model singlets,

$$\mathscr{M} = \prod_i \phi_i^{n_i}, \tag{A.1}$$

with $n_i \in \mathbb{N}$. $\mathscr{M}$ is constructed to be gauge invariant with respect to all gauge symmetries except the "anomalous" $U(1)_{\text{anom}}$. In a supersymmetric vacuum one then has

$$\frac{|\langle\phi_i\rangle|}{\sqrt{n_i}} = v, \tag{A.2}$$

where v is determined from the requirement that the FI term $\xi > 0$ in the D-term potential of the anomalous $U(1)_{\text{anom}}$ gets cancelled. That is,

$$0 \stackrel{!}{=} D_{\text{anom}} = \xi + \sum_i Q_{\text{anom}}^{(i)} |\langle\phi_i\rangle|^2 = \xi + v^2 \sum_i Q_{\text{anom}}^{(i)} n_i; \tag{A.3}$$

that is,

$$v = \sqrt{-\frac{\xi}{\sum_i Q_{\text{anom}}^{(i)} n_i}}. \tag{A.4}$$

On the other hand, the "anomalous" charge of the monomial $\mathscr{M}$ is

$$Q_{\text{anom}}(\mathscr{M}) = \sum_i Q_{\text{anom}}^{(i)} n_i < 0. \tag{A.5}$$

Hence, we obtain

$$|\langle\phi_j\rangle| = \sqrt{n_j}\sqrt{-\frac{\xi}{Q_{\text{anom}}(\mathscr{M})}}. \tag{A.6}$$

That is, if one compares the cases in which (i) the FI term ξ is cancelled by a single field and (ii) the FI term is cancelled by a monomial, there are $\sqrt{n_j}$ factors that enhance the flavon VEVs somewhat in case (ii).

B. Nonperturbative Terms in the Superpotential

In this appendix we discuss how to compute the $U(1)_{\text{anom}}$ charge of the nonperturbative term e^{-bS} in the case that the anomaly of $U(1)_{\text{anom}}$ is cancelled via the universal Green-Schwarz mechanism. We follow the notation of Appendix A.2 in [6].

The Kähler potential of the dilaton S reads

$$K\left(S, S^\dagger, V\right) = -\ln\left(S + S^\dagger - \delta_{\text{GS}} V\right). \tag{B.1}$$

Then, under $U(1)_{\text{anom}}$ gauge transformations with gauge parameter $\Lambda(x)$, the $U(1)_{\text{anom}}$ vector field V and the dilaton S shift according to

$$V \mapsto V + \frac{i}{2}\left(\Lambda(x) - \Lambda(x)^\dagger\right), \tag{B.2a}$$

$$S \mapsto S + \frac{i}{2}\delta_{\text{GS}}\Lambda(x), \tag{B.2b}$$

such that $K(S, S^\dagger, V)$ is invariant. Furthermore, in order to cancel the cubic anomaly $A_{U(1)_{\text{anom}}^3}$, the constant δ_{GS} has to satisfy

$$\delta_{\text{GS}} = \frac{1}{2\pi^2} A_{U(1)_{\text{anom}}^3} = \frac{1}{6\pi^2} \operatorname{tr} Q_{\text{anom}}^3, \tag{B.3}$$

where the trace sums over the $U(1)_{\text{anom}}$ charges of all matter superfields. Consequently, one can define a charge s for the nonperturbative term,

$$e^{-bS} \mapsto e^{-is\Lambda(x)} e^{-bS}, \tag{B.4}$$

with $b > 0$ and the charge s is given by

$$s = Q_{\text{anom}}\left(e^{-bS}\right) = \frac{b}{2}\delta_{\text{GS}} = \frac{b}{12\pi^2}\,\text{tr}\,Q_{\text{anom}}^3. \tag{B.5}$$

Depending on $\text{tr}\,Q_{\text{anom}}^3$ the charge s of e^{-bS} can be positive or negative. On the other hand, in certain string-derived models, in which the Green-Schwarz mechanism is universal, one has the relation

$$\text{tr}\,Q_{\text{anom}}^3 = \frac{1}{8}\,\text{tr}\,Q_{\text{anom}}, \tag{B.6}$$

using the fact that the generator of $U(1)_{\text{anom}}$ is normalized to $1/2$. Then one obtains

$$s = \frac{b}{96\pi^2}\,\text{tr}\,Q_{\text{anom}}. \tag{B.7}$$

We have chosen $U(1)_{\text{anom}}$ such that the FI term ξ is positive; that is,

$$\xi = \frac{g}{192\pi^2}\,\text{tr}\,Q_{\text{anom}} > 0; \tag{B.8}$$

see Appendix A. Consequently, the $U(1)_{\text{anom}}$ charge of the nonperturbative term e^{-bS} is positive as well; that is,

$$s = \frac{2b}{g}\xi > 0. \tag{B.9}$$

For instance, in the case of a condensing $SU(N_c)$ group with $N_f < N_c$ fundamental and antifundamental "matter" fields, Q and $\widetilde{Q}$, one has (see, e.g., [13, Equation (2.7)] of the published version)

$$\begin{aligned}\mathscr{W}_{\text{hid}} \supset \left(N_c - N_f\right)\frac{\Lambda^{(3Nc-N_f)/(N_c-N_f)}}{(\det M)^{1/(N_c-N_f)}} \\ + \left(\frac{\phi}{M_P}\right)^{q+\bar{q}} m_i^{\bar{j}} M_{\bar{j}}^i,\end{aligned} \tag{B.10}$$

where Λ denotes the renormalization group invariant scale and carries charge $Q_{\text{anom}}(\Lambda) = N_f(q + \bar{q})/(3N_c - N_f)$. q and $\bar{q}$ are the "anomalous" charges of Q and $\widetilde{Q}$, respectively. Inserting the VEV of the mesons $M_{\bar{j}}^i = Q^i\widetilde{Q}_{\bar{j}}$ (see [13, Equation (2.13)]), one obtains a term of the form (3).

Conflict of Interests

The authors declare that there is no conflict of interests regarding the publication of this paper.

Acknowledgments

The authors would like to thank Mu-Chun Chen and Graham Ross for useful discussions. Michael Ratz would like to thank the UC Irvine, where part of this work was done, for hospitality. This work was partially supported by the DFG cluster of excellence "Origin and Structure of the Universe" (http://www.universe-cluster.de) by Deutsche Forschungsgemeinschaft (DFG). The authors would like to thank the Aspen Center for Physics for hospitality and support. This research was done in the context of the ERC Advanced Grant Project "FLAVOUR" (267104).

References

[1] K. S. Babu, I. Gogoladze, and K. Wang, "Natural R-parity, μ-term, and fermion mass hierarchy from discrete gauge symmetries," *Nuclear Physics B*, vol. 660, no. 1-2, pp. 322–342, 2003.

[2] H. M. Lee, S. Raby, M. Ratz et al., "A unique $\mathbb{Z}_4^R$ symmetry for the MSSM," *Physics Letters B*, vol. 694, no. 4-5, pp. 491–495, 2011.

[3] M. B. Green and J. H. Schwarz, "Anomaly cancellations in supersymmetric $D = 10$ gauge theory and superstring theory," *Physics Letters B*, vol. 149, no. 1–3, pp. 117–122, 1984.

[4] M.-C. Chen, M. Fallbacher, and M. Ratz, "Supersymmetric unification and R symmetries," *Modern Physics Letters A*, vol. 27, no. 40, Article ID 1230044, 15 pages, 2012.

[5] M.-C. Chen, M. Ratz, and V. Takhistov, "R parity violation from discrete R symmetries," *Nuclear Physics B*, vol. 891, pp. 322–345, 2015.

[6] H. M. Lee, S. Raby, M. Ratz et al., "Discrete R symmetries for the MSSM and its singlet extensions," *Nuclear Physics B*, vol. 850, no. 1, pp. 1–30, 2011.

[7] R. Kappl, B. Petersen, S. Raby, M. Ratz, R. Schieren, and P. K. Vaudrevange, "String-derived MSSM vacua with residual R symmetries," *Nuclear Physics B*, vol. 847, no. 2, pp. 325–349, 2011.

[8] M. Leurer, Y. Nir, and N. Seiberg, "Mass matrix models," *Nuclear Physics B*, vol. 398, no. 2, pp. 319–342, 1993.

[9] P. Fayet and J. Iliopoulos, "Spontaneously broken supergauge symmetries and goldstone spinors," *Physics Letters B*, vol. 51, no. 5, pp. 461–464, 1974.

[10] W. Fischler, H. P. Nilles, J. Polchinski, S. Raby, and L. Susskind, "Vanishing renormalization of the D term in supersymmetric U(1) theories," *Physical Review Letters*, vol. 47, article 757, 1981.

[11] H. P. Nilles and P. K. S. Vaudrevange, "Geography of fields in extra dimensions: string theory lessons for particle physics," in *Perspectives on String Phenomenology*, vol. 22 of *Advanced Series on Directions in High Energy Physics*, World Scientific, 2015.

[12] C. D. Froggatt and H. B. Nielsen, "Hierarchy of quark masses, cabibbo angles and CP violation," *Nuclear Physics B*, vol. 147, no. 3-4, pp. 277–298, 1979.

[13] P. Binetruy and E. Dudas, "Gaugino condensation and the anomalous $U(1)$," *Physics Letters B*, vol. 389, no. 3, pp. 503–509, 1996.

[14] N. Arkani-Hamed, M. Dine, and S. P. Martin, "Dynamical supersymmetry breaking in models with a Green–Schwarz mechanism," *Physics Letters B*, vol. 431, no. 3-4, pp. 329–338, 1998.

[15] I. Affleck, M. Dine, and N. Seiberg, "Dynamical supersymmetry breaking in supersymmetric QCD," *Nuclear Physics, Section B*, vol. 241, no. 2, pp. 493–534, 1984.

[16] H. P. Nilles, "Dynamically broken supergravity and the hierarchy problem," *Physics Letters B*, vol. 115, no. 3, pp. 193–196, 1982.

[17] K. Intriligator, N. Seiberg, and D. Shih, "Dynamical SUSY breaking in meta-stable vacua," *Journal of High Energy Physics*, vol. 2006, article 21, 2006.

[18] M. Drees, "Supersymmetric models with extended Higgs sector," *International Journal of Modern Physics A*, vol. 4, no. 14, pp. 3635–3651, 1989.

Hindawi Publishing Corporation
Advances in High Energy Physics
Volume 2015, Article ID 980687, 12 pages
http://dx.doi.org/10.1155/2015/980687

Research Article

The Higgs Sector of the Minimal SUSY $B - L$ Model

Lorenzo Basso[1,2]

[1] *Universitè de Strasbourg, IPHC, 23 rue du Loess, 67037 Strasbourg, France*
[2] *CNRS, UMR7178, 67037 Strasbourg, France*

Correspondence should be addressed to Lorenzo Basso; lorenzo.basso@iphc.cnrs.fr

Received 23 April 2015; Revised 17 June 2015; Accepted 25 June 2015

Academic Editor: Kai Schmidt-Hoberg

I review the Higgs sector of the $U(1)_{B-L}$ extension of the minimal supersymmetric standard model (MSSM). I will show that the gauge kinetic mixing plays a crucial role in the Higgs phenomenology. Two light bosons are present, a MSSM-like one and a $B-L$-like one, which mix at one loop solely due to the gauge mixing. After briefly looking at constraints from flavour observables, new decay channels involving right-handed (s)neutrinos are presented. Finally, how model features pertaining to the gauge extension affect the model phenomenology, concerning the existence of R-Parity-conserving minima at loop level and the Higgs-to-diphoton coupling, will be reviewed.

1. Introduction

The recently discovered Higgs boson is considered as the last missing piece of the standard model (SM) of particle physics. Nonetheless, several firm observations univocally call for its extension, mainly, but not limited to, the presence of dark matter, the neutrino masses and mixing pattern, the stability of the SM vacuum, and the hierarchy problem. Supersymmetry (SUSY) has long been considered as the most appealing framework to extend the SM. Its minimal realisations (MSSM and its constrained versions (for a review, see [1])) start however to feel considerable pressure to accommodate the recent findings, especially the measured Higgs mass of 125 GeV. Despite not in open contrast with the MSSM, the degree of fine tuning required to achieve it is more and more felt as unnatural. In order to alleviate this tension, nonminimal SUSY realisations can be considered. One can either extend the MSSM by the inclusion of extra singlets (e.g., NMSSM [2]) or by extending its gauge group. Concerning the latter, one of the simplest possibilities is to add an additional Abelian gauge group. I will focus here on the presence of $U(1)_{B-L}$ group which can be a result of an $E_8 \times E_8$ heterotic string theory (and hence M-theory) [3–5]. This model, the minimal R-Parity-conserving $B - L$ supersymmetric standard model (BLSSM in short), was proposed in [6, 7] and neutrino masses are obtained via a type I seesaw mechanism. Furthermore, it could help to understand the origin of R-Parity and its possible spontaneous violation in supersymmetric models [6–8] as well as the mechanism of leptogenesis [9, 10].

It was early pointed out that the presence of two Abelian gauge groups in this model gives rise to kinetic mixing terms of the form

$$-\chi_{ab}\widehat{F}^{a,\mu\nu}\widehat{F}^{b}_{\mu\nu}, \quad a \neq b, \tag{1}$$

which are allowed by gauge and Lorentz invariance [11], as $\widehat{F}^{a,\mu\nu}$ and $\widehat{F}^{b,\mu\nu}$ are gauge-invariant quantities by themselves; see, for example, [12]. Even if these terms are absent at tree level at a particular scale, they will in general be generated by RGE effects [13, 14]. These terms can have a sizable effect on the mass spectrum of this model, as studied in detail in [15], and on the dark matter, where several scenarios would not work if kinetic mixing is neglected, as thoroughly investigated in [16]. In this work, I will review the properties of the Higgs sector of the model. Two light states exist, a MSSM-like boson and a $B-L$-like boson. After reviewing the model, I will show that a large portion of parameter space exists where the SM-like Higgs boson has a mass compatible with its measure, both in a "normal" ($M_{H_2} > M_{H_1} = 125\,\text{GeV}$) and in an "inverted" hierarchy ($M_{H_1} < M_{H_2} = 125\,\text{GeV}$), also in agreement with bounds from low energy observables and dark matter relic abundance. The phenomenological properties of

the two lightest Higgs bosons will be systematically investigated, where once again the gauge mixing is shown to be fundamental. The presence of extra D-terms arising from the new $U(1)_{B-L}$ sector, as compared to models based on the SM gauge symmetry, has a large impact on the model phenomenology. They affect both the vacuum structure of the model and the Higgs sector, in particular enhancing the Higgs-to-diphoton coupling. Both of these issues will be reviewed here, although the latter is disfavoured by recent data [17], to show model features beyond the MSSM.

2. The Model

For a detailed discussion of the masses of all particles as well as of the corresponding one-loop corrections, we refer to [15]. Attention will be paid to the main aspects of the $U(1)$ kinetic mixing since it has important consequence for the scalar sector. For the numerical investigations that will be shown, we used the `SPheno` version [22, 23] created with `SARAH` [24–28] for the BLSSM. For the standardised model definitions, see [29], while for a review of the model implementation in `SARAH`, see [30]. This spectrum calculator performs a two-loop RGE evaluation and calculates the mass spectrum at one loop. In addition, it calculates the decay widths and branching ratios (BRs) of all SUSY and Higgs particles as well as low energy observables like $(g-2)_\mu$. We will discuss the most constrained scenario with a universal scalar mass m_0, a universal gaugino mass $M_{1/2}$, and trilinear soft-breaking couplings proportional to the superpotential coupling ($T_i = A_0 Y_i$) at the GUT scale. Other input parameters are $\tan\beta$, $\tan\beta'$, $M_{Z'}$, Y_x, and Y_ν. They will be defined in the following section. The numerical study here presented has been performed by randomly scanning over the independent input parameters above described via the `SSP` toolbox [31], while low energy observables such as BR($\mu \to e\gamma$) and BR($\mu \to 3e$) have been evaluated with the `FlavourKit` package [32]. Furthermore, during the scans, all points have been checked with `HiggsBounds`-4.1.1 [33–36], both in the "normal" hierarchy and in the "inverted" hierarchy case.

2.1. Particle Content and Superpotential. The model consists of three generations of matter particles including right-handed neutrinos which can, for example, be embedded in $SO(10)$ 16-plets. Moreover, below the GUT scale, the usual MSSM Higgs doublets are present as well as two fields η and $\overline{\eta}$ responsible for the breaking of $U(1)_{B-L}$. The η field is also responsible for generating a Majorana mass term for the right-handed neutrinos and thus we interpret its $B-L$ charge as its lepton number. The same goes for $\overline{\eta}$, and we call these fields bileptons since they carry twice the lepton number of (anti)neutrinos. The quantum numbers of the chiral superfields with respect to $U(1)_Y \times SU(2)_L \times SU(3)_C \times U(1)_{B-L}$ are summarised in Table 1.

The superpotential is given by

$$\begin{aligned} W = {} & Y_u^{ij}\widehat{u}_i^c\widehat{Q}_j\widehat{H}_u - Y_d^{ij}\widehat{d}_i^c\widehat{Q}_j\widehat{H}_d - Y_e^{ij}\widehat{e}_i^c\widehat{L}_j\widehat{H}_d + \mu\widehat{H}_u\widehat{H}_d \\ & + Y_\nu^{ij}\widehat{\nu}_i^c\widehat{L}_j\widehat{H}_u - \mu'\widehat{\overline{\eta}}\widehat{\eta} + Y_x^{ij}\widehat{\nu}_i^c\widehat{\eta}\widehat{\nu}_j^c \end{aligned} \tag{2}$$

Table 1: Chiral superfields and their quantum numbers under $G_{SM} \otimes U(1)_{B-L}$, where $G_{SM} = (U(1)_Y \otimes SU(2)_L \otimes SU(3)_C)$.

Superfield	Spin-0	Spin-1/2	Generations	$G_{SM} \otimes U(1)_{B-L}$
$\widehat{Q}$	$\widetilde{Q}$	Q	3	$(1/6, \mathbf{2}, \mathbf{3}, 1/6)$
$\widehat{d}^c$	$\widetilde{d}^c$	d^c	3	$(1/3, \mathbf{1}, \overline{\mathbf{3}}, -1/6)$
$\widehat{u}^c$	$\widetilde{u}^c$	u^c	3	$(-2/3, \mathbf{1}, \overline{\mathbf{3}}, -1/6)$
$\widehat{L}$	$\widetilde{L}$	L	3	$(-1/2, \mathbf{2}, \mathbf{1}, -1/2)$
$\widehat{e}^c$	$\widetilde{e}^c$	e^c	3	$(1, \mathbf{1}, \mathbf{1}, 1/2)$
$\widehat{\nu}^c$	$\widetilde{\nu}^c$	ν^c	3	$(0, \mathbf{1}, \mathbf{1}, 1/2)$
$\widehat{H}_d$	H_d	$\widetilde{H}_d$	1	$(-1/2, \mathbf{2}, \mathbf{1}, 0)$
$\widehat{H}_u$	H_u	$\widetilde{H}_u$	1	$(1/2, \mathbf{2}, \mathbf{1}, 0)$
$\widehat{\eta}$	η	$\widetilde{\eta}$	1	$(0, \mathbf{1}, \mathbf{1}, -1)$
$\widehat{\overline{\eta}}$	$\overline{\eta}$	$\widetilde{\overline{\eta}}$	1	$(0, \mathbf{1}, \mathbf{1}, 1)$

and we have the additional soft SUSY-breaking terms:

$$\begin{aligned} \mathscr{L}_{SB} = {} & \mathscr{L}_{MSSM} - \lambda_{\widetilde{B}}\lambda_{\widetilde{B}'}M_{BB'} - \frac{1}{2}\lambda_{\widetilde{B}'}\lambda_{\widetilde{B}'}M_{B'} - m_\eta^2|\eta|^2 \\ & - m_{\overline{\eta}}^2|\overline{\eta}|^2 - m_{\nu^c,ij}^2(\widetilde{\nu}_i^c)^*\widetilde{\nu}_j^c - \eta\overline{\eta}B_{\mu'} + T_\nu^{ij}H_u\widetilde{\nu}_i^c\widetilde{L}_j \\ & + T_x^{ij}\eta\widetilde{\nu}_i^c\widetilde{\nu}_j^c, \end{aligned} \tag{3}$$

where i, j are generation indices. Without loss of generality, one can take B_μ and $B_{\mu'}$ to be real. The extended gauge group breaks to $SU(3)_C \otimes U(1)_{em}$ as the Higgs fields and bileptons receive vacuum expectation values (*vevs*):

$$\begin{aligned} H_d^0 &= \frac{1}{\sqrt{2}}(\sigma_d + v_d + i\phi_d), \\ H_u^0 &= \frac{1}{\sqrt{2}}(\sigma_u + v_u + i\phi_u) \\ \eta &= \frac{1}{\sqrt{2}}(\sigma_\eta + v_\eta + i\phi_\eta), \\ \overline{\eta} &= \frac{1}{\sqrt{2}}(\sigma_{\overline{\eta}} + v_{\overline{\eta}} + i\phi_{\overline{\eta}}). \end{aligned} \tag{4}$$

We define $\tan\beta' = v_\eta/v_{\overline{\eta}}$ in analogy to the ratio of MSSM *vevs* ($\tan\beta = v_u/v_d$).

2.2. Gauge Kinetic Mixing. As already mentioned in the Introduction, the presence of two Abelian gauge groups in combination with the given particle content gives rise to a new effect absent in any model with just one Abelian gauge group: gauge kinetic mixing. This can be seen most easily by inspecting the matrix of the anomalous dimension, which for our model at one loop reads

$$\gamma = \frac{1}{16\pi^2}\begin{pmatrix} \frac{33}{5} & 6\sqrt{\frac{2}{5}} \\ 6\sqrt{\frac{2}{5}} & 9 \end{pmatrix}, \tag{5}$$

with typical GUT normalisation of the two Abelian gauge groups, that is, $\sqrt{3/5}$ for $U(1)_Y$ and $\sqrt{3/2}$ for $U(1)_{B-L}$ [7].

Therefore, even if at the GUT scale the $U(1)$ kinetic mixing terms are zero, they are induced via RGE evaluation at lower scales. It turns out that it is more convenient to work with noncanonical covariant derivatives rather than with off-diagonal field-strength tensors as in (1). However, both approaches are equivalent [37]. Therefore, in the following, we consider covariant derivatives of the form $D_\mu = \partial_\mu - iQ_\phi^T GA$, where Q_ϕ is a vector containing the charges of the field ϕ with respect to the two Abelian gauge groups, G is the gauge coupling matrix

$$G = \begin{pmatrix} g_{YY} & g_{YB} \\ g_{BY} & g_{BB} \end{pmatrix}, \tag{6}$$

and A contains the gauge bosons $A = (A_\mu^Y, A_\mu^B)^T$.

As long as the two Abelian gauge groups are unbroken, we have still the freedom to perform a change of basis by means of a suitable rotation. A convenient choice is the basis where $g_{BY} = 0$, since in this case only the Higgs doublets contribute to the gauge boson mass matrix of the $SU(2)_L \otimes U(1)_Y$ sector, while the impact of η and $\overline{\eta}$ is only in the off-diagonal elements. Therefore, we choose the following basis at the electroweak scale [38]:

$$\begin{aligned} g'_{YY} &= \frac{g_{YY}g_{BB} - g_{YB}g_{BY}}{\sqrt{g_{BB}^2 + g_{BY}^2}} = g_1, \\ g'_{BB} &= \sqrt{g_{BB}^2 + g_{BY}^2} = g_{BL}, \\ g'_{YB} &= \frac{g_{YB}g_{BB} + g_{BY}g_{YY}}{\sqrt{g_{BB}^2 + g_{BY}^2}} = \overline{g}, \\ g'_{BY} &= 0. \end{aligned} \tag{7}$$

When unification at some large scale ($\sim 2 \cdot 10^{16}$ GeV) is imposed, that is, $g_1^{\mathrm{GUT}} = g_2^{\mathrm{GUT}} = g_{BL}^{\mathrm{GUT}}$ and $g_{YB}^{\prime(\mathrm{GUT})} = g_{BY}^{\prime(\mathrm{GUT})} = 0$, at SUSY scale, we get [15]

$$\begin{aligned} g_{BL} &= 0.548, \\ \overline{g} &\simeq -0.147. \end{aligned} \tag{8}$$

2.3. Tadpole Equations. The minimisation of the scalar potential is here described in the so-called tadpole method. We can solve the tree-level tadpole equations arising from the minimum conditions of the vacuum with respect to μ, B_μ, μ', and $B_{\mu'}$. Using $v_x^2 = v_\eta^2 + v_{\overline{\eta}}^2$ and $v^2 = v_d^2 + v_u^2$, we obtain

$$\begin{aligned} |\mu|^2 = \frac{1}{8}&\left(\left(2\overline{g}g_{BL}v_x^2\cos\left(2\beta'\right) - 4m_{H_d}^2 + 4m_{H_u}^2\right)\right. \\ &\left.\cdot\sec\left(2\beta\right) - 4\left(m_{H_d}^2 + m_{H_u}^2\right) - \left(g_1^2 + \overline{g}^2 + g_2^2\right)v^2\right), \end{aligned} \tag{9}$$

$$\begin{aligned} B_\mu = -\frac{1}{8}&\left(-2\overline{g}g_{BL}v_x^2\cos\left(2\beta'\right) + 4m_{H_d}^2 - 4m_{H_u}^2\right. \\ &\left.+\left(g_1^2 + \overline{g}^2 + g_2^2\right)v^2\cos\left(2\beta\right)\right)\tan\left(2\beta\right), \end{aligned} \tag{10}$$

$$\begin{aligned} \left|\mu'\right|^2 = \frac{1}{4}&\left(-2\left(g_{BL}^2v_x^2 + m_\eta^2 + m_{\overline{\eta}}^2\right)\right. \\ &\left.+\left(2m_\eta^2 - 2m_{\overline{\eta}}^2 + \overline{g}g_{BL}v^2\cos\left(2\beta\right)\right)\sec\left(2\beta'\right)\right), \end{aligned} \tag{11}$$

$$\begin{aligned} B_{\mu'} = \frac{1}{4}&\left(-2g_{BL}^2v_x^2\cos\left(2\beta'\right) + 2m_\eta^2 - 2m_{\overline{\eta}}^2 + \overline{g}g_{BL}v^2\right. \\ &\left.\cdot\cos\left(2\beta\right)\right)\tan\left(2\beta'\right), \end{aligned} \tag{12}$$

$M_{Z'} \simeq g_{BL}v_x$, and, thus, we find an approximate relation between $M_{Z'}$ and μ'

$$\begin{aligned} M_{Z'}^2 \simeq &-2\left|\mu'\right|^2 \\ &+\frac{4\left(m_{\overline{\eta}}^2 - m_\eta^2\tan^2\beta'\right) - v^2\overline{g}g_{BL}\cos\beta\left(1 + \tan\beta'\right)}{2\left(\tan^2\beta' - 1\right)}. \end{aligned} \tag{13}$$

For the numerical results, the one-loop corrected equations are used, which lead to a shift of the solutions in (9)–(12).

2.4. The Scalar Sector. In this model, 2 MSSM complex doublets and 2 bilepton complex singlets are present, yielding 4 *CP*-even, 2 *CP*-odd, and 2 charged physical scalars.

Concerning the *CP*-even scalars, the MSSM and bilepton sectors are almost decoupled, mixing exclusively due to the gauge kinetic mixing. In first approximation, the mass matrix is block-diagonal and has mass eigenstates that mimic the MSSM case. In practice, it turns out that only two Higgs bosons are light (hereafter called H_1 and H_2, one per sector), while the other two are very heavy (above the TeV scale). The lightest scalars are well defined states, being either almost exclusively doublet-like or bilepton-like. It is worth stressing that their mixing is small (see Figure 4) and solely due to the gauge kinetic mixing (see also [39]).

Concerning the physical pseudoscalars A^0 and A_η^0, their masses are given by

$$\begin{aligned} m_{A^0}^2 &= \frac{2B_\mu}{\sin 2\beta}, \\ m_{A_\eta^0}^2 &= \frac{2B_{\mu'}}{\sin 2\beta'}. \end{aligned} \tag{14}$$

For completeness, we note that the mass of charged Higgs boson reads as in the MSSM as

$$m_{H^+}^2 = B_\mu\left(\tan\beta + \cot\beta\right) + m_W^2. \tag{15}$$

In this model, the *CP*-odd and charged Higgses are typically very heavy. In (10), we see that, compared to the MSSM, there is a nonnegligible contribution from the gauge kinetic mixing. LHC searches limit $\tan\beta' < 1.5$ and $v_x \gtrsim 7$ TeV, since [40, 41]

$$M_{Z'} \gtrsim 3.5\ \mathrm{TeV} \tag{16}$$

at 95% C.L. Notice that recent reanalysis of LEP precision data also constrains $v_x \gtrsim 7$ TeV at 99% C.L. [42]. A consequence of this strong constraint in the BLSSM is that the first terms in

(10)–(12) can be large, pushing for CP-odd and charged Higgs masses in the TeV range.

The very large bound on the Z' mass is in contrast with the non-SUSY version of the model, where the gauge couplings are free parameters and can be much smaller, hence yielding lower mass bounds. The latter need to be evaluated as a function of both gauge couplings [43].

Next, we describe the sneutrino sector, which shows two distinct features compared to the MSSM. Firstly, it gets enlarged by the superpartners of the right-handed neutrinos. Secondly, even more drastically, a splitting between the real and imaginary parts of each sneutrino occurs resulting in twelve states: six scalar sneutrinos and six pseudoscalar ones [44, 45]. The origin of this splitting is the $Y_x^{ij}\widetilde{\nu}_i^c\widetilde{\eta}\widetilde{\nu}_j^c$ term in the superpotential (see (2)), which is $\Delta L = 2$ operator after the breaking of $U(1)_{B-L}$. In the case of complex trilinear couplings or μ-terms, a mixing between the scalar and pseudoscalar particles occurs, resulting in 12 mixed states and consequently in a 12×12 mass matrix.

To gain some feeling for the behaviour of the sneutrino masses, we can consider a simplified setup: neglecting kinetic mixing as well as left-right mixing, the masses of the R-sneutrinos at the SUSY scale can be expressed as

$$\begin{aligned} m^2_{\widetilde{\nu}^S} &\simeq m^2_{\nu^c} + M^2_{Z'}\left(\frac{1}{4}\cos\left(2\beta'\right) + \frac{2Y_x^2}{g^2_{BL}}\sin\beta'^2\right) \\ &\quad + M_{Z'}\frac{\sqrt{2}Y_x}{g_{BL}}\left(A_x\sin\beta' - \mu'\cos\beta'\right), \\ m^2_{\widetilde{\nu}^P} &\simeq m^2_{\nu^c} + M^2_{Z'}\left(\frac{1}{4}\cos\left(2\beta'\right) + \frac{2Y_x^2}{g^2_{BL}}\sin\beta'^2\right) \\ &\quad - M_{Z'}\frac{\sqrt{2}Y_x}{g_{BL}}\left(A_x\sin\beta' - \mu'\cos\beta'\right). \end{aligned} \tag{17}$$

In addition, we treat the parameters $A_x, m^2_{\nu^c}, M_{Z'}, \mu', Y_x$, and $\tan\beta'$ as independent. The different effects on the sneutrino masses can easily be understood by inspecting (17). The first two terms give always a positive contribution whereas the third one gives a contribution that can be potentially large which differs in sign between the scalar and pseudoscalar states, therefore inducing a large mass splitting between the states. Further, this contribution can either be positive or negative depending on the sign of $A_x\sin\beta' - \mu'\cos\beta'$. For example, choosing Y_x and μ' positive, one finds that the CP-even (CP-odd) sneutrino is the lightest one for $A_x < 0$ ($A_x > 0$). This is pictorially shown in Figure 1, as a function of the GUT-scale input parameter A_0, for a choice of the other parameters. One notices that the CP-even (CP-odd) sneutrino is the lightest one when the 125 GeV Higgs boson is predominantly H_1 (H_2). It is worth pointing out here that, as will be described in the following section, when $M_{H_1} = 125$ GeV, the next-to-lightest Higgs boson can decay into pairs of CP-even sneutrinos, but not into similar channel with CP-odd sneutrinos. Being H_2 predominantly a bilepton field, when this decay is open, it saturates its BRs; see Figure 3. Regarding the decay into CP-odd sneutrinos, this channel is accessible (i.e., $\widetilde{\nu}^P$ is light enough) only in the region where H_2

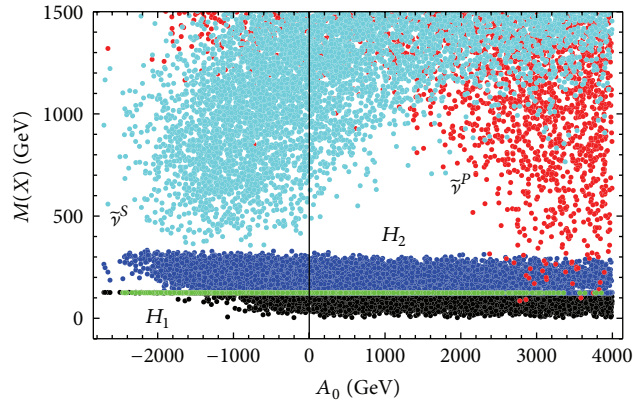

Figure 1: Masses of CP-even ($\widetilde{\nu}^S$, cyan) and CP-odd ($\widetilde{\nu}^P$, red) R-sneutrinos as a function of A_0. For comparison, also the masses of the lightest (H_1, black) and next-to-lightest (H_2, blue) Higgs bosons are shown. Configurations when $M_{H_1} = 125$ GeV are shown in green.

is the SM-like Higgs boson, that is, mainly coming from the doublets. In this case, however, this decay channel is mitigated by the small scalar mixing and is not overwhelming (unlike for H_1, now mainly from the bileptons).

Depending on the parameters, either type of sneutrinos can get very light. For the LSP, it can be a suitable dark matter candidate [16] and yield extra fully invisible decay channels to the Higgs bosons, thereby increasing their invisible widths. In the case of the decay into the CP-odd sneutrino, since this can happen mainly for the SM-like Higgs boson, one should account for the constraints on the former [17]. Eventually, the R-sneutrinos could also get tachyonic or develop dangerous R-Parity-violating *vevs*. While the first possibility is taken into account in our numerical evaluation by `SPheno`, and such points are excluded from our scans, the second case will be reviewed in the following subsection.

The last important sector for considerations that will follow is the one of the charged sleptons. See [46] for further details. New SUSY breaking D-term contributions to the masses appear, which can be parametrised as a function of the Z' mass and of $\tan\beta'$ as

$$\frac{Q^{B-L}}{2}\frac{M_{Z'}\left(\tan^2\beta' - 1\right)}{1 + \tan^2\beta'}. \tag{18}$$

Their impact is larger for the sleptons than for the squarks by a factor of 3 due to the different $B - L$ charges (Q^{B-L}). It is possible to vary the stau mass by $\pm\mathcal{O}(100)$ GeV with respect to the MSSM case while keeping the impact on the squarks under control. Having different sfermion masses in the BLSSM as compared to the MSSM has a net impact on the Higgs phenomenology, in particular in enhancing the $h\gamma\gamma$ coupling while keeping unaltered the SM-like Higgs coupling to gluons. As described at the end of this review, the new D-terms coming from the B–L sector can further reduce the stau mass entering in the $h\gamma\gamma$ effective interaction (while ensuring a pole mass of $\sim$ 250 GeV, compatible with exclusions) (with pole mass we denote the one-loop corrected mass at

$Q = M_{\text{SUSY}} = \sqrt{\tilde{t}_1\tilde{t}_2}$, while in the loop, leading to the effective $h\gamma\gamma$ coupling, the running $\overline{\text{DR}}$ tree-level mass at $Q = m_h$ enters, being h the SM-like Higgs boson; i.e., $m_h = 125\,\text{GeV}$) leading this mechanism to work also in the constrained version of the model. This mechanism has been recently reanalysed also in [47] in the very same model.

2.5. The Issue of R-Parity Conservation. We have encountered so far several neutral scalar fields which could develop *vev*, beside the Higgs bosons. If *vevs* of fields charged under QCD and electromagnetism are forbidden because the latter are good symmetries, R-sneutrino *vevs*, which are not by themselves problematic, would unavoidably break R-Parity. The issue of conserving R-Parity is of fundamental importance, since this is a built-in symmetry in our model where $B - L$ is gauged. We will therefore restrain ourselves to parameter configurations where the global minimum is R-Parity conserving.

When all neutral scalar fields are allowed to get *vev*, it is not trivial even at the tree level to find which is the deeper global minimum and whether it is of a "good" type, here defined as having the correct broken symmetries and being R-Parity conserving. One possible way to study this issue is to start from a simplified set of input parameters yielding a correct tree-level global minimum when only the Higgs fields get *vev*. and then look for the true global minimum when all other neutral fields (mainly R-sneutrinos) acquire *vev*, both at the tree level and at loop level. See [48] for further details.

At the tree level there seems to exist regions where the BLSSM has a stable, R-Parity-conserving global minimum with the correct broken and unbroken gauge groups. For this to happen one needs the R-sneutrino Yukawa coupling Y_x to be not so large and the trilinear parameter A_0 to be not large compared to the soft scalar mass m_0, as, intuitively, large Y_x and A_0 can lead to large negative contributions to the potential energy for large values of v_x, as well as reducing the effective R-sneutrino masses, as described above and clear from Figure 1.

It turns out that when loop corrections are taken into account, few points all over such regions of parameters exist where R-Parity is not preserved anymore, or where $SU(2)_L$ or $U(1)_{B-L}$ is unbroken. This is apparently due to a very finely tuned breaking of $SU(2)_L$ and $U(1)_{B-L}$ which often does not survive loop corrections. The reason for this is that, besides the known large contributions of third generation (s)fermions, the additional new particles of the $B - L$ sector also play an important role. As previously described for the charged sleptons sector, new SUSY breaking D-term contributions to the masses appear; see (18). Since, as shown in (16), the experimental bounds require $M_{Z'}$ to be in the multi-TeV range, these contributions can be much larger than in the MSSM sector, resulting in the observed importance of the corresponding loop contributions. Furthermore, these contributions are also responsible for the restoration of $U(1)_{B-L}$ at the one-loop level.

Ultimately, overall safe regions of parameters cannot be found where the correct vacuum structure can be ensured. At the same time, if naive trends can be spotted for bad points to appear, these have nonetheless to be checked case by case due to the highly nontrivial scalar potential, and it might be possible that neighbour configurations still hold a valid global minimum. We will not check the validity of our scans from the vacuum point of view in the following, being confident that if any point is ruled out, a neighbour one yielding a very similar phenomenology can be found, which is allowed.

3. A Quick Look at Flavour Observables

Before moving to the Higgs phenomenology, we briefly show the impact on the BLSSM model when considering the constraints arising from low energy observables. For a review of the observables as well as for the impact on general SUSY models encompassing a seesaw mechanism, see [49, 50].

We consider here only the two most constraining ones, $\text{BR}(\mu \to e\gamma)$ and $\text{BR}(\mu \to 3e)$. The present exclusions are $\text{BR}(\mu \to e\gamma) < 5.7 \cdot 10^{-13}$ [18] and $\text{BR}(\mu \to 3e) < 1 \cdot 10^{-12}$ [19]. In Figure 2 we plot these branching ratios as a function of the mass of the lightest (in black) and next-to-lightest (in red) SM-like neutrino, which display some pattern for evading the bounds. In particular, they are required to be rather light, below 0.5 eV, while the model, due to the limited scans here performed, seems to prefer configurations with neutrinos heavier than 0.01 eV, hence the preferred region in between. Lighter mass values are nonetheless also allowed.

For convenience, the impact of satisfying the earlier bounds will be shown only in the inverted hierarchy case, due to the smaller density of configurations therein. Instead, points not allowed in the normal hierarchy case are automatically dropped.

Regarding the long-lasting $(g-2)_\mu$ discrepancy, in the setup investigated here charginos and charged Higgses are too heavy, same for the Z' boson, while the neutralino and sneutrino are too weakly coupled, to give a significant enhancement over the SM prediction.

4. Higgs Phenomenology

We review here the phenomenology of the Higgs sector, showing a first survey of its phenomenological features. First, results when normal hierarchy is imposed are presented. Then, we will show that the inverted hierarchy is also possible on a large portion of the parameter space. Without aim for completeness, the results are here presented as the starting point for a more thorough investigation. Finally, how model features pertaining to the extended gauge sector impinge on the Higgs phenomenology and in particular how the Higgs-to-diphoton branching ratio can be easily enhanced in this model, despite the experimental data now converging to a more SM-like behaviour than in the recent past, are described.

4.1. Normal Hierarchy. In this subsection we discuss the normal hierarchy case, with the lightest Higgs boson being the SM-like one (i.e., predominantly from the doublets), and a heavier Higgs boson predominantly from the bilepton fields (those carrying $B-L$ number and responsible for the $U(1)_{B-L}$

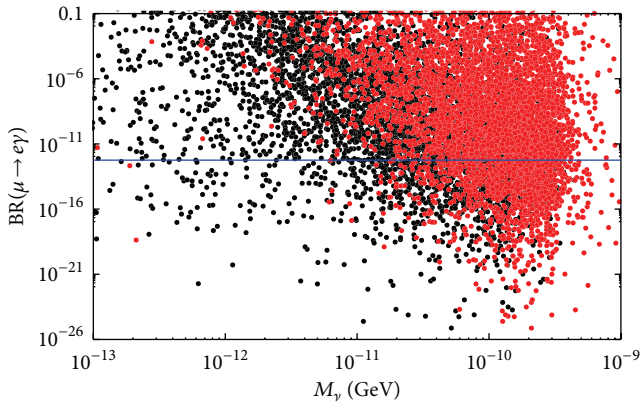

(a)

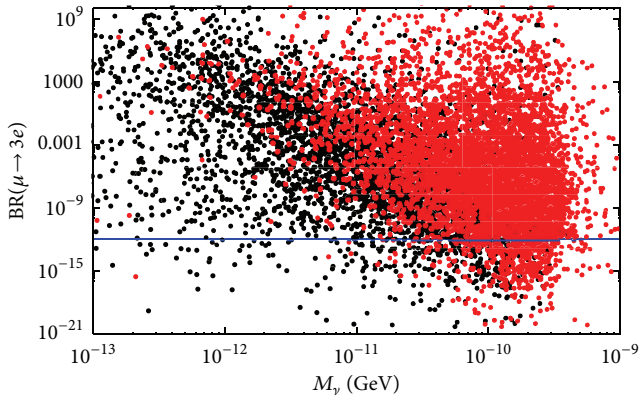

(b)

FIGURE 2: (a) BR($\mu \to e\gamma$) and (b) BR($\mu \to 3e$) as a function of the light neutrino masses in GeV (black: ν_1, red: ν_2). The blue horizontal lines represent the actual experimental limits, from [18] and [19], respectively. The parameters have been chosen as $m_0 \in [0.4, 2]$ TeV, $M_{1/2} \in [1.0, 2.0]$ TeV, $\tan\beta \in [5, 40]$, $A_0 \in [-4.0, 4.0]$ TeV, $\tan\beta' \in [1.05, 1.15]$, $M_{Z'} \in [2.5, 3.5]$ TeV, $Y_x \in \mathbf{1} \cdot [0.002, 0.4]$, and $Y_\nu \in \mathbf{1} \cdot [0.05, 5] \times 10^{-6}$.

spontaneous breaking). Their mixing is going to be small and solely due to the kinetic mixing.

In Figure 3 we first inspect the heavy Higgs boson branching ratios. Besides the standard decay modes, the decay into a pair of SM Higgs bosons exists, as well as two new characteristic channels of this model, comprising right-handed (s)neutrinos:

(1) $H_2 \to H_1 H_1$. Its BR can be up to 40% before the top quark threshold and around 30% afterwards.

(2) $H_2 \to \nu_h \nu_h$. A similar decay channel exists for the Z' boson. The BRs are $\mathcal{O}(10)$%, up to 20% depending on the heavy Higgs and neutrino masses.

(3) $H_2 \to \tilde{\nu}^S \tilde{\nu}^S$, where, $\tilde{\nu}^S$ is the CP-even sneutrino and the LSP, hence providing fully invisible decays of the heavy Higgs. If kinematically open, it saturates the Higgs BRs. Notice that only points with very light CP-even sneutrinos are shown, possible only for very large and negative A_0 (see Figure 1).

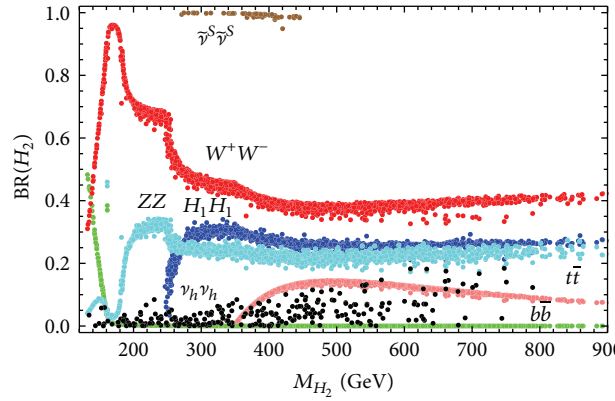

FIGURE 3: Branching ratios for H_2 with $M_{H_2} > M_{H_1} = 125$ GeV. The CP-even sneutrino channel (brown) is superimposed.

While the first two channels exist also in the non-SUSY version of the model (however, in the non-SUSY $B - L$ model, the Higgs mixing angle is a free parameter, directly impacting these branching ratios) (see, e.g., [51]), the last one, involving the CP-even sneutrino, is truly new and rather intriguing. This is because the sneutrino is light and it can be a viable LSP candidate if its mass is smaller than H_2, as in this case [16]. It however implies that the heavy Higgs is predominantly bilepton-like, with a light Higgs very much SM-like. This can be seen in Figure 4, where the points with large BR($H_2 \to \tilde{\nu}^S \tilde{\nu}^S$) (in red) have the lowest mixing between H_2 and the SM scalar doublet fields, of the order of 0.1%. It immediately follows that this channel will have very small cross section at the LHC, when considering SM-like Higgs production mechanisms. This is true for all heavy Higgs masses $M_{H_2} > 140$ GeV. The 125 GeV Higgs is well SM-like, with tiny reduction of its couplings to the SM particle content. On the other hand, the heavy Higgs is feebly mixed with the doublets, suppressing its interactions with the SM particles and hence its production cross section. This can be seen in Figure 5(a). Considering only the gluon-fusion production mechanism, and multiplying it by the relevant BR, we get the cross sections for the choice of channels displayed therein. The most constraining channels, $H \to WW \to \ell\nu jj$ and $H \to WW \to 2\ell 2\nu$, are also compared to the exclusions at the LHC for $\sqrt{s} = 8$ TeV from [20] and [21], respectively. The $H \to ZZ$ channels are well below current exclusions, which are hence not shown.

We see that all (starting from $M_{H_2} > 130$ GeV) the displayed configurations are allowed by the current searches (the exclusions shown by solid curves of the same color as the depicted channel). This is because of the suppression of the heavy Higgs boson cross sections due to the small scalar mixing.

In the lower plot the cross sections for the new channels are displayed. Those pertaining to model configurations for which the heavy Higgs boson decays to the CP-even sneutrino (LSP), yielding a fully invisible decay mode, are displayed in red. Contrary to all other cases, the production of the heavy Higgs for this channel is via vector boson fusion

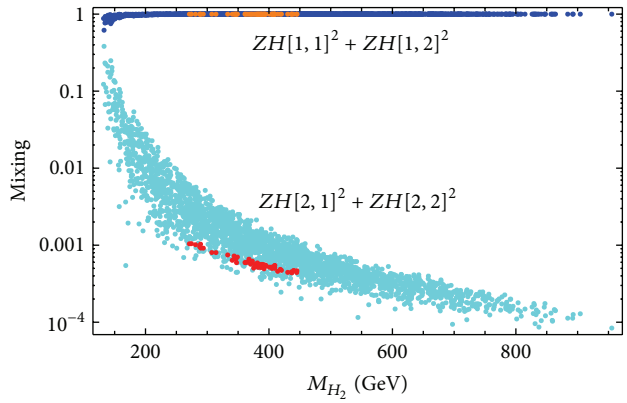

FIGURE 4: Mixing between Higgs boson mass eigenstates (blue-orange: H_1, cyan-red: H_2) and scalar doublet fields, as a function of M_{H_2}. $ZH[i, j]$ is the scalar mixing matrix. Orange/red points are the subset corresponding to BR($H_2 \to \tilde{\nu}^S\tilde{\nu}^S$) > 90%.

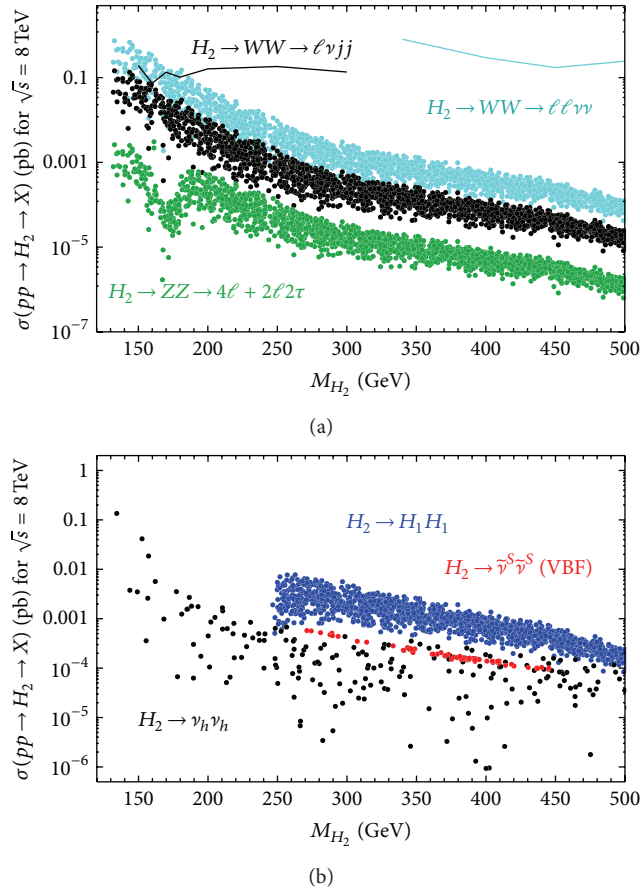

FIGURE 5: Cross sections at $\sqrt{s} = 8$ TeV for (a) the SM-like channels and (b) the new channels, as a function of the heavy Higgs mass. The solid lines above are the exclusion curves from [20, 21].

as searched for at the LHC [52]. Typical cross sections range between 0.1 fb and 1 fb. The $H_2 \to H_1H_1$ channel is shown in blue and it can yield cross sections of $1 \div 10$ fb for $250 < M_{H_2} < 400$ GeV. Last is the $H_2 \to \nu_h\nu_h$ channel. It can be sizable only for very light H_2 masses, $\sim 10 \div 100$ fb for $140 < M_{H_2} < 160$ GeV, although the further decay chain of the heavy neutrinos has to be accounted for. The latter can give spectacular multileptonic final states of the heavy Higgs boson ($4\ell 2\nu$ and $3\ell 2j\nu$) or high jet multiplicity ones ($2\ell 4j$), via $\nu_h \to \ell^{\mp}W^{\pm}$ and $\nu_h \to \nu Z$ in a 2 : 1 ratio (modulo threshold effects). Further, these decays are typically seesaw-suppressed and can therefore give rise to displaced vertices [53].

4.2. Inverted Hierarchy. In this subsection we discuss the inverted hierarchy case, where H_2 is the SM-like boson and a lighter Higgs boson exists.

We start once again by presenting the BRs for the next-to-lightest Higgs boson in Figure 6. This time, however, this is the SM-like boson, hence predominantly from the doublets. It has the same new channels as the heavy Higgs in the normal hierarchy, the only difference being the *CP*-odd R-sneutrino instead of the *CP*-even one. This is simply because the inverted hierarchy can happen only for large positive A_0 values, where only the *CP*-odd R-sneutrino can be light; see Figure 1. The configurations not allowed by the low energy observables or by `HiggsBounds` are displayed as gray points. We see that H_2 may have sizable decays into pairs of the lighter Higgs bosons, yielding 4*b*-jets final states. This decay is still allowed with rates up to few percent. Further, rare decays into pairs of heavy neutrinos are also present, with BRs below the permil level. This channel can give rise to rare multilepton/jets decays for the SM-like Higgs boson, which are searched for at the LHC, even in combination with searches for displaced vertices [54]. The last available channel is the decay into pairs of *CP*-odd R-sneutrinos. Being the LSP, it will increase the invisible decay width and hence give larger-than-expected widths for the SM-like boson. Its rate is obviously constrained, and a precise evaluation of the allowed range is needed. It however goes beyond the scope of the present review and we postpone it to a future publication.

Regarding the lightest Higgs boson (H_1), this will obviously decay predominantly into pairs of *b*-jets, see Figure 7. Notice that due to its large bilepton fraction it can also decay into pairs of very light RH neutrinos, at sizable rates depending on the neutrino masses. As in Figure 6, the nonallowed configurations are displayed as gray points. We see that the pattern of decays is not affected by the inclusion of the constraints, in the sense that this channel stays viable. Once again, the latter will yield multilepton/jet final state, which will be very soft and hence very challenging for the LHC. However, also in this case displaced vertices may appear.

As in the previous section, we show in Figure 8 the mixing between the Higgs mass eigenstates and the doublet fields as a function of the light Higgs mass, to show that H_2 is here rather SM-like. Once more, the gray points displayed here are excluded by the low energy observables and by `HiggsBounds`.

Finally, the production cross sections for the lightest Higgs boson can be evaluated. In Figure 9 we compare

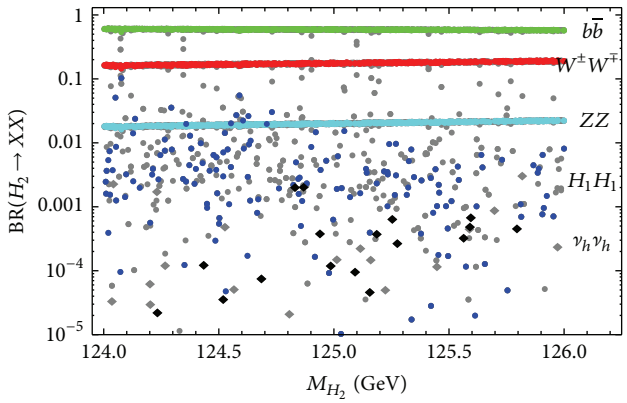

FIGURE 6: Branching ratios for the 125 GeV Higgs boson (H_2). The decay into heavy neutrinos is displayed with diamonds. All other decays are displayed with circles. Gray points are excluded by the low energy observables and by `HiggsBounds`. The decay into *CP*-odd sneutrinos is not shown.

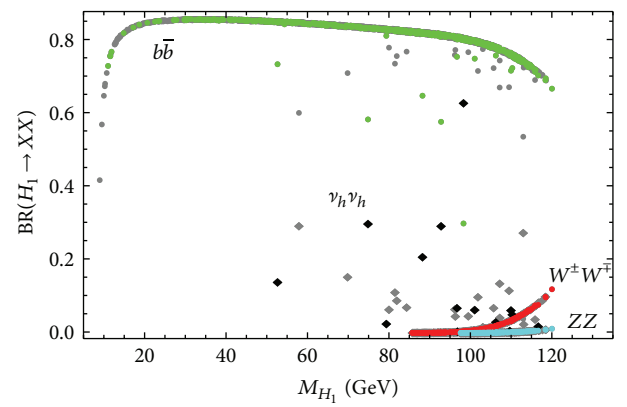

FIGURE 7: Same as in Figure 6 for the lightest Higgs boson (H_1).

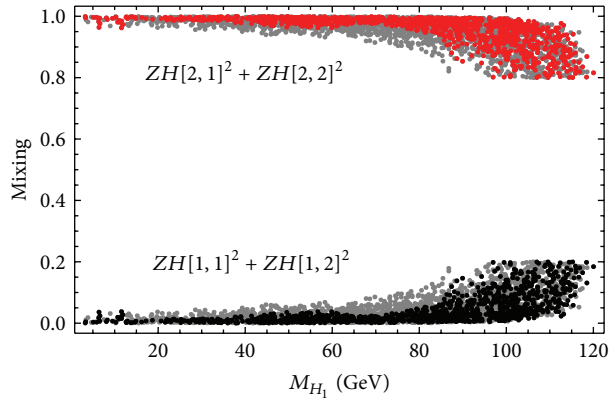

FIGURE 8: Mixing between scalar mass eigenstates and Higgs doublets (black: H_1, red: H_2) and scalar doublet fields, as a function of M_{H_1}. $ZH[i, j]$ is the scalar mixing matrix. Gray points are excluded by the low energy observables and by `HiggsBounds`.

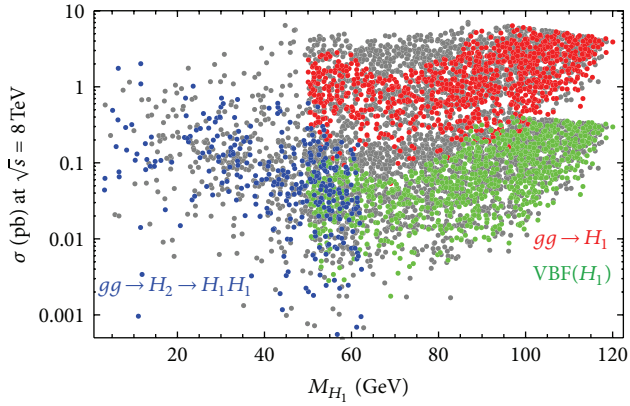

FIGURE 9: Cross sections at $\sqrt{s} = 8$ TeV for different production mechanisms. Gluon-fusion (in red) and vector-boson-fusion (in green) mechanisms are displayed only for $M_{H_1} > 50$ GeV for simplicity. Gray points are excluded by the low energy observables and by `HiggsBounds`.

the direct production (for the main SM production mechanisms, gluon fusion and vector boson fusion) with the pair production via H_2 decays only via gluon fusion, $gg \to H_2 \to H_1H_1$. When the latter channel is kinematically open, that is, $2M_{H_1} < 125$ GeV, the lightest Higgs boson pair production has cross sections up to 1 pb at the LHC at $\sqrt{s} = 8$ TeV, and it can give rare $4b$, $2b2V$, or $4V$ ($V = W, Z$) decays of the SM-like Higgs boson. A thorough analysis of the phenomenology of the Higgs sector in the BLSSM for the upcoming LHC run 2, based on the first investigations shown here, will be performed soon.

4.3. Enhancement of the Diphoton Rate. A feature of gauge-extended models is that new SUSY-breaking D-terms arise, which give further contributions to the sparticle masses. In the case of the model under consideration, we showed discussing (18) that these terms can be large and that they bring larger corrections to sleptons than to squarks. We already discussed how the vacuum structure of the BLSSM is affected by this. Here, we discuss the impact of the new D-terms on the Higgs phenomenology, focusing on the Higgs-to-diphoton decay, despite being disfavoured by most recent data [17], as an illustrative case. See [46] for further details.

To start our discussion let us briefly review the partial decay width of the Higgs boson h into two photons within the MSSM and its singlet extensions. This can be written as (see, e.g., [55])

$$\Gamma_{h\to\gamma\gamma} = \frac{G_\mu \alpha^2 m_h^3}{128\sqrt{2}\pi^3} \left| \sum_f N_c Q_f^2 g_{hff} A_{1/2}^h(\tau_f) + g_{hWW} A_1^h(\tau_W) + \frac{m_W^2 g_{hH^+H^-}}{2c_W^2 m_{H^\pm}^2} A_0^h(\tau_{H^\pm}) \right.$$

$$+\sum_{\chi_i^\pm}\frac{2m_W}{m_{\chi_i^\pm}}g_{h\chi_i^+\chi_i^-}A_{1/2}^h\left(\tau_{\chi_i^\pm}\right)+\sum_{\tilde{e}_i}\frac{g_{h\tilde{e}_i\tilde{e}_i}}{m_{\tilde{e}_i}^2}A_0^h\left(\tau_{\tilde{e}_i}\right)$$
$$+\sum_{\tilde{q}_i}\frac{g_{h\tilde{q}_i\tilde{q}_i}}{m_{\tilde{q}_i}^2}3Q_{\tilde{q}_i}^2A_0^h\left(\tau_{\tilde{q}_i}\right)\Bigg|^2, \tag{19}$$

corresponding to the contributions from charged SM fermions, W bosons, charged Higgs, charginos, charged sleptons, and squarks, respectively. The amplitudes A_i at the lowest order for the spin-1, spin-1/2, and spin-0 particle contributions can be found, for instance, in [55]. g_{hXX} denotes the coupling between the Higgs boson and the particle in the loop and Q_X is its electric charge. In the SM, the largest contribution is given by the W-loop, while the top-loop leads to a small reduction of the decay rate. In the MSSM, it is possible to get large contributions due to sleptons and squarks, although it is difficult to realise such a scenario in a constrained model with universal sfermion masses [56–58]. In singlet or triplet extension of the MSSM also the chargino and charged Higgs can enhance the loop significantly [59, 60]. However, this is only possible for large singlet couplings which lead to a cut-off well below the GUT scale. In contrast, it is possible to enhance the diphoton ratio in the BLSSM due to light staus even in the case of universal boundary conditions at the GUT scale. We show this by calculating explicitly the contributions of the stau:

$$A\left(\tilde{\tau}\right)=\frac{1}{3}\frac{\partial\det m_{\tilde{\tau}}^2}{\partial\log v}\simeq-\frac{2}{3}\cdot\frac{2m_\tau^2\left(A_\tau-\mu\tan\beta\right)^2}{\left(m_E^2+D_R\right)\left(m_L^2+D_L\right)+m_\tau^2\mu\tan\beta\left(2A_\tau-\mu\tan\beta\right)}. \tag{20}$$

Here, D_L and D_R represent the D-term contributions of the left- and right-handed stau and we have neglected subleading contributions. Given that $2A_\tau < \mu\tan\beta$, for fixed values of the other parameters, D_R and D_L can be used to enhance the $\gamma\gamma$ rate by suppressing the denominator.

We turn now to a fully numerical analysis to demonstrate the mechanism to enhance the Higgs-to-diphoton rate as a feature of the model with an extended gauge sector. This is a result of reducing the stau mass at the Higgs mass scale via extra D-terms as shown discussing (18). We recall here that this mechanism leaves the stop mass and hence, as we will show, the Higgs-to-gluons effective coupling nearly unchanged. In Table 2 we have collected two possible scenarios that provide SM-like Higgs particle in the mass range preferred by LHC results displaying an enhanced diphoton rate. In the first point, the lightest CP-even scalar eigenstate is the SM-like Higgs boson while the light bilepton is roughly twice as heavy. In Figure 10 we show that all the features arise from the extended gauge sector: it is sufficient to change only $\tan\beta'$ to obtain an enhanced diphoton signal $R_{\gamma\gamma}^1 \equiv [\sigma(gg \to h_1)\cdot BR(h_1 \to \gamma\gamma)]_{B-L}/[\sigma(gg \to h_1)\cdot BR(h_1 \to \gamma\gamma)]_{\mathrm{SM}}$ and the correct dark matter relic density while keeping the mass of the SM-like Higgs nearly unchanged. The dark matter candidate in this scenario is the lightest neutralino that is mostly a bileptino (the superpartner of the bileptons). The correct abundance for $\tan\beta' \simeq 1.156$ is obtained due to a coannihilation with the light stau. In the second point, the SM-like Higgs is accompanied by a light scalar around 98 GeV which couples weakly to the SM gauge bosons, compatibly with the LEP excess [61–63]. In this case, the LSP is a CP-odd sneutrino which annihilates very efficiently due to large Y_x. This usually results in a small relic density. To get an abundance which is large enough to explain the dark matter relic, the mass of the sneutrino has to be tuned below m_W [16]. This can be achieved by slightly increasing $\tan\beta'$ and by tuning the Majorana Yukawa couplings Y_x, which tends to increase the SM-like Higgs mass for the given point. It is worth mentioning that a neutralino LSP with the correct relic density in the stau coannihilation region can also be found in this scenario. Notice that both points yield rates consistent with observations in the WW^*/ZZ^* channels (measured at the LHC) (being $c_{hZZ} \sim 1$), as well as an effective Higgs-to-gluon coupling close to 1.

Table 2: The input parameter used: Point I: $m_0 = 673$ GeV, $M_{1/2} = 2220$ GeV, $A_0 = -1842$ GeV, $\tan\beta = 42.2$, $\tan\beta' = 1.1556$, $M_{Z'} = 2550$ GeV, and $Y_x = \mathbf{1}\cdot 0.42$ (neutralino LSP); Point II: $m_0 = 742$ GeV, $M_{1/2} = 1572$ GeV, $A_0 = 3277$ GeV, $\tan\beta = 37.8$, $\tan\beta' = 1.140$, $M_{Z'} = 2365$ GeV, and $Y_x = \mathrm{diag}(0.40, 0.40, 0.13)$ (CP-odd sneutrino LSP). c_{SVV} denotes the coupling squared of the Higgs fields to vector bosons normalised to the SM values.

	Point I	Point II
m_{h_1} [GeV]	125.2	98.2
m_{h_2} [GeV]	186.9	123.0
$m_{\tilde{\tau}}$ [GeV]	267.0	237.3
Doublet fr. [%]	99.5	8.7
Bilepton fr. [%]	0.5	91.3
c_{h_1gg}	0.992	0.087
c_{h_1ZZ}	1.001	0.085
c_{h_2gg}	0.005	0.911
c_{h_2ZZ}	0.005	0.921
$\Gamma(h_1)$ [MeV]	4.13	0.22
$R_{\gamma\gamma}^1$	1.57	0.085
$R_{b\bar{b}}^1$	1.03	0.089
$R_{WW^*}^1$	0.98	0.05
$\Gamma(h_2)$ [MeV]	4.8	3.58
$R_{\gamma\gamma}^2$	0.005	1.79
$R_{b\bar{b}}^2$	0.006	0.95
$R_{WW^*}^2$	0.01	0.88
LSP mass [GeV]	253.9	82.9
Ωh^2	0.10	10^{-2}

5. Conclusions

In this review I described the $U(1)_{B-L}$ extension of the MSSM, focusing in particular on the scalar sector, described in detail. The fundamental role that the gauge kinetic mixing plays in this sector has been underlined.

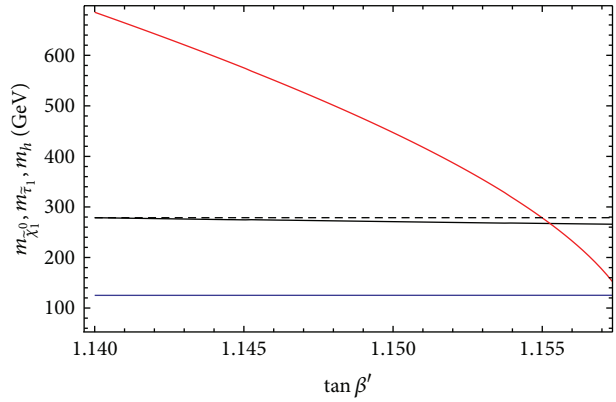

(a)

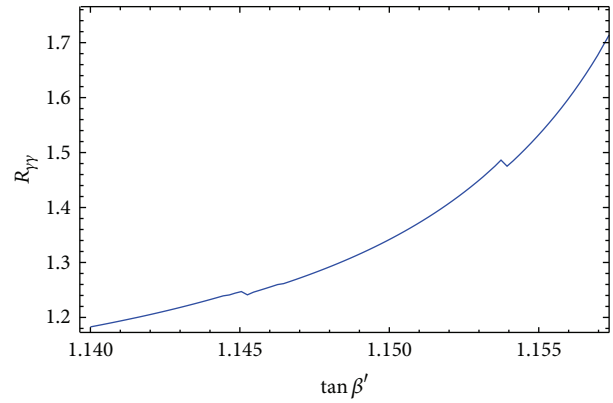

(b)

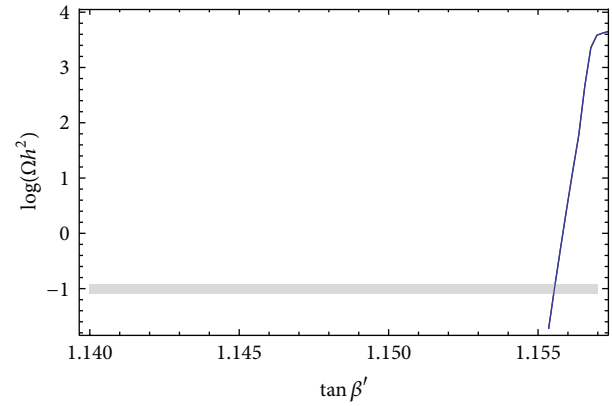

(c)

Figure 10: (a) The mass of the SM-like Higgs (bottom (blue line)), of the stau (middle (black) line, where the dashed line represents a reference unchanged value), and of the lightest neutralino (top (red) line); (b) the diphoton branching ratio; (c) the neutralino relic density as a function of $\tan\beta'$. The other parameters have been chosen as $m_0 = 673\,\text{GeV}$, $M_{1/2} = 2220\,\text{GeV}$, $\tan\beta = 42.2$, $A_0 = -1842.6$, $M_{Z'} = 2550\,\text{GeV}$, and $Y_x = \mathbf{1} \cdot 0.42$.

The comparison to the most constraining low energy observables showed that a preferred region for the light neutrino masses exists to evade these bounds. Then, I presented a first systematic investigation of the phenomenology of the Higgs sector of this model, showing that both the normal hierarchy and the inverted hierarchy of the two lightest Higgs bosons are naturally possible in a large portion of the parameter space. Particular attention has been devoted to analysis of the new decay channels comprising both the *CP*-even and *CP*-odd R-sneutrinos, which are a peculiarity of the BLSSM. Based on these first findings, a thorough analysis of the Higgs sector in the BLSSM at the upcoming LHC run 2 will be soon

prepared. The fit of the SM-like Higgs boson to the LHC data will also be performed with `HiggsSignals` [64].

Finally, I described how in the BLSSM model (and in general in gauge-extended MSSM models) the Higgs-to-diphoton decay can be easily enhanced. Despite being disfavoured by most recent data, this feature is a consequence of the potentially large new SUSY-breaking D-terms arising from the $B - L$ sector. At the same time these terms affect also the vacuum structure of the model, where naive R-Parity-conserving configurations at the tree level could develop deeper R-Parity-violating global minima, or partially restore the $SU(2)_L \times U(1)_{B-L}$ symmetry at one loop. It is however possible to still find R-Parity-conserving global minima on the whole parameter space, which can either accommodate an enhancement of the Higgs-to-diphoton decay or fit the most recent Higgs data.

Conflict of Interests

The author declares that there is no conflict of interests regarding the publication of this paper.

Acknowledgments

The author would like to thank S. Moretti and C. H. Shepherd-Themistocleous for helpful discussions in the early stages of this work. He is also really grateful to all his collaborators, and in particular to Florian Staub. He further acknowledges support from the Theorie-LHC France initiative of the CNRS/IN2P3 and from the French ANR 12 JS05 002 01 BATS@LHC.

References

[1] J. Ellis, F. Luo, K. A. Olive, and P. Sandick, "The Higgs mass beyond the CMSSM," *The European Physical Journal C*, vol. 73, article 2403, 2013.

[2] U. Ellwanger, C. Hugonie, and A. M. Teixeira, "The next-to-minimal supersymmetric standard model," *Physics Reports*, vol. 496, no. 1-2, pp. 1–77, 2010.

[3] W. Buchmüller, K. Hamaguchi, O. Lebedev, and M. Ratz, "Supersymmetric Standard Model from the heterotic string (II)," *Nuclear Physics B*, vol. 785, no. 1-2, pp. 149–209, 2007.

[4] M. Ambroso and B. A. Ovrut, "THE B-L/electroweak hierarchy in smooth heterotic compactifications," *International Journal of Modern Physics A*, vol. 25, no. 13, p. 2631, 2010.

[5] M. Ambroso and B. A. Ovrut, "The mass spectra, hierarchy and cosmology of B-L MSSM heterotic compactifications," *International Journal of Modern Physics A*, vol. 26, no. 9, pp. 1569–1627, 2010.

[6] S. Khalil and A. Masiero, "Radiative $B - L$ symmetry breaking in supersymmetric models," *Physics Letters B*, vol. 665, no. 5, pp. 374–377, 2008.

[7] P. Fileviez Perez and S. Spinner, "Fate of R parity," *Physical Review D*, vol. 83, no. 3, Article ID 035004, 7 pages, 2011.

[8] V. Barger, P. Fileviez Perez, and S. Spinner, "Minimal gauged $U(1)_{B-L}$ model with spontaneous R parity violation," *Physical Review Letters*, vol. 102, Article ID 181802, 2009.

[9] J. Pelto, I. Vilja, and H. Virtanen, "Leptogenesis $B - L$ in gauged supersymmetry with MSSM Higgs sector," *Physical Review D*, vol. 83, Article ID 055001, 2011.

[10] K. S. Babu, Y. Meng, and Z. Tavartkiladze, "New ways to leptogenesis with gauged B–L symmetry," *Physics Letters B*, vol. 681, no. 1, pp. 37–43, 2009.

[11] B. Holdom, "Two U(1)'s and ϵ charge shifts," *Physics Letters B*, vol. 166, no. 2, pp. 196–198, 1986.

[12] K. S. Babu, C. Kolda, and J. March-Russell, "Implications of generalized Z-Z′ mixing," *Physical Review D: Particles, Fields, Gravitation and Cosmology*, vol. 57, no. 11, pp. 6788–6792, 1998.

[13] F. del Aguila, G. D. Coughlan, and M. Quirós, "Gauge coupling renormalisation with several U(1) factors," *Nuclear Physics B*, vol. 307, no. 3, pp. 633–648, 1988.

[14] F. del Aguila, J. Gonzalez, and M. Quiros, "Renormalization group analysis of extended electroweak models from the heterotic string," *Nuclear Physics B*, vol. 307, no. 3, pp. 571–632, 1988.

[15] B. O'Leary, W. Porod, and F. Staub, "Mass spectrum of the minimal SUSY $B - L$ model," *Journal of High Energy Physics*, vol. 2012, no. 5, article 042, 2012.

[16] L. Basso, B. O'Leary, W. Porod, and F. Staub, "Dark matter scenarios in the minimal SUSY $B - L$ model," *Journal of High Energy Physics*, vol. 2012, no. 9, article 54, 2012.

[17] V. Khachatryan, A. M. Sirunyan, A. Tumasyan et al., "Precise determination of the mass of the Higgs boson and tests of compatibility of its couplings with the standard model predictions using proton collisions at 7 and 8 TeV," *The European Physical Journal C*, vol. 7, article 212, 2014.

[18] J. Adam, X. Bai, A. M. Baldini et al., "New constraint on the existence of the $\mu^+ \to e^+\gamma$ decay," *Physical Review Letters*, vol. 110, Article ID 201801, 2013.

[19] U. Bellgardt, G. Otter, R. Eichler et al., "Search for the decay $\mu \to e^+e^+e^-$," *Nuclear Physics B*, vol. 299, no. 1, pp. 1–6, 1988.

[20] CMS Collaboration, "Search for the standard model Higgs boson in the H to WW to lnujj decay channel in pp collisions at the LHC," Tech. Rep. CMS-PAS-HIG-13-027, CERN, Geneva, Switzerland, 2012.

[21] S. Chatrchyan, V. Khachatryan, A. M. Sirunyan et al., "Search for a standard-model-like Higgs boson with a mass in the range 145 to 1000 GeV at the LHC," *The European Physical Journal C*, vol. 73, article 2469, 2013.

[22] W. Porod, "SPheno, a program for calculating supersymmetric spectra, SUSY particle decays and SUSY particle production at e^+e^- colliders," *Computer Physics Communications*, vol. 153, no. 2, pp. 275–315, 2003.

[23] W. Porod and F. Staub, "SPheno 3.1: extensions including flavour, CP-phases and models beyond the MSSM," *Computer Physics Communications*, vol. 183, no. 11, pp. 2458–2469, 2012.

[24] F. Staub, "Sarah," http://arxiv.org/abs/0806.0538.

[25] F. Staub, "From superpotential to model files for FeynArts and CalcHep/CompHep," *Computer Physics Communications*, vol. 181, no. 6, pp. 1077–1086, 2010.

[26] F. Staub, "Automatic calculation of supersymmetric renormalization group equations and loop corrections," *Computer Physics Communications*, vol. 182, no. 3, pp. 808–833, 2011.

[27] F. Staub, "SARAH 3.2: dirac gauginos, UFO output, and more," *Computer Physics Communications*, vol. 184, no. 7, pp. 1792–1809, 2013.

[28] F. Staub, "SARAH 4 : a tool for (not only SUSY) model builders," *Computer Physics Communications*, vol. 185, no. 6, pp. 1773–1790, 2014.

[29] L. Basso, A. Belyaev, D. Chowdhury et al., "Proposal for generalised supersymmetry les Houches Accord for see-saw models and PDG numbering scheme," *Computer Physics Communications*, vol. 184, no. 3, pp. 698–719, 2013.

[30] F. Staub, "Exploring new models in all detail with SARAH," http://arxiv.org/abs/1503.04200.

[31] F. Staub, T. Ohl, W. Porod, and C. Speckner, "A tool box for implementing supersymmetric models," *Computer Physics Communications*, vol. 183, no. 10, pp. 2165–2206, 2012.

[32] W. Porod, F. Staub, and A. Vicente, "A flavor kit for BSM models," *The European Physical Journal C*, vol. 74, article 2992, 2014.

[33] P. Bechtle, O. Brein, S. Heinemeyer, G. Weiglein, and K. E. Williams, "HiggsBounds: confronting arbitrary Higgs sectors with exclusion bounds from LEP and the Tevatron," *Computer Physics Communications*, vol. 181, no. 1, pp. 138–167, 2010.

[34] P. Bechtle, O. Brein, S. Heinemeyer, G. Weiglein, and K. E. Williams, "HiggsBounds 2.0.0: confronting neutral and charged Higgs sector predictions with exclusion bounds from LEP and the Tevatron," *Computer Physics Communications*, vol. 182, no. 12, pp. 2605–2631, 2011.

[35] P. Bechtle, O. Brein, S. Heinemeyer et al., "Recent developments in HiggsBounds and a preview of HiggsSignals," PoS CHARGED, http://arxiv.org/abs/1301.2345.

[36] P. Bechtle, O. Brein, S. Heinemeyer et al., "HiggsBounds-4 : improved tests of extended Higgs sectors against exclusion bounds from LEP, the Tevatron and the LHC," *The European Physical Journal C*, vol. 74, article 2693, 2014.

[37] R. M. Fonseca, M. Malinsky, W. Porod, and F. Staub, "Running soft parameters in SUSY models with multiple U(1) gauge factors," *Nuclear Physics B*, vol. 854, no. 1, pp. 28–53, 2012.

[38] P. H. Chankowski, S. Pokorski, and J. Wagner, "Z′ and the Appelquist-Carrazzone decoupling," *The European Physical Journal C—Particles and Fields*, vol. 47, no. 1, pp. 187–205, 2006.

[39] W. Abdallah, S. Khalil, and S. Moretti, "Double Higgs peak in the minimal SUSY $B - L$ model," *Physical Review D*, vol. 91, no. 1, Article ID 014001, 6 pages, 2015.

[40] G. Aad, B. Abbott, J. Abdallah et al., "Search for high-mass dilepton resonances in pp collisions at $\sqrt{s} = 8$ TeV with the ATLAS detector," *Physical Review D*, vol. 90, Article ID 052005, 2014.

[41] V. Khachatryan, A. M. Sirunyan, A. Tumasyan et al., "Search for physics beyond the standard model in dilepton mass spectra in proton-proton collisions at $\sqrt{s} = 8$ TeV," *Journal of High Energy Physics*, vol. 2015, no. 4, article 025, 2015.

[42] G. Cacciapaglia, C. Csáki, G. Marandella, and A. Strumia, "The minimal set of electroweak precision parameters," *Physical Review D*, vol. 74, no. 3, Article ID 033011, 12 pages, 2006.

[43] L. Basso, K. Mimasu, and S. Moretti, "Non-exotic Z' signals in l^+l^-, bb and $t\bar{t}$ final states at the LHC," *Journal of High Energy Physics*, vol. 2012, no. 11, article 060, 2012.

[44] M. Hirsch, H. V. Klapdor-Kleingrothaus, and S. G. Kovalenko, "B-L-violating masses in softly broken supersymmetry," *Physics Letters B*, vol. 398, no. 3-4, pp. 311–314, 1997.

[45] Y. Grossman and H. E. Haber, "Sneutrino mixing phenomena," *Physical Review Letters*, vol. 78, no. 18, pp. 3438–3441, 1997.

[46] L. Basso and F. Staub, "Enhancing $h \to \gamma\gamma$ with staus in supersymmetric models with an extended gauge sector," *Physical Review D*, vol. 87, no. 1, Article ID 015011, 6 pages, 2013.

[47] A. Hammad, S. Khalil, and S. Moretti, "Higgs boson decays into $\gamma\gamma$ and $Z\gamma$ in the MSSM and BLSSM," http://arxiv.org/abs/1503.05408.

[48] J. E. Camargo-Molina, B. O'Leary, W. Porod, and F. Staub, "Stability of R parity in supersymmetric models extended by $U(1)_{B-L}$," *Physical Review D*, vol. 88, Article ID 015033, 2013.

[49] A. Abada, M. E. Krauss, W. Porod, F. Staub, A. Vicente, and C. Weiland, "Lepton flavor violation in low-scale seesaw models: SUSY and non-SUSY contributions," *Journal of High Energy Physics*, vol. 2014, no. 11, article 048, 2014.

[50] A. Vicente, "Lepton flavor violation beyond the MSSM," http://arxiv.org/abs/1503.08622.

[51] L. Basso, S. Moretti, and G. M. Pruna, "Phenomenology of the minimal $B - L$ extension of the standard model: the Higgs sector," *Physical Review D*, vol. 83, Article ID 055014, 2011.

[52] CMS Collaboration, "Search for invisible decays of Higgs bosons in the vector boson fusion production mode," Tech. Rep. CMS-PAS-HIG-14-038, CERN, Geneva, Switzerland, 2015, http://cds.cern.ch/record/2007270.

[53] L. Basso, A. Belyaev, S. Moretti, and C. H. Shepherd-Themistocleous, "Phenomenology of the minimal $B - L$ extension of the standard model: Z' and neutrinos," *Physical Review D*, vol. 80, no. 5, Article ID 055030, 14 pages, 2009.

[54] L. Basso, A. Belyaev, J. Fiaschi, S. Moretti, I. Tomalin, and M. Thomas,In preparation.

[55] A. Djouadi, "The anatomy of electroweak symmetry breaking: tome I: the Higgs boson in the Standard Model," *Physics Reports*, vol. 457, no. 1–4, pp. 1–216, 2008.

[56] M. Carena, S. Gori, N. R. Shah, and C. E. M. Wagner, "A 125 GeV SM-like Higgs in the MSSM and the $\gamma\gamma$ rate," *Journal of High Energy Physics*, vol. 2012, no. 3, article 014, 2012.

[57] U. Ellwanger, "A Higgs boson near 125 GeV with enhanced diphoton signal in the NMSSM," *Journal of High Energy Physics*, vol. 2012, no. 3, article 044, 2012.

[58] R. Benbrik, M. Gomez Bock, S. Heinemeyer, O. Stål, G. Weiglein, and L. Zeune, "Confronting the MSSM and the NMSSM with the discovery of a signal in the two photon channel at the LHC," *European Physical Journal C*, vol. 72, article 2171, 2012.

[59] K. Schmidt-Hoberg and F. Staub, "Enhanced $h \to \gamma\gamma$ rate in MSSM singlet extensions," *Journal of High Energy Physics*, vol. 2012, no. 10, article 195, 2012.

[60] A. Delgado, G. Nardini, and M. Quiros, "Large diphoton Higgs rates from supersymmetric triplets," *Physical Review D*, vol. 86, no. 11, Article ID 115010, 7 pages, 2012.

[61] ALEPH Collaboration, DELPHI Collaboration, L3 Collaboration, OPAL Collaboration, and The LEP Working Group for Higgs Boson Searches, "Search for the Standard Model Higgs boson at LEP," *Physics Letters B*, vol. 565, Article ID 0306033, pp. 61–75, 2003.

[62] G. Bélanger, U. Ellwanger, J. F. Gunion, Y. Jiang, S. Kraml, and J. H. Schwarz, "Higgs bosons at 98 and 125 GeV at LEP and the LHC," *Journal of High Energy Physics*, vol. 2013, no. 1, article 069, 2013.

[63] M. Drees, "Supersymmetric explanation of the excess of Higgs-like events at the LHC and at LEP," *Physical Review D*, vol. 86, Article ID 115018, 2012.

[64] P. Bechtle, S. Heinemeyer, O. Stal, T. Stefaniak, and G. Weiglein, "HiggsSignals: confronting arbitrary Higgs sectors with measurements at the Tevatron and the LHC," *The European Physical Journal C*, vol. 74, article 2711, 2014.

Hindawi Publishing Corporation
Advances in High Energy Physics
Volume 2015, Article ID 764875, 7 pages
http://dx.doi.org/10.1155/2015/764875

Review Article

Supersymmetry: Early Roots That Did Not Grow

Cecilia Jarlskog

Division of Mathematical Physics, Physics Department, LTH, Lund University, 22100 Lund, Sweden

Correspondence should be addressed to Cecilia Jarlskog; cecilia.jarlskog@matfys.lth.se

Received 24 March 2015; Accepted 1 May 2015

Academic Editor: Florian Staub

This paper is about early roots of supersymmetry, as found in the literature from 1940s and early 1950s. There were models where the power of "partners" in alleviating divergences in quantum field theory was recognized. However, other currently known remarkable features of supersymmetry, such as its role in the extension of the Poincaré group, were not known. There were, of course, no supersymmetric nonabelian quantum field theories in those days.

1. Introduction

During several years I was collecting material to produce a book which was subsequently published under the title *Portrait of Gunnar Källén: A Physics Shooting Star and Poet of Early Quantum Field Theory* [1]. I found to my great surprise that Källén's very first published paper [2] had a fundamental element of supersymmetry in it: the fact that spin-1/2 fermions and spin-0 bosons, taken together in equal numbers of degrees of freedom, give a far better-behaved field theory! Källén's paper was published when he was a 23-year-old second-year doctoral student in Lund, Sweden. He had been sent to Pauli in Zürich, Switzerland, to attend Pauli's summer course of 1949. The acknowledgement of Källén's paper reads as follows:

> *"I want to express my respectful gratitude to professor W. Pauli, Zürich, who has suggested this investigation to me, and to thank him and Dr. R. Jost and Dr. J. Luttinger for many helpful discussions."*

2. Källén's Work

Källén considers the vacuum polarization in quantum electrodynamics (QED) to orders e^2 and e^4, in a model containing not only n Dirac fields but also N spin-0 particles, all with charge e and interacting with an external electromagnetic field. He informs the readers that the e^2 case has been treated (and in fact published in the same year, 1949) by Jost and Rayski [3]. These authors, who were both in Zürich, in their paper "express their gratitude to Professor W. Pauli for his kind interest in this work as well as for much valuable aid." Källén informs the reader that Jost and Rayski have shown that to the order e^2 the "nongauge invariant (and divergent) terms compensate each other if one uses a suitable mixture of spinor and scalar fields." The mixture is

$$N = 2n$$
$$\sum_{i=1}^{N} M_i^2 = 2\sum_{i=1}^{n} m_i^2, \tag{1}$$

where M_i (m_i) denote the masses of the scalars (spinors). The first relation that there be as many bosonic as fermionic degrees of freedom is exactly the basic ingredient of supersymmetry. The second relation includes the degeneracy condition of supersymmetry $M_i = m_i$ but it is more general. Källén studies what happens at the order e^4, which is, of course, a much more difficult task. After impressive calculations, he finds that the first relation alone is enough for removal of divergences in the fourth order. There are no divergences in higher than the fourth order and an overall charge renormalization is all that is needed.

The paper by Jost and Rayski [3] gives credit to work published in the previous year by Umezawa et al. [4] and by Rayski [5] for having shown that

> *"by coupling the electromagnetic field to several charged fields of spinor and scalar (or pseudoscalar) types the gauge invariance of the vacuum polarization and the vanishing of the ph.s.e. [meaning photon self-energy] may be achieved (at least in the second order of approximation e^2) due to some compensations. It is premature to decide whether such compensations posses any deeper meaning or whether they should be considered merely as accidental."*

Jost and Rayski do not discuss the "partners" any further but deal with comparison of charge renormalization of spinors and scalars in this scenario.

It should be emphasized that the self-energy of the photon was a major issue in those days. Indeed a nonzero photon mass could easily emerge from calculations, as was shown in a seminal paper by Wentzel [6].

To conclude this section, Pauli was very pleased with Källén's work. He expressed his appreciation in several letters (to Rudolf Peierls, Oskar Klein, and others). As mentioned before, Källén's work had started when he was attending Pauli's summer course in Zürich. Pauli was a major "pole of attraction" to many distinguished physicists as well as young researchers.

3. Regularization and Renormalization

An insight into the situation in 1949 is obtained by considering what was going on in Zürich. Indeed the previous two years had been extremely turbulent and exciting in the world of physics, due to two remarkable experimental discoveries crying for theoretical explanations. These were

(1) the discovery in 1947 of the Lamb-shift [7] by Lamb[1] and Retherford[2],

(2) the discovery in 1948 of the anomalous magnetic moment of the electron [8] by Foley and Kusch[3]. Note that this anomaly was quickly calculated by Schwinger who announced his famous factor $\alpha/2\pi$ in a one-page letter [9] which appeared in Physical Review, next to the experimental discovery.

These discoveries, which showed departure from predictions of Dirac theory, attracted the attention of some of the greatest theorists of that time, among them H. A. Bethe, R. P. Feynman, N. M. Kroll, J. Schwinger, S.-I. Tomonaga, and V. F. Weisskopf. Through these efforts, regularization and renormalization took the central stage in relativistic quantum field theory.

Returning to Zürich, Pauli who was keen on writing review-type articles, going through the details in order to understand what is going on, was quick to publish a paper in 1949, together with F. Villars [10]. This paper, published under the title "On the Invariant Regularization in Relativistic Quantum Theory," came to play a major role in the thinking of field theorists for decades to come. The paper begins by noting that

> *"In spite of many successes of the new relativistically invariant formalism of quantum electrodynamics, which is based on the idea of "renormalization" of mass and charge, there are still some problems of uniqueness left, which need further clarification."*

The authors then point out the inherent ambiguities in calculations in quantum electrodynamics, due to presence of divergent integrals. Actually a number of prescriptions had been put forward on how to deal with these infinities, usually by introducing cut-offs[4]. Regularization and renormalization were the key concepts and it was essential that the regularization prescription should respect Lorentz as well as gauge invariance.

In their article, Pauli and Villars specify two distinct paths to regularization:

> *"In order to overcome these ambiguities we apply in the following the method of regularization... with the help of an introduction of auxiliary masses. This method has already a long history. Much work has been done to compensate the infinities in the self-energy of the electron with the help of auxiliary fields ... Some authors assumed formally a negative energy of the free auxiliary particles, while others did not need these artificial assumptions and could obtain the necessary compensations by using the different sign of the self-energy of the electron due to its interaction with different kinds of fields (for instance scalar fields vs. vector fields)."*

Pauli and Villars call the first kind of regularization (involving fictitious particles) "*formalistic*." Some of the hypothetical particles thus introduced are ghosts (with negative probabilities) and their masses are taken to go to infinity at the end of computation in order to remove them from the physical sector. This formalistic prescription amounted to introducing some simple relations which nowadays can be found in many textbooks on field theory:

$$\sum_i C_i = 0; \qquad \sum_i C_i M_i^2 = 0, \ldots. \tag{2}$$

Here the C_i denotes the square of the coupling constant of the fermion i to the photon and M_i stands for the mass of that fermion. For the case of traditional quantum electrodynamics (describing the interactions of light with electrons) which was of interest one takes $C_1 = 1$ and $M_1 = m_e$ where m_e is the mass of the electron. The relation $\sum_i C_i = 0$ shows that some of the fictitious fermions are ghost-like, with negative square of their coupling constants.

Pauli and Villars call the second option "*realistic*." In this case[5] Nature herself provides the regulators, in the form of

what in supersymmetry language is called the partners. In comparing the two approaches they note the following:

> *"It seems very likely that the "formalistic" standpoint used in this paper and by other workers can only be a transitional stage of the theory, and that the auxiliary masses will eventually either be entirely eliminated, or the "realistic" standpoint will be so much improved that the theory will not contain any further accidental compensations."*

The first (formalistic) option is indeed easy to use and is the only one which is used in the Pauli-Villars paper. An immediate question which arises is as follows: what happened to the second alternative, the "realistic standpoint," fermions accompanied by their bosonic partners?

4. Yukawa, the Intellectual Father of Scalars

In 1940s and 1950s scalar particles enjoyed a great deal of popularity among theorists in Japan. This can be traced back to the work of H. Yukawa[6] who proposed that the strong force is mediated by a scalar particle (and its antiparticle), $U^{\pm}$. Using Wigner's estimate of the range of the nuclear force, he found that the mass of U should be about 200 times the mass of the electron (see Yukawa's Nobel Lecture [11]).

The sequence of events from 1935 to 1949, when Yukawa was awarded the Nobel Prize, as well as what happened afterwards, is truly amazing. Indeed particles with the expected mass and charge were there: the muons, $\mu^{\pm}$ (initially called the mesotrons and later on the mu-mesons). However, these penetrating particles turned out to have no strong interactions! The pions were discovered much later, in 1947 (for a more detailed discussion see below).

At the time of his Nobel Prize Yukawa was well aware that the picture was far more complicated. In his Nobel Lecture he noted the following [11]:

> *"In this way, meson theory has changed a great deal during these fifteen years. Nevertheless, there remain still many questions unanswered. Among other things, we know very little about mesons heavier than π-mesons. We do not know yet whether some of the heavier mesons are responsible for nuclear forces at very short distances. The present form of meson theory is not free from the divergence difficulties, although recent development of relativistic field theory has succeeded in removing some of them. We do not yet know whether the remaining divergence difficulties are due to our ignorance of the structure of elementary particles themselves [12]. We shall probably have to go through another change of the theory, before we shall be able to arrive at the complete understanding of the nuclear structure and of various phenomena, which will occur in high energy regions."*

Little did Yukawa, or anyone else, know about quantum chromodynamics (QCD) and its gluons as mediators of the strong force. In spite of all this, light mesons play an important role in the treatment of strong interactions at very low energies (chiral dynamics).

5. Scalars in Japan and "Mixed Fields"

In 1940s there were several towering figures in the Japanese theoretical community, among them S. Sakata (1911–1970), S-I. Tomonaga (1906–1979), and H. Yukawa (1907–1981). Following Yukawa, proposing new scalars became popular in Japan. As a token of importance of scalars in Japan we note that the 1965 Nobel Laureate in Physics, Tomonaga[7], in spite of not having been directly involved, discussed this subject in his Nobel Lecture [13]. He wrote the following:

> *"In the meantime, in 1946, Sakata [14] proposed a promising method of eliminating the divergence of the electron mass by introducing the idea of a field of cohesive force. It was the idea that there exists unknown field, of the type of the meson field which interacts with the electron in addition to the electromagnetic field. Sakata named this field the cohesive force field, because the apparent electronic mass due to the interaction of this field and the electron, though infinite, is negative and therefore the existence of this field could stabilize the electron in some sense. Sakata pointed out the possibility that the electromagnetic mass and the negative new mass cancel each other and that the infinity could be eliminated by suitably choosing the coupling constant between this field and the electron. Thus the difficulty which had troubled people for a long time seemed to disappear insofar as the mass was concerned. (It was found later that Pais [15] proposed the same idea in the U.S. independently of Sakata.)*
> *That is to say, according to our result, the Sakata theory led to the cancellation of infinities for the mass but not for the scattering process. It was also known that the infinity of vacuum polarization type was not cancelled by the introduction of the cohesive force field."*

Pais had an earlier publication in Physical Review [15] in which he promised a forthcoming article which appeared in Trans. Roy. Acad. Sciences of Netherlands 19, number 1 (1947).

Returning to Japan, a key player in proposing "mixed fields," harmonious existence of fermions and bosons, was H. Umezawa[8] (1924–1995) and an excellent account of the status of the mixed fields, as of 1950, can be found in an article, "On the applicability of the method of the mixed fields in the theory of the elementary particles," that he wrote together with Sakata [16]. Fortunately, Umezawa produced an excellent book (translated from Japanese) entitled *Quantum Field Theory* [17] which not only teaches field theory but is also a rich source of historical information. Umezawa considers the case of mixed fields in a few places in his book. As an example, the equations presented on page 255 must look familiar to researchers in the field of supersymmetry[9]!

Taken altogether, one is impressed by the amount of work done on this subject in Japan .

The mixed fields had in turn their roots. Perhaps the earliest one was the introduction of a "subtractive" vector field, proposed by F. Bopp [18, 19]. This amounted to replacing the $1/r$ Coulomb potential with $(1/r)(1 - \exp(-\kappa r))$, or later on, in the relativistic version, introducing a cut-off in the propagator, namely, $1/k^2 - 1/(k^2 - \kappa^2)$, κ being the cut-off mass.

The mixed fields cancellations worked in the case of vacuum polarization because all charged particles are running in the loop. So the divergence created by the singularities in the electron propagators is compensated by those of its scalar partners. However, in the mixed fields models the photon did not have any fermionic partner!

6. Interplay Theory: Experiment

Carl D. Anderson (the discoverer of the positron[10] and one of the discoverers of the muon) has described the circumstances concerning the discovery of the positron [20] as follows:

> *"... it has often been stated in the literature that the discovery of the positron was a consequence of its theoretical prediction by Dirac, but this is not true. The discovery of positron was wholly accidental. ... The aim of the experiment that led to the discovery of the positron was simply to measure directly the energy spectrum of the secondary electrons produced in the atmosphere and other materials by the incoming cosmic radiation which at that time (1930) was thought to consist primarily of a beam of photons or gamma rays ..."*

Anderson emphasizes the importance of being familiar with theory by noting that if one had known the Dirac theory one

> *"could have discovered the positron in a single afternoon. The reason for this is that the Dirac theory could have provided an excellent guide as to just how to proceed to form positron-electron pairs out of a beam of gamma-ray photons. History did not proceed in such a direct and efficient manner, probably because the Dirac theory, in spite of its successes, carried with it so many novel and seemingly unphysical ideas, such as negative mass, negative energy, infinite charge density, etc. Its highly esoteric character was apparently not in tune with most of the scientific thinking of that day. Furthermore, positive electrons apparently were not needed to explain any other observations."*

The discovery of the muon involved a long process and it took almost two decades to know its nature. Already in 1929 the so-called penetrating radiation from outer space was discovered by Walther Bothe[11] and W. Kolhörster. It took a few years before one could show that the penetrating radiation consisted of new kind of particles which were neither protons nor electrons [20]. Stated briefly, by 1939, in spite of observation of range, curvature, ionization, and penetrating power of the mesotrons one was not quite sure what they were [21]. It was found, however, that the mesotrons did not interact much with matter [22]. By 1947 it was definitively established [23] that the observed mesotrons were not relevant for transmitting strong interactions; a large fraction of negative mesotrons, instead of being captured by nuclei, decayed; the capture rates were by about 12 orders of magnitude smaller than expected! On the interplay of theory and experiment in this case Anderson says that

> *"This novel suggestion of Yukawa was unknown to the workers engaged in the experiments on the muon until after the muon's existence was established. ... It is interesting to speculate on just how much Yukawa's suggestion, had it been known, would have influenced the progress of the experimental work on muon. My own opinion is that this influence would have been considerable even though Dirac's theory, which was much more specific than Yukawa's, did not have an effect on the positron's discovery. My reason for believing this is that for a period of almost two years there was strong and accumulating evidence for the muon's existence and it was only the caution of the experimental workers that prevented an earlier announcement of its existence. I believe that a theoretical idea like Yukawa's would have appealed to the people carrying out the experiments and would have provided them with a belief that maybe after all there is some need for a particle as strange as a muon, especially if it could help explain something as interesting as the enigmatic nuclear force. ..."*

The discovery of charged pions was announced in 1947 (and that of neutral pions a couple of years later) by researchers working at Bristol [24, 25] and Cecil F. Powell received the 1950 Nobel Prize in Physics for "his development of the photographic method of studying nuclear processes and his discoveries regarding mesons made with this method."

In his Nobel Lecture [26–28], Powell has nothing to say about any theoretical influence. He ends his talk by stating that

> *"In the years which have passed, the study of what might, in the early days, have been regarded as a trivial phenomenon has, in fact, led us to the discovery of many new forms on matter and many new processes of fundamental physical importance. It has contributed to the development of a picture of the material universe as a system in a state of perpetual change and flux; a picture which stands in great contrast with that of our predecessors with their fixed and eternal atoms. At the present time a number of widely divergent hypotheses, none of which is generally accepted, have been advanced to account for the origin of the cosmic radiation. It will indeed be of great*

> *interest if the contemporary studies of the primary radiation lead us - as the Thomsons suggested, and as present tendencies seem to indicate - to the study of some of the most fundamental problems in the evolution of the cosmos."*

Professor Donald Perkins, in Oxford, UK, who was a member of the Bristol group[12] has confirmed that the discovery of pions had nothing to do with theory but could simply be described by [29] "ignorant experimentalists looking for anything of interest in emulsions exposed to cosmic radiation." The kaons were also discovered in 1947 and that eventually led to a new exciting period in the history of particle physics (θ – τ-puzzle, parity violation) during which there were fruitful close contacts between theory and experiment.

In the case of supersymmetry, there have been close contacts between theorists and experimentalists. It remains to be seen what the outcome of these joint efforts is going to be. This time around the community is well prepared to receive supersymmetry, if it exists. In this connection, it is of some interest to look back at our history.

7. The Rich Heritage of Relativistic Quantum Field Theory and Its Future

Richard Feynman, in a talk given in 1979, made the following statement:

> *"We have a theory which is called quantum electrodynamics which is our pride and joy."*

Indeed, Relativistic quantum electrodynamics (QED) is one of the crown jewels of human achievements in physics. It emerged at the end of 1920s through efforts to describe the interactions of light quanta with electrons. However, two decades of work by a large number of researchers was required to reformulate it and to be able to make sense out of it. Naturally, there were several earlier milestones on the road that led to QED. It is perhaps appropriate to briefly remind ourselves of a few of them:

(i) Introduction of the quantum of action h by Max Planck (1900).

(ii) Einstein's theory of special relativity (1905).

(iii) Einstein's introduction of light as a "quantum *particle*," $E = h\nu$ (1905).

(iv) "Creation of quantum mechanics"[13] by Heisenberg (1925) and Schrödinger's version of it (1926).

(v) Dirac's introduction of annihilation and creation operators for photons (1927) and his first-order relativistic description of the electron (1928).

(vi) Quantization rules for bosons, using commutators, and for fermions, using anticommutators as well as a formal derivation of the Pauli principle (1928).

These theoretical breakthroughs took us to the end of 1920s when it was realized that QED, in spite of all its successes, faced insurmountable-looking difficulties, such as infinite corrections to the energy levels of atoms. The conclusion drawn by some researchers was that QED, of those days, will not be applicable to any problem where relativistic effects are important.

On the status of field theory later on, one of the leading field theorists of our time, Steven Weinberg writes ([30], p. 281) the following:

> *"During 1930s it was widely believed that these infinities signified the breakdown of quantum electrodynamics at energies above a few MeV. ... [after the war] ... The great success of calculations in quantum electrodynamics using the renormalization idea generated a new enthusiasm for quantum electrodynamics."*

However, by the end of 1950s and in 1960s quantum theory came under fierce attack, at least in some theoretical circles. By that time, the number of hadrons had increased so much that it raised the question whether they were all "elementary particles," each with its own field. The pion-nucleon coupling constant was found to be so large that it did not allow physicists to apply their favorite approach, perturbation theory. What was there to be done? Indeed, a group of theorists advocated departure from field theory altogether. It was argued that

> *"there is no reason why some particles should be on a different footing from others. The elementary particle concept is unnecessary, at least for baryons and mesons."*

Some distinguished physicists declared field theory as dead and buried, as far as hadrons were concerned. Why it worked well for quantum electrodynamics was considered as a puzzle. As we know from later history, field theory retaliated by striking back with stronger force than ever before and gave us the electroweak theory as well as QCD!

What we wish to know now is whether supersymmetry is realized in Nature. Viki Weisskopf liked to say *"predicting is difficult, especially when it concerns the future,"* a statement that he attributed to Niels Bohr. Indeed we all have "feelings" and "wishes." We would like to tell Mother Nature how She should behave, but She has already made up Her mind and it is for us to find out what Her feelings and wishes have been. In any case, discovery of supersymmetry need not signify any departure from our current framework: relativistic local quantum field theory.

Concerning the future, I would like to quote Steven Weinberg who writes ([30], p. 289)

> *"My own view is that all of the successful field theories of which we are so proud-electrodynamics, the electroweak theory, quantum chromodynamics and even General Relativity-are in truth effective field theories, only with a much larger characteristic energy, something like the Planck energy,* 10^{19} *GeV."*

Let us hope that Mother Nature will soon reveal some of Her instructive secrets, for us to be able to proceed further on the "right path."

Conflict of Interests

The author declares that there is no conflict of interests regarding the publication of this paper.

Endnotes

1. In 1955 there were two Nobel Laureates in Physics, one of them being Willis Lamb who received the Prize for this discovery. In his Nobel Lecture, he mentions that this effect had been seen about ten years earlier by other researchers [31, 32] but, unfortunately, as he puts it, had not been taken seriously. This was perhaps fortunate for him as he could do a much more accurate measurement, using newly developed microwave techniques.

2. Unfortunately sometimes in the scientific literature one sees Retherford incorrectly spelled as Rutherford, thereby giving the credit to the latter who had passed away about ten years earlier, in 1937. Robert Curtis Retherford (1912–1981) was a graduate student of Willis Lamb.

3. Polykarp Kusch was the second Nobel Laureate in Physics in 1955, for "his precision determination of the magnetic moment of the electron."

4. See, for example, Feynman's article "Relativistic cut-off for quantum electrodynamics" [33] where he mentions several by then existing cut-off procedures, some similar to his own, especially that of F. Bopp [18, 19].

5. Pauli and Villars, in their paper, give credit to Rayski as an inventor of auxiliary fictitious particles. The authors state that "*Rayski made this proposal in the summer of 1948 during his investigations on the photon self-energy of Bosons (see [6]). With his friendly consent we later resumed his work and generalized the method for arbitrary external fields (not necessarily light waves).*" Note, however, that Pauli and Villars consistently refer to J. Rayski as G. Rayski. This could be due to the fact that he, when he had been in the USA, had translated his first name, Jerzy, into English and had published under the name George Rayski. Jerzy Rayski (1917–1993) from Krakow, Poland, had spent one year during 1949–1950 in Zürich. He relates some of his recollections in [34].

6. Yukawa received the 1949 Nobel Prize in Physics "for his prediction of the existence of mesons on the basis of theoretical work on nuclear forces."

7. The 1965 Nobel Prize in Physics was awarded to Sin-Itiro Tomonaga, Julian Schwinger, and Richard P. Feynman "for their fundamental work in quantum electrodynamics, with deep-ploughing consequences for the physics of elementary particles."

8. For information about Umezawa see, for example, G. Vitiello on "Hiroomi Umezawa and Quantum Field Theory" [35]. I wish to thank Professor Vitiello for sending his article to me.

9. These are

$$k - 2l + 3m = 0$$

$$\sum_i^k \left(\kappa_i^{(s)}\right)^2 - 2\sum_i^l \left(\kappa_i^{(f)}\right)^2 + 3\sum_i^m \left(\kappa_i^{(v)}\right)^2 = 0, \qquad (*)$$

   where k, l, and m denote the number of (charged) scalar, spin-1/2, and spin-1 fields, respectively, and κ_i denotes the appropriate mass.

10. The Sixth General Assembly of IUPAP (the International Union of Pure and Applied Physics) which took place in Amsterdam, in 1948, unanimously recommended the use of the term electron for both $e^{\pm}$ and the terms positon and negaton for denoting e^+ and e^-, respectively. In the long run, however, the physics community did not follow this recommendation.

11. In 1954 Walther Bothe received a Nobel Prize in Physics for "the coincidence method and his discoveries made therewith."

12. I wish to thank Professors Don Perkins and Gösta Ekspong, who both were among the young members of the Bristol group, for inspiring correspondence on their work at Bristol. Powell refers to their work in his Nobel Lecture [26–28]; however, in his list of references, Ekspong's former last name (Carlson) is misspelled (as Carison).

13. This is quoting the Prize motivation that the Nobel Prize in Physics 1932 was awarded to Werner Heisenberg "for the creation of quantum mechanics, ..."

References

[1] C. Jarlskog, Ed., *Portrait of Gunnar Källén—A Physics Shooting Star and Poet of Early Quantum Field Theory*, Springer, Berlin, Germany, 2014.

[2] G. Källén, "Higher approximation in the external field for the problem of vacuum polarization," *Helvetica Physica Acta*, vol. 22, no. 6, pp. 637–658, 1949.

[3] R. Jost and J. Rayski, "Remarks on the problem of the vacuum polarization and the photon-self-energy," *Helvetica Physica Acta*, vol. 22, no. 4, pp. 457–466, 1949.

[4] H. Umezawa, Y. Yukawa, and E. Yamada, "The problem of vacuum polarization," *Progress of Theoretical Physics*, vol. 3, no. 3, pp. 317–318, 1948.

[5] J. Rayski, "On simultaneous interaction of several fields and the self-energy problem," *Acta Physica Polonica*, vol. 9, pp. 129–140, 1948.

[6] G. Wentzel, "New aspects of the photon self-energy problem," *Physical Review*, vol. 74, no. 9, pp. 1070–1075, 1948.

[7] W. E. Lamb and R. C. Retherford, "Fine structure of the hydrogen atom by a microwave method," *Physical Review*, vol. 72, no. 3, pp. 241–243, 1947.

[8] H. M. Foley and P. Kusch, "On the intrinsic moment of the electron," *Physical Review*, vol. 73, no. 4, article 412, 1948.

[9] J. Schwinger, "On quantum-electrodynamics and the magnetic moment of the electron," *Physical Review*, vol. 73, no. 4, pp. 416–417, 1948.

[10] W. Pauli and F. Villars, "On the invariant regularization in relativistic quantum theory," *Reviews of Modern Physics*, vol. 21, pp. 434–444, 1949.

[11] H. Yukawa, Nobel Lecture, 1949.

[12] H. Yukawa, "Quantum theory of non-local fields. Part I. Free fields," *Physical Review*, vol. 77, pp. 219–226, 1950.

[13] S.-I. Tomonaga, Nobel Lecture, 1965.

[14] S. Sakata and T. Inoue, "On the correlation between mesons and Yukawa's particles," *Progress of Theoretical Physics*, vol. 1, pp. 143–150, 1946.

[15] A. Pais, "On the theory of the electron and of the nucleon," *Physical Review*, vol. 68, no. 9-10, pp. 227–228, 1945.

[16] S. Sakata and H. Umezawa, "On the applicability of the method of the mixed fields in the theory of the elementary particles," *Progress of Theoretical Physics*, vol. 5, no. 4, pp. 682–691, 1950.

[17] H. Umezawa, *Quantum Field Theory*, North-Holland, Amsterdam, The Netherlands, 1956.

[18] F. Bopp, "Lineare theorie des elektrons. II," *Annalen der Physik*, vol. 434, no. 7-8, pp. 573–608, 1943.

[19] F. Bopp, "Eine lineare theorie des elektrons," *Annalen der Physik*, vol. 430, no. 5, pp. 345–384, 1940.

[20] C. D. Anderson, "Early work on the positron and muon," *The American Journal of Physics*, vol. 29, no. 12, pp. 825–830, 1961.

[21] S. H. Neddermeyer and C. D. Anderson, "Nature of cosmic-ray particles," *Reviews of Modern Physics*, vol. 11, no. 3-4, pp. 191–207, 1939.

[22] J. G. Wilson, "Absorption of penetrating cosmic ray particles in gold," *Proceedings of the Royal Society of London Series A: Mathematical and Physical Sciences*, vol. 172, no. 951, pp. 517–529, 1939.

[23] M. Conversi, E. Pancini, and O. Piccioni, "On the disintegration of negative mesons," *Physical Review*, vol. 71, no. 3, pp. 209–210, 1947.

[24] C. M. G. Lattes, H. Muirhead, G. P. S. Occhialini, and C. F. Powell, "Processes involving charged mesons," *Nature*, vol. 159, no. 4047, pp. 694–697, 1947.

[25] C. M. G. Lattes, G. P. S. Occhialini, and C. F. Powell, "Observations on the tracks of slow mesons in photographic emulsions," *Nature*, vol. 160, pp. 453–456, 1947.

[26] C. F. Powell, Nobel Lecture, 1950.

[27] D. H. Perkins, "Nuclear disintegration by meson capture," *Nature*, vol. 159, no. 4030, pp. 126–127, 1947.

[28] A. G. Carlson, J. E. Hooper, and D. T. King, "LXIII. Nuclear transmutations produced by cosmic-ray particles of great energy—part V. The neutral mesons," *Philosophical Magazine Series 7*, vol. 41, no. 318, pp. 701–724, 1950.

[29] D. H. Perkins, Private communication, 2015.

[30] S. Weinberg, "Living with infinities," in *Portrait of Gunnar Källén—A Physics Shooting Star and Poet of Early Quantum Field Theory*, C. Jarlskog, Ed., pp. 279–292, Springer, Berlin, Germany, 2014.

[31] W. V. Houston, "A new method of analysis of the structure of Hα and Dα," *Physical Review*, vol. 51, no. 6, pp. 446–449, 1937.

[32] R. C. Williams, "The fine structures of Hα and Dα under varying discharge conditions," *Physical Review*, vol. 54, pp. 558–567, 1938.

[33] R. P. Feynman, "Relativistic cut-off for quantum electrodynamics," *Physical Review Letters*, vol. 74, no. 10, pp. 1430–1438, 1948.

[34] J. Rayski, "Search for generalized, quantizable dynamical models," *Reports on Mathematical Physics*, vol. 25, no. 3, pp. 255–274, 1988.

[35] G. Vitiello, "Hiroomi umezawa and quantum field theory," *NeuroQuantology*, vol. 9, no. 3, pp. 402–412, 2011.

Hindawi Publishing Corporation
Advances in High Energy Physics
Volume 2015, Article ID 760729, 12 pages
http://dx.doi.org/10.1155/2015/760729

Research Article

Two-Loop Correction to the Higgs Boson Mass in the MRSSM

Philip Diessner,[1] Jan Kalinowski,[2] Wojciech Kotlarski,[1,2] and Dominik Stöckinger[1]

[1]*Institut für Kern- und Teilchenphysik, TU Dresden, 01069 Dresden, Germany*
[2]*Faculty of Physics, University of Warsaw, Pasteura 5, 02093 Warsaw, Poland*

Correspondence should be addressed to Wojciech Kotlarski; wojciech.kotlarski@fuw.edu.pl

Received 24 April 2015; Accepted 23 June 2015

Academic Editor: Mark D. Goodsell

We present the impact of two-loop corrections on the mass of the lightest Higgs boson in the minimal R-symmetric supersymmetric standard model (MRSSM). These shift the Higgs boson mass up by typically 5 GeV or more. The dominant corrections arise from strong interactions, and from the gluon and its $N = 2$ superpartners, the sgluon and Dirac gluino, and these corrections further increase with large Dirac gluino mass. The two-loop contributions governed purely by Yukawa couplings and the MRSSM λ, Λ parameters are smaller. We also update our earlier analysis which showed that the MRSSM can accommodate the measured Higgs and W boson masses. Including the two-loop corrections increases the parameter space where the theory prediction agrees with the measurement.

1. Introduction

The recent discovery at the LHC of a particle consistent with the long sought Higgs boson seemingly completes the Standard Model (SM). The mass of the particle is measured with an astonishingly high accuracy of $m_H = 125.09 \pm 0.24\,\text{GeV}$ [1]. The precise determination of this mass is of paramount importance not only within the context of the Standard Model, but also for finding the path beyond it. In fact, a number of experimental observations suggest that the SM cannot be the ultimate theory and many theoretical scenarios for the beyond SM (BSM) physics have been proposed in past decades. In some models of BSM, in particular in supersymmetric extensions of the SM, the Higgs boson mass can be predicted. However, the current experimental accuracy is far better than theoretical predictions for Higgs boson mass in any given model of BSM physics. From the point of view of theory, the best accuracy has been achieved in the minimal supersymmetric extension of the SM (MSSM), in which the discovery of the Higgs boson and the determination of its mass have given a new impetus to the theoretical efforts. The most recent improvements comprise the inclusion of leading three-loop corrections [2, 3], resummation of leading logarithms beyond the two-loop level [4, 5], inclusion of the external momenta of two-loop self-energies [6, 7], and the evaluation of the $\mathcal{O}(\alpha_t^2)$-contributions in the complex MSSM [8, 9]. The MSSM two-loop corrections controlled by Yukawa couplings and α_s have been known for quite some time for the real MSSM (see the above references for an overview of the literature).

The absence of any direct signal of supersymmetric particle production at the LHC and the observed Higgs boson mass of ~125 GeV being rather close to the upper value of ~135 GeV achievable in the MSSM are a strong motivation to consider nonminimal SUSY scenarios. In fact, nonminimal SUSY models can lift the Higgs boson mass (at the tree-level by new F- or D-term contributions or at the loop level from additional new states), which makes these models more natural by reducing fine-tuning. They can also weaken SUSY limits either by predicting compressed spectra or by reducing the expected missing transverse energy or by reducing production cross sections. The comparison of the measured Higgs boson mass with the theoretically predicted values in any given model is therefore highly desirable. Although the theoretical calculations for the SM-like Higgs boson mass in such models are less advanced, progress is being made in the development of highly automated tools which greatly facilitate the computations in nonminimal SUSY models: `SARAH` [10–12] automatically generates spectrum generators similar to `SPheno` [13, 14]; `FlexibleSUSY`

[15] automatically generates spectrum generators similar to `Softsusy` [16].

In a recent paper [17] we considered the MRSSM, a highly motivated supersymmetric model with continuous R-symmetry [18, 19] distinct from the MSSM. Since R-symmetry forbids soft Majorana gaugino masses as well as the higgsino mass term, additional superfields are needed. The MRSSM has been constructed in [20] as a minimal viable model of this type. It contains adjoint chiral superfields with R-charge 0 for each gauge sector and two additional Higgs weak iso-doublet superfields with R-charge 2. It has been also argued that R-symmetry generically forbids large contributions to CP- and flavor-violating observables due to the absence of chirality-changing Dirac gluino couplings [20, 21], relaxing flavor constraints on the sfermion sector, although recently it has been shown that the dramatic chirality-flip suppression of [20] can only work in a limited number of scenarios, and in general a certain correlation between flavor structure of fermion masses and superpartner spectrum is required [22]. Also, Dirac gluinos suppress the production cross section for squarks, making squarks below the TeV scale generically compatible with LHC data. Furthermore, models with R-symmetry and/or Dirac gauginos contain promising dark matter candidates [23–25], and the collider physics of the extra, non-MSSM-like states has been studied [26–34].

In [17] the complete next-to-leading order computation and discussion of the lightest Higgs boson and W boson masses have been performed. We showed that the model can accommodate measured values of these observables for interesting regions of parameter space with stop masses of order 1 TeV (a similar analysis has been done in [35], where also a welcome reduction of the level of fine-tuning was found). The outcome of the paper was not obvious since in the MRSSM (i) the lightest Higgs boson tree-level mass is typically reduced compared to the MSSM due to mixing with additional scalars, (ii) the stop mixing is absent, and (iii) R-symmetry necessarily introduces an $SU(2)$ scalar triplet, which can increase m_W already at the tree-level. Nevertheless, we identified benchmark points BMP1, BMP2, and BMP3 illustrating different viable parameter regions for $\tan\beta = 3, 10, 40$, respectively, and also verified that they are not excluded by further experimental constraints from Higgs observables, collider, and low-energy physics.

These promising results motivate a more precise computation of the Higgs boson mass in the MRSSM and a more precise parameter analysis. Technically, this is facilitated by the Mathematica package `SARAH`, recently updated by providing `SPheno` routines, which calculate two-loop corrections to the CP-even Higgs scalars masses in the effective potential approximation and the gaugeless limit [36]. This is the level of precision of the established MSSM predictions except for the refinements mentioned above. It is also the level of precision at which the proof [37] applies that the employed regularization by dimensional reduction preserves supersymmetry. First applications of the improved `SARAH` version to the calculations of the Higgs boson masses in the R-parity violating MSSM [38] and next-to-minimal SSM [39] have been published.

Since a judicious choice of the model parameters was needed to meet experimental constraints and an estimate of unknown two-loop contributions was presented, it is of immediate interest to verify our findings at higher precision with the new `SARAH` version. The aim of the current paper is to calculate two-loop corrections for the Higgs boson mass in the same MRSSM setup as in [17] and present an update of the results obtained there.

The paper is organized as follows. After a short recapitulation of the MRSSM setup in Section 2, we explain in Section 3 our calculation framework and discuss the dependence of two-loop corrections on parameters that entered already at the one-loop level. The dependence on parameters that enter only at the two-loop level is investigated in Section 4. In Section 5 we provide an update to the analysis presented in [17] using the two-loop corrected masses of Higgses, before concluding in Section 6.

2. The MRSSM

The MRSSM has been constructed in [20] as a minimal supersymmetric model with unbroken continuous R-symmetry. The superpotential of the model reads as

$$\begin{aligned} W = {} & \mu_d \widehat{R}_d \cdot \widehat{H}_d + \mu_u \widehat{R}_u \cdot \widehat{H}_u + \Lambda_d \widehat{R}_d \cdot \widehat{T} \widehat{H}_d + \Lambda_u \widehat{R}_u \\ & \cdot \widehat{T} \widehat{H}_u + \lambda_d \widehat{S} \widehat{R}_d \cdot \widehat{H}_d + \lambda_u \widehat{S} \widehat{R}_u \cdot \widehat{H}_u - Y_d \widehat{d} \widehat{q} \cdot \widehat{H}_d \\ & - Y_e \widehat{e} \widehat{l} \cdot \widehat{H}_d + Y_u \widehat{u} \widehat{q} \cdot \widehat{H}_u, \end{aligned} \tag{1}$$

where $\widehat{H}_{u,d}$ are the MSSM-like Higgs weak iso-doublets and $\widehat{S}, \widehat{T}, \widehat{R}_{u,d}$ are the singlet, weak iso-triplet, and $\widehat{R}$-Higgs weak iso-doublets, respectively. The usual MSSM μ-term is forbidden; instead $\mu_{u,d}$-terms involving R-Higgs fields are allowed. Λ, λ-terms are similar to the usual Yukawa terms, where $\widehat{R}$-Higgs and $\widehat{S}$ or $\widehat{T}$ play the role of the quark/lepton doublets and singlets.

The usual soft mass terms of the MSSM scalar fields are allowed just like in the MSSM. In contrast, A-terms and soft Majorana gaugino masses are forbidden by R-symmetry. The fermionic components of the chiral adjoint, $\widehat{\Phi}_i = \widehat{\mathcal{O}}, \widehat{T}, \widehat{S}$ for each standard model gauge group $i = SU(3), SU(2), U(1)$, respectively, are paired with standard gauginos $\widetilde{g}, \widetilde{W}, \widetilde{B}$ to build Dirac fermions and the corresponding mass terms. The Dirac gaugino masses generated by D-type spurions produce additional terms with the auxiliary $\mathcal{D}$-fields in the Lagrangian,

$$\begin{aligned} V_D = {} & M_B^D \left(\widetilde{B} \widetilde{S} - \sqrt{2} \mathcal{D}_B S \right) + M_W^D \left(\widetilde{W}^a \widetilde{T}^a - \sqrt{2} \mathcal{D}_W^a T^a \right) \\ & + M_O^D \left(\widetilde{g}^a \widetilde{O}^a - \sqrt{2} \mathcal{D}_g^a O^a \right) + \text{h.c.}, \end{aligned} \tag{2}$$

which after being eliminated through their equations of motion lead to the appearance of Dirac masses in the scalar sector as well. For our phenomenological studies of two-loop

effects we take the soft-breaking scalar mass terms that have been considered in [17]

$$\begin{aligned} V_{\mathrm{SB}}^{\mathrm{EW}} &= m_{H_d}^2\left(\left|H_d^0\right|^2+\left|H_d^-\right|^2\right)+m_{H_u}^2\left(\left|H_u^0\right|^2+\left|H_u^+\right|^2\right) \\ &\quad+\left[B_\mu\left(H_d^-H_u^+-H_d^0H_u^0\right)+\mathrm{h.c.}\right] \\ &\quad+m_{R_d}^2\left(\left|R_d^0\right|^2+\left|R_d^+\right|^2\right)+m_{R_u}^2\left|R_u^0\right|^2+m_{R_u}^2\left|R_d^-\right|^2 \\ &\quad+m_S^2|S|^2+m_T^2\left|T^0\right|^2+m_T^2\left|T^-\right|^2+m_T^2\left|T^+\right|^2 \\ &\quad+m_O^2|O|^2+\widetilde{d}_{L,i}^*m_{q,ij}^2\widetilde{d}_{L,j}+\widetilde{d}_{R,i}^*m_{d,ij}^2\widetilde{d}_{R,j} \\ &\quad+\widetilde{u}_{L,i}^*m_{q,ij}^2\widetilde{u}_{L,j}+\widetilde{u}_{R,i}^*m_{u,ij}^2\widetilde{u}_{R,j}+\widetilde{e}_{L,i}^*m_{l,ij}^2\widetilde{e}_{L,j} \\ &\quad+\widetilde{e}_{R,i}^*m_{e,ij}^2\widetilde{e}_{R,j}+\widetilde{\nu}_{L,i}^*m_{l,ij}^2\widetilde{\nu}_{L,j}, \end{aligned} \tag{3}$$

where the holomorphic mass terms for adjoint scalars, which might lead to tachyonic states, have been neglected (see also [40, 41] for discussions that these terms can be subdominant within a broad definition of gauge mediation).

The electroweak symmetry breaking (EWSB) is triggered by nonzero vacuum expectation values of $R = 0$ neutral EW scalars, which are parameterized as

$$\begin{aligned} H_d^0 &= \frac{1}{\sqrt{2}}\left(v_d+\phi_d+i\sigma_d\right), \\ H_u^0 &= \frac{1}{\sqrt{2}}\left(v_u+\phi_u+i\sigma_u\right), \\ T^0 &= \frac{1}{\sqrt{2}}\left(v_T+\phi_T+i\sigma_T\right), \\ S &= \frac{1}{\sqrt{2}}\left(v_S+\phi_S+i\sigma_S\right); \end{aligned} \tag{4}$$

R-Higgs bosons carry R-charge 2 and therefore do not develop vacuum expectation values. We stress that in general the mixing of ϕ_T, ϕ_S with ϕ_u and ϕ_d leads to a reduction of the lightest Higgs boson mass at the tree-level compared to the MSSM.

3. Higgs Mass Dependence on λ, Λ Superpotential Parameters

We now present the MRSSM Higgs boson mass prediction at the two-loop level. We use the same renormalization scheme as in [17], where all SUSY parameters are defined in the $\overline{\mathrm{DR}}$ scheme and $m_{H_d}^2$, $m_{H_u}^2$, v_S, and v_T are determined by minimizing the effective potential at the two-loop order. The discussion is divided into two parts. In the present section we begin with the one-loop contributions, which are dominated by terms of $\mathcal{O}(\alpha_{t,b,\lambda})$, where α_λ collectively denotes squares of the superpotential couplings $\lambda_{u,d}$ and $\Lambda_{u,d}$. We then discuss the two-loop contributions of $\mathcal{O}(\alpha_{t,b,\lambda}^2)$, that is, ones which depend on parameters which already play a role at the one-loop level. In the subsequent section we then discuss those two-loop corrections which involve new parameters.

In the usual MSSM, the one-loop contributions to the Higgs boson mass are dominated by top/stop contributions. In the MRSSM, these contributions are also important, but they are simpler since stop mixing is forbidden by R-symmetry (corresponding to the MSSM parameter $X_t \equiv A_t - \mu/\tan\beta = 0$). This implies that the top/stop contributions cannot reach values as high as in the MSSM for a given stop mass scale. However, as mentioned above, the MRSSM superpotential contains new terms governed by $\lambda_{u,d}$ and $\Lambda_{u,d}$ which have a Yukawa-like structure. References [17, 35] have given a useful analytical approximation for these contributions. In the limit $\lambda = \lambda_u = -\lambda_d$, $\Lambda = \Lambda_u = \Lambda_d$, $v_S \approx v_T \approx 0$, and large $\tan\beta$, we get

$$\begin{aligned} \Delta m_{H_1,\mathrm{eff.pot},\lambda}^2 &= \frac{2v^2}{16\pi^2}\Bigg[\frac{\Lambda^2\lambda^2}{2} \\ &\quad+\frac{4\lambda^4+4\lambda^2\Lambda^2+5\Lambda^4}{8}\log\frac{m_{R_u}^2}{Q^2} \\ &\quad+\left(\frac{\lambda^4}{2}-\frac{\lambda^2\Lambda^2}{2}\frac{m_S^2}{m_T^2-m_S^2}\right)\log\frac{m_S^2}{Q^2} \\ &\quad+\left(\frac{5}{8}\Lambda^4+\frac{\lambda^2\Lambda^2}{2}\frac{m_T^2}{m_T^2-m_S^2}\right)\log\frac{m_T^2}{Q^2} \\ &\quad-\left(\frac{5}{4}\Lambda^4-\lambda^2\Lambda^2\frac{\left(M_W^D\right)^2}{\left(M_B^D\right)^2-\left(M_W^D\right)^2}\right)\log\frac{\left(M_W^D\right)^2}{Q^2} \\ &\quad-\left(\lambda^4+\lambda^2\Lambda^2\frac{\left(M_B^D\right)^2}{\left(M_B^D\right)^2-\left(M_W^D\right)^2}\right)\log\frac{\left(M_B^D\right)^2}{Q^2}\Bigg]. \end{aligned} \tag{5}$$

This result shows a behavior proportional to λ^4, Λ^4, and $\log m_{\mathrm{soft}}^2$. This is similar to the top/stop contributions as λ's and Y_t appear in a similar fashion in superpotential.

We expect therefore that the two-loop result will depend on these model parameters (which already entered at the one-loop level) in a manner similar to the pure top quark/squarks two-loop contributions, that is, similar to the MSSM $\mathcal{O}(\alpha_t^2)$ contributions without stop mixing.

In Figures 1 and 2 the dependence of the lightest Higgs boson mass calculated at tree-, one-, and two-loop levels for two benchmarks BMP1 and BMP3 on different model parameters is shown. All parameters except the ones shown on the horizontal axes are set to the values of the benchmark points defined in [17] (see Table 2). Indeed λ, Λ behavior of the two-loop corrections is very similar to the one of the corresponding one-loop corrections. The numerical impact of the two-loop λ, Λ-contributions is rather small, typically less than 1 GeV, except for very large $|\lambda_u|, |\Lambda_u| > 1$, where they can reach several GeV. Particularly, the strong λ_u dependence for large λ_u is already manifest for the tree-level mass; this is due to the mixing with the singlet state already present in the tree-level mass matrix.

One should remember that very large one-loop contributions are required to bring the predicted Higgs boson mass

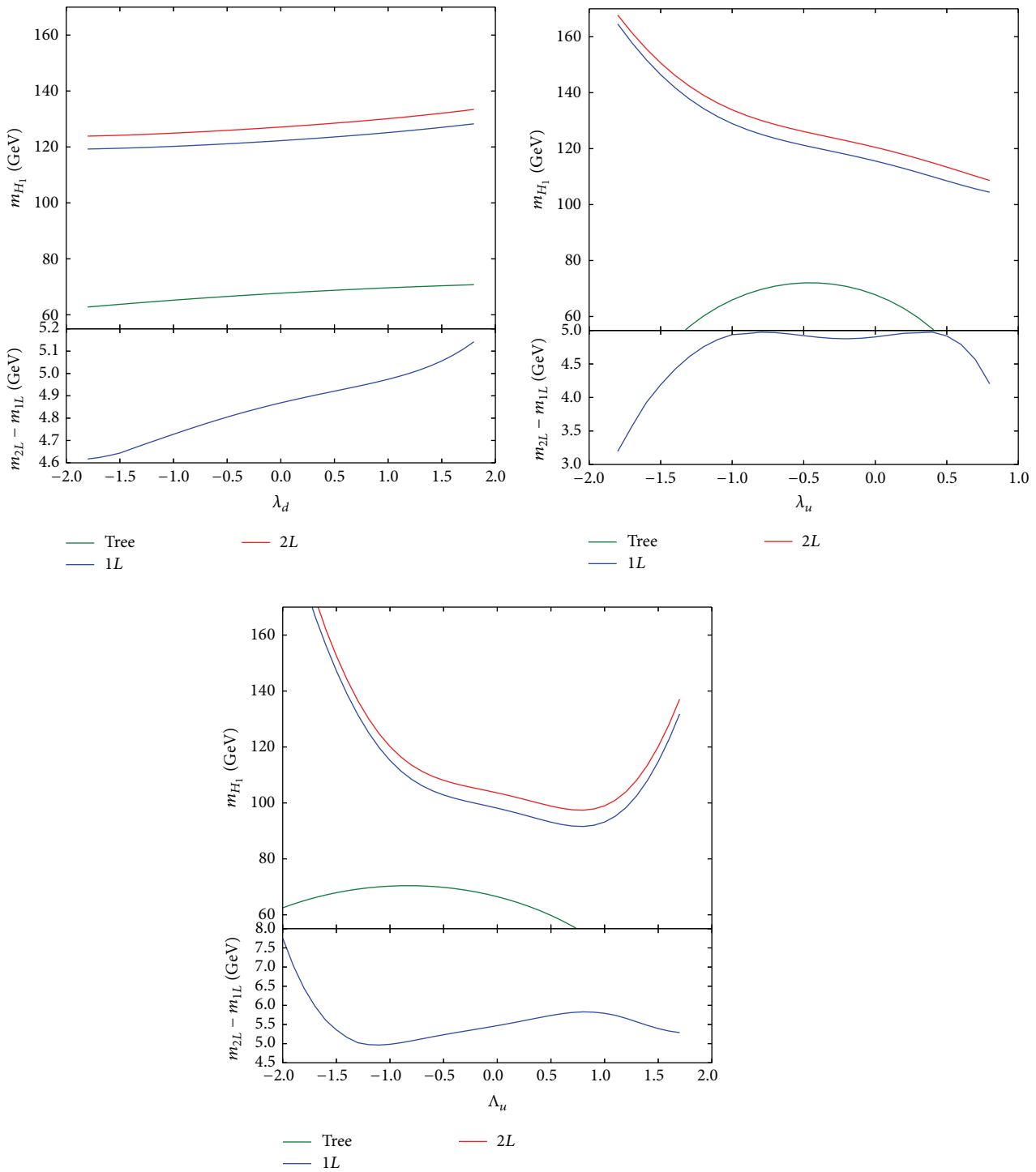

FIGURE 1: Lightest MRSSM Higgs boson mass m_{H_1} and the difference $m_{2L} - m_{1L}$ between masses calculated at the two-loop and one-loop level, as a function of λ_d, λ_u, and Λ_u, respectively. In the upper parts of the figure lines from top to bottom correspond to two-loop, one-loop, and tree-level calculations. All other parameters are set to the values of benchmark point BMP1 with $\tan\beta = 3$ (see Table 2).

close to the experimental one. In the preferred parameter regions, λ, Λ are large but still moderate enough not to blow up the two-loop contributions. Although the large values of Λ couplings will lead to Landau poles at scales below the GUT scale; this is not problem for our phenomenological approach, and even in top-down approaches as in [40] perturbativity up to the GUT scale is not required.

Overall, the total two-loop contributions (including the ones to be discussed in the subsequent section) are in the range between 4 and 5 GeV, except in the very large λ, Λ regions. This is in agreement with the estimate given in [17],

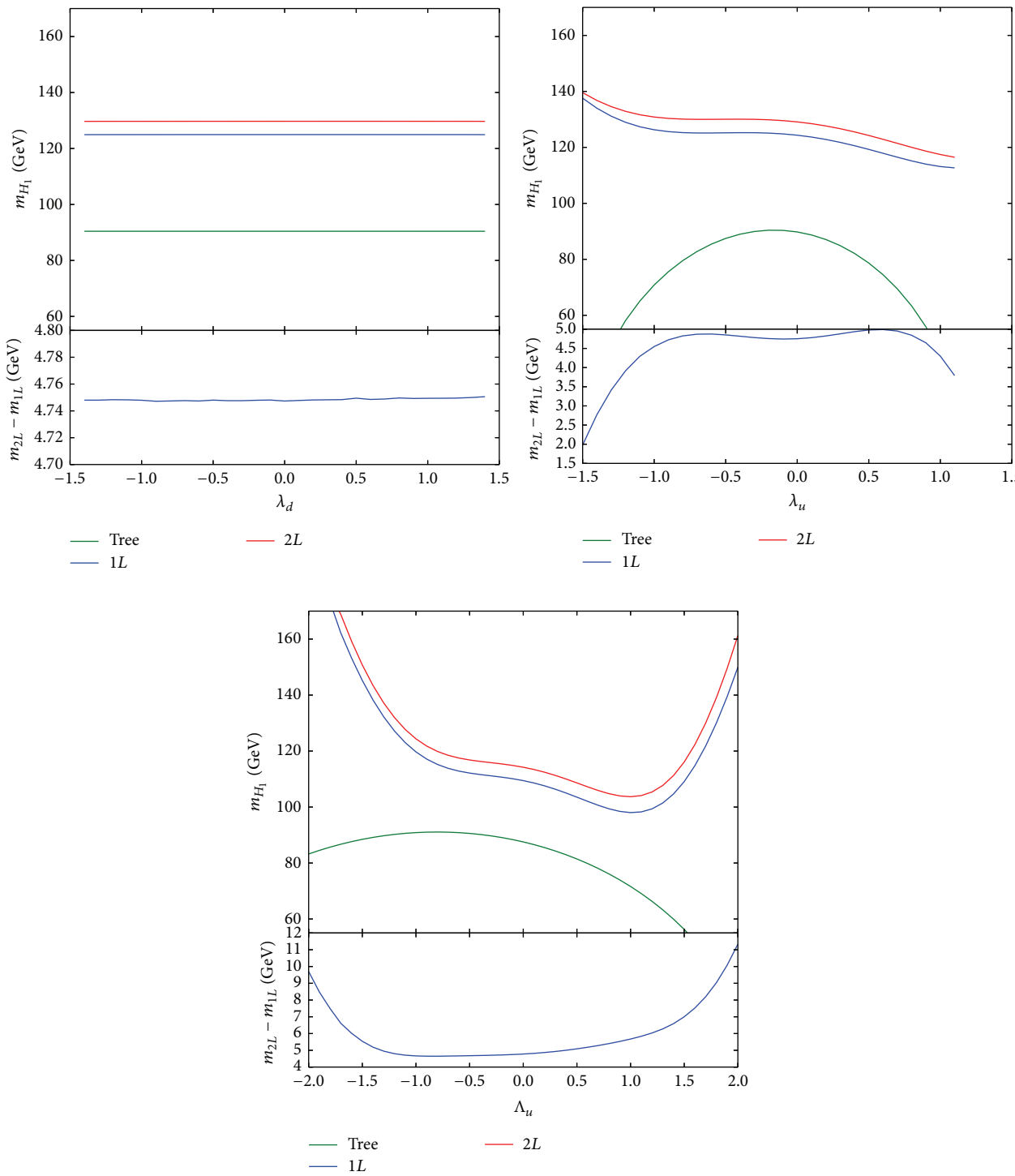

FIGURE 2: As in Figure 1, but for benchmark point BMP3 with $\tan\beta = 40$ (see Table 2).

and it confirms the validity of the perturbative expansion in spite of the large one-loop corrections.

4. QCD Corrections and the Two-Loop Corrected Higgs Boson Mass

At two-loop level the strongly interacting sector and the strong coupling α_s appear directly in the Higgs boson mass predictions. These two-loop corrections involve not only the gluon but also the Dirac gluino and the sgluon, the scalar component of the octet superfield $\widehat{O}$. They can be expected to be sizable, and they depend on the gluino Dirac mass and sgluon soft mass parameters. These parameters already play a role at lower order, appearing in corrections to Y_t (through threshold corrections to $\widehat{\alpha}_s$), though the influence on, for

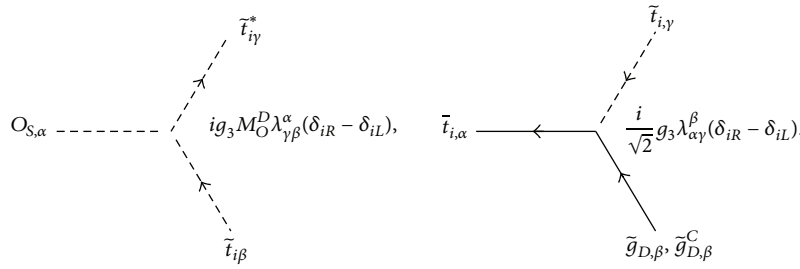

Figure 3: Feynman rules needed to evaluate diagrams of Figure 4. In the right diagram, the charge-conjugated gluino $\tilde{g}^C_{D,\beta}$ applies in the case of $i = L$, $\tilde{g}_{D,\beta}$ in the case of $i = R$.

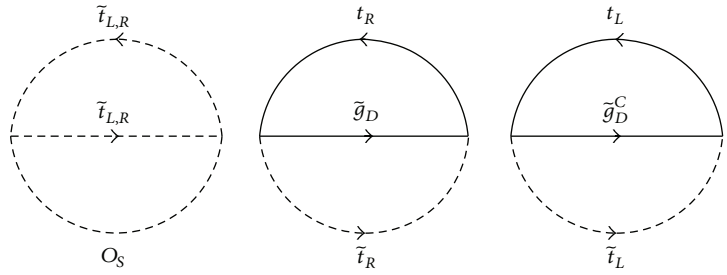

Figure 4: Two-loop diagrams contributing to the Higgs boson mass via (6) which depend on the Dirac mass M_O^D and the soft sgluon mass m_O. We only draw diagrams involving top/stop; similar diagrams exist for all quark/squark flavors.

example, $\overline{\text{DR}}$ top mass is negligible. The gluino Dirac mass parameter M_O^D appears not only directly as the gluino mass but via (2), also in couplings and mass terms of sgluons, inducing the mass splitting. In [17] a simplifying assumption was made that masses of the scalar and pseudoscalar components of (complex) sgluon field were equal, since it was unimportant for that analysis between the real and imaginary parts of the sgluon field, $O = (1/\sqrt{2})(O_S + iO_A)$. The masses of the scalar sgluons O_S and pseudoscalar sgluons O_A are related by the tree-level formula $m^2_{O_S} = 4(M_O^D)^2 + m^2_{O_A}$, where $m^2_{O_A}$ is equal to the soft-breaking parameter m_O^2 [26, 28]. The relevant vertices and Feynman rules are depicted in Figure 3. We assume real M_O^D, so only the scalar O_S acquires the direct coupling to sfermions proportional to M_O^D, via (2).

The structure of the strong corrections is thus markedly different from the MSSM case, where only the Majorana gluino and the gluon appear. In the following, we study the magnitude and the behavior of the corrections as a function of the parameters M_O^D and m_O^2.

4.1. Analytic Formulas. As in the previous section, we begin with an analytic approximation for the leading contributions of $\mathcal{O}(\alpha_t\alpha_s)$, that is, two-loop strong corrections proportional to Y_t^2. This provides us with qualitative insight and serves as a check of the code. Generally, in the gaugeless limit (in which the two electroweak gauge couplings $g_{1,2}$ are neglected), the two-loop corrections from gluinos and sgluons contribute only to the diagonal part of $\{\phi_d, \phi_u\}$ submatrix of the scalar Higgs boson mass matrix. In the MRSSM $\mathcal{O}(\alpha_t\alpha_s)$ terms contribute only to $\phi_u\phi_u$ element. This already constitutes a difference to the MSSM, where μ-term violates R-symmetry and Peccei-Quinn symmetry leading to couplings of stops to ϕ_d.

Figure 4 shows two-loop diagrams contributing to the Higgs boson mass at $\mathcal{O}(\alpha_t\alpha_s)$ that explicitly depend on m_O and/or M_O^D. These diagrams provide the following contribution to the effective potential:

$$V^{(2)}_{\text{eff}} = \frac{8g_3^2}{\left(16\pi^2\right)^2}\left(M_O^D\right)^2 \sum_{i=L,R} f_{SSS}\left(m^2_{\tilde{t}_i}, m^2_{\tilde{t}_i}, m^2_{O_S}\right) + \frac{8g_3^2}{\left(16\pi^2\right)^2} \sum_{i=L,R} f_{FFS}\left(m_t^2, m^2_{\tilde{t}_i}, m^2_{\tilde{g}_D}\right), \tag{6}$$

where the functions f_{SSS} and f_{FFS} are defined in [42]. The effective potential $V^{(2)}_{\text{eff}}$ depends on v_u through stop masses, which in the gaugeless limit approach

$$m^2_{\tilde{t}_L\tilde{t}_L} \longrightarrow m_q^2 + \frac{1}{2}Y_t^2 v_u^2, \qquad m^2_{\tilde{t}_R\tilde{t}_R} \longrightarrow m_u^2 + \frac{1}{2}Y_t^2 v_u^2. \tag{7}$$

Equation (6) can be obtained from [42] by applying translation rules from real fields to complex ones. Many such rules can be found in [36]; an additional rule needed here for the case of a Lagrangian $\mathscr{L} \ni -c\Phi_1|\Phi_2|^2$, where $\Phi_1, c \in \mathbb{R}$, $\Phi_2 \in \mathbb{C}$, is $V_{SSS} = (1/2)|c|^2 f_{SSS}(m_1^2, m_2^2, m_2^2)$.

An important difference to the MSSM is that contributions with fermion mass insertions, corresponding to $\overline{FF}S$-type contributions in [42], are not present in the MRSSM. Such contributions vanish due to the lack of L-R mixing between squarks. Hence the gluino mass appears in a simpler

way than in the MSSM. Likewise, the sgluon only enters via the *SSS*-type diagram of Figure 4. An *SS*-type diagram vanishes due to the color structure.

The corresponding two-loop contribution to $\phi_u\phi_u$ Higgs boson mass matrix element in zero-momentum approximation is then given by (as pointed out in [36], in SARAH and SPheno the two-loop tadpole contributions are included directly in vacuum minimization condition and not in (8))

$$\left[\Delta m^2_{H_1}\right]_{\phi_u\phi_u} = \left(\frac{\partial^2}{\partial v_u \partial v_u} - \frac{1}{v_u}\frac{\partial}{\partial v_u}\right) V^{(2)}_{\text{eff}}. \tag{8}$$

For large $\tan\beta$, corrections of order $\mathcal{O}(\alpha_b\alpha_s)$ cannot be neglected any more. But since they contribute only to $\phi_d\phi_d$ matrix element, their impact on mass of the lightest Higgs, which stems mainly from $\phi_u\phi_u$ element, is small. Results of (6) were compared with the results of two-loop routines from the SARAH-generated SPheno module.

4.2. Numerical Analysis. We now turn to the numerical analysis of the complete two-loop corrections to the SM-like Higgs boson mass, using the full evaluation within the framework of SARAH and SPheno. Figures 5(a) and 5(b) focus on the gluino and sgluon mass dependence, which arises mainly from the $\mathcal{O}(\alpha_t\alpha_s)$ corrections; they show the two-loop corrections as a function of the gluino mass parameter for two different values of the soft sgluon mass, $m_O = 2$ and 10 TeV for two benchmarks BMP1 and BMP3; other parameters are fixed at benchmark values. For comparison, the two-loop result without the sgluon contribution is shown as well (i.e., without the first diagram of Figure 4). We also plot the MSSM prediction with strong stop mixing and without any sfermion mixing at tree-level.

Figures 5(a) and 5(b) show that the dependence in the MRSSM without sgluon contributions is very similar to the one in the MSSM without stop mixing. The corresponding thin solid red and thin dashed light blue curves in Figure 5 show a characteristic drop for large gluino masses. This is understandable as in the MSSM without sfermion mixing the gluino contribution is precisely the same as in the MRSSM and given by the two corresponding diagrams in Figure 4. The Dirac or Majorana nature of the gluino does not matter since the Dirac partner, the octet superfield $\widehat{O}$, has no direct couplings to quark superfields. A few TeV gluino masses slightly increase the Higgs boson mass, but for larger values of M_O^D the f_{FFS} function becomes negative and drives the correction downwards.

In the full MRSSM calculations, including the sgluon diagrams strongly changes the behavior. Surprisingly, the full MRSSM two-loop contributions resemble the MSSM contributions with large stop mixing. In both cases, large gluino masses strongly enhance the Higgs boson mass, however, for different reasons. In the MSSM the increase can be traced back to the additional $\overline{FF}S$-type diagram which is directly proportional to M_O^D and which vanishes in the limit of no stop mixing. In the MRSSM, on the other hand, the sgluon diagram grows with M_O^D due to both the sgluon-stop-stop coupling, which scales like M_O^D, and an increase in the scalar (but not pseudoscalar) sgluon mass. Due to the sgluon contributions the total two-loop contributions to the Higgs boson mass in the MRSSM are larger than the ones in the MSSM. They are further increased by heavy sgluons.

Figure 5(c) compares the numerical impact of individual contributions by successively switching off contributions. It allows us to read off the contributions from sgluon, gluino, and gluon, of $\mathcal{O}(\alpha_t^2, \alpha_t\alpha_b)$, and the remaining two-loop contributions (particularly λ, Λ contributions). The gluon diagrams alone contribute approximately +4 GeV. The negative gluino and the positive sgluon corrections together amount to an additional upward shift of the Higgs boson mass, which can reach several GeV for large Dirac gluino masses. The remaining contributions are far smaller and amount to around −1 GeV for $\mathcal{O}(\alpha_t^2, \alpha_t\alpha_b)$ contributions and +0.5 GeV for the remaining contributions.

5. Update of Benchmarks

In this section we present an update of the analysis of [17], using the more precise evaluation of the Higgs boson mass. Reference [17] studied the mass predictions of W and lightest Higgs bosons in the MRSSM and showed that agreement with experimental data is possible, in spite of tree-level shifts from violations of custodial symmetry and from mixing with other Higgs states, respectively.

Table 2 shows benchmark parameter points defined in that reference. They exemplify parameter regions in which m_W and m_{H_1} agree with experiment. They are characterized by large $|\Lambda| \approx 1$, rather light Dirac higgsinos and gauginos, and they have $\tan\beta = 3, 10, 40$, respectively.

For all three benchmark points the two-loop correction to m_{H_1} is around +5 GeV. As discussed in the previous sections, the largest part of this is due to $\mathcal{O}(\alpha_t\alpha_s)$ corrections. The MRSSM-specific corrections of $\mathcal{O}(\alpha_\Lambda^2)$ are small since the values of Λ_u, though large, are still not as large as needed to make these corrections dominate; see Figures 1 and 2 for two out of three benchmarks. The magnitude of the total two-loop correction is consistent with the theory error estimate given in [17].

The upward shift of m_{H_1} implies that it is easier to obtain agreement with the measured value; that is, smaller values of $|\Lambda_u|$ are sufficient. In Table 3 we provide new, slightly modified benchmark points, whose definitions differ only in the values of Λ_u. The two-loop Higgs boson mass prediction agrees well with experiment, and the good agreement of m_W with experiment is unchanged. Likewise, both the old and the new set of benchmark points pass checks against HiggsBounds [43–45] and HiggsSignals [46, 47].

In Figure 6 we give an update to some of the subfigures from Figures 4 and 5 of [17]. These show the predictions of m_W and m_{H_1} as contour lines in several two-dimensional parameter spaces. The Higgs boson mass is evaluated at the two-loop level. As discussed before, with the exception of the regions of very large Λ, there is a general positive contribution to the lightest Higgs boson mass between 4 and 5 GeV. Accordingly, the contour lines, in particular the central green region in which the Higgs boson mass agrees

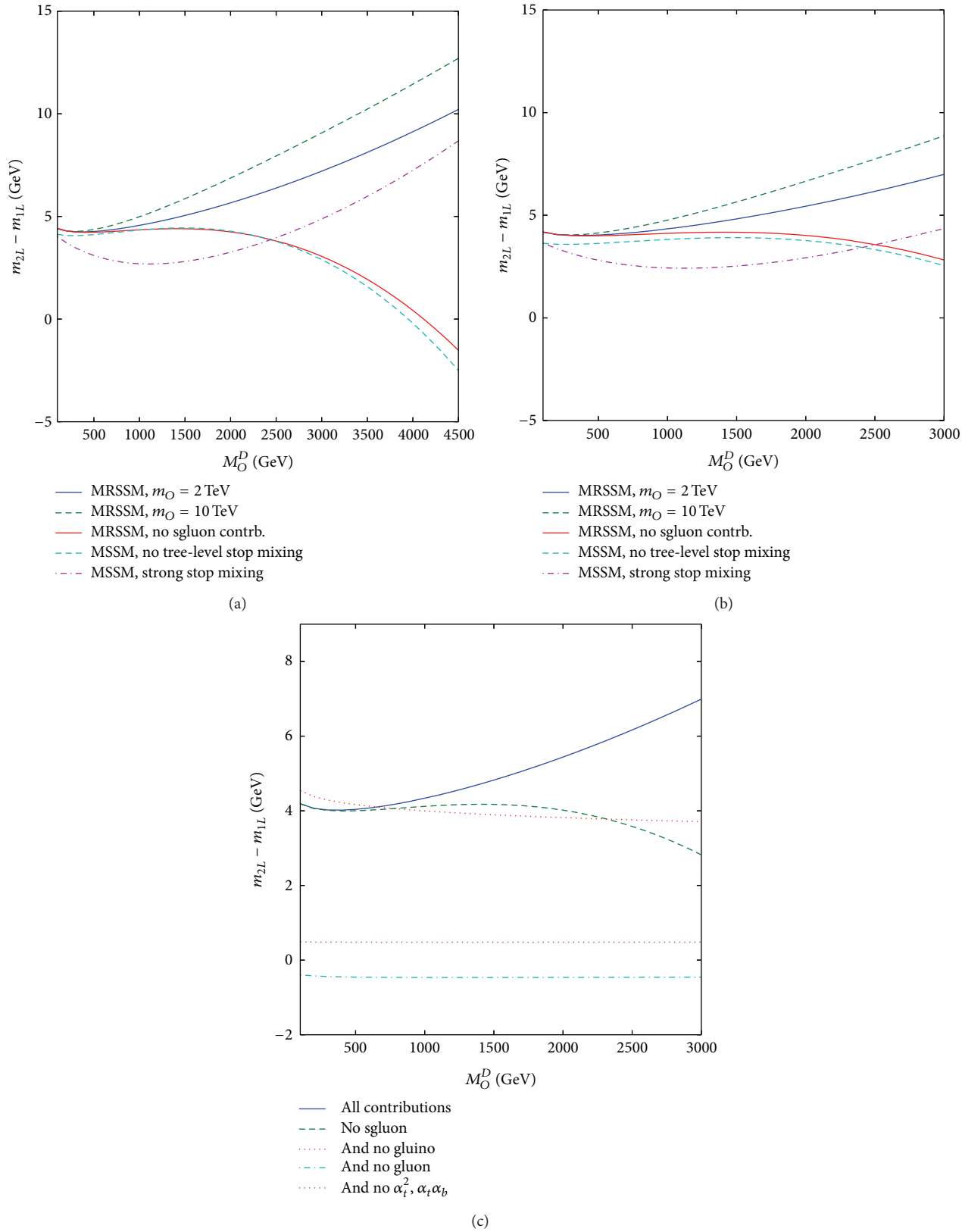

Figure 5: Two-loop contributions to the SM-like Higgs boson mass depending on the gluino mass in the MRSSM for BMP1 (a) and BMP3 (b) and two different values of the soft sgluon mass parameter m_O = 2 TeV (thick solid blue line) and 10 TeV (thick dashed green line) with all contributions, respectively, and without the sgluon contributions (thin solid red line). For comparison also the MSSM contributions for no (thin dashed light blue line) and maximal (purple dotted line) stop mixing are plotted. The chosen MSSM parameters are given in Table 1. For BMP3 and m_O = 2 TeV (c) shows the result, when successively switching off dominating and subdominating contributions.

Table 1: Definition of the fixed parameters for the MSSM points in Figures 5(a), 5(b) and 5(c). All parameters in GeV or GeV^2, where appropriate. The stop mixing parameter X_t is given for both cases of no and large stop mixing.

	$\tan\beta$	M_1	M_2	μ	m_A	$m^2_{q,u,d;(3,3)}$	$m^2_{q,u,d}$	$m^2_{l,e}$	$A_{\tau,b}$	X_t
BMP1	3	600	500	400	700	1000^2	2000^2	1000^2	0	0/2000
BMP3	40	250	500	400	700	1000^2	2000^2	1000^2	0	0/2000

Table 2: Benchmark points of [17]. Dimensionful parameters are given in GeV or GeV^2, as appropriate. The first two parts define input parameters. The third part shows parameters derived from electroweak symmetry breaking after solving the tadpole equations at two loops. The last part gives the theory predictions for the Higgs boson mass at the two-loop level and further quantities relevant to comparison with experiment.

	BMP1	BMP2	BMP3
$\tan\beta$	3	10	40
B_μ	500^2	300^2	200^2
λ_d, λ_u	1.0, −0.8	1.1, −1.1	0.15, −0.15
Λ_d, Λ_u	−1.0, −1.2	−1.0, −1.0	−1.0, −1.15
M_B^D	600	1000	250
$m^2_{R_u}$	2000^2	1000^2	1000^2
μ_d, μ_u		400, 400	
M_W^D		500	
M_O^D		1500	
m^2_T, m^2_S, m^2_O		3000^2, 2000^2, 1000^2	
$m^2_{Q;1,2}, m^2_{Q;3}$		2500^2, 1000^2	
$m^2_{D;1,2}, m^2_{D;3}$		2500^2, 1000^2	
$m^2_{U;1,2}, m^2_{U;3}$		2500^2, 1000^2	
m^2_L, m^2_E		1000^2	
$m^2_{R_d}$		700^2	
v_S	4.96	0.67	−0.30
v_T	−0.34	−0.20	−0.34
$m^2_{H_d}$	673^2	743^2	1160^2
$m^2_{H_u}$	-535^2	-542^2	-541^2
m_{H_1}	130.3 GeV	130.3 GeV	129.8 GeV
m_W	80.400 GeV	80.384 GeV	80.393 GeV
HiggsBounds's obsratio	0.67	0.68	0.67
HiggsSignals' p value	0.03	0.03	0.03

Table 3: Adapted benchmark points; other parameters are as given in Table 2.

	BMP1′	BMP2′	BMP3′
Λ_u	−1.11	−0.85	−1.03
v_S	5.2	1.01	−0.22
v_T	−0.25	−0.02	−0.21
$m^2_{H_d}$	674^2	764^2	1160^2
$m^2_{H_u}$	-502^2	-512^2	-516^2
m_{H_1}	125.3 GeV	125.5 GeV	125.4 GeV
m_W	80.397 GeV	80.381 GeV	80.386 GeV
HiggsBounds's obsratio	0.61	0.65	0.87
HiggsSignals' p value	0.72	0.66	0.72

with experiment, shift to slightly lower values of Λ. Also, the overlap region, where Higgs and W boson masses agree with experiment, is enlarged.

6. Conclusions

In this work we have presented the impact of two-loop corrections on the mass of the lightest Higgs boson in the MRSSM. The calculation has been performed using the framework of SARAH in the approximation of the vanishing electroweak gauge couplings and external momenta of the Higgs self-energies. The code has been cross-checked with an analytic calculation of the most important new corrections. We have separately analyzed the impact of contributions involving λ, Λ-couplings, which already appear in the one-loop corrections, and of the strong corrections involving gluon, Dirac gluino, and sgluon exchange.

In the previous work [17] and the present paper we have found that the lightest Higgs boson mass in the MRSSM differs from the one in the usual MSSM in several respects. At tree-level the additional mixing with additional scalar states reduces the MRSSM Higgs mass below the MSSM value. At the one-loop level, the top/stop contributions cannot be as large as in the MSSM, because stop mixing is forbidden by R-symmetry. However, the new contributions from the superpotential λ, Λ-terms have a similar structure as the top/stop contributions. If λ, Λ-couplings are similar in magnitude to the top Yukawa coupling, the lightest Higgs boson mass can easily be in the ballpark of the experimentally allowed range.

The two-loop corrections governed by these λ, Λ-couplings, however, amount to only 1 GeV or less in parameter regions in which the Higgs boson mass agrees with experiment. The most important two-loop contributions are the strong corrections of $\mathcal{O}(\alpha_t\alpha_s)$. As we have shown the Dirac gluino and gluon contributions alone are very similar to the MSSM strong contributions for vanishing stop mixing. The inclusion of the sgluons changes the picture. The sgluon contributions are positive and rise with the Dirac gluino mass, such that the total $\mathcal{O}(\alpha_t\alpha_s)$ corrections of the MRSSM are larger than the ones of the MSSM, independently of the magnitude of stop mixing.

Overall, the MRSSM two-loop corrections to the lightest Higgs boson mass are typically positive. For example, for the benchmark parameter points proposed in [17], the two-loop corrections to the Higgs boson mass amount to approximately +5 GeV, within the error estimate of that reference. Since perturbation theory shows a converging behavior and since λ, Λ-corrections are subdominant (for $|\lambda|, |\Lambda|$ less than

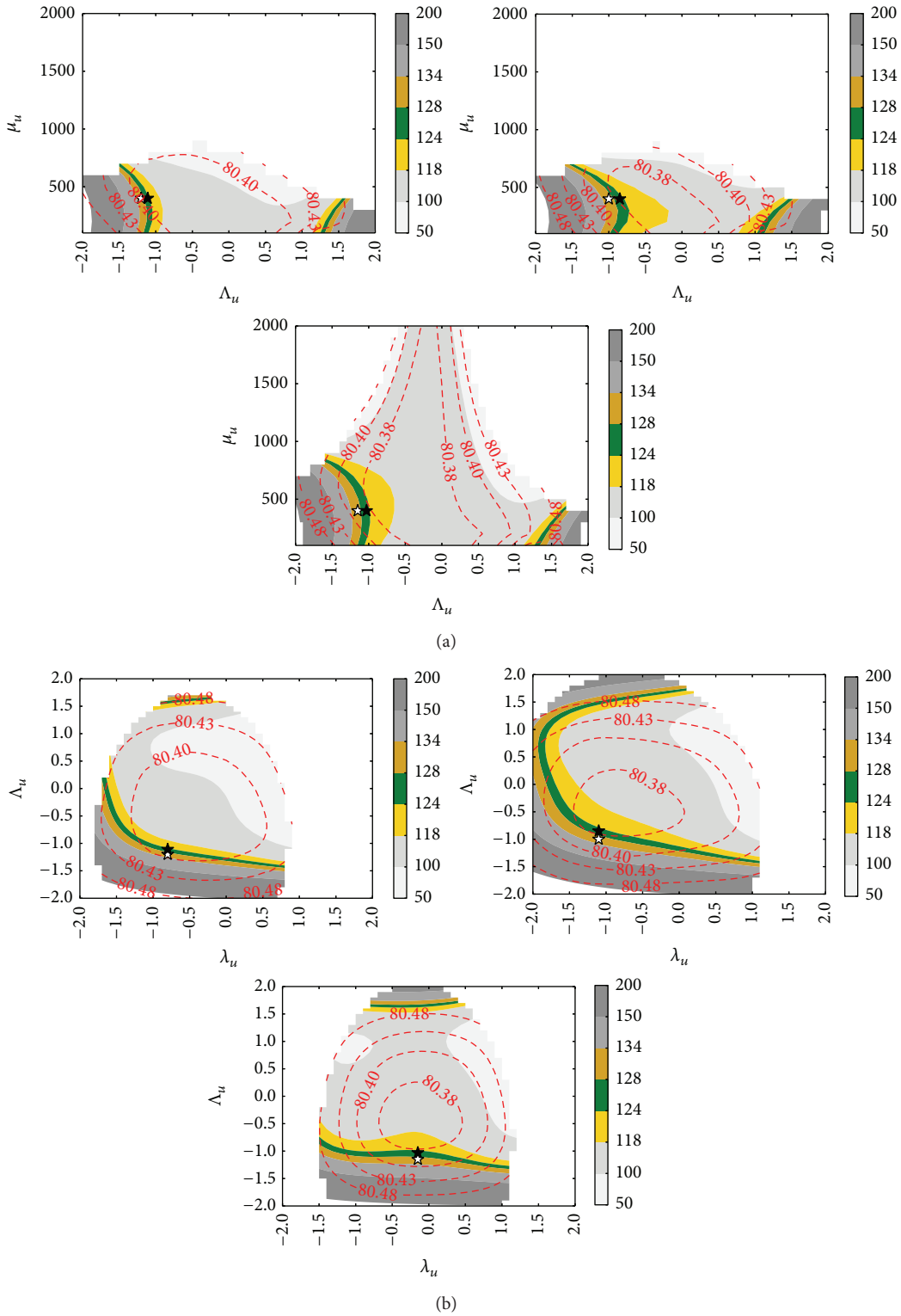

FIGURE 6: Contour plots showing the behavior of m_{H_1} given by the color map and m_W by the red contour lines: (a) for BMP1, (b) for BMP3, for different combinations of model parameters. The white stars mark the original benchmark points from [17], whereas the black ones show the adapted points after taking into account the two-loop corrections.

around 1.2), we estimate the remaining theory uncertainty to be not larger than the one of the MSSM.

The positive two-loop corrections make it easier to achieve agreement between the theory prediction for the lightest Higgs boson mass and the measured value. We have provided an update of the analysis of [17], showing parameter regions of simultaneous agreement of the Higgs and W boson mass predictions with experiment. Compared to [17], the allowed parameter regions are slightly larger and located at smaller values of λ, Λ-couplings.

Conflict of Interests

The authors declare that there is no conflict of interests regarding the publication of this paper.

Acknowledgments

The authors would like to thank Kilian Nickel and Florian Staub for communication about SARAH. This work is supported in part by the Polish National Science Centre Grants under OPUS-2012/05/B/ST2/03306, DEC-2012/05/B/ST2/02597, the European Commission through the Contract PITN-GA-2012-316704 (HIGGSTOOLS), the German DAAD PPP Poland Project 56269947 "Dark Matter at Colliders," and DFG Research Training Group 1504 and the DFG Grant STO 876/4-1.

References

[1] G. Aad, B. Abbott, J. Abdallah et al., "Combined measurement of the Higgs boson mass in pp collisions at $\sqrt{s} = 7$ and 8 TeV with the ATLAS and CMS experiments," *Physical Review Letters*, vol. 114, Article ID 191803, 2015.

[2] R. Harlander, P. Kant, L. Mihaila, and M. Steinhauser, "Higgs boson mass in supersymmetry to three loops," *Physical Review Letters*, vol. 100, no. 19, Article ID 191602, 4 pages, 2008.

[3] P. Kant, R. V. Harlander, L. Mihaila, and M. Steinhauser, "Light MSSM Higgs boson mass to three-loop accuracy," *Journal of High Energy Physics*, vol. 2010, article 104, 2010.

[4] T. Hahn, S. Heinemeyer, W. Hollik, H. Rzehak, and G. Weiglein, "High-precision predictions for the light *CP*-even higgs boson mass of the minimal supersymmetric standard model," *Physical Review Letters*, vol. 112, no. 14, Article ID 141801, 2014.

[5] P. Draper, G. Lee, and C. E. M. Wagner, "Precise estimates of the Higgs mass in heavy supersymmetry," *Physical Review D—Particles, Fields, Gravitation and Cosmology*, vol. 89, no. 5, Article ID 055023, 2014.

[6] G. Degrassi, S. Di Vita, and P. Slavich, "Two-loop QCD corrections to the MSSM Higgs masses beyond the effective-potential approximation," *The European Physical Journal C*, vol. 75, no. 2, article 61, 2015.

[7] S. Borowka, T. Hahn, S. Heinemeyer, G. Heinrich, and W. Hollik, "Momentum-dependent two-loop QCD corrections to the neutral Higgs-boson masses in the MSSM," *European Physical Journal C*, vol. 74, no. 8, article 2994, 2014.

[8] W. Hollik and S. Paßehr, "Two-loop top-Yukawa-coupling corrections to the Higgs boson masses in the complex MSSM," *Physics Letters B*, vol. 733, pp. 144–150, 2014.

[9] W. Hollik and S. Paßehr, "Higgs boson masses and mixings in the complex MSSM with two-loop top-Yukawa-coupling corrections," *Journal of High Energy Physics*, vol. 2014, article 171, 2014.

[10] F. Staub, "Automatic calculation of supersymmetric renormalization group equations and loop corrections," *Computer Physics Communications*, vol. 182, no. 3, pp. 808–833, 2011.

[11] F. Staub, "SARAH 3.2: dirac gauginos, UFO output, and more," *Computer Physics Communications*, vol. 184, no. 7, pp. 1792–1809, 2013.

[12] F. Staub, "SARAH 4: a tool for (not only SUSY) model builders," *Computer Physics Communications*, vol. 185, no. 6, pp. 1773–1790, 2014.

[13] W. Porod, "SPheno, a program for calculating supersymmetric spectra, SUSY particle decays and SUSY particle production at e^+e^- colliders," *Computer Physics Communications*, vol. 153, no. 2, pp. 275–315, 2003.

[14] W. Porod and F. Staub, "SPheno 3.1: extensions including flavour, CP-phases and models beyond the MSSM," *Computer Physics Communications*, vol. 183, no. 11, pp. 2458–2469, 2012.

[15] P. Athron, J.-H. Park, D. Stöckinger, and A. Voigt, "FlexibleSUSY—a spectrum generator generator for supersymmetric models," *Computer Physics Communications*, vol. 190, pp. 139–172, 2015.

[16] B. C. Allanach, "SOFTSUSY: a program for calculating supersymmetric spectra," *Computer Physics Communications*, vol. 143, no. 3, pp. 305–331, 2002.

[17] P. Diessner, J. Kalinowski, W. Kotlarski, and D. Stöckinger, "Higgs boson mass and electroweak observables in the MRSSM," *Journal of High Energy Physics*, vol. 2014, article 124, 2014.

[18] P. Fayet, "Supergauge invariant extension of the Higgs mechanism and a model for the electron and its neutrino," *Nuclear Physics B*, vol. 90, pp. 104–124, 1975.

[19] A. Salam and J. Strathdee, "Supersymmetry and fermion-number conservation," *Nuclear Physics B*, vol. 87, no. 1, pp. 85–92, 1975.

[20] G. D. Kribs, E. Poppitz, and N. Weiner, "Flavor in supersymmetry with an extended R symmetry," *Physical Review D: Particles, Fields, Gravitation and Cosmology*, vol. 78, no. 5, Article ID 055010, 2008.

[21] W. Buchmüller and D. Wyler, "*CP* violation and *R* invariance in supersymmetric models of strong and electroweak interactions," *Physics Letters B*, vol. 121, no. 5, pp. 321–325, 1983.

[22] E. Dudas, M. Goodsell, L. Heurtier, and P. Tziveloglou, "Flavour models with Dirac and fake gluinos," *Nuclear Physics B*, vol. 884, pp. 632–671, 2014.

[23] M. R. Buckley, D. Hooper, and J. Kumar, "Phenomenology of Dirac neutralino dark matter," *Physical Review D*, vol. 88, no. 6, Article ID 063532, 2013.

[24] E. J. Chun, J.-C. Park, and S. Scopel, "Dirac gaugino as leptophilic dark matter," *Journal of Cosmology and Astroparticle Physics*, vol. 2010, no. 2, article 015, 2010.

[25] G. Belanger, K. Benakli, M. Goodsell, C. Moura, and A. Pukhov, "Dark matter with Dirac and Majorana gaugino masses," *Journal of Cosmology and Astroparticle Physics*, vol. 2009, no. 8, article 027, 2009.

[26] P. J. Fox, A. E. Nelson, and N. Weiner, "Dirac gaugino masses and supersoft supersymmetry breaking," *Journal of High Energy Physics*, vol. 2002, no. 8, article 035, 2002.

[27] T. Plehn and T. M. P. Tait, "Seeking sgluons," *Journal of Physics G: Nuclear and Particle Physics*, vol. 36, no. 7, Article ID 075001, 2009.

[28] S. Choi, M. Drees, J. Kalinowski, J. Kim, E. Popenda, and P. M. Zerwas, "Color-octet scalars of N=2 supersymmetry at the LHC," *Physics Letters B*, vol. 672, no. 3, pp. 246–252, 2009.

[29] S. Choi, D. Choudhury, A. Freitas, J. Kalinowski, J. Kim, and P. M. Zerwas, "Dirac neutralinos and electroweak scalar bosons of $N = 1/N = 2$ hybrid supersymmetry at colliders," *Journal of High Energy Physics*, vol. 2010, no. 8, article 025, 2010.

[30] S. Choi, D. Choudhury, A. Freitas, J. Kalinowski, and P. Zerwas, "The extended Higgs system in R-symmetric supersymmetry theories," *Physics Letters B*, vol. 697, no. 3, pp. 215–221, 2011.

[31] K. Benakli, M. D. Goodsell, and F. Staub, "Dirac gauginos and the 125 GeV Higgs," *Journal of High Energy Physics*, vol. 2013, no. 6, article 073, 2013.

[32] G. Aad, T. Abajyan, B. Abbott et al., "Search for pair-produced massive coloured scalars in four-jet final states with the ATLAS detector in proton-proton collisions at $\sqrt{s} = 7$ TeV," *The European Physical Journal C*, vol. 73, no. 1, article 2263, 2013.

[33] ATLAS Collaboration, "Search for anomalous production of events with same-sign dileptons and b jets in 14.3 fb^{-1} of pp collisions at $\sqrt{s} = 8$ TeV with the ATLAS detector," Tech. Rep. ATLAS-CONF 2013-051, 2013.

[34] W. Kotlarski, A. Kalinowski, and J. Kalinowski, "Searching for sgluons in the same-sign leptons final state at the lhc," *Acta Physica Polonica B*, vol. 44, no. 11, pp. 2149–2154, 2013.

[35] E. Bertuzzo, C. Frugiuele, T. Gregoire, and E. Ponton, "Dirac gauginos, R symmetry and the 125 GeV Higgs," *Journal of High Energy Physics*, vol. 2015, no. 4, article 089, 2015.

[36] M. D. Goodsell, K. Nickel, and F. Staub, "Two-loop Higgs mass calculations in supersymmetric models beyond the MSSM with SARAH and SPheno," *European Physical Journal C*, vol. 75, no. 1, article 32, 2015.

[37] W. Hollik and D. Stöckinger, "MSSM Higgs-boson mass predictions and two-loop non-supersymmetric counterterms," *Physics Letters, Section B: Nuclear, Elementary Particle and High-Energy Physics*, vol. 634, no. 1, pp. 63–68, 2006.

[38] H. K. Dreiner, K. Nickel, and F. Staub, "On the two-loop corrections to the Higgs mass in trilinear R-parity violation," *Physics Letters B*, vol. 742, pp. 261–265, 2015.

[39] M. D. Goodsell, K. Nickel, and F. Staub, "Two-loop corrections to the Higgs masses in the NMSSM," *Physical Review D*, vol. 91, no. 3, Article ID 035021, 2015.

[40] S. D. L. Amigo, A. E. Blechman, P. J. Fox, and E. Poppitz, "R-symmetric gauge mediation," *Journal of High Energy Physics*, vol. 2009, no. 1, article 018, 2009.

[41] K. Benakli and M. D. Goodsell, "Dirac gauginos in general gauge mediation," *Nuclear Physics B*, vol. 816, no. 1-2, pp. 185–203, 2009.

[42] S. P. Martin, "Two-loop effective potential for a general renormalizable theory and softly broken supersymmetry," *Physical Review D*, vol. 65, no. 11, Article ID 116003, 2002.

[43] P. Bechtle, O. Brein, S. Heinemeyer, G. Weiglein, and K. E. Williams, "HiggsBounds: confronting arbitrary Higgs sectors with exclusion bounds from LEP and the Tevatron," *Computer Physics Communications*, vol. 181, no. 1, pp. 138–167, 2010.

[44] P. Bechtle, O. Brein, S. Heinemeyer, G. Weiglein, and K. E. Williams, "HiggsBounds 2.0.0: confronting neutral and charged Higgs sector predictions with exclusion bounds from LEP and the Tevatron," *Computer Physics Communications*, vol. 182, no. 12, pp. 2605–2631, 2011.

[45] P. Bechtle, O. Brein, S. Heinemeyer et al., "HiggsBounds-4: improved tests of extended Higgs sectors against exclusion bounds from LEP, the Tevatron and the LHC," *European Physical Journal C*, vol. 74, no. 3, pp. 1–32, 2014.

[46] P. Bechtle, S. Heinemeyer, O. Stål, T. Stefaniak, and G. Weiglein, "HiggsSignals: confronting arbitrary Higgs sectors with measurements at the Tevatron and the LHC," *The European Physical Journal C*, vol. 74, no. 2, article 2711, 2014.

[47] P. Bechtle, S. Heinemeyer, O. Stål, T. Stefaniak, and G. Weiglein, "Probing the standard model with higgs signal rates from the tevatron, the LHC and a future ILC," *Journal of High Energy Physics*, vol. 2014, 39 pages, 2014.

Hindawi Publishing Corporation
Advances in High Energy Physics
Volume 2015, Article ID 982167, 24 pages
http://dx.doi.org/10.1155/2015/982167

Review Article

Searches for Prompt R-Parity-Violating Supersymmetry at the LHC

Andreas Redelbach

Physikalisches Institut, Universität Würzburg, Emil-Hilb-Weg 22, 97074 Würzburg, Germany

Correspondence should be addressed to Andreas Redelbach; andreas.redelbach@physik.uni-wuerzburg.de

Received 27 March 2015; Accepted 30 May 2015

Academic Editor: Mark D. Goodsell

Searches for supersymmetry (SUSY) at the LHC frequently assume the conservation of R-parity in their design, optimization, and interpretation. In the case that R-parity is not conserved, constraints on SUSY particle masses tend to be weakened with respect to R-parity-conserving models. We review the current status of searches for R-parity-violating (RPV) supersymmetry models at the ATLAS and CMS experiments, limited to 8 TeV search results published or submitted for publication as of the end of March 2015. All forms of renormalisable RPV terms leading to prompt signatures have been considered in the set of analyses under review. Discussing results for searches for prompt R-parity-violating SUSY signatures summarizes the main constraints for various RPV models from LHC Run I and also defines the basis for promising signal regions to be optimized for Run II. In addition to identifying highly constrained regions from existing searches, also gaps in the coverage of the parameter space of RPV SUSY are outlined.

1. Introduction

One of the primary objectives of the detectors at the LHC is the search for new particles and phenomena not described by the Standard Model (SM) of particle physics. Weak-scale supersymmetry (SUSY) [1–9] is a well-motivated and well-studied example of a theory beyond the SM (BSM) used to guide many of these searches. One attractive feature of SUSY is that it can solve the SM hierarchy problem [10–15] if the gluino, higgsino, and top squark masses are not much higher than the TeV scale. Closely related to this is the paradigm of naturalness, and see, for example, [16, 17].

In this document, we review constraints on SUSY models in the presence of lepton- or baryon-number violating interactions ($\not{L}$ and $\not{B}$, resp.) at the end of LHC Run I. These interactions are present in generic SUSY models with minimal particle content. They are renormalizable and are described by the following superpotential terms:

$$W_{\not{L}\mathrm{RPV}} = \frac{1}{2}\lambda_{ijk}L_iL_j\overline{E}_k + \lambda'_{ijk}L_iQ_j\overline{D}_k + \varepsilon_iL_iH_2, \quad (1a)$$

$$W_{\not{B}\mathrm{RPV}} = \frac{1}{2}\lambda''_{ijk}\overline{U}_i\overline{D}_j\overline{D}_k. \quad (1b)$$

In this notation, L_i and Q_i indicate the lepton and quark SU(2)-doublet superfields, respectively, while $\overline{E}_i$, $\overline{U}_i$, and $\overline{D}_i$ are the corresponding singlet superfields. The indices i, j, and k refer to quark and lepton generations. The Higgs SU(2)-doublet superfield H_2 contains the Higgs field that couples to up-type quarks. The λ_{ijk}, λ'_{ijk}, and λ''_{ijk} parameters are new Yukawa couplings, referred to as *trilinear* R-parity-violating couplings. The ε_i parameters have dimensions of mass and are present in models with *bilinear* R-parity violation (bRPV). The terms in (1a) and (1b) are forbidden in many models of SUSY by the imposition of R-parity conservation (RPC) [10, 18–21] in order to prevent rapid proton decay. However, proton decay can also be prevented by suppressing only one of $W_{\not{L}\mathrm{RPV}}$ or $W_{\not{B}\mathrm{RPV}}$, in which case some R-parity-violating interactions remain in the theory.

Introducing RPV couplings in the minimal supersymmetric Standard Model (MSSM) can significantly weaken mass and cross section limits from collider experiments and also provide a rich phenomenology; see, for example, the articles [22–24] or [25, 26]. A systematic phenomenological overview of possible signatures for specific RPV scenarios is summarized in [26] going through all possible mass

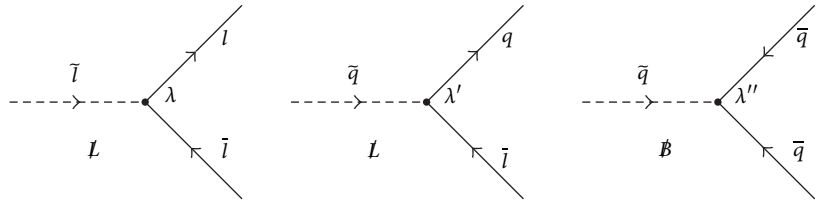

Figure 1: Feynman diagrams associated with the trilinear R-parity-violating superpotential interactions involving λ, λ', or λ''. $(\tilde{q})q$ and $(\tilde{l})l$ denote (s)quarks and (s)leptons, respectively. Arrows on the (s)quark and (s)lepton lines are displayed to indicate the flow of the baryon or lepton number.

orderings and determining the dominant decay signatures. Many papers have investigated signatures beyond the focus of most searches for SUSY at the LHC. Among such challenging scenarios are highly collimated LSP decay products [27, 28], same-sign dilepton signatures [29, 30], taus and b-jets with reduced missing transverse energy [31], resonances of dijets [32, 33], high object multiplicities [34], or, more specifically, a charged lepton plus multiple jets [35].

In this note, we review the current constraints from various ATLAS and CMS searches for SUSY based on approximately 20 fb^{-1} of pp collision data with $\sqrt{s} = 8$ TeV collected in 2012. This review is organized as follows: After a short overview of R-parity-violating parameters and previous constraints of RPV SUSY in Section 2, the main characteristics of analyses searching for RPV SUSY at ATLAS and CMS are presented in Section 3. The next sections focus on the results assuming the dominance of particular R-parity-violating couplings: After the results for bRPV scenarios in Section 4, several limits for simplified models assuming LLE, LQD, or a combination of LQD and LLE relevant for resonance production are discussed in Sections 5, 6, and 7, respectively. In order to constrain models based on UDD couplings, Section 8 summarizes several results both from ATLAS and from CMS searches. Finally, conclusions from R-parity-violating searches at LHC Run I are drawn and some implications for strategies to investigate uncovered parts of the RPV SUSY parameter space for Run II are outlined.

2. R-Parity-Violating Parameters and Constraints

For each particle, R-parity is defined as $P_R = (-1)^{3(B-L)+2s}$ in terms of the corresponding spin, baryon, and leptons numbers. All Standard Model particles and the Higgs bosons have even R-parity, while all supersymmetric particles (sparticles) have odd R-parity. As described, for example, in [36], an extension of the minimal supersymmetric Standard Model (MSSM) with R-parity-violating interactions, does not extend the number of the supersymmetric particles. Direct phenomenological consequences of R-parity-violating interactions are as follows:

(i) The lightest supersymmetric particle (LSP) is not necessarily stable.

(ii) Sparticles can also be produced in odd numbers; in particular single-sparticle production is possible.

Conversely, in R-parity-conserving models, only pair production of SUSY particles is possible in collision processes, with the stable LSP being a possible candidate for dark matter. An excellent review of LHC Run I searches with one focus on RPC SUSY is given by [37]. In this section a short overview of RPV parameters and also of constraints previous to LHC searches is given.

2.1. Parameters for RPV SUSY. The number of R-parity-violating parameters can be obtained from (1a) and (1b): Counting the possible generation indices in the terms ε_i and λ'_{ijk} leads to 3 and 27 parameters, respectively. As explained, for example, in [22], antisymmetries in the summation over gauge indices, suppressed in the notation of (1a) and (1b), lead to $\lambda_{ijk} = -\lambda_{jik}$ and $\lambda''_{ijk} = -\lambda''_{ikj}$. Due to these antisymmetric relations, 9 independent R-parity-violating parameters of type LLE and UDD arise, respectively. The structure of trilinear R-parity-violating couplings leads to Feynman diagrams as illustrated in Figure 1 from [22].

Possible signatures implied in various RPV scenarios are summarized in [26]. Although the majority of R-parity-violating analyses focus on neutralino ($\tilde{\chi}_1^0$) LSPs, alternative types of LSPs have been studied in [48] and within the framework of bRPV models also in [49]. It is also interesting to note that constraints for RPV couplings from theoretical considerations have been discussed, for example, in [22]: In contrast to fixing individual RPV couplings explicitly, the assumption of spontaneous breaking of R-parity can lead to high predictivity for the actual values of these couplings. One possible mechanism is based on right-handed sneutrino fields aquiring vacuum expectation values thus generating RPV couplings; see [22] and references therein. In this context also the $\mu\nu$SSM [50] as a natural extension of (1a) and (1b) is relevant, leading to interesting implications for LHC signatures, as recently discussed in [51]. Constraints for RPV couplings can also be derived from flavor symmetries, investigating, for example, flavor symmetry groups related to the Yukawa couplings and hierarchy of fermion masses. Within the so-called minimal flavor violation model [52], the size of the small R-parity-violating terms is determined by flavor parameters, and in the absence of neutrino masses only the UDD terms remain in the superpotential equation (1a) and (1b). Recently, implications of fundamental symmetries on R-parity-violation have been reviewed in [53], emphasizing, for example, that the simplest supersymmetric theories based on local $B - L$ predict that R-parity must be a broken symmetry.

2.2. Pre-LHC Constraints. A very large number of bounds for the trilinear R-parity-violating couplings have been deduced from studies of low and intermediate energy processes. In particular, rare decays, involving flavor violation, constitute constraints on RPV couplings. Processes that violate lepton number or baryon number also provide strong limits on R-parity-violating couplings. Presenting these indirect bounds is beyond the scope of this review, referring the reader to corresponding reviews; see for example [22, 54]. Many indirect bounds on the trilinear couplings assume *single coupling dominance*, where a single R-parity-violating coupling dominates over all the others.

However, it is important to note in general these bounds on R-parity-violating couplings are relaxed for increased masses of SUSY particles involved; see, for example, [55]. In this context it is illustrative to look at the strong constraint derived from nonobservation of proton decay; see [56]:

$$\lambda'_{11k} \cdot \lambda''_{11k} \lesssim 10^{-23} \left(\frac{m_{\tilde{q}}}{100\,\text{GeV}} \right)^2, \tag{2}$$

where $m_{\tilde{q}}$ is the typical squark mass. As already noted before, it is sufficient to eliminate only one of $W_{\not L\text{RPV}}$ or $W_{\not B\text{RPV}}$ from (1a) and (1b) to forbid proton decay. The form of the above constraint also shows the anticorrelation between the mass scale of intermediate SUSY particles and the size of their RPV couplings. It is interesting to note that a possible solution to circumvent proton decay has also been established in the minimal flavor violation model [52].

Various results of analyses searching for nonvanishing R-parity-violating couplings have been obtained in pre-LHC collider experiments. Constraints from existing searches for RPV SUSY can be classified, for example, by the category of contributing RPV couplings:

(i) LEP results [57–62] have investigated various *trilinear RPV* couplings, typically leading to mass limits at the scale of 100 GeV.

(ii) HERA searches have mainly focused on signatures from λ'_{ijk} couplings assuming the dominance of a single coupling [63–66]. A very distinctive signature from a narrow-width resonance in sparticle production with subsequent decay can be possible for a nonzero LQD coupling or a combination of LQD and LLE couplings. Therefore couplings of λ'_{ijk}-type at HERA would allow resonant single squark production, corresponding to high sensitivities in different search channels. Expressing the limits in terms of the sparticle masses, squark masses above 200 GeV have been excluded.

(iii) Several searches at the Tevatron [67] have constrained various *trilinear couplings* and/or sparticle masses even stronger. The signatures studied at the Tevatron include searches for multileptons [68, 69] (via LLE) or multijets [70] and pairs of dijets [71] (via UDD, resp.). Also resonant sparticle production [72–74] with subsequent decay (via a combination of LQD and LLE couplings) has been considered.

Since several of these signatures investigated at the Tevatron have set the strongest collider-based RPV limits before the LHC, we shortly mention some of these limits as benchmarks in comparison to LHC constraints to be discussed later. Using the multijet final state, the CDF collaboration has excluded gluino masses up to approximately 150 GeV for light-flavor models [70]. Based on the search for pairs of dijets, as predicted from decays in stop-quark pair production, stop masses up to 100 GeV have been excluded [71]. The CDF experiment has also set a limit on the expected cross section at approximately 100 fb from multilepton search results [69]. In a benchmark scenario of resonant sneutrino production and subsequent lepton-flavor violating (LFV) decay into different charged lepton flavors, τ-sneutrino masses around 500 GeV have been excluded [73].

Prior to LHC searches, no direct exclusion limits from LEP, HERA, or Tevatron have been obtained for bRPV models. However, several studies have investigated bRPV phenomenology at the Tevatron [67, 75–77], elaborating, for example, signatures of multileptons or displaced vertices.

Significantly reducing the size of R-parity-violating couplings generically leads to late LSP decays. Since the corresponding part of the RPV parameter space for small R-parity-violating couplings does not predict prompt signatures at the LHC, no further details used in the searches for late decays are discussed here. It should however be mentioned that a number of analyses at ATLAS [78–82] and CMS [83–87] have probed signatures related to long-lived sparticles and displaced vertices expected in such cases deriving also strong limits on SUSY masses. A phenomenological overview of these searches for long-lived sparticles has recently been presented, for example, in [88].

3. Overview of Analyses Searching for RPV SUSY

Both ATLAS [89] and CMS [90] are multipurpose detectors designed for the study of pp and heavy-ion collisions at the LHC. They provide nearly full-solid angle coverage around the interaction point. Each detector uses a right-handed coordinate system with its origin at the nominal interaction point in the centre of the corresponding detector and the z-axis along the beam pipe. Cylindrical coordinates (r, ϕ) are used in the transverse plane, ϕ being the azimuthal angle around the beam pipe. The pseudorapidity is defined in terms of the polar angle θ as $\eta = -\ln\tan(\theta/2)$.

3.1. Strategies for Simulating and Selecting Events. The 8 TeV pp data set, after the application of beam, detector, and data quality requirements, has an integrated luminosity of approximately 20 fb^{-1} both for ATLAS and for CMS detectors. It is interesting to note that the average number of pp interactions occurring in the same bunch crossing at 8 TeV varies between approximately 10 and 30, necessitating systematic studies of related pile-up effects. The trigger system of ATLAS and CMS consists a hardware-based systems, with subsequent software-based systems. Using so-called high level triggers,

the events of interest are finally recorded. For each analysis, a combination of different triggers is used, before the offline selection of events is done. The main requirements of the latter are summarized for each analysis in Sections 3.3 and 3.4. In order to ensure the quality of reconstruction, various requirements on transverse momenta p_T and criteria for the isolation to other objects have been developed at the LHC detectors, with more details presented in [89, 90]. After reconstruction of final states, the most relevant physical objects for prompt RPV SUSY analyses can shortly be classified as follows.

Electrons, muons, and hadronically decaying τ-leptons are collectively referred to as charged leptons. Depending on the specific analysis, it is possible to discriminate hadronic jets according to their flavor contents: In particular, b-tagged jets can often be distinguished from jets consisting of only light quark-flavors. The missing transverse energy per event E_T^{miss} is computed using the transverse momenta of identified objects.

SUSY R-parity-violating signal samples are generated using different event generators, for example, HERWIG++ [91] or PYTHIA [92, 93]. The events are subsequently simulated within the framework of fast or full simulation, where, for the details of the specific setup of event generation or simulation, the corresponding analysis papers should be considered.

Unless otherwise stated, signal cross sections are calculated to next-to-leading order in the strong coupling constant, adding the resummation of soft gluon emission at next-to-leading-logarithmic accuracy (NLO+NLL) [94–98]. The nominal cross section and the uncertainty are taken from an envelope of cross section predictions using different PDF sets and factorisation and renormalisation scales, as described in [99].

Each analysis is based on a number of *signal regions* (SRs), each designed to maximize the sensitivity to different final state topologies in terms of the chosen discriminating variables. Additionally, a number of control regions are constructed to constrain the dominant backgrounds. These control regions are designed to have a high purity and a small statistical uncertainty in terms of the background process of interest and also to contain only a small fraction of the potential SUSY signal. Practically, control regions are often introduced to estimate the rate of SM processes, using data-driven methods or also normalization of Monte Carlo simulations.

3.2. Strategies for Presentation of Results. The large number of free mass parameters for sparticles in the MSSM is already severely constrained by many experimental bounds; see, for example, the discussion in [36]. As a consequence, several approaches to study SUSY particle spectra have been developed.

Within the phenomenological MSSM *pMSSM* [100], the high number of free SUSY parameters is reduced with realistic requirements on the flavor and CP structure, without imposing any SUSY-breaking scheme. In this framework also SUSY spectra consistent with various experimental constraints, as, for example, the LHC results for the Higgs mass, can be addressed [101, 102].

The approach of *simplified models* [103, 104] is commonly used in searches for SUSY at the LHC. In this case the decay cascades are modeled simply by setting the masses of most SUSY particles to multi-TeV values, effectively decoupling them for the reach at the LHC. This also implies selection of specific production channels, while other mixed production modes, for example, scalar plus fermionic SUSY particle, are typically neglected. The decay cascades of the remaining particles to the LSP, typically with zero or one intermediate step, are characterized only by the masses of the participating particles, allowing studies of the search sensitivity to the SUSY masses and decay kinematics.

In an alternative approach, *complete SUSY models,* for example, mSUGRA/CMSSM [105–110] or minimal GMSB [111–116], are simulated. These models typically impose boundary conditions at a high energy scale and determine the SUSY masses near the TeV scale by evaluating renormalization group equations. Due to the minimal number of input parameters at the high energy scale, it is realistic to scan the parameter space effectively.

One common strategy for obtaining results is to compute the level of agreement between the background prediction and data using the p value for the number of observed events to be consistent with the background-only hypothesis. To do so, the number of events in each signal region is described using a Poisson probability density function. The statistical and systematic uncertainties on the expected background values are modelled with nuisance parameters constrained by a Gaussian function with a width corresponding to the size of the uncertainty considered.

Since no significant excess of events over the SM expectations is observed in any signal region of the R-parity analyses, upper limits at 95% CL on the number of BSM events for each signal region can be derived in a *model-independent* way. Here the CL_s prescription [117] is used. Normalising these events by the integrated luminosity of the data sample, they can be interpreted as upper limits on the visible BSM cross section (σ_{vis}), where σ_{vis} is defined as the product of acceptance, reconstruction efficiency, and production cross section. If a limit on non-SM events ($N_{\text{non-SM}}$) has been obtained in a BSM analysis, the visible signal cross section can also be determined as $\sigma_{\text{vis}} = N_{\text{non-SM}}/L$.

Model-dependent limits will be discussed in detail in Sections 4 to 8. For many models, the limits are calculated from asymptotic formulae [118] with a simultaneous fit to all signal regions based on the profile likelihood method. Alternatively, the limit can also be obtained from pseudo experiments; further details can be found in each paper.

The systematic uncertainties on the signal expectations originating from detector effects and the theoretical uncertainties on the signal acceptance are included. The impact of the theoretical uncertainties on the signal cross section is shown on the limit plots obtained. The $\pm 1\sigma_{\text{theory}}^{\text{SUSY}}$ lines around the observed limits are obtained by changing the SUSY cross section by one standard deviation ($\pm 1\sigma$). All mass

limits on supersymmetric particles quoted later are derived from the $-1\sigma^{\text{SUSY}}_{\text{theory}}$ theory line. The band around the expected limit shows the $\pm 1\sigma$ uncertainty, including all statistical and systematic uncertainties except the theoretical uncertainties on the SUSY cross section. If several SRs contribute to exclusion limits in a model investigated, the general strategy is to obtain limits by performing a statistical combination of the most sensitive signal regions.

3.3. Details for RPV Searches at ATLAS. In this section the main requirements for signal selections developed in ATLAS searches for R-parity-violating SUSY are summarized, also introducing relevant kinematic variables. Some of these analyses have been optimized also for RPC scenarios; however the focus of this review is on RPV-related signal regions. Each of these analyses has investigated RPV-related constraints in at least two different RPV models or several SRs have been developed particularly for RPV signatures. (When finalizing this review, a recent ATLAS analysis [119] has also considered stop *LQD*-type decays to light charged lepton plus b-quark, constraining stop masses up to 1 TeV.)

(i) Multilepton Analysis (ATLAS). In this case at least four charged leptons in every signal event are required, at least two of which must be electrons or muons, in the following referred to as "light leptons." The events are separated into signal regions based on the number of light leptons observed [40], and the absence of a Z boson candidate among the pairs of light leptons facilitates suppression of backgrounds in R-parity-violating searches. The SM background is further reduced using the missing transverse momentum E_T^{miss} and the effective mass m_{eff}, defined in this case as the scalar sum of the E_T^{miss}, the p_T of all selected charged leptons, and the p_T of reconstructed jets. In most signal regions, events with a pair of light leptons forming a Z boson candidate are vetoed, and possible $Z \to \ell^+\ell^-\gamma$ and $Z \to \ell^+\ell^-\ell^+\ell^-$ candidates are also rejected. Three signal regions are based on threshold requirements only for E_T^{miss}, thus being useful in particular for RPC searches for low sparticle masses. Additionally, in the SRs used for RPV results, either high E_T^{miss} *or* high m_{eff} is required: thus, a selected event may have one quantity below the threshold, but never both. As the SRs used have disjoint selection criteria, they are statistically combined when setting constraints on the specific SUSY models considered in [40].

(ii) Same-Sign/Three-Lepton Analysis (ATLAS). The search [38] requires two light leptons with same charge or three light leptons in conjunction with requirements on the number of jets. It designed in particular for SUSY models where pair-produced Majorana particles (e.g., gluinos) can decay semileptonically with a large branching ratio. The effective mass, m_{eff}, is a key discriminating variable, defined by this analysis as the sum of E_T^{miss} and the p_T values of the signal leptons and all signal jets. If the event contains a third light lepton the event is regarded as three-lepton event, otherwise it is a two-lepton event. Five nonoverlapping signal regions have been defined in total. The signal regions SR3b and SR1b use leptons, large m_{eff}, and also the presence of b-jets to suppress the SM background. There is no explicit E_T^{miss} requirement in SR3b, implying that this SR does not depend on the assumption of a stable LSP escaping the detector unseen. SR1b additionally uses the transverse mass, m_T, to reject background events with W bosons, defined as

$$m_T = \sqrt{2p_T^l E_T^{\text{miss}} \left(1 - \cos\left[\Delta\phi\left(\mathbf{l}, \mathbf{p}_T^{\text{miss}}\right)\right]\right)}, \tag{3}$$

where p_T^l is the larger of the p_T values of the two charged leptons and $\mathbf{p}_T^{\text{miss}}$ is the missing transverse momentum vector.

(iii) Tau Plus Jets Analysis (ATLAS). Requiring at least one tau lepton in events with jets and large E_T^{miss} the search [39] can also be sensitive to RPV models with relatively high multiplicities of taus. The search channels are separated by the numbers of taus and light charged leptons involved, leading to $e\tau$, $\mu\tau$, and $\tau\tau$ channels, respectively. The following kinematical variables are introduced to suppress background processes: the transverse mass formed by E_T^{miss} and the p_T of the tau lepton in the $e\tau$ and $\mu\tau$ channels,

$$m_T^\tau = \sqrt{2p_T^\tau E_T^{\text{miss}} \left(1 - \cos\left(\Delta\phi\left(\boldsymbol{\tau}, \mathbf{p}_T^{\text{miss}}\right)\right)\right)}. \tag{4}$$

Similarly the transverse mass m_T^l formed by E_T^{miss} and the p_T of the light lepton (e or μ) is used. Two variants of H_T-related variables have been defined as the scalar sum of the transverse momenta of the tau, light lepton, and signal jets: H_T includes all signal jet ($p_T > 30$ GeV) candidates, whereas H_T^{2j} only considers two jets with the largest transverse momenta in the event. In this analysis the effective mass uses H_T^{2j}, that is, $m_{\text{eff}} = H_T^{2j} + E_T^{\text{miss}}$. Moreover a requirement on the minimal azimuthal angle $\Delta\phi$ ($\text{jet}_{1,2}$, p_T^{miss}) between p_T^{miss} and either of the two leading jets is used to remove multijet events. As a result, also upper limits on the visible cross section have been obtained for the bRPV-related SRs of type $e\tau$, $\mu\tau$, and $\tau\tau$, respectively.

(iv) Multijet Analysis (ATLAS). Two complementary search strategies have been developed in this analysis [44]: The *jet-counting analysis* is searching for an excess in events with ≥6 jets or ≥7 jets, using the predictable scaling of the number of n-jet events ($n = 6, 7$) as a function of the transverse momentum (p_T) requirement placed on the nth leading jet in p_T for background processes. It is interesting to note that this scaling relation differs significantly between the signal and the background. That analysis technique provides the opportunity to enhance sensitivity to specific heavy-flavor compositions in the final state and to explore various assumptions on the branching ratios of the benchmark signal processes studied. The number of jets, the p_T requirement used in the selection of jets, and the number of b-tagged jets are optimized separately for each signal model.

The second approach in [44] consists of a data-driven template-based analysis using a topological observable called the *total-jet-mass* of large-radius (R) jets. This analysis method is based on templates of the event-level observable

Table 1: Overview of ATLAS analyses designed to probe prompt RPV models. The signature descriptions are indicative only, and further details can be found in the analysis documentation in each case.

Short name	Signature	Variables	Ref.
$4L_A$	$4(e,\mu,\tau)+E_T^{\text{miss}}$	$m_{\text{eff}}, E_T^{\text{miss}}, Z_{\text{veto}}$	[40]
SS/$3L_A$	$\ell^{\pm}\ell^{\pm}$ or 3ℓ	$N_{\text{jets}}, N_{b\text{-jets}}, E_T^{\text{miss}}, m_{\text{eff}}$	[38]
τ_A	$\tau + E_T^{\text{miss}} \geq 4j$	$m_T^{\tau}, m_T^{l}, H_T, H_T^{2j}, E_T^{\text{miss}}, m_{\text{eff}}, p_T^{\text{miss}}$	[39]
Multi-j_A	$\geq 6j$	jet p_T, M_J^{Σ}, $N_{b\text{-jets}}$, $\lvert\Delta\eta\rvert$	[44]
$l_i l_j$ reson$_A$	$e\mu$, $e\tau$, $\mu\tau$ resonance	$\lvert\Delta\phi_{ij}\rvert, m_{ij}$ $(i \neq j)$	[43]

Table 2: Schematic overview of RPV model parameters investigated by ATLAS analyses. The signature descriptions are also indicated in Table 1 with corresponding references.

RPV type	RPV couplings	Production	LSP	Analysis
LLE	$\lambda_{12k}, \lambda_{k33}$ $(k=1,2)$	$\widetilde{\chi}_1^{\pm}$, slepton, sneutrino, gluino	$\widetilde{\chi}_1^0$	$4L_A$
UDD	λ''_{323}	Gluino	$\widetilde{t}_1$	SS/$3L_A$
*b*RPV	ε_i $(i=1,2,3)$	Strong/electroweak (mSUGRA)	$\widetilde{\chi}_1^0$	SS/$3L_A$, τ_A
UDD	λ''_{ijk}	Gluino	$\widetilde{\chi}_1^0$	Multi-j_A
LQD + *LLE*	λ'_{311} and λ_{i3j} $(i \neq j)$	τ-sneutrino	$\widetilde{\nu}_{\tau}$	$l_i l_j$ reson$_A$

formed by the scalar sum of the four leading large R jet masses in the event, which is significantly larger for the signal than for the SM backgrounds. The total-jet-mass analysis uses a topological observable M_J^{Σ} as the primary distinguishing characteristic between signal and background. The observable M_J^{Σ} [120–122] is defined as the scalar sum of the masses of the four leading large-radius jets reconstructed with a radius parameter $R = 1.0$, $p_T > 100$ GeV and $|\eta| < \eta_{\text{cut}}$, and

$$M_J^{\Sigma} = \sum_{\substack{p_T > 100\,\text{GeV} \\ |\eta| \leq \eta_{\text{cut}}}}^{4} m_{\text{jet}}. \tag{5}$$

As explained, for example, in [44], four-jet (or more) events are used, because four large-R jets cover a significant portion of the central region of the calorimeter and are very likely to capture most signal quarks within their area. As a second discriminating variable for the design of SRs and CRs the pseudorapidity difference $|\Delta\eta|$ between the two leading large-R jets is used. This is motivated by different angular distributions among jets expected from signal events as compared to backgroud processes. For the definition of SRs also the p_T thresholds of the third and fourth jet have been included. Using the results from simulation studies, it has been demonstrated that M_J^{Σ} typically has higher sensitivity than the kinematic variable H_T. The latter is essentially a measure of the transverse energy (or transverse momenta) in the event, whereas the M_J^{Σ} mass intrinsically also contains angular information to be used in high-multiplicity jet events. This analysis technique focuses primarily on the ten-quark models as further discussed in Section 8.1. The total-jet-mass analysis is designed to be independent of the flavor composition of the signal process and as a data-driven method it essentially removes any reliance on MC simulations of these hadronic final states. No explicit veto is applied to events with leptons or E_T^{miss}.

Also model-independent upper limits on non-SM contributions have been derived separately for each analysis in [44].

(v) LFV Resonance Analysis (ATLAS). The reconstruction of a narrow-width resonance from its decay products essentially relies on the invariant mass determined from the corresponding momenta. In this case the decay products are given by charged leptons of different flavor [43]. Therefore the selection for signal events requires exactly two leptons ($l_i^+ l_j^-$ with $i \neq j$), of opposite charge and of different flavor. Good discrimination against background is obtained requiring that the two leptons are back-to-back in the azimuthal plane with $|\Delta\phi_{\ell\ell'}| > 2.7$, where $\Delta\phi_{\ell\ell'}$ is the ϕ difference between the two leptons. In events containing a hadronically decaying τ, it is additionally required that the transverse energy E_T of the τ candidate is less than the corresponding E_T of the light signal lepton due to the energy carried by the τ-neutrino.

In order to reconstruct the four-momenta of hadronically decaying τ-leptons, also the momenta of the emerging τ-neutrino have to be taken into account. A collinear neutrino approximation is used to determine the dilepton invariant mass (m_{ij}) in the $e\tau_{\text{had}}$ and $\mu\tau_{\text{had}}$ channels. This approximation is well justified since the hadronic decay of a high-energetic τ lepton from a heavy resonance, the neutrino, and the resultant jet are nearly collinear. The four-vector of the neutrino is reconstructed from the $\vec{p}_T^{\,\text{miss}}$ and η of the τ_{had} jet. Four-vectors of the electron or muon, τ_{had} candidate, and neutrino are then used to calculate the *dilepton invariant mass* m_{ij}. The minimal requirement on m_{ij} for signal events is $m_{ij} > 200$ GeV. Finally, the expected and observed upper limits are obtained as a function of $\widetilde{\nu}_{\tau}$ mass.

For further reference, the ATLAS analyses considered are summarized in Table 1 indicating the signatures and main variables for signal selections. An overview relating ATLAS analysis and corresponding RPV model investigated, is presented in Table 2.

3.4. Details for RPV Searches at CMS. An overview of CMS analysis strategies used in the search for prompt RPV is given below.

(i) Multilepton Plus b-Jets Analysis (CMS). In this analysis, events with three or more charged leptons are selected, requiring two light leptons, which may be electrons or muons [41]. Accepting only opposite-sign, same-flavor pairs of electrons or muons with an invariant mass $m_{\ell\ell} > 12\,\text{GeV}$ reduces backgrounds, for example, from Drell-Yan processes and low-mass resonances. Signal regions are defined with different requirements on the total number of light leptons and the number of hadronically decaying τ candidates in the event. Since no Z bosons are expected in the signal models under investigation, events in which any selected dilepton pair has an invariant mass consistent with that of the Z boson are rejected thus providing good suppression of Z-related backgrounds. Moreover, at least one b-tagged jet is required in the signal regions. Additional discrimination against background events is obtained with cuts on the S_T distribution. As was discussed in [41], that distribution has high sensitivity to the mass of the parent particle, produced in pair production.

Several kinematic regions relevant to results are introduced in [41], relating to different assumptions on stop masses in comparison to neutralino LSP masses. Relatively light stops (with respect to masses of $\widetilde{\chi}_1^0$) would correspond to region A, while the case of heaviest stop masses (in comparison to $m(\widetilde{\chi}_1^0)$) is included in region E. It is interesting to note that, for example, in region B stop four-body decays $\widetilde{t}_1 \to t\mu t\bar{b}$ or $t\nu b\bar{b}$ are possible.

(ii) SS-Leptons Analysis (CMS). The analysis [46] targets at topologies with same-sign leptons and additional jets from strong production processes. Events with at least two isolated same-sign leptons (ee, $e\mu$, or $\mu\mu$) and at least two jets are selected. The lepton pairs are required to have an invariant mass above 8 GeV and also events with a third lepton are rejected if the lepton forms an opposite-sign same-flavor pair with one of the first two leptons for which the invariant mass of the pair ($m_{\ell\ell}$) satisfies $m_{\ell\ell} < 12\,\text{GeV}$ or $76 < m_{\ell\ell} < 106\,\text{GeV}$. Signal regions are defined with different requirements on E_T^{miss}, H_T, the number of jets, and the number of b-tagged jets.

For each model considered, limits are obtained by performing a statistical combination of the most sensitive signal regions. The search region dedicated to RPV results is based on the selection of $n_{\text{jets}} \geq 2$, $n_{b\text{-jets}} \geq 2$, and $H_T > 500\,\text{GeV}$ without explicit requirement on E_T^{miss} [46].

(iii) τ Plus b-Jets Analysis (CMS). Different assumptions for the decays of stops have motivated the search for signatures of τ-leptons and b-jets [42]. Selected events are required to contain a light lepton and a hadronically decaying τ_h of opposite electric charge thus leading to the signal channels $e\tau_h$ and $\mu\tau_h$. Events are vetoed if another light lepton is found, passing the kinematic, identification, and isolation criteria, which has an opposite electric charge from the selected light lepton. The b-tagged jet with the highest p_T is selected, and then the remaining four jets with the highest p_T are selected whether or not they are b-tagged. The S_T distribution is finally used to extract the limits, where S_T is defined as the scalar sum of the p_T of the light lepton, the τ_h, and the five jets.

(iv) $\geq 4j$ from Jet Pairs Analysis (CMS). This analysis [47] has been designed to search for pairs of jets where each jet decays to two jets, respectively. The strategy followed in this analysis first requires that signal events contain at least four jets. The leading four jets, ordered in p_T, are used to create three unique combinations of dijet pairs per event. A distance variable is implemented to select the jet pairing that best corresponds to the two resonance decays, $\Delta R = \sqrt{(\Delta\eta)^2 + (\Delta\phi)^2}$, where $\Delta\eta$ and $\Delta\phi$ are the differences in η and ϕ between the two jets, respectively. This variable exploits the smaller relative distance between daughter jets from the same parent decays compared to that between uncorrelated jets. For each dijet pair configuration the value of ΔR_{dijet} is calculated:

$$\Delta R_{\text{dijet}} = \sum_{i=1,2} \left|\Delta R^i - 1\right|, \tag{6}$$

where ΔR^i represents the separation between two jets in dijet pair i and an offset of 1 is used to maximize the signal efficiency. The configuration that minimizes the value ΔR_{dijet} is selected, with ΔR_{min} representing the minimum ΔR_{dijet} for the event.

Once a dijet pair configuration is chosen, two additional quantities are used to suppress the backgrounds from SM multijet events and incorrect signal pairings: The pseudorapidity difference between the two dijet systems $\Delta\eta_{\text{dijet}}$, and the absolute value of the fractional mass difference $\Delta m/m_{\text{av}}$, where Δm is the difference between the two dijet masses and m_{av} is their average value. As discussed in [47] the $\Delta m/m_{\text{av}}$ quantity is small with a peak at zero in signal events where the correct pairing is chosen, while for SM multijet background or incorrectly paired signal events, this distribution is much broader. An additional kinematic variable Δ is calculated for each dijet pair:

$$\Delta = \left(\sum_i^{1,2} \left|p_T^i\right|\right) - m_{\text{av}}, \tag{7}$$

where p_T sum is over the two jets in the dijet configuration. This type of variables has been used extensively in hadronic resonance searches at the Tevatron and the LHC; see, for example, [123] and references therein. Requiring a minimum value of Δ results in a lowering of the peak position value of the m_{av} distribution from background SM multijet events. With this selection the fit to the background can be extended to lower values of m_{av}, making a wider range of supersymmetric particle masses accessible to the search [47].

(v) Multijet Analysis (CMS). This search targets jets final states with high multiplicities from pair-produced three-jet resonances [45]. Signal events have to contain at least six jets with additional requirements on p_T thresholds. The *jet-ensemble technique* [70] is used to combine the six

Table 3: Overview of CMS analyses constraining prompt RPV models. The signature descriptions are indicative only, and the reader is referred to the analysis documentation for further details in each case.

Short name	Signature	Variables	Ref.
$3L/b_C$	$\geq 3\ell + b$-jets	$S_T, m_{\ell\ell}$	[41]
SS_C	$\ell^{\pm}\ell^{\pm}$	$N_{\text{jets}}, N_{b\text{-jets}}, H_T$	[46]
τb_C	$\tau + b$-jets	$N_e = 1$ or $N_\mu = 1, S_T$	[42]
Pair-j_C	$\geq 4j$ from jet pairs	$\Delta m, \Delta\eta_{\text{dijet}}, \Delta$, 4th jet p_T	[47]
Multi-j_C	$\geq 6j$	Δ, 4th jet p_T, 6th jet p_T, S_T	[45]

Table 4: Overview of RPV model parameters investigated by CMS analyses. The signature descriptions are also indicated in Table 3 with corresponding references.

RPV type	RPV couplings	Production	LSP	Analysis
LLE/LQD	$\lambda_{122}, \lambda_{233}, \lambda'_{233}$	Stop	$\widetilde{\chi}_1^0$	$3L/b_C$
UDD	λ''_{323}	Gluino	$\widetilde{t}_1$	SS_C
LQD	λ'_{3jk} $(j,k=1,2), \lambda'_{333}$	Stop	$\widetilde{\chi}_1^0, \widetilde{t}_1$	τb_C
UDD	$\lambda''_{312}, \lambda''_{323}$	Stop	$\widetilde{t}_1$	Pair-j_C
UDD	$\lambda''_{112}, \lambda''_{113}, \lambda''_{223}$	Gluino	$\widetilde{\chi}_1^0$	Multi-j_C

highest-jets p_T in each event into all possible unique triplets. To maximize sensitivity to the presence of a three-jet resonance, an additional requirement is placed on each jet triplet to suppress SM backgrounds and remove incorrectly combined signal triplets. This selection criterion is based on the constant invariant mass of correctly reconstructed signal triplets and also on the observed linear correlation between the invariant mass and scalar sum of jet p_T for background triplets and incorrectly combined signal triplets:

$$M_{jjj} < \left(\sum_{i=1}^{3} p_T^i\right) - \Delta, \tag{8}$$

where M_{jjj} is the triplet invariant mass, p_T sum is over the three jets in the triplet (triplet scalar p_T), and Δ is an empirically determined parameter. The peak position of the M_{jjj} distribution in data depends on the value of Δ, where $\Delta = 110$ GeV is found to be the optimal choice, yielding the lowest value of the peak of M_{jjj}.

The use of b-jet identification facilitates a heavy-flavor search in addition to the inclusive search for three-jet resonances. High-mass signal events lead to a more spherical shape than background events, which typically contain back-to-back jets. In order to significantly reduce the background in the high-mass searches, a sphericity variable, $S = (3/2)(\lambda_2 + \lambda_3)$, is used, where the λ_i variables are eigenvalues of the following tensor [92]:

$$S^{\alpha\beta} = \frac{\sum_i p_i^\alpha p_i^\beta}{\sum_i |p_i|^2}. \tag{9}$$

Here α and β label separate jets, and the sphericity S is calculated using all jets in each event. In summary, the SRs in this analysis are defined using M_{jjj}, Δ, and also cuts on the fourth jet p_T, sixth jet p_T, and S_T. To optimize sensitivity for the heavy flavor search, a region of low or high mass M_{jjj} for the underlying resonance mass has been developed, respectively.

This overview of CMS RPV analyses is completed with Tables 3 and 4. Using these tables, the signatures and main variables for signal selections per analysis are indicated and also the information which analyses are used to constrain which RPV SUSY models is presented. As can be noted from Table 4, most of these analyses from CMS have also investigated at least two different RPV-based models.

4. Bilinear R-Parity Violation

In the bRPV model, the terms with coefficients ε_i $(i = 1, 2, 3)$ lead to lepton-number violating interactions between lepton and Higgs superfields. An overview of bRPV phenomenology can be found, for example, in [124, 125]. Note that also for the soft SUSY breaking terms additional bRPV terms $-B_i\varepsilon_i\widetilde{L}_i H_2$ and $m^2_{\ell_i H}\widetilde{L}_i H_1^\dagger$ [126] arise, leading to extra parameters. In general, there is no basis where both sets of bilinear RPV terms $\varepsilon_i L_i H_2$ and $B_i\varepsilon_i\widetilde{L}_i H_2$ can be eliminated at the same time. Taking into account the mixing of sneutrinos and scalar neutral Higgs fields, the electroweak symmetry is broken when these scalar fields acquire vacuum expectation values. Another characteristic consequence of bRPV is the generation of neutrino masses via neutralino-neutrino mixing; see, for example, [127].

Requiring both that electroweak symmetry breaking is consistent with Higgs results and at the same time that predictions agree with data from neutrino oscillations effectively constrains the parameter space of bRPV. A corresponding fitting routine is implemented in the SPheno code [128] fulfilling these experimental constraints in determining bRPV couplings, spectra, and decays. Note also that in general all the resulting bRPV parameters are nonvanishing and are not related in a trivial way. As discussed, for example, in [129], one expects strong correlations between neutralino decay properties measurable at high-energy collider experiments and neutrino mixing angles determined in low-energy neutrino oscillation experiments, such as

$$\tan^2\theta_{\text{atm}} \simeq \frac{\text{BR}\left(\widetilde{\chi}_1^0 \longrightarrow \mu W\right)}{\text{BR}\left(\widetilde{\chi}_1^0 \longrightarrow \tau W\right)}. \tag{10}$$

Due to the small size of the bRPV couplings, the production processes and the SUSY cascade decays are usually the same as in corresponding RPC scenarios. The fundamental difference in high-energy collision processes arises from decays of the LSP. Focusing on prompt LSP decays can lead to two-body decays of a neutralino LSP into gauge boson plus lepton, as described below.

4.1. bRPV mSUGRA Model. The analyses of [130] and subsequently [129, 131] have investigated the corresponding phenomenology and expected sensitivities at the LHC. Assuming

a neutralino LSP is sufficiently heavy, its most relevant two-body decay modes have been discussed:

(i) $\tilde{\chi}_1^0 \rightarrow W\tau$.

(ii) $\tilde{\chi}_1^0 \rightarrow We$.

(iii) $\tilde{\chi}_1^0 \rightarrow W\mu$.

(iv) $\tilde{\chi}_1^0 \rightarrow Z\nu$.

(v) $\tilde{\chi}_1^0 \rightarrow h^0\nu$.

Notably, for a large part of the parameter space, the decays to $W\tau$ and $W\mu$ (see also (10)) tend to be dominant, requiring consistency with neutrino oscillations. The exact magnitude of the individual LSP branching ratios also depend on its couplings, that is, if it corresponds mainly to a bino-, wino-, or higgsino-like state. Ideally, the searches for bRPV SUSY signatures could utilize the subsequent decay products of gauge or Higgs bosons; see, for example, [129]. Reconstructing such bosons accompanying the leptonic partner from LSP decays would allow reconstructing LSP masses and also indicate its two-body decays to possibly reveal RPV of bilinear type. Depending on the number of charged leptons in the LSP decays, the phenomenology of final states can be classified as *leptonic*, *semileptonic*, or *invisible decays* [130]. The latter decay mode $\tilde{\chi}_1^0 \rightarrow \nu\nu\nu$ would mimic RPC SUSY signal with large E_T^{miss}. Moreover it has been emphasized in [129] that reducing the LSP mass can lead to significantly late LSP decays. In the context of mSUGRA the LSP mass is mainly driven by the input parameter $m_{1/2}$, leading to an approximate displacement of decays of 1 mm (in the rest frame of the LSP) for $m_{1/2} \approx 300$ GeV.

Similar to RPC mSUGRA models, the most relevant production processes are given by

(i) $\tilde{g}$-$\tilde{g}$ production is most relevant in the region of low $m_{1/2}$;

(ii) squark-$\tilde{g}$ processes are most significant for low $m_{1/2}$ and m_0;

(iii) contributions from squark-(anti)-squark are most relevant for low m_0 and relatively high $m_{1/2}$;

(iv) electroweak gaugino-gaugino-based production tends to be dominant for highest input mass scales of m_0 and $m_{1/2}$;

In the minimal supergravity model [105–110], the SUSY breaking sector at the high scale of unification connects to the MSSM at the electroweak scale dominantly through gravitational-strength interactions. In a minimal form, one common mass scale $m_{1/2}$ appears for the three gauginos, one mass scale m_0 for all scalars, and one coupling for all scalar three-field interactions A_0, so that all gauginos are degenerated and also all squark, sleptons, and Higgs-related mass values become degenerate at the unification mass scale. In addition to these three input parameters, also the ratio of the vevs of the two neutral Higgses, $\tan\beta$, and the sign of the Higgs mass term, $\text{sign}(\mu)$, are necessary to define the mSUGRA model. After fixing this set of 5 parameters as boundary conditions for mSUGRA, the renormalization group evolution for SUSY-breaking masses and trilinear parameters will finally determine the SUSY mass spectrum at LHC energies.

Taking into account the Higgs boson mass observed at 125 GeV, bRPV mSUGRA signal models have been analyzed. Similar to Higgs-aware signal models of RPC mSUGRA investigated, for example, in [132], the input parameters are chosen as $\tan\beta = 30$, $A_0 = -2m_0$, and $\text{sign}(\mu) = 1$ with varying values of the mass scales m_0 and $m_{1/2}$. Referring to the same input parameters with respect to RPC mSUGRA also implies the same masses and essentially the same cross sections in comparison to each RPC-based production process. Due to the smallness of bRPV couplings, other production processes are highly suppressed, so that RPC- and bRPV-based production processes are almost in one-to-one correspondence in mSUGRA.

4.2. Results for bRPV Searches. In the ATLAS SS/3L$_A$ analysis [38] the parameter space of bRPV mSUGRA has been strongly constrained. Based on the limits from Figure 2, values of $m_{1/2}$ are excluded between 200 GeV and 490 GeV at 95% CL for m_0 values below 2.2 TeV. This limit corresponds to a lower bound of approximately 1.3 TeV for gluino masses in bRPV mSUGRA. Signal models with $m_{1/2} < 200$ GeV are not considered in this analysis because the lepton acceptance is significantly reduced due to the increased LSP lifetime in that region. The sensitivity is dominated by the signal region SR3b selecting same-sign or three leptons and requiring additionally $\geq$ 3 b-jets, $\geq 5\,N_{\text{jets}}$ and $m_{\text{eff}} > 350$ GeV, respectively. High sensitivity in particular in signal region SR3b is also a result of the high number of leptons and also of b-jets from LSP decays in conjunction with low requirements for missing transverse energy. It is interesting to note that, in SR3b, a 95% CL upper limit on the (observed) visible cross section at 0.19 fb has been obtained, establishing a model-independent limit.

The ATLAS τ_A analysis [39] has demonstrated that searching for hadronically decaying τ-leptons in addition to jets, E_T^{miss}, and light leptons has a high sensitivity for bRPV at low m_0. In this part of the parameter space, the number of taus from RPC decays of relatively light staus is high. Adding also τ-leptons from bRPV LSP decays, the number of taus is even more pronounced in this case. Notably, several SRs, based on $\tau+\mu$, $\tau+e$, and 2τ, have been optimized particularly for bRPV. Performing a statistical combination of these SRs, the 95% CL limits on mSUGRA mass parameters in Figure 2 have been obtained. As a result from [39], values of $m_{1/2}$ up to 680 GeV are excluded for low m_0, while the exclusion along the m_0 axis reaches a maximum of 920 GeV for $m_{1/2} = 360$ GeV. For the results in SRs relevant for bRPV searches also limits on visible cross sections have been derived, corresponding to upper limits on the observed σ_{vis} of 0.52 fb, 0.26 fb, and 0.20 fb in the $\tau + \mu$, $\tau + e$, and 2τ channels, respectively. Although the expected σ_{vis} are the same for $\tau + \mu$ and $\tau + e$, the higher number of events observed in the SR($\tau + \mu$) effectively leads to a weaker limit of 0.52 fb with respect to 0.26 fb in SR($\tau + e$).

Moreover, the ATLAS search for leptons in SUSY strong production [133], optimized for RPC models, has also obtained exclusion limits for this bRPV mSUGRA model.

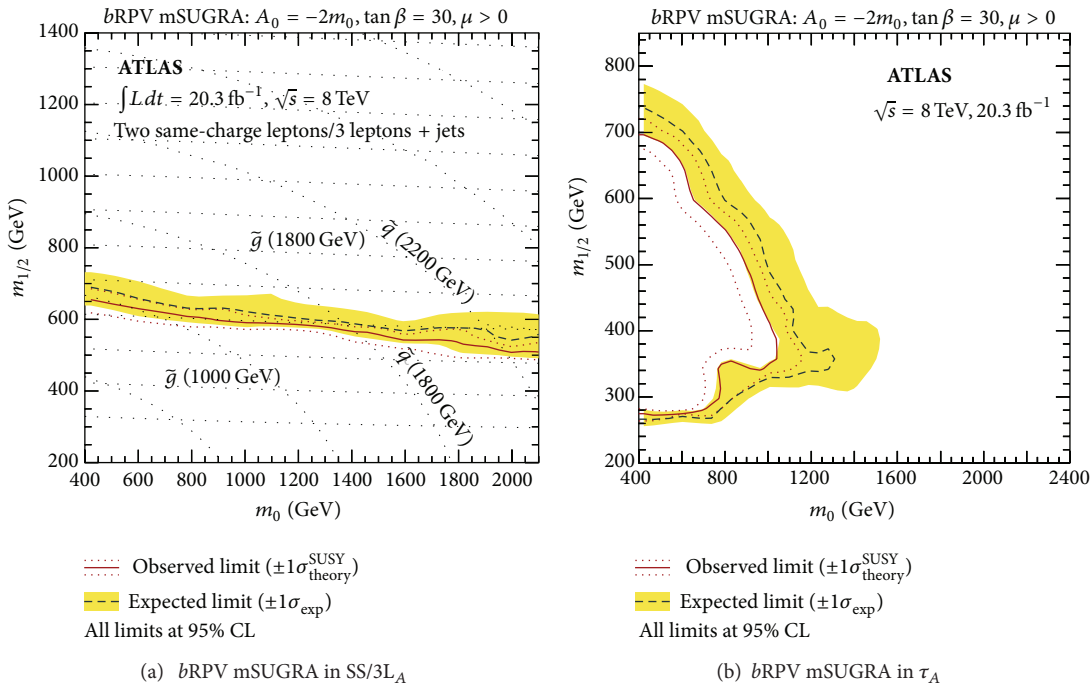

(a) bRPV mSUGRA in SS/3L$_A$ (b) bRPV mSUGRA in τ_A

FIGURE 2: Observed and expected exclusion limits for the bRPV mSUGRA model obtained in the SS/3L ATLAS analysis (left, from [38]) and in the τ_A analysis (right, from [39]).

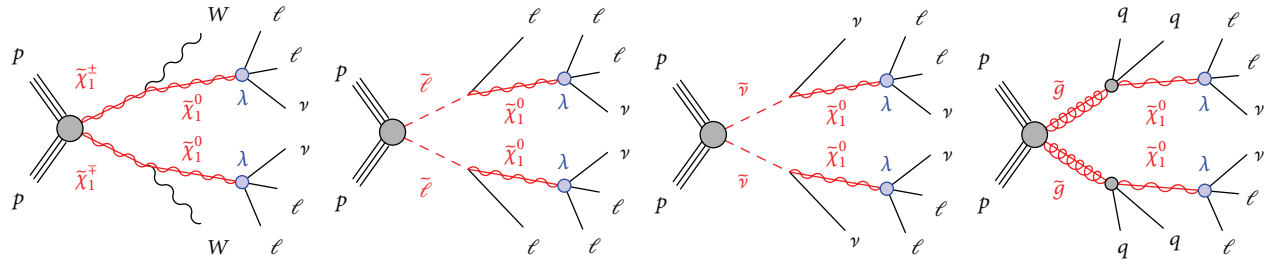

(a) Chargino NLSP (b) Slepton NLSP (c) Sneutrino NLSP (d) Gluino NLSP

FIGURE 3: Representative diagrams for the RPV simplified models based on electroweak or gluino production (from [40]).

Comparing the expected limits to the SS/3L analysis, they are comparable for both analyses in the range of low m_0, whereas, for the highest values of m_0, the SS/3L analysis reaches slightly stronger expected limits. In terms of observed limits, both analyses are actually comparable in the high m_0 regime, while [133] obtains a stronger limit in the case of low values of m_0. In particular for $m_0 = 400$ GeV an observed exclusion of $m_{1/2} \approx 750$ GeV corresponding to $m_{\tilde{g}} \approx 1.7$ TeV has been obtained. It is interesting to note that, within the SRs investigated in [133], the hard single-lepton channel has the highest sensitivity to the bRPV mSUGRA model.

5. *LLE* Models

5.1. LLE Simplified Models. In the RPV simplified models studied in [40], a bino-like $\tilde{\chi}_1^0$ is assumed to decay into two charged leptons and a neutrino via the λ_{ijk} term. Four event topologies are tested, resulting from different choices for the next-to-lightest SUSY particles (NLSPs): a chargino ($\tilde{\chi}_1^\pm$) NLSP; slepton NLSPs, referring to mass-degenerate charged sleptons; sneutrino NLSPs, referring to mass-degenerate sneutrinos; and a gluino NLSP. In the slepton case, both the left-handed and the right-handed sleptons (L-sleptons and R-sleptons, resp.) have been considered, as the different production cross sections for the two cases substantially affect the analysis sensitivity. The assumed decays of each NLSP choice are described in Table 5 and illustrated in Figure 3. The masses of the NLSP and LSP are varied, while other sparticles are assumed to be decoupled.

In the paper [41], *LLE* couplings have been investigated in the context of stop-pair production: The corresponding simplified model assumes stop decays to a top quark and intermediate on- or off-shell bino, $\tilde{t}_1 \to \tilde{\chi}_1^0 + t$. The bino decays to two leptons and a neutrino through the leptonic RPV interactions, $\tilde{\chi}_1^{0*} \to \ell_i + \nu_j + \ell_k$ and $\nu_i + \ell_j + \ell_k$, where the indices i, j, k refer to those appearing in (1a). The stop is assumed to be right-handed and RPV couplings

Table 5: Sparticle decays in the SUSY RPV simplified models considered in [40]. The neutralino LSP is assumed to decay to two charged leptons and a neutrino. For the chargino model, the $W^{\pm}$ from the $\widetilde{\chi}_1^{\pm}$ decay may be virtual as indicated by the superscript $(*)$.

RPV model NLSP	Decay
Chargino	$\widetilde{\chi}_1^{\pm} \to W^{\pm(*)}\widetilde{\chi}_1^0$
L-slepton	$\widetilde{\ell}_L \to \ell\widetilde{\chi}_1^0$
	$\widetilde{\tau}_L \to \tau\widetilde{\chi}_1^0$
R-slepton	$\widetilde{\ell}_R \to \ell\widetilde{\chi}_1^0$
	$\widetilde{\tau}_R \to \tau\widetilde{\chi}_1^0$
Sneutrino	$\widetilde{\nu}_l \to \nu_\ell\widetilde{\chi}_1^0$
	$\widetilde{\nu}_\tau \to \nu_\tau\widetilde{\chi}_1^0$
Gluino	$\widetilde{g} \to q\bar{q}\widetilde{\chi}_1^0$
	$q \in u, d, s, c$

are large enough that all decays are prompt. Results for the corresponding simplified mass spectra and leptonic RPV couplings λ_{122} or λ_{233} are investigated in Section 5.3.

5.2. LLE RPV Results with Electroweak or $\widetilde{g}$ Production. The *LLE* simplified models produce events with four leptons in the final state, and thus it is natural to constrain them with the ATLAS search for SUSY in events with four or more charged leptons [40]. Up to two of the leptons may be hadronically decaying taus, and the search was specifically optimised to give good sensitivity across the full range of *LLE*-mediated $\widetilde{\chi}_1^0$ decays.

In all cases, the observed limit is determined mainly by the production cross section of the signal process, with stronger constraints on models where λ_{121} or λ_{122} dominate, and less stringent limits for tau-rich decays via λ_{133} or λ_{233}. Limits on models with different combinations of λ_{ijk} parameters can generically be expected to lie between these extremes. The limits are in many cases nearly insensitive to the $\widetilde{\chi}_1^0$ mass, except where the $\widetilde{\chi}_1^0$ is significantly less massive than the NLSP as inferred from Figure 4. Where the NLSP $\to$ LSP cascade may also produce leptons, the observed limit may also become weaker as $m_{\widetilde{\chi}_1^0}$ approaches the NLSP mass, and the cascade product momenta decrease considerably.

When the mass of the $\widetilde{\chi}_1^0$ LSP is at least as large as 20% of the NLSP mass, and assuming tau-rich LSP decays, lower limits can be placed on sparticle masses, excluding gluinos with masses less than 950 GeV; wino-like charginos with masses less than 450 GeV; and L(R)-sleptons with masses less than 300 (240) GeV. If instead the LSP decays only to electrons and muons, the equivalent limits are approximately 1350 GeV for gluinos, 750 GeV for charginos, and 490 (410) GeV for L(R)-sleptons, and a lower limit of 400 GeV can also be placed on sneutrino masses. These results significantly improve upon previous searches at the LHC, where gluino masses of up to 1 TeV [134] and chargino masses of up to 540 GeV [135] were excluded.

The model-independent limits on σ_{vis} for RPV-related SRs all lie below 0.5 fb: In signal regions requiring at least three light leptons, the observed 95% CL upper limits on the *visible cross sections* are below 0.2 fb. (It is interesting to note that the ATLAS search for multileptons based on 7 TeV data [135] has obtained limits of approximately 1 fb on σ_{vis} considering also four-body decays of a stau LSP as motivated, e.g., by [136].)

5.3. LLE RPV Results for $\widetilde{t}_1$ Production. The limits obtained in [41] are mostly independent of the bino mass, leading to an exclusion of models with the stop mass below 1020 GeV when λ_{122} is nonzero, and below 820 GeV when λ_{233} is nonzero. These limits are shown in Figure 5. There is a change in kinematics at the line $m_{\widetilde{\chi}_1^0} = m_{\widetilde{t}_1} - m_t$, below which the stop decay is two-body, while above it is a four-body decay. Near this line, the $\widetilde{\chi}_1^0$ and top are produced almost at rest, which results in low-momentum leptons, corresponding to reduced acceptance. This loss of acceptance is more visible in the $\lambda_{233} \neq 0$ case and causes the loss of sensitivity near the line at $m_{\widetilde{\chi}_1^0} = 800$ GeV. The analysis [41] has also explained that this effect is more pronounced in the observed limit because the data has a larger statistical uncertainty in the relevant signal regions than the simulated signal samples.

6. *LQD* Models

6.1. Simplified LQD Models for $\widetilde{t}_1$ Production. In addition to the simplified model for stop pair production introduced in the previous Section 5.1, RPV decays via λ'_{233} are also considered in the simplified model of [41]. The same assumptions on stop decays to a top quark and intermediate on- or off-shell bino, $\widetilde{t}_1 \to \widetilde{\chi}_1^0 + t$, are made, only the *LQD*-related decay of $\widetilde{\chi}_1^0$ to one lepton and two quarks leads to different final states in comparison to LSP decays via *LLE* as already discussed in the previous section. A possible signal process is illustrated in the Feynman diagram, Figure 6. Due to the high number of W-bosons indicated in the final states of that process, also a relatively large number of charged (light) leptons can be expected, in conjunction with many b-jets.

In another simplified model investigated in [42], two different decay channels of directly produced top squarks are considered. In the first case the two-body lepton number violating decay $\widetilde{t}_1 \to \tau b$ via the coupling constant λ'_{333} is investigated; see also [22] for related phenomenological studies.

In the second part of the search the focus is on a scenario in which the dominant RPC decay of the top squark is $\widetilde{t}_1 \to \widetilde{\chi}_1^{\pm} b$. This requires the mass splitting between the top squark and the chargino to be less than the mass of the top quark, so it is chosen to be 100 GeV. The chargino is assumed to be a pure higgsino and to be nearly degenerate in mass with the neutralino. In particular, the decay $\widetilde{\chi}_1^{\pm} \to \widetilde{\nu}\tau^{\pm} \to qq\tau^{\pm}$ via an intermediate τ-sneutrino is considered. This RPV decay of the sneutrino is possible via the *LQD*-type coupling λ'_{3jk}, where the cases $j, k = 1, 2$ are taken into account.

6.2. Results for $\widetilde{t}_1$ Production. The analysis [41] has probed regions in the mass plane of neutralino versus stop masses assuming pair production of $\widetilde{t}_1$ and nonvanishing λ'_{233}. As discussed before, in that analysis several different kinematic regions in the mass plane are relevant also in the final results

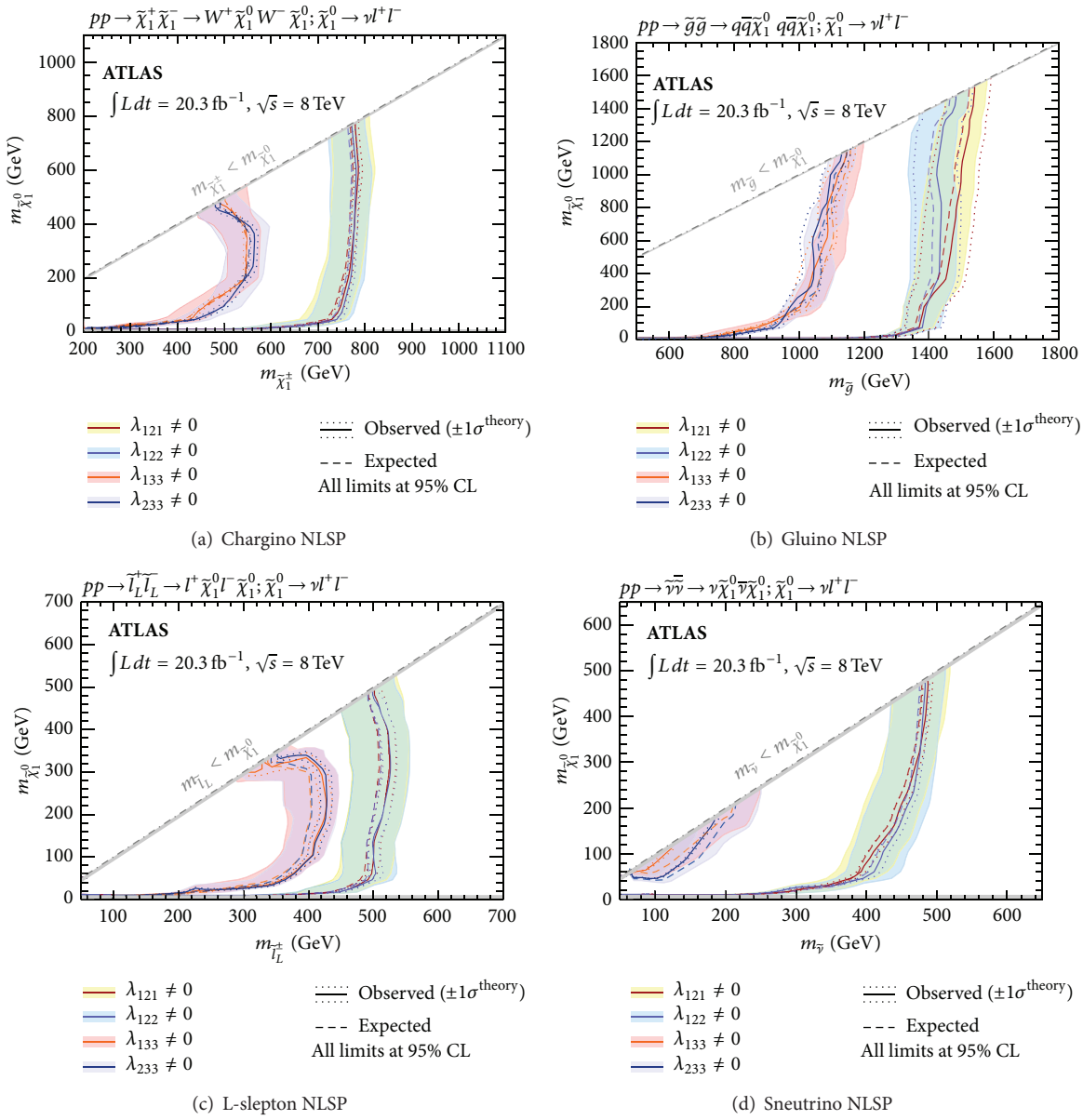

FIGURE 4: Observed and expected 95% CL exclusion limit contours for the *LLE* RPV (a) chargino NLSP, (b) gluino NLSP, (c) left-handed slepton NLSP, and (d) sneutrino NLSP simplified models (from [40]).

of Figure 7. The most significant effect is when the decay $\tilde{\chi}_1^0 \to \mu + t + b$ is suppressed, reducing the number of leptons in the final state. The different regions where this effect is pronounced primarily lead the shape of the exclusion for λ'_{233}. As a result, stop masses up to approximately 800 GeV can be excluded in this model.

In the search for b-jets and τ-leptons from CMS [42], constraints for the masses of pair-produced stops have been derived. An upper bound at 95% confidence level is set on $\sigma\mathcal{B}^2$, where σ is the cross section for pair production of top squarks and $\mathcal{B}$ is the branching fraction for the top squark decay to a $\tilde{\chi}_1^\pm$ and a bottom quark, with a subsequent decay of the chargino via $\tilde{\chi}_1^\pm \to \tilde{\nu}\tau^\pm \to qq\tau^\pm$. Expected and observed upper limits on $\sigma\mathcal{B}^2$ as a function of the stop mass are shown in Figure 8 for the top squark search from [42]. As a result, top squarks undergoing a chargino-mediated decay involving the coupling λ'_{3jk} with masses in the range 200–580 GeV are excluded, in agreement with the expected exclusion limit in the range 200–590 GeV. In the derivation of these upper limits $\mathcal{B} = 100\%$ is assumed.

Since the other simplified model investigated in [42] leads to direct decays of stops after $\tilde{t}_1$ pair-production, the underlying stop mass essentially determines the results. The limits corresponding to top squarks decaying directly through the coupling λ'_{333} exclude masses of $\tilde{t}_1$ below 740 GeV, in agreement with the expected limit at 750 GeV.

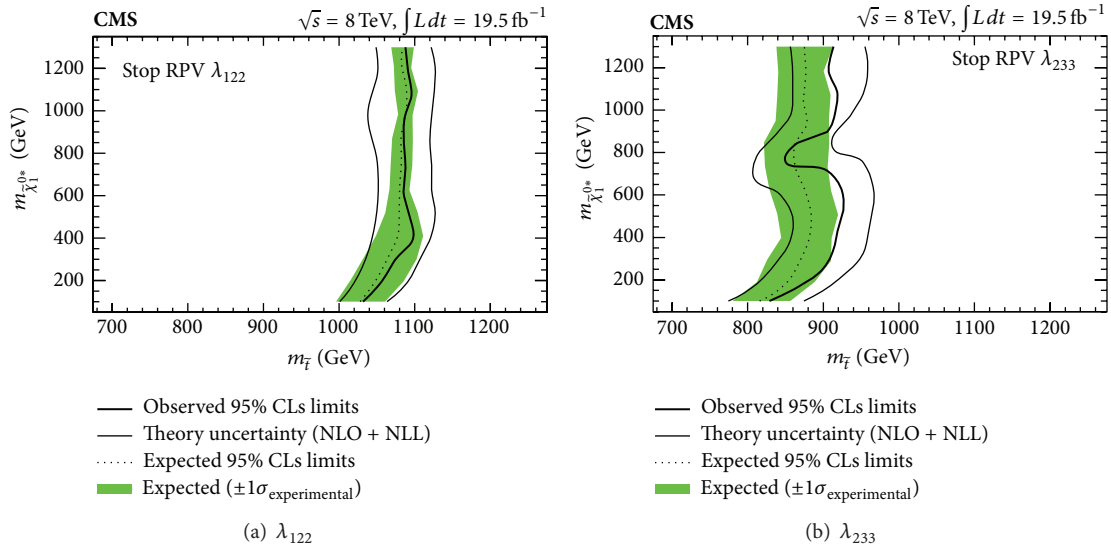

(a) λ_{122} (b) λ_{233}

FIGURE 5: The 95% confidence level limits in the stop and bino mass plane for models with RPV couplings λ_{122} and λ_{233}. The region to the left of the curve is excluded (from [41]).

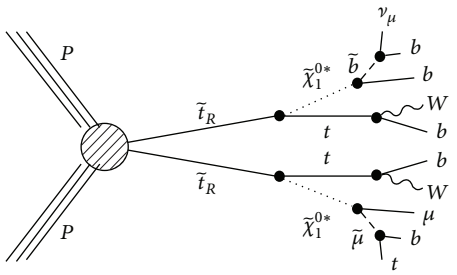

FIGURE 6: Signal process for stop-pair production with LSP decays mediated via λ'_{233} (from [41]).

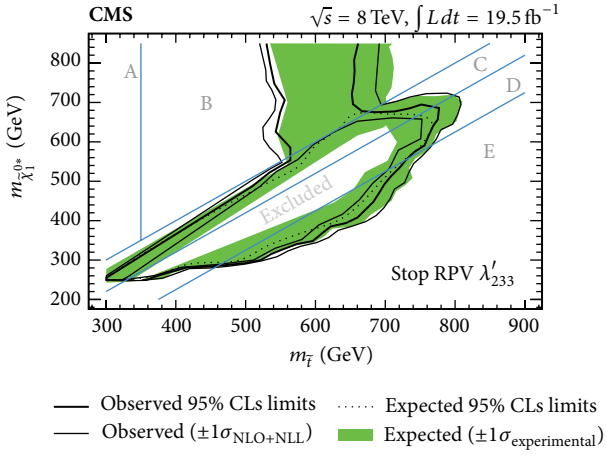

FIGURE 7: The 95% CL limits in the stop and bino mass plane for stop-pair production and RPV coupling λ'_{233} (from [41]). The different kinematic regions, A, B, C, D, and E are defined in [41].

7. Resonance Production and Decay

If *LQD* couplings are present at hadron colliders, resonant production of sleptons is possible. The decay products from such a slepton resonance can also depend on additional RPV couplings. If also *LLE* couplings occur, then leptonic final states can be investigated, whereas jets are expected if only *LQD* terms are assumed. In order to allow for considerable production rates and also for significant decay rates into charged leptons, τ-sneutrinos emerge as candidates for resonance searches. (It is interesting to note that also a search for RPV resonances from second generation sleptons has been performed by CMS at 7 TeV [137]. Assuming the coupling λ'_{211}, the search investigated two same-sign muons and at least two jets in the final state.) In the case of $\tilde{\nu}_\tau$, the corresponding bounds for its coupling of type *LQD* and also *LLE* are relatively weak. Therefore the analysis [43] searching for resonances using leptonic final states has focused on τ-sneutrinos, as described in more detail below.

7.1. Resonance via Tau Sneutrino. As illustrated in Figure 9, a τ-sneutrino ($\tilde{\nu}_\tau$) may be produced in pp collisions by $d\bar{d}$ annihilation and subsequently decay to $e\mu$, $e\tau$, or $\mu\tau$. Although only $\tilde{\nu}_\tau$ is considered in [43] to facilitate comparisons with previous searches performed at the Tevatron, the results of this analysis in principle apply to any sneutrino flavor.

7.2. Resonance Searches. Expected and observed upper limits are set as a function of $\tilde{\nu}_\tau$ mass. The likelihood of observing the number of events in data as a function of the expected number of signal and background events is constructed from a Poisson distribution for each bin in the $\tilde{\nu}_\tau$ mass. Signal cross sections are calculated to next-to-leading order for $\tilde{\nu}_\tau$.

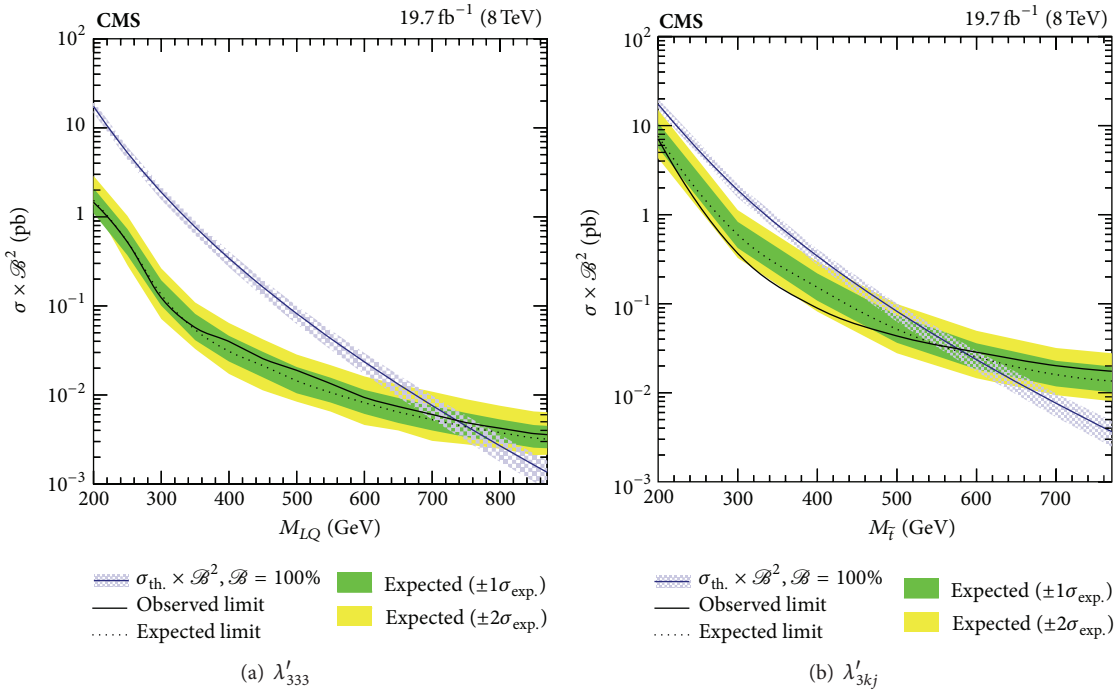

(a) λ'_{333} (b) λ'_{3kj}

FIGURE 8: The expected (observed) combined upper limits on the third-generation LQ pair production cross section σ times the square of the branching fraction, $\mathscr{B}^2$. These limits also apply to top squarks decaying directly via the coupling λ'_{333} (a). The limits (b) apply to top squarks with a chargino-mediated decay through the coupling λ'_{3kj} (from [42]).

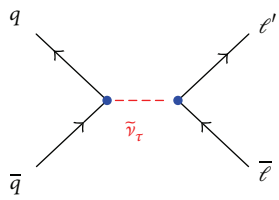

FIGURE 9: Feynman diagram illustrating resonant production and decay of $\tilde{\nu}_\tau$. l_i and l_j can be e, μ, or τ, where $i \neq j$. The blue dots indicate RPV couplings λ'_{311} and λ_{i3j} ($i \neq j$), respectively (from [43]).

Figure 10 shows the observed and expected cross section times branching ratio limits as a function of the $\tilde{\nu}_\tau$ mass. For a $\tilde{\nu}_\tau$ mass of 1 TeV, the observed limits on the production cross section times branching ratio are 0.5 fb, 2.7 fb, and 9.1 fb for the $e\mu$, $e\tau$, and $\mu\tau$ channels, respectively. Theoretical predictions of cross section times branching ratio are also shown, assuming $\lambda'_{311} = 0.11$ and $\lambda_{i3k} = 0.07$ ($i \neq k$) for the $\tilde{\nu}_\tau$, consistent with benchmark couplings used in previous searches. For these benchmark couplings, the lower limits on the $\tilde{\nu}_\tau$ mass are 2.0 TeV, 1.7 TeV, and 1.7 TeV for the $e\mu$, $e\tau$, and $\mu\tau$ channels, respectively.

These results considerably extend previous constraints from the Tevatron and LHC experiments. Based on the similar assumptions for RPV couplings, that is, $\lambda'_{311} = 0.10$ and $\lambda_{i3k} = 0.05$ ($i \neq k$), the CDF experiment [73] has obtained lower limits for τ-sneutrino masses at 558 GeV, 442 GeV, and 441 GeV for the $e\mu$, $e\tau$, and $\mu\tau$ channels, respectively.

8. *UDD* Models

In this section results from searches for signatures from *UDD* couplings are presented. Both ATLAS and CMS have investigated several different topologies as motivated by a number of simplified models.

8.1. $\tilde{g}$ Production with Multijets at ATLAS. Pair-produced massive new particles with decays to a total of six quarks, as well as cascade decays with at least ten quarks, are considered in the design of the analysis [44]. Three-body decays of the type shown in Figure 11 are given by effective RPV vertices allowed by the baryon-number-violating λ''_{ijk} couplings with off-shell squark propagators. For both models, all squark masses are set to 5 TeV and thus gluinos decay directly to three quarks or to two quarks and a neutralino through standard RPC couplings. In the ten-quark cascade decay model, the neutralinos each decay to three quarks via an off-shell squark and the RPV *UDD* decay vertex with coupling λ''_{ijk}. In this model, the neutralino is the LSP.

All possible λ'' flavor combinations are allowed to proceed with equal probability. The analysis maintains approximately equal sensitivity to all flavor modes. All samples are produced assuming that the gluino and neutralino widths are narrow and that their decays are prompt.

It is interesting to compare limits based on different assumptions for the branching ratios into heavy flavor jets. Figure 12 illustrates the variation for the observed mass limit when the decays into b-jets are absent or assumed at 100 percent, respectively.

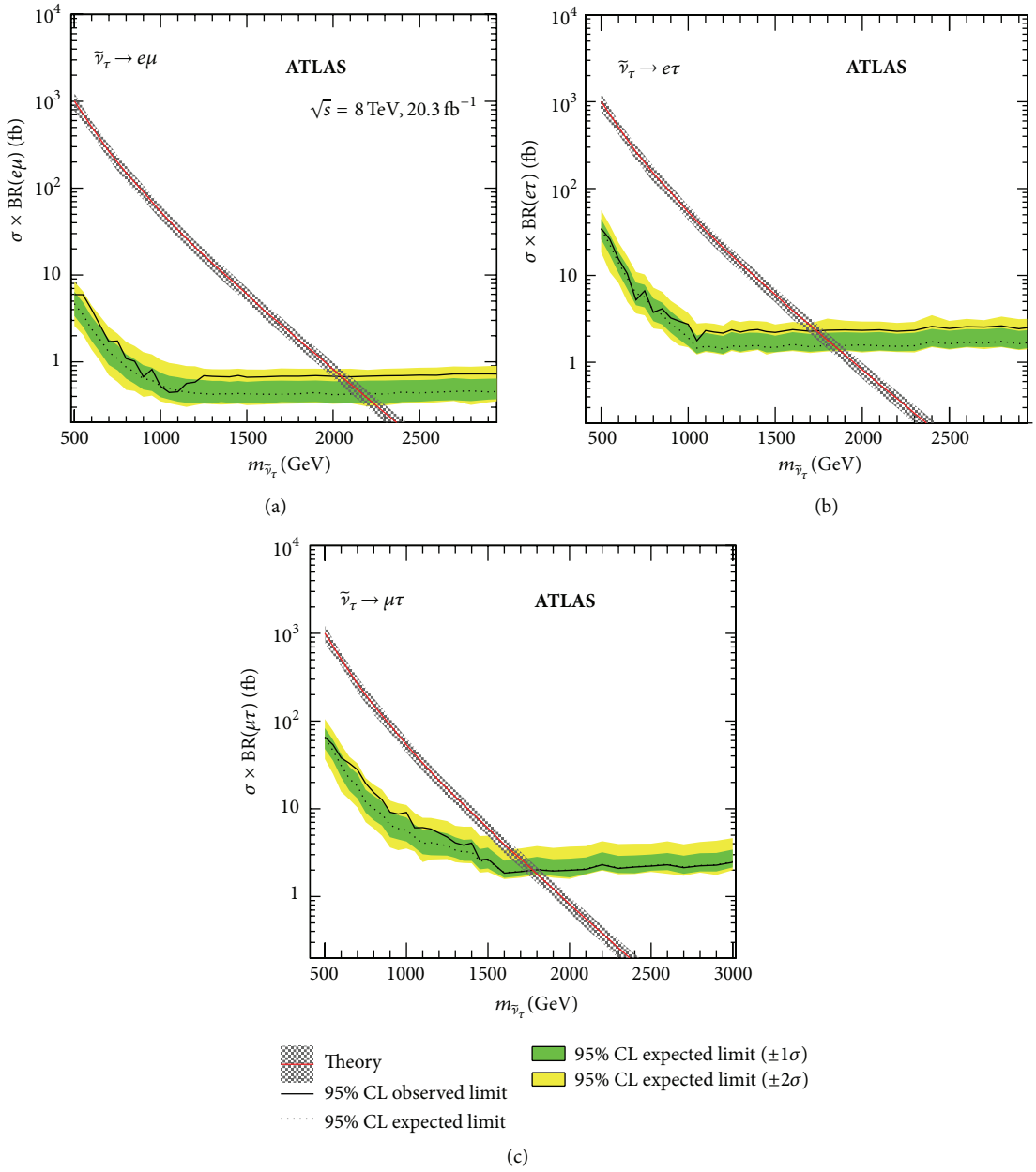

FIGURE 10: The 95% CL limits on cross section times branching ratio as a function of $\tilde{\nu}_\tau$ mass for $e\mu$ (a), $e\tau$ (b), and $\mu\tau$ (c) (from [43]). Theory curves correspond to $\lambda'_{311} = 0.11$ and $\lambda_{i3k} = 0.07$ for $\tilde{\nu}_\tau$.

More generally, excluded masses as a function of the branching ratios of the decays are presented in Figure 13 where each bin shows the maximum gluino mass that is excluded for the given decay mode. It is illustrative to recognize the observed mass limit from Figure 12(a) can also be found in the lower left corner of Figure 13.

The interpretations of the results of the jet-counting and total-jet-mass analyses are displayed together in Figure 14 for the ten-quark model. This figure allows for the direct comparison of the results of the various analyses. Without b-tagging requirements, the jet-counting analysis sets slightly lower expected limits than the total-jet-mass analysis. With b-tagging requirements, the limits are stronger for the jet-counting analysis. The observed limits from the total-jet-mass analysis and jet-counting analysis with b-tagging requirements are also comparable.

Exclusion limits at the 95% CL are set extending up to $m_{\tilde{g}} = 917$ GeV in the case of pair-produced gluino decays to six light quarks and up to $m_{\tilde{g}} = 1$ TeV in the case of cascade decays to ten quarks for moderate $m_{\tilde{g}} - m_{\tilde{\chi}^0_1}$ mass splittings.

It is interesting to note that strong model-independent limits have been obtained in [44]. Within the jet-counting method, the 95% CL upper limits obtained on the (observed) *visible signal cross section* vary from 0.2 fb to 2.6 fb, depending

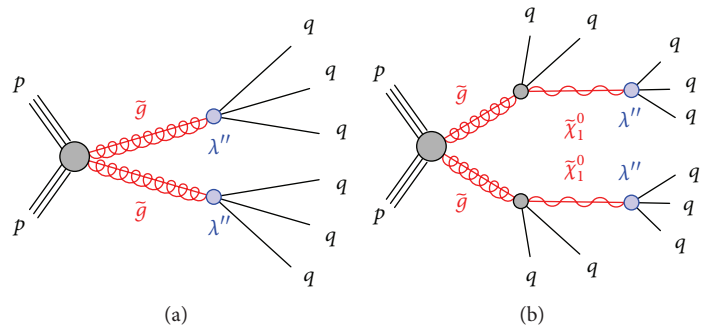

FIGURE 11: Diagrams for multijet processes considered for the analysis [44]. The gray shaded circles represent effective vertices that include off-shell propagators, and the blue shaded circles represent effective RPV vertices allowed by *UDD* λ''_{ijk} couplings with off-shell propagators (from [44]).

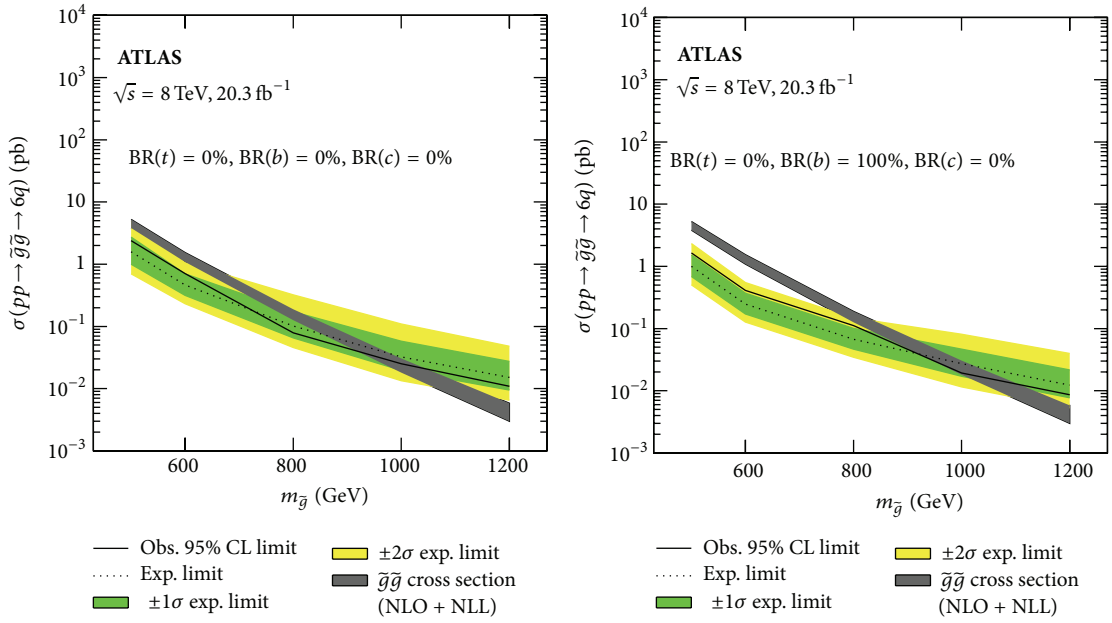

FIGURE 12: Observed mass exclusions at the 95% CL for BR(b) = 0% (a) and BR(b) = 100% (b) (from [44]).

on the requirements on jet p_T and number of b-jets for different SRs. Notably the strongest limit of 0.2 fb has been derived in the SR requiring at least seven jets, with p_T above 180 GeV and one b-tagged jet.

8.2. $\tilde{g}$ Production with Leptonic Final States at ATLAS. In the gluino-mediated top squark $\to$ bs (RPV) model investigated in [38], top squarks are assumed to decay with the *UDD* coupling $\lambda''_{323} = 1$. The final state is therefore $\tilde{g}\tilde{g} \to bbbb\ ss\ WW$, characterized by the presence of four b-quarks and only moderate missing transverse momentum.

Results are interpreted in the parameter space of the gluino and top squark masses (see Figure 15). Gluino masses below 850 GeV are excluded at 95% CL, almost independently of the stop mass. The sensitivity is dominated by SR3b. The SR3b signal region is sensitive to various models with same-sign or $\geq$ 3 leptons and $\geq$ 3b-quarks. This is also demonstrated in the gluino-mediated top squark $\to$ bs (RPV) model, where $m_{\tilde{g}} < 850$ GeV is excluded by SR3b alone in the absence of a large E_T^{miss} signature.

It is important to mention that for the same simplified model, a similar bound of $m_{\tilde{g}} > 900$ GeV has been obtained in the ATLAS search for (7–10) jets and E_T^{miss} [138]. The latter exclusion limit tends to be extended for relatively light or heavy stops.

As a model-independent limit from SR3b, the limit on the visible cross section $\sigma_{\text{vis}}^{95} = 0.19$ fb has been obtained at the 95% CL. It is interesting to note that SR3b is also the most sensitive signal region constraining bRPV mSUGRA.

8.3. $\tilde{g}$ Production with Multijets at CMS. The signal is modeled in [45] with pair-produced gluinos where each

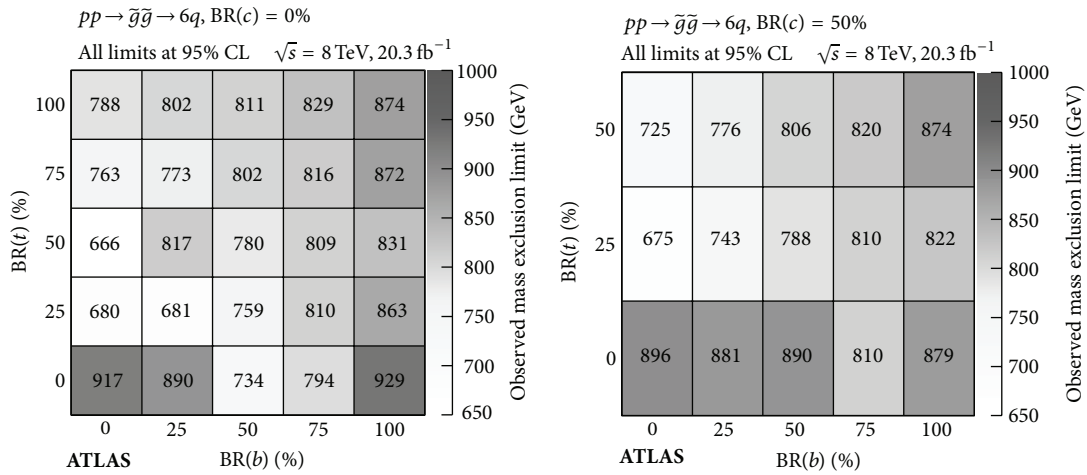

(a) BR(c) = 0%: observed (b) BR(c) = 50%: observed

FIGURE 13: Observed mass exclusions at the 95% CL in the BR(t) versus BR(b) space for BR(c) = 0% (a) and BR(c) = 50% (b). Each point in this space is individually optimized and fit. Masses below these values are excluded in the six-quark model. Bin centers correspond to evaluated models (from [44]).

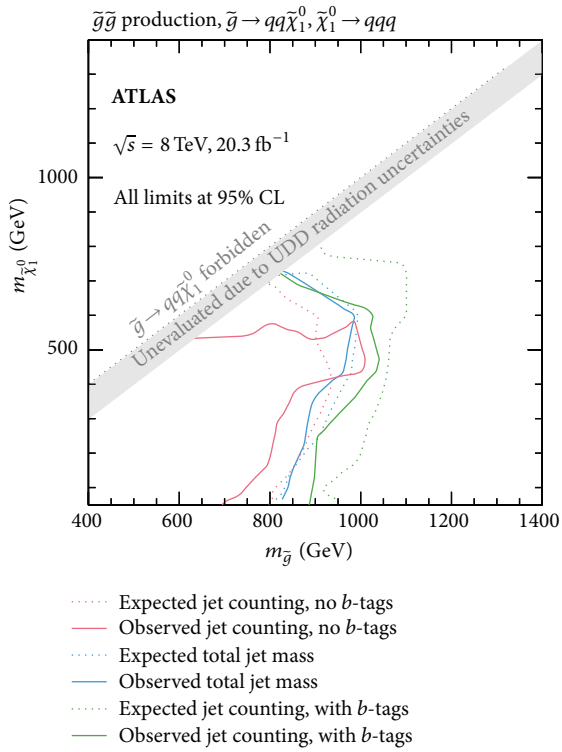

FIGURE 14: Expected and observed exclusion limits in the $(m_{\tilde{g}} - m_{\tilde{\chi}_1^0})$ plane for the ten-quark model for the jet-counting analysis (with and without b-tagged jets) and the total-jet-mass analysis (from [44]).

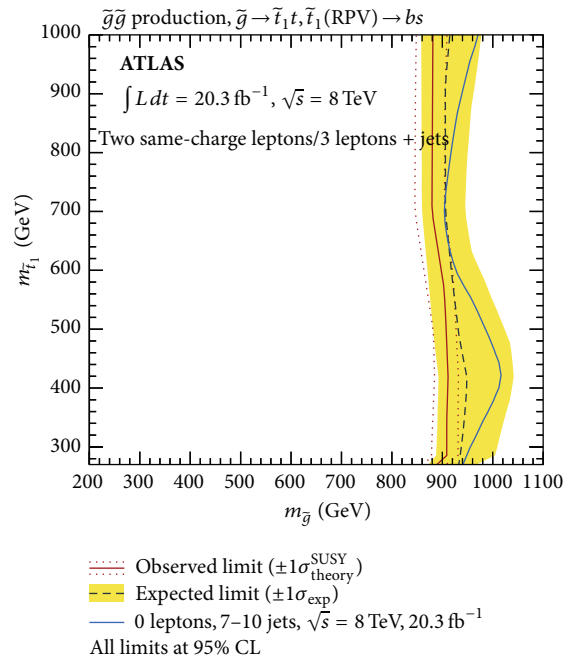

FIGURE 15: Observed and expected exclusion limits on gluino-mediated top squark production, obtained with 20.3 fb^{-1} of pp collisions at $\sqrt{s}$ = 8 TeV, for the top squark decay modes via λ''_{323} (from [38]).

gluino decays to three quarks through *UDD*-type couplings. Two different scenarios, an inclusive search and also a heavy-flavor search, are considered in that analysis. For the first case, the coupling λ''_{112} is set to a non-zero value, giving a branching fraction of 100% for the gluino decay to three light-flavor quarks. The second case, represented by λ''_{113} or λ''_{223}, investigates gluino decays to one b quark and two light-flavor quarks. In these simplified models, all superpartners except the gluino are taken to be decoupled, the natural width of the gluino resonance is assumed to be much smaller than

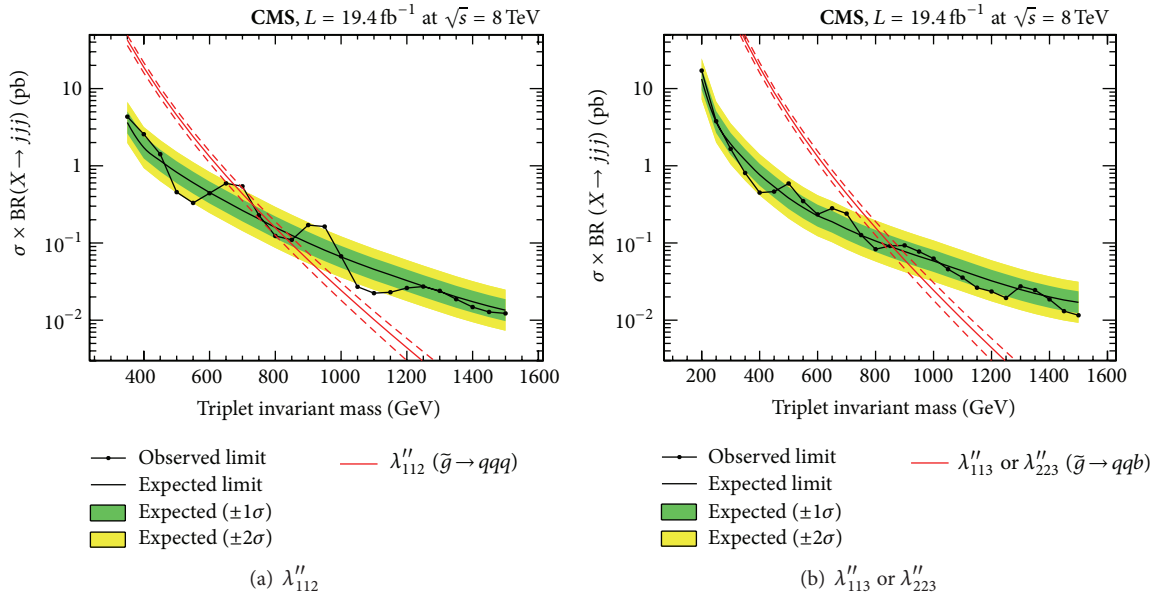

(a) λ''_{112} (b) λ''_{113} or λ''_{223}

FIGURE 16: Observed and expected 95% CL cross section limits as a function of mass for the inclusive (a) and heavy-flavor searches (b). The limits for the heavy-flavor search cover two mass ranges, one for low-mass gluinos ranging from 200 to 600 GeV, and one for high-mass gluinos covering the complementary mass range up to 1500 GeV (from [45]).

the mass resolution of the detector, and no intermediate particles are produced in the gluino decay.

As is also illustrated in Figure 16, several constraints on $\tilde{g}$-masses have been derived in [45]. The production of gluinos undergoing RPV decays into light-flavor jets is excluded at 95% CL for gluino masses below 650 GeV, with a less conservative exclusion of 670 GeV based upon the theory value at the central scale. The respective expected limits are 755 and 795 GeV. Gluinos whose decay includes a heavy-flavor jet are excluded for masses between 200 and 835 GeV, with the less conservative exclusion up to 855 GeV from the central theoretical value. The respective expected limits are 825 and 860 GeV. In the heavy-flavor search the limits extend to higher masses because of the reduction of the background.

8.4. $\tilde{g}$ Production with Same-Sign Leptons at CMS. In this analysis [46], a simplified model based on gluino pair production followed by the decay of each gluino to three quarks is considered. It is interesting to note that the analogous model is also taken into account in [38], as mentioned above. Moreover, *UDD*-like decays can in principle be motivated also from the SUSY model with minimal flavor violation [52]. In [46], the focus is on the decay mode $\tilde{g} \to tbs$. Due to its Majorana nature, the corresponding antiparticles emerge with equal probability in the decay of $\tilde{g}$. Such decays lead to same-sign W-boson pairs in the final state in 50% of the cases.

The signal process is illustrated in Figure 17. In comparison to the decays $\tilde{g} \to tsd$, yielding also same-sign W-boson pairs, the mode tbs is investigated. Due to two extra b quarks in the final state a higher signal selection efficiency can finally be obtained. The key parameter of the model is $m_{\tilde{g}}$ determining the production cross section and the final state kinematics. The dedicated search region RPV2 with the high-lepton p_T selection is used to place an upper limit on the production cross section.

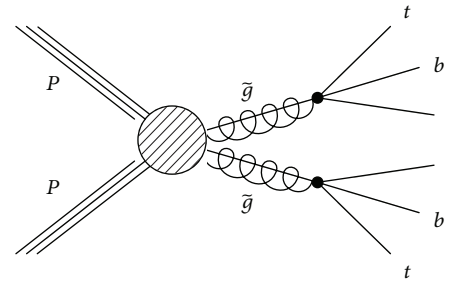

FIGURE 17: Signal process for $\tilde{g} \to tbs$ assuming gluino pair-production and λ''_{323} coupling.

The result is shown in Figure 18. In this scenario, the gluino mass is probed up to approximately 900 GeV. A similar exclusion limit from the corresponding ATLAS search has been obtained, as discussed in Section 8.2.

8.5. $\tilde{t}_1$ Production with Jet Pairs at CMS. The analysis [47] has been optimized by studying two simplified models with stop pair production: first, the coupling λ''_{312} is assumed leading to two light-flavor jets in the decay of each $\tilde{t}_1$.

Considering λ''_{323} nonzero in the second simplified model, one b-jet and one light-flavor jet are generated per $\tilde{t}_1$. In both of the above cases, the branching ratio of the top squark decay to two jets is set to 100% and all superpartners except the top squarks are taken to be decoupled, so that no intermediate particles are produced in the top squark decay.

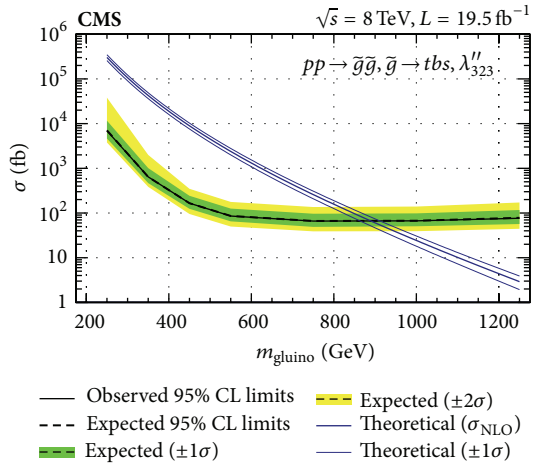

FIGURE 18: 95% CL upper limit on the gluino production cross section for a RPV simplified model, $pp \to \tilde{g}\tilde{g}, \tilde{g} \to tbs$ (from [46]).

Figure 19 shows the observed and expected 95% CL upper limits obtained in [47] based on results from the low-mass and high-mass SRs, respectively. In that case the top squark mass corresponds to m_{av}. The vertical dashed blue line at a top squark mass of 300 GeV indicates the transition from the low- to the high-mass limits, and at this mass point the limits are shown for both analyses. The production of top squarks decaying via λ''_{312} into light-flavor jets is excluded at 95% CL for top squark masses from 200 to 350 GeV. Stops decaying via λ''_{323} coupling, thus leading to a heavy-flavor jet, are excluded for masses between 200 and 385 GeV.

9. Conclusions

Results of searches for signatures of prompt R-parity violation at 8 TeV at LHC experiments have probed RPV SUSY at the highest collider energies so far. No significant deviations have been found in the corresponding ATLAS and CMS analyses, implying strong constraints on superpartner masses and/or RPV couplings. A common assumption for many interpretations are $\tilde{\chi}_1^0$ LSPs with varying assumptions on dominant R-parity-violating couplings and in particular NLSP types. Using simplified models with RPC production of NLSPs and subsequent decays via LSPs and *LLE* interactions, the following approximate upper limits on superpartner masses have been obtained:

(i) Gluino masses $m(\tilde{g}) > 950$ GeV.

(ii) Light stop masses $m(\tilde{t}_1) > 820$ GeV.

(iii) Wino-like chargino masses $m(\tilde{\chi}_1^{\pm}) > 450$ GeV.

(iv) Charged slepton masses $m(\tilde{l}) > 240$ GeV.

(v) Sneutrino masses $m(\tilde{\nu}) > 400$ GeV.

Resonance searches have mainly focused on analyzing heavy narrow resonances of tau-sneutrinos, excluding masses up to 2.0 TeV, thus extending previous limits from Tevatron significantly. Limits based on dominant *LQD* couplings have been investigated in models with stop-pair production, constraining stop masses up to 1 TeV. Relaxing the assumption of dominance of a single R-parity-violating coupling has, for example, been investigated in the *UDD* multijet analysis by ATLAS: Variation of corresponding branching ratios to different heavy quarks has led to upper limits of gluino masses within the range 666 GeV $< m(\tilde{g}) <$ 929 GeV. In contrast to trilinear RPV models, searches for bilinear RPV have assumed mSUGRA boundary conditions, yielding the first collider-based observed limits for bRPV models: requiring mSUGRA parameters consistent with the observed mass of the Higgs boson, limits from bRPV searches exclude gluino masses in that model around 1.3 TeV.

The strongest model-independent limits for observed visible cross sections have been derived at approximately 0.2 fb. It is interesting to note that such a strong constraint has been obtained in the following searches:

(i) Multileptons in SRs requiring at least three light leptons.

(ii) Same-sign or three leptons in combination with at least three b-jets.

(iii) Two hadronically decaying taus in conjunction with jets and E_T^{miss}.

(iv) Seven jets, with p_T above 180 GeV and one b-tagged jet.

Summarizing the relevant signal regions defined for these searches at the ATLAS and CMS experiments also facilitates identifying possible new targets for future analysis optimization. This should include improved reconstruction of highly collimated objects with low E_T^{miss}, relevant in scenarios predicting strongly boosted final states.

Obviously the whole parameter space of RPV SUSY has not been covered in LHC searches. Various options in particular for investigating *LQD* couplings remain and should be subject of systematic studies. Indeed most of the limits for prompt RPV from Run I have been obtained assuming either *LLE* or *UDD* couplings in simplified models. Therefore it would be interesting not only to vary the types of RPV couplings, but also to consider approaches for studying complete SUSY mass spectra with different R-parity-violating couplings. As an example, extending pMSSM models with RPV decays would lead to significantly different final states topologies in comparison to the RPC-based pMSSM models analyzed frequently. Also considering alternative options for the nature of both the NLSP and the LSP would modify some of the model-dependent results mentioned before. As an example, the assumption of a stau LSP has only been investigated in the analysis of 7 TeV data implying different final states with respect to $\tilde{\chi}_1^0$ LSPs. It would also be interesting to search for various types of heavy sparticle RPV resonances using the increased future energies at the LHC.

Since the largest cross sections are predicted for supersymmetric strong production processes for LHC Run II, signatures from gluino and/or squark production typically offer high potential for future RPV searches. Increasing the luminosity will also enhance the sensitivity for searches focusing on electroweak production processes. Ultimately,

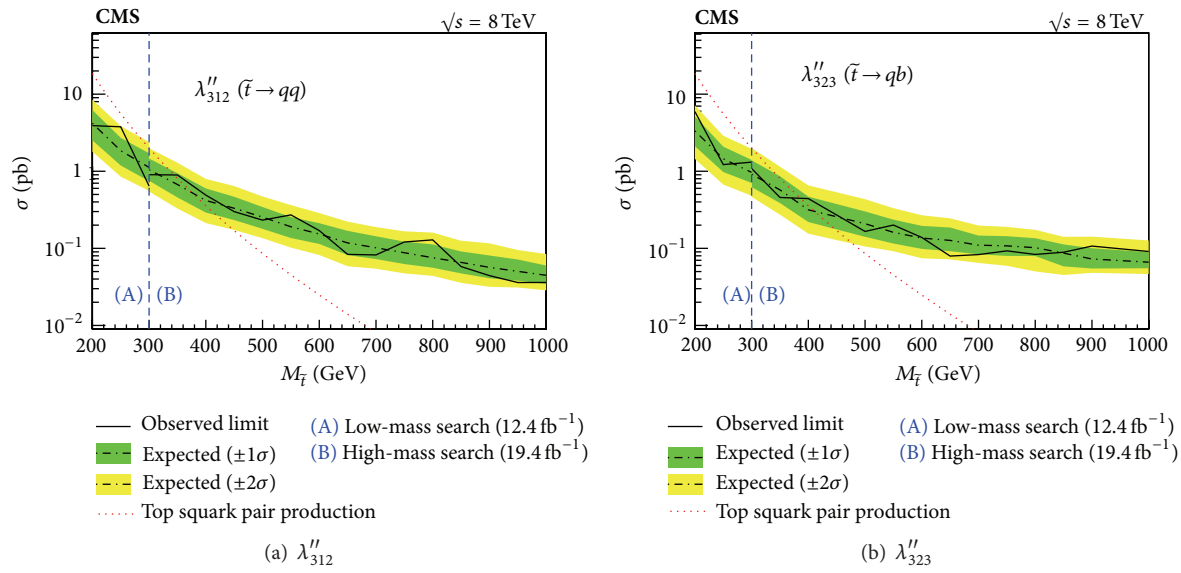

FIGURE 19: Observed and expected 95% CL cross section limits as a function of top squark mass for the inclusive (a) and heavy-flavor (b) searches for R-parity-violating stop decays (from [47]).

the results for RPV SUSY in Run II can become crucial for the question of supersymmetry at the weak scale.

Conflict of Interests

The author declares that there is no conflict of interests regarding the publication of this paper.

Acknowledgments

The author is grateful to J. Boyd, M. Flowerdew, T. Lari, and V. Mitsou for their comments on this paper. This work was supported by the German BMBF within the research network FSP-101 "Physics on the TeV Scale with ATLAS at the LHC" and by the German Helmholtz Alliance "Physics at the Terascale."

References

[1] H. Miyazawa, "Baryon number changing currents," *Progress of Theoretical Physics*, vol. 36, no. 6, pp. 1266–1276, 1966.

[2] P. Ramond, "Dual theory for free fermions," *Physical Review D*, vol. 3, pp. 2415–2418, 1971.

[3] Y. A. Gol'fand and E. P. Likhtman, "Extension of the algebra of Poincaré group generators and violation of P invariance," *JETP Letters*, vol. 13, pp. 323–326, 1971, *Pisma Zhurnal Eksperimentalnoi i Teoreticheskoi Fiziki*, vol. 13, pp. 452–455, 1971.

[4] A. Neveu and J. H. Schwarz, "Factorizable dual model of pions," *Nuclear Physics B*, vol. 31, no. 1, pp. 86–112, 1971.

[5] A. Neveu and J. H. Schwarz, "Quark model of dual pions," *Physical Review D*, vol. 4, no. 4, pp. 1109–1111, 1971.

[6] J.-L. Gervais and B. Sakita, "Field theory interpretation of supergauges in dual models," *Nuclear Physics, Section B*, vol. 34, no. 2, pp. 632–639, 1971.

[7] D. V. Volkov and V. P. Akulov, "Is the neutrino a goldstone particle?" *Physics Letters B*, vol. 46, no. 1, pp. 109–110, 1973.

[8] J. Wess and B. Zumino, "A lagrangian model invariant under supergauge transformations," *Physics Letters B*, vol. 49, no. 1, pp. 52–54, 1974.

[9] J. Wess and B. Zumino, "Supergauge transformations in four dimensions," *Nuclear Physics B*, vol. 70, no. 1, pp. 39–50, 1974.

[10] S. Dimopoulos and H. Georgi, "Softly broken supersymmetry and SU(5)," *Nuclear Physics B*, vol. 193, no. 1, pp. 150–162, 1981.

[11] E. Witten, "Dynamical breaking of supersymmetry," *Nuclear Physics B*, vol. 188, no. 3, pp. 513–554, 1981.

[12] M. Dine, W. Fischler, and M. Srednicki, "Supersymmetric technicolor," *Nuclear Physics, Section B*, vol. 189, no. 3, pp. 575–593, 1981.

[13] S. Dimopoulos and S. Raby, "Supercolor," *Nuclear Physics B*, vol. 192, no. 2, pp. 353–368, 1981.

[14] N. Sakai, "Naturalnes in supersymmetric GUTS," *Zeitschrift für Physik C*, vol. 11, no. 2, pp. 153–157, 1981.

[15] R. K. Kaul and P. Majumdar, "Cancellation of quadratically divergent mass corrections in globally supersymmetric spontaneously broken gauge theories," *Nuclear Physics B*, vol. 199, no. 1, pp. 36–58, 1982.

[16] R. Barbieri and G. F. Giudice, "Upper bounds on supersymmetric particle masses," *Nuclear Physics B*, vol. 306, no. 1, pp. 63–76, 1988.

[17] B. de Carlos and J. Casas, "One-loop analysis of the electroweak breaking in supersymmetric models and the fine-tuning problem," *Physics Letters B*, vol. 309, no. 3-4, pp. 320–328, 1993.

[18] P. Fayet, "Supersymmetry and weak, electromagnetic and strong interactions," *Physics Letters B*, vol. 64, no. 2, pp. 159–162, 1976.

[19] P. Fayet, "Spontaneously broken supersymmetric theories of weak, electromagnetic and strong interactions," *Physics Letters B*, vol. 69, no. 4, pp. 489–494, 1977.

[20] G. R. Farrar and P. Fayet, "Phenomenology of the production, decay, and detection of new hadronic states associated with supersymmetry," *Physics Letters B*, vol. 76, no. 5, pp. 575–579, 1978.

[21] P. Fayet, "Relations between the masses of the superpartners of leptons and quarks, the goldstino coupling and the neutral currents," *Physics Letters B*, vol. 84, no. 4, pp. 416–420, 1979.

[22] R. Barbier, C. Bérat, M. Besançon et al., "*R*-parity-violating supersymmetry," *Physics Reports*, vol. 420, pp. 1–202, 2005.

[23] B. Allanach and B. Gripaios, "Hide and seek with natural supersymmetry at the LHC," *Journal of High Energy Physics*, vol. 2012, no. 5, article 062, 2012.

[24] M. Asano, K. Rolbiecki, and K. Sakurai, "Can R-parity violation hide vanilla supersymmetry at the LHC?" *Journal of High Energy Physics*, vol. 2013, no. 1, article 128, 2013.

[25] H. Dreiner and G. G. Ross, "R-parity violation at hadron colliders," *Nuclear Physics B*, vol. 365, no. 3, pp. 597–613, 1991.

[26] H. Dreiner, F. Staub, A. Vicente, and W. Porod, "General MSSM signatures at the LHC with and without *R*-parity," *Physical Review D*, vol. 86, no. 3, Article ID 035021, 16 pages, 2012.

[27] P. W. Graham, S. Rajendran, and P. Saraswat, "Supersymmetric crevices: missing signatures of *R*-parity violation at the LHC," *Physical Review D*, vol. 90, Article ID 075005, 2014.

[28] C. Brust, P. Maksimovic, A. Sady, P. Saraswat, M. T. Walters, and Y. Xin, "Identifying boosted new physics with non-isolated leptons," *Journal of High Energy Physics*, vol. 2015, no. 4, article 079, 2015.

[29] J. Berger, M. Perelstein, M. Saelim, and P. Tanedo, "The same-sign dilepton signature of RPV/MFV SUSY," *Journal of High Energy Physics*, vol. 2013, no. 4, article 77, 2013.

[30] M. Saelim and M. Perelstein, "RPV SUSY with same-sign dileptons at LHC-14," http://arxiv.org/abs/1309.7707.

[31] J. A. Evans and Y. Kats, "LHC searches examined via the RPV MSSM," in *Proceedings of the the European Physical Society Conference on High Energy Physics (EPS-HEP '13)*, p. 287, 2013.

[32] C. Brust, A. Katz, and R. Sundrum, "SUSY stops at a bump," *Journal of High Energy Physics*, vol. 2012, no. 8, article 059, 2012.

[33] R. Franceschini and R. Torre, "RPV stops bump off the background," *The European Physical Journal C*, vol. 73, article 2422, 2013.

[34] J. A. Evans, Y. Kats, D. Shih, and M. J. Strassler, "Toward full LHC coverage of natural supersymmetry," *Journal of High Energy Physics*, vol. 2014, no. 7, article 101, 2014.

[35] M. Lisanti, P. Schuster, M. Strassler, and N. Toro, "Study of LHC searches for a lepton and many jets," *Journal of High Energy Physics*, vol. 2012, article 81, 2012.

[36] S. P. Martin, "A supersymmetry primer," *Adv.Ser.Direct.High Energy Phys*, vol. 21, Article ID 9709356, pp. 1–153, 2010.

[37] E. Halkiadakis, G. Redlinger, and D. Shih, "Status and implications of beyond-the-standard-model searches at the LHC," *Annual Review of Nuclear and Particle Science*, vol. 64, pp. 319–342, 2014.

[38] G. Aad, B. Abbott, J. Abdallah et al., "Search for supersymmetry at $N\sqrt{s} = 8$ TeV in final states with jets and two same-sign leptons or three leptons with the ATLAS detector," *Journal of High Energy Physics*, vol. 2014, no. 6, article 035, 2014.

[39] G. Aad, B. Abbott, J. Abdallah et al., "Search for supersymmetry in events with large missing transverse momentum, jets, and at least one tau lepton in 20 fb^{-1} of $\sqrt{s} = 8$ TeV proton-proton collision data with the ATLAS detector," *Journal of High Energy Physics*, vol. 2014, no. 9, article 103, 2014.

[40] G. Aad, B. Abbott, J. Abdallah et al., "Search for supersymmetry in events with four or more leptons in $\sqrt{s} = 8$ TeV pp collisions with the ATLAS," *Physical Review D*, vol. 90, Article ID 052001, 2014.

[41] S. Chatrchyan, V. Khachatryan, A. M. Sirunyan et al., "Search for top squarks in *R*-parity-violating supersymmetry using three or more leptons and *b*-tagged jets," *Physical Review Letters*, vol. 111, Article ID 221801, 2013.

[42] CMS Collaboration, "Search for pair production of third-generation scalar leptoquarks and top squarks in proton-proton collisions at $\sqrt{s} = 8$ TeV," *Physics Letters B*, vol. 739, pp. 229–249, 2014.

[43] G. Aad, B. Abbott, J. Abdallah et al., "Search for a heavy neutral particle decaying to $e\mu$, $e\tau$, or $\mu\tau$ in pp collisions at $\sqrt{s} = 8$ TeV with the ATLAS detector," *Physical Review Letters*, vol. 115, no. 3, Article ID 031801, 18 pages, 2015.

[44] G. Aad, B. Abbott, J. Abdallah et al., "Search for massive supersymmetric particles decaying to many jets using the ATLAS detector in pp collisions at $\sqrt{s} = 8$ TeV," *Physical Review D*, vol. 91, no. 11, Article ID 112016, 2015.

[45] S. Chatrchyan, V. Khachatryan, A. M. Sirunyan et al., "Searches for light- and heavy-flavour three-jet resonances in pp collisions at $\sqrt{s} = 8$ TeV," *Physics Letters B*, vol. 730, pp. 193–214, 2014.

[46] S. Chatrchyan, V. Khachatryan, A. M. Sirunyan et al., "Search for new physics in events with same-sign dileptons and jets in pp collisions at $\sqrt{s} = 8$ TeV," *Journal of High Energy Physics*, vol. 2014, article 163, 2014.

[47] V. Khachatryan, A. M. Sirunyan, A. Tumasyan et al., "Search for pair-produced resonances decaying to jet pairs in proton–proton collisions at $\sqrt{s} = 8$ TeV," *Physics Letters B*, vol. 747, pp. 98–119, 2015.

[48] H. Dreiner and S. Grab, "All possible lightest supersymmetric particles in R−parity violating mSUGRA models and their signals at the LHC," in *Proceedings of the 7th International Conference on Supersymmetry and the Unification of Fundamental Interactions (SUSY '08)*, vol. 1200 of *AIP Conference Proceedings*, pp. 358–361, Boston, Mass, USA, June 2008.

[49] M. Hirsch and W. Porod, "Neutrino properties and the decay of the lightest supersymmetric particle," *Physical Review D*, vol. 68, Article ID 115007, 2003.

[50] D. Lopez-Fogliani and C. Muñoz, "Proposal for a supersymmetric standard model," *Physical Review Letters*, vol. 97, no. 4, Article ID 041801, 4 pages, 2006.

[51] V. A. Mitsou, "Exploring neutrino physics at LHC via *R*-parity violating SUSY," *Journal of Physics: Conference Series*, vol. 631, Article ID 012074, 2015.

[52] C. Csáki, Y. Grossman, and B. Heidenreich, "Minimal flavor violation supersymmetry: a natural theory for *R*-parity violation," *Physical Review D*, vol. 85, no. 9, Article ID 095009, 22 pages, 2012.

[53] R. N. Mohapatra, "Supersymmetry and R-parity: an overview," *Physica Scripta*, vol. 90, no. 8, Article ID 088004, 2015.

[54] Y. Kao and T. Takeuchi, "Single-coupling bounds on *R*-parity violating supersymmetry, an update," http://arxiv.org/abs/0910.4980.

[55] H. K. Dreiner, "An introduction to explicit *R*-parity violation," *Pramana*, vol. 51, no. 1-2, pp. 123–133, 1998.

[56] I. Hinchliffe and T. Kaeding, "*B*- and *L*-violating couplings in the minimal supersymmetric standard model," *Physical Review D*, vol. 47, no. 1, pp. 279–284, 1993.

[57] The DELPHI Collaboration, "Search for supersymmetric particles assuming R -parity non-conservation in $e^+ e^-$ - collisions at $\sqrt{s} = 192$ to 208 GeV," *The European Physical Journal C—Particles and Fields*, vol. 36, no. 1, pp. 1–23, 2004.

[58] G. Abbiendi, C. Ainsley, P. Åkesson et al., "Search for R-parity violating decays of sfermions at LEP," *The European Physical Journal C*, vol. 33, pp. 149–172, 2004.

[59] A. Heister, S. Schael, R. Barate et al., "Search for supersymmetric particles with R-parity violating decays in e^+e^- collisions at $\sqrt{s}$ up to 209 GeV," *The European Physical Journal C*, vol. 31, no. 1, pp. 1–16, 2003.

[60] N. Sousa and A. N. Schellekens, "Orientation matters for NIMreps," *Nuclear Physics B*, vol. 653, no. 3, pp. 339–368, 2003.

[61] P. Achard, O. Adriani, M. Aguilar-Benite et al., "Search for R-parity violating decays of supersymmetric particles in e^+e^- collisions at LEP," *Physics Letters B*, vol. 524, no. 1-2, pp. 65–80, 2002.

[62] The DELPHI Collaboration, "Searches for supersymmetric particles in e^+ e^- collisions up to 208 GeV and interpretation of the results within the MSSM," *The European Physical Journal C—Particles and Fields*, vol. 31, no. 4, pp. 421–479, 2003.

[63] H1 Collaboration, "A search for squarks of Rp-violating SUSY at HERA," *Zeitschrift für Physik C*, vol. 71, pp. 211–226, 1996.

[64] H1 Collaboration, C. Adloff, V. Andreev, B. Andrieu et al., "Searches at HERA for squarks in R-parity violating supersymmetry," *The European Physical Journal C—Particles and Fields*, vol. 20, no. 4, pp. 639–657, 2001.

[65] D. Boscherini, "Results on searches beyond the standard model at HERA," http://arxiv.org/abs/hep-ex/0205101.

[66] M. Schneider, "Search for new particles at HERA," http://arxiv.org/abs/hep-ex/0201042.

[67] B. Allanach, H. Baer, S. Banerjee et al., "Searching for R-parity violation at run-II of the tevatron," http://arxiv.org/abs/hep-ph/9906224.

[68] V. M. Abazov, B. Abbott, M. Abolins et al., "Search for R-parity violating supersymmetry via the $LL\overline{E}$ couplings λ_{121}, λ_{122} or λ_{133} in $p\overline{p}$ collisions at $\sqrt{s}$ = 1.96 TeV," *Physics Letters B*, vol. 638, no. 5-6, pp. 441–449, 2006.

[69] A. Abulencia, J. Adelman, T. Affolder et al., "Search for anomalous production of multilepton events in $p\overline{p}$ collisions at $\sqrt{s}$ = 1.96 TeV," *Physical Review Letters*, vol. 98, Article ID 131804, 2007.

[70] T. Aaltonen, B. Álvarez González, S. Amerio et al., "First search for multijet resonances in $\sqrt{s}$ = 1.96 TeV $\overline{p}p$ collisions," *Physical Review Letters*, vol. 107, no. 4, Article ID 042001, 7 pages, 2011.

[71] T. Aaltonen, S. Amerio, D. Amidei et al., "Search for pair-production of strongly-interacting particles decaying to pairs of jets in $p\overline{p}$ collisions at $\sqrt{s}$ = 1.96 TeV," *Physical Review Letters*, vol. 111, no. 3, Article ID 031802, 2013.

[72] Y. Tu, "Search for high-mass resonances decaying into leptons of different flavor ($e\mu, e\tau, \mu\tau$)," http://arxiv.org/abs/0809.0296.

[73] T. Aaltonen, J. Adelman, B. Á. González et al., "Search for R-parity violating decays of sneutrinos to $e\mu$, $\mu\tau$, and $e\tau$ pairs in $p\overline{p}$ collisions at $\sqrt{s}$ = 1.96 TeV," *Physical Review Letters*, vol. 105, Article ID 191801, 2010.

[74] V. M. Abazov, B. Abbott, M. Abolins et al., "Search for sneutrino production in $e\mu$ final states in 5.3 fb^{-1} of $p\overline{p}$ collisions at $\sqrt{s}$ = 1.96 TeV," *Physical Review Letters*, vol. 105, Article ID 191802, 2010.

[75] A. Datta, B. Mukhopadhyaya, and F. Vissani, "Tevatron signatures of an R-parity violating supersymmetric theory," *Physics Letters B*, vol. 492, no. 3-4, pp. 324–330, 2000.

[76] M. Magro, F. de Campos, O. Eboli, W. Porod, D. Restrepo, and J. W. F. Valle, "Probing neutrino mass with multilepton production at the Tevatron in the simplest R-parity violation model," *Journal of High Energy Physics*, vol. 2003, no. 9, article 071, 2003.

[77] F. de Campos, O. J. P. Éboli, M. B. Magro, W. Porod, D. Restrepo, and J. W. F. Valle, "Probing neutrino mass with displaced vertices at the Fermilab Tevatron," *Physical Review D*, vol. 71, Article ID 075001, 2005.

[78] G. Aad, B. Abbott, J. Abdallah et al., "Searches for heavy long-lived charged particles with the ATLAS detector in proton-proton collisions at $\sqrt{s}$ = 8 TeV," *Journal of High Energy Physics*, vol. 2015, article 68, 2015.

[79] ATLAS Collaboration, "Search for long-lived, heavy particles in final states with a muon and a multi-track displaced vertex in proton-proton collisions at sqrt(s) = 8TeV with the ATLAS detector," Tech. Rep. ATLAS-CONF-2013-092, 2013, http://cds.cern.ch/record/1595755.

[80] G. Aad, B. Abbott, J. Abdallah et al., "Search for nonpointing and delayed photons in the diphoton and missing transverse momentum final state in 8 TeV pp collisions at the LHC using the ATLAS detector," *Physical Review D*, vol. 90, no. 11, Article ID 112005, 2014.

[81] G. Aad, T. Abajyan, B. Abbott et al., "Search for charginos nearly mass-degenerate with the lightest neutralino based on a disappearing-track signature in pp collisions at $\sqrt{(s)}$ = 8 TeV with the ATLAS detector," *Physical Review D*, vol. 88, no. 11, Article ID 112006, 23 pages, 2013.

[82] G. Aad, T. Abajyan, B. Abbott et al., "Search for long-lived stopped R-hadrons decaying out of time with pp collisions using the ATLAS detector," *Physical Review D*, vol. 88, no. 11, Article ID 112003, 2013.

[83] S. Chatrchyan, V. Khachatryan, A. M. Sirunyan et al., "Searches for long-lived charged particles in pp collisions at $\sqrt{s}$ = 7 and 8 TeV," *Journal of High Energy Physics*, vol. 2013, no. 7, article 122, 2013.

[84] CMS Collaboration, "Search for long-lived particles in events with photons and missing energy in proton-proton collisions at $\sqrt{s}$ = 7 TeV," *Physics Letters B*, vol. 722, no. 4-5, pp. 273–294, 2013.

[85] V. Khachatryan, A. M. Sirunyan, A. Tumasyan et al., "Search for displaced supersymmetry in events with an electron and a muon with large impact parameters," *Physical Review Letters*, vol. 114, no. 6, Article ID 061801, 2015.

[86] V. Khachatryan, A. M. Sirunyan, A. Tumasyan et al., "Search for long-lived neutral particles decaying to quark-antiquark pairs in proton-proton collisions at $\sqrt{s}$ = 8 TeV," *Physical Review D*, vol. 91, no. 1, Article ID 012007, 21 pages, 2015.

[87] V. Khachatryan, A. M. Sirunyan, A. Tumasyan et al., "Search for decays of stopped long-lived particles produced in proton-proton collisions at $\sqrt{s}$ = 8 TeV," *The European Physical Journal C*, vol. 75, article 151, 2015.

[88] Z. Liu and B. Tweedie, "The fate of long-lived superparticles with hadronic decays after LHC Run 1," *Journal of High Energy Physics*, vol. 2015, no. 6, article 042, 2015.

[89] G. Aad, E. Abat, J. Abdallah et al., "The ATLAS experiment at the CERN large Hadron collider," *Journal of Instrumentation*, vol. 3, Article ID S08003, 2008.

[90] S. Chatrchyan, G. Hmayakyan, V. Khachatryan et al., "The CMS experiment at the CERN LHC," *Journal of Instrumentation*, vol. 3, Article ID S08004, 2008.

[91] M. Bähr, S. Gieseke, M. A. Gigg et al., "Herwig++ physics and manual," *The European Physical Journal C*, vol. 58, no. 4, pp. 639–707, 2008.

[92] T. Sjöstrand, S. Mrenna, and P. Z. Skands, "PYTHIA 6.4 physics and manual," *Journal of High Energy Physics*, vol. 2006, no. 5, article 026, 2006.

[93] T. Sjöstrand, S. Mrenna, and P. Z. Skands, "A brief introduction to PYTHIA 8.1," *Computer Physics Communications*, vol. 178, no. 11, pp. 852–867, 2008.

[94] W. Beenakker, R. Höpker, M. Spira, and P. Zerwas, "Squark and gluino production at hadron colliders," *Nuclear Physics B*, vol. 492, pp. 51–103, 1997.

[95] A. Kulesza and L. Motyka, "Threshold resummation for squark-antisquark and gluino-pair production at the LHC," *Physical Review Letters*, vol. 102, no. 11, Article ID 111802, 4 pages, 2009.

[96] A. Kulesza and L. Motyka, "Soft gluon resummation for the production of gluino-gluino and squark-antisquark pairs at the LHC," *Physical Review D*, vol. 80, no. 9, Article ID 095004, 23 pages, 2009.

[97] W. Beenakker, S. Brensing, M. Kramer et al., "Soft-gluon resummation for squark and gluino hadroproduction," *Journal of High Energy Physics*, vol. 2009, no. 12, article 041, 2009.

[98] W. Beenakker, S. Brensing, M. Krämer et al., "Squark and gluino hadroproduction," *International Journal of Modern Physics A*, vol. 26, no. 16, pp. 2637–2664, 2011.

[99] M. Kramer, A. Kulesza, R. van der Leeuw et al., "Supersymmetry production cross sections in pp collisions at $\sqrt{s} = 7$ TeV," http://arxiv.org/abs/1206.2892.

[100] S. S. AbdusSalam, B. C. Allanach, F. Quevedo, F. Feroz, and M. Hobson, "Fitting the phenomenological MSSM," *Physical Review D*, vol. 81, no. 9, Article ID 095012, 31 pages, 2010.

[101] A. Arbey, M. Battaglia, A. Djouadi, and F. Mahmoudi, "An update of the constraints on the phenomenological MSSM from the new LHC Higgs results," *Physics Letters B*, vol. 720, pp. 153–160, 2013.

[102] B. Dumont, J. F. Gunion, and S. Kraml, "Phenomenological MSSM in view of the 125 GeV Higgs data," *Physical Review D*, vol. 89, Article ID 055018, 2014.

[103] J. Alwall, P. C. Schuster, and N. Toro, "Simplified models for a first characterization of new physics at the LHC," *Physical Review D*, vol. 79, Article ID 075020, 2009.

[104] D. Alves, N. Arkani-Hamed, S. Arora et al., "Simplified models for LHC new physics searches," *Journal of Physics G*, vol. 39, Article ID 105005, 2012.

[105] A. H. Chamseddine, R. L. Arnowitt, and P. Nath, "Locally supersymmetric grand unification," *Physical Review Letters*, vol. 49, no. 14, pp. 970–974, 1982.

[106] R. Barbieri, S. Ferrara, and C. A. Savoy, "Gauge models with spontaneously broken local supersymmetry," *Physics Letters B*, vol. 119, no. 4-6, pp. 343–347, 1982.

[107] L. E. Ibáñez, "Locally supersymmetric SU(5) grand unification," *Physics Letters B*, vol. 118, no. 1–3, pp. 73–78, 1982.

[108] L. Hall, J. Lykken, and S. Weinberg, "Supergravity as the messenger of supersymmetry breaking," *Physical Review D*, vol. 27, no. 10, pp. 2359–2378, 1983.

[109] N. Ohta, "Grand unified theories based on local supersymmetry," *Progress of Theoretical Physics*, vol. 70, no. 2, pp. 542–549, 1983.

[110] G. L. Kane, C. Kolda, L. Roszkowski, and J. D. Wells, "Study of constrained minimal supersymmetry," *Physical Review D*, vol. 49, no. 11, pp. 6173–6210, 1994.

[111] M. Dine and W. Fischler, "A phenomenological model of particle physics based on supersymmetry," *Physics Letters B*, vol. 110, no. 3-4, pp. 227–231, 1982.

[112] L. Alvarez-Gaumé, M. Claudson, and M. B. Wise, "Low-energy supersymmetry," *Nuclear Physics B*, vol. 207, no. 1, pp. 96–110, 1982.

[113] C. R. Nappi and B. A. Ovrut, "Supersymmetric extension of the SU(3)×SU(2)×U(1) model," *Physics Letters B*, vol. 113, pp. 175–179, 1982.

[114] M. Dine and A. E. Nelson, "Dynamical supersymmetry breaking at low energies," *Physical Review D*, vol. 48, no. 3, pp. 1277–1287, 1993.

[115] M. Dine, A. E. Nelson, and Y. Shirman, "Dynamical supersymmetry breaking simplified," *Physical Review D*, vol. 51, pp. 1362–1370, 1995.

[116] M. Dine, A. E. Nelson, Y. Nir, and Y. Shirman, "New tools for low energy dynamical supersymmetry breaking," *Physical Review D*, vol. 53, no. 5, pp. 2658–2669, 1996.

[117] A. L. Read, "Presentation of search results: the CL_s technique," *Journal of Physics G: Nuclear and Particle Physics*, vol. 28, no. 10, pp. 2693–2704, 2002.

[118] G. Cowan, K. Cranmer, E. Gross, and O. Vitells, "Asymptotic formulae for likelihood-based tests of new physics," *The European Physical Journal C*, vol. 71, article 1554, 2011.

[119] The ATLAS Collaboration, "A search for B–L R-Parity violating scalar top decays in $\sqrt{s} = 8$ TeV pp collisions with the ATLAS experiment," Tech. Rep. ATLAS-CONF-2015-015, ATLAS-COM-CONF-2015-017, 2015.

[120] A. Hook, E. Izaguirre, M. Lisanti, and J. G. Wacker, "High multiplicity searches at the LHC using jet masses," *Physical Review D*, vol. 85, Article ID 055029, 2012.

[121] S. El Hedri, A. Hook, M. Jankowiak, and J. G. Wacker, "Learning how to count: a high multiplicity search for the LHC," *Journal of High Energy Physics*, vol. 2013, no. 8, article 136, 2013.

[122] T. Cohen, M. Jankowiak, M. Lisanti, H. K. Lou, and J. G. Wacker, "Jet substructure templates: data-driven QCD backgrounds for fat jet searches," *Journal of High Energy Physics*, vol. 2014, no. 5, article 005, 2014.

[123] S. Chatrchyan, V. Khachatryan, A. M. Sirunyan et al., "Search for pair-produced dijet resonances in four-jet final states in pp collisions at $\sqrt{s} = 7$ TeV," *Physical Review Letters*, vol. 110, no. 14, Article ID 141802, 2013.

[124] W. Porod, M. Hirsch, J. Romão, and J. Valle, "Testing neutrino mixing at future collider experiments," *Physical Review D*, vol. 63, no. 11, Article ID 115004, 16 pages, 2001.

[125] M. A. Díaz, M. Hirsch, W. Porod, J. C. Romão, and J. W. F. Valle, "Solar neutrino masses and mixing from bilinear R-parity broken supersymmetry: analytical versus numerical results," *Physical Review D*, vol. 68, Article ID 0302021, 2003, Erratum in: *Physical Review D*, vol. 71, Article ID 059904, 2005.

[126] B. Allanach, C. Balazs, G. Belanger et al., "SUSY Les Houches Accord 2," *Computer Physics Communications*, vol. 180, no. 1, pp. 8–25, 2009.

[127] J. Romao, M. Diaz, M. Hirsch, W. Porod, and J. Valle, "Supersymmetric solution to the solar and atmospheric neutrino problems," *Physical Review D*, vol. 61, Article ID 071703, 2000.

[128] W. Porod, "SPheno, a program for calculating supersymmetric spectra, SUSY particle decays and SUSY particle production at e^+e^- colliders," *Computer Physics Communications*, vol. 153, no. 2, pp. 275–315, 2003.

[129] F. de Campos, O. Eboli, M. Hirsch et al., "Probing neutrino oscillations in supersymmetric models at the Large Hadron Collider," *Physical Review D*, vol. 82, Article ID 075002, 2010.

[130] F. de Campos, O. J. P. Éboli, M. B. Magro et al., "Probing bilinear R-parity violating supergravity at the LHC," *Journal of High Energy Physics*, vol. 2008, no. 5, article 048, 2008.

[131] F. de Campos, O. Eboli, M. Magro et al., "Probing neutralino properties in minimal supergravity with bilinear R-parity violation," *Physical Review D*, vol. 86, no. 7, Article ID 075001, 8 pages, 2012.

[132] G. Aad, B. Abbott, J. Abdallah et al., "Search for squarks and gluinos with the ATLAS detector in final states with jets and missing transverse momentum using $\sqrt{s} = 8$ TeV proton-proton collision data," *Journal of High Energy Physics*, vol. 2014, article 176, 2014.

[133] G. Aad, B. Abbott, J. Abdallah et al., "Search for squarks and gluinos in events with isolated leptons, jets and missing transverse momentum at $\sqrt{s} = 8$ TeV with the ATLAS detector," *Journal of High Energy Physics*, vol. 2015, article 116, 2015.

[134] S. Chatrchyan, V. Khachatryan, A. M. Sirunyan et al., "Search for anomalous production of multilepton events in pp collisions at $\sqrt{s} = 7$ TeV," *Journal of High Energy Physics*, vol. 2012, no. 6, article 169, 2012.

[135] G. Aad, T. Abajyan, B. Abbott et al., "Search for R-parity-violating supersymmetry in events with four or more leptons in $\sqrt{s} = 7$ TeV pp collisions with the ATLAS detector," *Journal of High Energy Physics*, vol. 2012, no. 12, article 124, 2012.

[136] K. Desch, S. Fleischmann, P. Wienemann, H. Dreiner, and S. Grab, "Stau as the lightest supersymmetric particle in R-parity violating SUSY models: discovery potential with early LHC data," *Physical Review D*, vol. 83, no. 1, Article ID 015013, 25 pages, 2011.

[137] CMS Collaboration, CMS-PAS-SUS-13-005, http://cds.cern.ch/record/1547780.

[138] G. Aad, T. Abajyan, B. Abbott et al., "Search for new phenomena in final states with large jet multiplicities and missing transverse momentum at $\sqrt{s} = 8$ TeV proton-proton collisions using the ATLAS experiment," *Journal of High Energy Physics*, vol. 2013, no. 10, article 130, 2013.

Hindawi Publishing Corporation
Advances in High Energy Physics
Volume 2015, Article ID 509847, 16 pages
http://dx.doi.org/10.1155/2015/509847

Research Article

Two Higgs Bosons near 125 GeV in the Complex NMSSM and the LHC Run I Data

Stefano Moretti[1] and Shoaib Munir[2]

[1] *School of Physics & Astronomy, University of Southampton, Southampton SO17 1BJ, UK*
[2] *Asia Pacific Center for Theoretical Physics, San 31, Hyoja-dong, Nam-gu, Pohang 790-784, Republic of Korea*

Correspondence should be addressed to Shoaib Munir; s.munir@apctp.org

Received 24 April 2015; Revised 14 July 2015; Accepted 30 July 2015

Academic Editor: Mark D. Goodsell

We analyse the impact of explicit CP-violation in the Higgs sector of the Next-to-Minimal Supersymmetric Standard Model (NMSSM) on its consistency with the Higgs boson data from the Large Hadron Collider (LHC). Through detailed scans of the parameter space of the complex NMSSM for certain fixed values of one of its CP-violating (CPV) phases, we obtain a large number of points corresponding to five phenomenologically relevant scenarios containing ~125 GeV Higgs boson(s). We focus, in particular, on the scenarios where the visible peaks in the experimental samples can actually be explained by two nearly mass-degenerate neutral Higgs boson states. We find that some points corresponding to these scenarios give an overall slightly improved fit to the data, more so for nonzero values of the CPV phase, compared to the scenarios containing a single Higgs boson near 125 GeV.

1. Introduction

The Higgs sector of the NMSSM [1–4] (see, e.g., [5, 6] for reviews) contains two additional neutral mass eigenstates besides the three of the Minimal Supersymmetric Standard Model (MSSM). This is due to the presence of a Higgs singlet superfield besides the two doublet superfields of the MSSM. When all the parameters in the Higgs and sfermion sectors of the NMSSM are real, one of these new Higgs states is a scalar and the other a pseudoscalar. Hence, in total three scalars, $H_{1,2,3}$, and two pseudoscalars, $A_{1,2}$, make up the neutral Higgs boson content of the model. This extended Higgs sector of the NMSSM boasts some unique phenomenological possibilities, which are either precluded or experimentally ruled out in the MSSM. For example, in the NMSSM either of the two lightest CP-even Higgs bosons, H_1 or H_2, can play the role of the ~125 GeV Standard Model- (SM-) like Higgs boson, $H_{\rm obs}$, observed at the LHC [7–9].

Of particular interest in the NMSSM is the possibility that the SM-like Higgs boson can obtain a large tree-level mass in a *natural* way, that is, without requiring large radiative corrections from the supersymmetric sectors. This happens in a specific region of the parameter space, which we refer to as the natural NMSSM, where there is a significant singlet-doublet mixing and $H_{\rm obs}$ is typically H_2. This scenario was used to explain [10–12] the enhancement in $H_{\rm obs} \to \gamma\gamma$ channel in the early LHC data. However, when the singlet-doublet mixing is too large, the properties of H_2 can deviate appreciably from an exact SM-like behaviour, resulting in a reduction of its fermionic partial decay widths. An alternative possibility in a very similar parameter space region is that of both H_1 and H_2 simultaneously having masses near 125 GeV [13–16]. In that case, the observed excess at the LHC could actually be due to a superposition of these two states, when their individual signal peaks cannot be resolved separately. One of these two Higgs bosons, typically H_1, is the singlet-like neutral state. Moreover, in [17] it was noted that the lighter one of the two pseudoscalars, A_1, when it is singlet-like, could also be nearly mass-degenerate with a SM-like H_1 near 125 GeV, instead of or even along with H_2. However, such a pseudoscalar can only contribute visibly to the measured signal strength near 125 GeV if it is produced in association with $b\bar{b}$ pair.

One of the most important yet unresolved issues in particle physics is that of the observed matter-antimatter

asymmetry in the universe. A plausible explanation for this asymmetry is electroweak (EW) baryogenesis [18, 19]. The necessary conditions for successful EW baryogenesis include the following [20]: (1) baryon number violation, (2) CP-violation, and (3) departure from equilibrium at the critical temperature of the EW symmetry breaking (EWSB) phase transition, implying that it is strongly first order. In the SM, a strongly first order EW phase transition is not possible given the measured mass of the Higgs boson at the LHC. Besides, the only source of CP-violation in the SM, the Cabibbo-Kobayashi-Maskawa matrix, is insufficient. Therefore, beyond the SM, a variety of sources of CP-violation have been proposed in the literature (for a review, see [21] and references therein). In the context of supersymmetry (SUSY), a strongly first order phase transition is possible in the MSSM only if the lightest stop has a mass below that of the top quark. This possibility has now been ruled out by SUSY searches at the LHC [22–24]. Also, the MSSM Higgs sector does not violate CP at the tree level but does so only at higher orders [25–32]. The CPV phases, transmitted radiatively to the Higgs sector via couplings to the sfermions, are tightly constrained by the measurements of fermion electric dipole moments (EDMs) [33–35]. However, these EDM constraints can be relaxed under certain conditions [27, 28, 36–41].

The NMSSM has been shown to accommodate a strongly first order EW phase transition without a light stop [42–47]. Additionally, in this model, CP-violation can be invoked explicitly in the Higgs sector even at the tree level by assuming the Higgs self-couplings, λ and κ, to be complex. Beyond the Born approximation, the phase of the SUSY-breaking Higgs-sfermion-sfermion couplings, $A_{\tilde{f}}$, where f denotes a SM fermion, is also induced in the Higgs sector, as in the MSSM. In the presence of the associated complex phases, the five neutral Higgs bosons are CP-indefinite states, due to the mixing between the scalar and pseudoscalar interaction eigenstates. CPV phases can therefore influence the phenomenology of the NMSSM Higgs bosons by, for example, modifying their mass spectrum as well as their production and decay rates [48], similarly to the MSSM [49–59]. The impact of these phases in the complex NMSSM (cNMSSM), that is, the CPV NMSSM, on the necessary conditions for successful EW phase transition was also studied some time ago [60]. The consistency of scenarios yielding the correct baryon asymmetry with the LHC Higgs boson data still remains to be studied in depth though. However, even leaving aside these considerations, the possibly distinct phenomenological scenarios that the cNMSSM can yield make it a particularly interesting model for exploration at the Run II of the LHC.

The cNMSSM has therefore been the subject of several studies recently and, in particular, some important theoretical developments have been made in the model. The dominant 1-loop corrections to the neutral Higgs sector from the (s)quark and gauge sectors were studied in [61–64], in the renormalisation group equations-improved effective potential approach. The corrections from the gaugino sector were included in [65] and, more inclusively, recently in [66]. In the Feynman diagrammatic approach, the complete 1-loop Higgs mass matrix was derived in [67] and $\mathcal{O}(\alpha_t\alpha_s)$ contributions to it were calculated in [68]. As far as the phenomenology of the Higgs bosons in the cNMSSM is concerned, the consistency of several CPV scenarios with the early results on H_{obs} from the LHC data was studied in detail in [48, 67]. Another distinct phenomenological scenario, possible only for nonzero CPV phases, has also been studied in [65].

The CMS and ATLAS collaborations have recently updated their measurements of H_{obs} signal rates in $\tau^+\tau^-$ and $b\bar{b}$ channels [69, 70]. The fact that these rates also tend to favour a SM-like H_{obs} is increasingly jeopardising the above-mentioned natural NMSSM scenario with large singlet-doublet mixing but only with one Higgs boson, either H_1 or H_2, around 125 GeV. This makes the scenario with both H_1 and H_2 contributing to the observed ~125 GeV signal all the more important, since it may potentially satisfy better the current Higgs boson data while still leaving plenty of room for new physics. In case of the cNMSSM, since the five neutral Higgs bosons are CP-mixed states, the scenario with mass-degenerate H_1 and H_2 can entail both the corresponding possibilities in the real NMSSM (rNMSSM), that is, mass-degenerate H_1, H_2 or H_1/H_2, A_1.

In this study we therefore analyse and compare the prospects for scenarios with two mass-degenerate Higgs bosons against those with a single Higgs boson near 125 GeV in the Z_3-invariant cNMSSM. We perform scans of the relevant parameter space [13] of the model using the public program NMSSMCALC [71] to search for all possible ~125 GeV Higgs boson scenarios, with the CPV phase of the coupling κ set to five different values, including 0°, the rNMSSM limit, in each case. The condition for mass-degeneracy between two Higgs bosons is imposed by requiring them to lie within 2.5 GeV of each other, which is consistent with the current mass resolution of the LHC [72], taking into account the uncertainties in the theoretical mass prediction. We then use fits to the Higgs boson data from the LHC Run I, both with $\sqrt{s} = 7$ TeV and $\sqrt{s} = 8$ TeV, as well as the Tevatron, performed using the program HiggsSignals [73], as the sole criterion for comparing the present likelihood of each of these scenarios. We also discuss how these mass-degenerate Higgs bosons can be identified at the LHC based on the signal rate double ratios introduced in [74].

The paper is organised as follows. In the next section we will briefly revisit the Higgs sector of the cNMSSM. In Section 3 we will provide details of our numerical scans and our procedure for fitting the model predictions for the Higgs boson(s) to the LHC data. In Section 4 we will discuss the results of our analysis and in Section 5 we will present our conclusions.

2. The Higgs Sector of the cNMSSM

The NMSSM contains a singlet Higgs superfield, $\widehat{S}$, besides the two $SU(2)_L$ doublet superfields,

$$\widehat{H}_u = \begin{pmatrix} \widehat{H}_u^+ \\ \widehat{H}_u^0 \end{pmatrix}, \qquad \widehat{H}_d = \begin{pmatrix} \widehat{H}_d^0 \\ \widehat{H}_d^- \end{pmatrix}, \tag{1}$$

of the MSSM. The superpotential of the NMSSM is written as

$$W_{\mathrm{NMSSM}} = \text{MSSM Yukawa terms} + \lambda \widehat{S} \widehat{H}_u \widehat{H}_d + \frac{\kappa}{3} \widehat{S}^3, \quad (2)$$

where λ and κ are dimensionless Yukawa couplings. This superpotential is scale invariant, since the term $\mu \widehat{H}_u \widehat{H}_d$ appearing in the MSSM superpotential has been removed by imposing a discrete Z_3 symmetry. In this model, an effective μ-term, $\mu_{\mathrm{eff}} = \lambda s$, is instead generated when the singlet field acquires a vacuum expectation value (VEV), s, which is naturally of the order of the SUSY-breaking scale.

The tree-level Higgs potential of the NMSSM, obtained from the superpotential in (2), is written in terms of the neutral scalar components of the Higgs superfields, H_u, H_d, and S, as

$$\begin{aligned} V_0 = & \left| \lambda \left(H_u^+ H_d^- - H_u^0 H_d^0 \right) + \kappa S^2 \right|^2 \\ & + \left(m_{H_u}^2 + |\lambda S|^2 \right) \left(\left| H_u^0 \right|^2 + \left| H_u^+ \right|^2 \right) \\ & + \left(m_{H_d}^2 + |\lambda S|^2 \right) \left(\left| H_d^0 \right|^2 + \left| H_d^- \right|^2 \right) \\ & + \frac{g^2}{4} \left(\left| H_u^0 \right|^2 + \left| H_u^+ \right|^2 - \left| H_d^0 \right|^2 - \left| H_d^- \right|^2 \right)^2 \\ & + \frac{g_2^2}{2} \left| H_u^+ H_d^{0*} + H_u^0 H_d^{-*} \right|^2 + m_S^2 |S|^2 \\ & + \left(\lambda A_\lambda \left(H_u^+ H_d^- - H_u^0 H_d^0 \right) S + \frac{1}{3} \kappa A_\kappa S^3 + \text{h.c.} \right), \end{aligned} \quad (3)$$

where $g^2 \equiv (g_1^2 + g_2^2)/2$, with g_1 and g_2 being the $U(1)_Y$ and $SU(2)_L$ gauge couplings, respectively, and A_λ and A_κ are the soft SUSY-breaking Higgs trilinear couplings. The scalar fields H_u, H_d, and S are developed around their respective VEVs, v_u, v_d, and s, as

$$\begin{aligned} H_d^0 &= \begin{pmatrix} \frac{1}{\sqrt{2}} \left(v_d + H_{dR} + i H_{dI} \right) \\ H_d^- \end{pmatrix}, \\ H_u^0 &= e^{i\theta} \begin{pmatrix} H_u^+ \\ \frac{1}{\sqrt{2}} \left(v_u + H_{uR} + i H_{uI} \right) \end{pmatrix}, \\ S &= \frac{e^{i\varphi}}{\sqrt{2}} \left(s + S_R + i S_I \right). \end{aligned} \quad (4)$$

The Higgs coupling parameters appearing in the potential in (3) can very well be complex, implying $\lambda \equiv |\lambda| e^{i\phi_\lambda}$, $\kappa \equiv |\kappa| e^{i\phi_\kappa}$, $A_\lambda \equiv |A_\lambda| e^{i\phi_{A_\lambda}}$, and $A_\kappa \equiv |A_\kappa| e^{i\phi_{A_\kappa}}$. As a result, V_0, evaluated at the vacuum, contains the phase combinations

$$\begin{aligned} \phi_\lambda' &\equiv \phi_\lambda + \theta + \varphi, \\ \phi_\kappa' &\equiv \phi_\kappa + 3\varphi, \\ & \phi_\lambda' + \phi_{A_\lambda}, \\ & \phi_\kappa' + \phi_{A_\kappa}. \end{aligned} \quad (5)$$

For correct EWSB, the Higgs potential should have a minimum at nonvanishing v_u, v_d, and s, which is ensured by requiring

$$\left\langle \frac{\delta V_0}{\delta \Phi} \right\rangle = 0 \quad \text{for } \Phi = H_{dR}, H_{uR}, S_R, H_{dI}, H_{uI}, S_I. \quad (6)$$

Through the above minimisation conditions the phase combinations $\phi_\lambda' + \phi_{A_\lambda}$ and $\phi_\kappa' + \phi_{A_\kappa}$ can be determined up to a twofold ambiguity by $\phi_\lambda' - \phi_\kappa'$. Thus, $\phi_\lambda' - \phi_\kappa'$ is the only physical CP phase appearing in the NMSSM Higgs sector at the tree level. Also, using these conditions, the soft mass parameters $m_{H_u}^2$, $m_{H_d}^2$, and m_S^2 can be traded for the corresponding Higgs field VEVs.

The neutral Higgs mass matrix is obtained by taking the second derivative of V_0 evaluated at the vacuum. This 5×5 matrix, $\mathscr{M}_0^2$, in the $\mathbf{H}^T = (H_{dR}, H_{uR}, S_R, H_I, S_I)$ basis, from which the massless Nambu-Goldstone mode has been rotated away, can be diagonalised using an orthogonal matrix, O, as $O^T \mathscr{M}_0^2 O = \mathrm{diag}\left(m_{H_1}^2 \;\; m_{H_2}^2 \;\; m_{H_3}^2 \;\; m_{H_4}^2 \;\; m_{H_5}^2 \right)$. This yields the physical tree-level masses corresponding to the five mass eigenstates:

$$\left(H_1, H_2, H_3, H_4, H_5 \right)_a^T = O_{ai} \left(H_{dR}, H_{uR}, S_R, H_I, S_I \right)_i^T, \quad (7)$$

such that $m_{H_1}^2 \leq m_{H_2}^2 \leq m_{H_3}^2 \leq m_{H_4}^2 \leq m_{H_5}^2$. The elements, O_{ai}, of the mixing matrix then govern the couplings of the Higgs bosons to all the particles in the model.

The tree-level Higgs mass matrix is subject to higher order corrections from the SM fermions, from the gauge and chargino/neutralino sectors and the Higgs sector itself, as well as the sfermion sector, in case of which they are dominated by the stop contributions. Upon the inclusion of these corrections, $\Delta\mathscr{M}^2$, the Higgs mass matrix gets modified, so that

$$\mathscr{M}_H^2 = \mathscr{M}_0^2 + \Delta\mathscr{M}^2. \quad (8)$$

Explicit expressions for $\mathscr{M}_0^2$ as well as $\Delta\mathscr{M}^2$ can be found in [65–67]. Thus, beyond the Born approximation, the CPV phases of the gaugino mass parameters, $M_{1,2}$, and of $A_{\tilde{f}}$ are also radiatively induced in the Higgs sector of the NMSSM.

Therefore, when studying the phenomenology of the Higgs bosons, one needs to take into account also the parameters from the other sectors of the model. However, the most general NMSSM contains more than 130 parameters at the EW scale. Assuming the matrices for the sfermion masses and for the trilinear scalar couplings to be diagonal considerably reduces the number of free parameters. One can further exploit the fact, mentioned above, that the corrections to the Higgs boson masses from the sfermions are largely dominated by the stop sector. For our numerical analysis in the following sections, we will thus impose the following

supergravity-inspired universality conditions on the model parameters at the EW scale:

$$M_0 \equiv M_{Q_{1,2,3}} = M_{U_{1,2,3}} = M_{D_{1,2,3}} = M_{L_{1,2,3}} = M_{E_{1,2,3}},$$
$$M_{1/2} \equiv 2M_1 = M_2 = \frac{1}{3}M_3, \quad (9)$$
$$A_0 \equiv A_{\tilde{t}} = A_{\tilde{b}} = A_{\tilde{\tau}},$$

where $M^2_{Q_{1,2,3}}$, $M^2_{U_{1,2,3}}$, $M^2_{D_{1,2,3}}$, $M^2_{L_{1,2,3}}$, and $M^2_{E_{1,2,3}}$ are the squared soft masses of the sfermions, $M_{1,2,3}$ those of the gauginos, and $A_{\tilde{t},\tilde{b},\tilde{\tau}}$ the soft trilinear couplings. Altogether, the input parameters of the cNMSSM then include M_0, $|M_{1/2}|$, $|A_0|$, $\tan\beta(\equiv v_u/v_d)$, $|\lambda|$, $|\kappa|$, μ_{eff}, $|A_\lambda|$, $|A_\kappa|$, $\theta_{1/2}$, $\theta_{\tilde{f}}$, ϕ'_λ, and ϕ'_κ, where $\theta_{1/2}$ and $\theta_{\tilde{f}}$ are the phases of the unified parameters $M_{1/2}$ and A_0, respectively.

3. Numerical Analysis

As noted in the Introduction, nonzero CPV phases can modify appreciably the masses and decay widths of the neutral Higgs bosons compared to the CP-conserving case for a given set of the remaining free parameters. In the case of H_{obs} candidate in the model, whether H_1 or H_2 or even H_3, the CPV phases are thus strongly constrained by the LHC mass and signal rate measurements. This was analysed in detail in [48], where the scenarios with mass-degenerate Higgs bosons were, however, not taken into account. In the present study we thus test whether the said modifications in the Higgs boson properties with nonzero values of the phase ϕ'_κ (by which we imply ϕ_κ, which is the actual physically meaningful phase, since φ can be absorbed into ϕ'_κ by a field redefinition) can lead to a relatively improved consistency with the experimental data.

The reason for choosing ϕ'_κ as the only variable phase while setting $\theta_{1/2}$, $\theta_{\tilde{f}}$, and ϕ'_λ to 0° is that it is virtually unconstrained by the measurements of fermionic EDMs [63, 64, 67]. Furthermore, our aim here is to analyse the scenarios with a generic CPV phase and compare them with the rNMSSM limit rather than measure the effect of any of the individual phases. Note however that since only the difference $\phi'_\lambda - \phi'_\kappa$ enters the Higgs mass matrix at the tree level, the impact of a variation in ϕ'_λ is also quantified by that due to the variation in ϕ'_κ at this level. At higher orders though, a variation in ϕ'_λ has an impact on the sfermion and neutralino/chargino sectors which is independent of ϕ'_κ.

In our numerical analysis, we used the program NMSSMCALC-v1.03 [71] for computing the Higgs boson mass spectrum and decay branching ratios (BRs) for a given model input point. The public distribution of NMSSMCALC contains two separate packages, one for the rNMSSM only and the other for the cNMSSM. Some supersymmetric corrections to the Higgs boson decay widths are currently only available in the rNMSSM and hence are not included in the cNMSSM package. For consistency among our rNMSSM and cNMSSM results, we therefore set $\phi_\kappa = 0°$ in the cNMSSM package for the rNMSSM case instead of using the dedicated rNMSSM package. Furthermore, using the cNMSSM code also for the rNMSSM limit makes it convenient to draw a one-on-one correspondence between $\phi_\kappa = 0°$ case and each of $\phi_\kappa > 0°$ cases in a given scenario. This is because in the cNMSSM package, even in the rNMSSM limit, the five neutral Higgs bosons are ordered by their masses and not separated on the basis of their CP-identities. Thus, the scenario with mass-degenerate H_1, H_2, which we will henceforth refer to as the $H_{\text{obs}} = H_1 + H_2$ scenario, takes into account both the ~125 GeV H_1, H_2 and the ~125 GeV H_1, A_1 solutions of the rNMSSM without distinguishing between them. If one, conversely, uses the rNMSSM package, these two scenarios ought to be considered separately. The same is true also for the $H_{\text{obs}} = H_2 + H_3$ scenario, wherein H_2, H_3 are mass-degenerate.

The program NMSSMCALC allows one the option to include only the complete 1-loop contributions in the Higgs mass matrix or to add also the 2-loop $\mathcal{O}(\alpha_t\alpha_s)$ corrections to it. In our analysis, for a better theoretical precision, we evaluated the Higgs boson masses at the 2-loop level. In the NMSSMCALC input, one also needs to choose between the modified dimensional regularisation ($\overline{\text{DR}}$) and on-shell renormalisation schemes for calculating contributions from the top/stop sector in the program. We opted for the $\overline{\text{DR}}$ scheme for each scenario. Note though that further inclusion of $\mathcal{O}(\alpha_b\alpha_s)$, $\mathcal{O}(\alpha_t + \alpha_b + \alpha_\tau)^2$, and the recently calculated NMSSM-specific $\mathcal{O}(\alpha_\lambda + \alpha_\kappa)^2$ 2-loop corrections [75] in NMSSMCALC may have a nonnegligible impact on the Higgs boson masses and observables [76]. We, however, maintain that such contributions will only result in a slight shifting of the parameter configurations yielding solutions of our interest here, but our overall results and conclusions should still remain valid.

We performed six sets of scans of the cNMSSM parameter space by linking NMSSMCALC with the MultiNest-v2.18 [77–79] package. MultiNest performs a multimodal sampling of a theoretical model's parameter space based on Bayesian evidence estimation. However, we use this package not for drawing Bayesian inferences about the various NMSSM scenarios considered but simply to avoid a completely random sampling of the 9-dimensional model parameter space. In the program, we therefore defined a Gaussian likelihood function for H_{obs} in a given scan, assuming the experimental measurement of its mass to be 125 GeV and allowing up to ±2 GeV error in its model prediction. We set the enlargement factor reduction parameter to 0.3 and the evidence tolerance factor to a rather small value of 0.2, so that while the package was sampled more concentratedly near the central mass value, a sufficiently large number of points were collected before the scan converged. In each of the first two sets of scans we required H_1 to be H_{obs}. In the third set we imposed this requirement of consistency with H_{obs} mass on H_2, in the fourth set on H_3, in the fifth set on both H_1 and H_2, and in the sixth set on both H_2 and H_3. Each of the six sets further contained five separate scans corresponding to $\phi_\kappa = 0°$, 3°, 10°, 30°, and 60°.

The scanned ranges of the nine free parameters (after fixing the phases) of the natural NMSSM, which are uniform across all its five scenarios considered, are given in Table 1(a). Only large values of λ and κ are used in this model (with the upper cut-off on them imposed to avoid the Landau pole).

Table 1: Ranges of the NMSSM parameters scanned, with fixed ϕ_κ, for (a) each $H_{\rm obs}$ scenario in the natural NMSSM and (b) the low-λ-NMSSM scenario.

(a)

Parameter	Natural NMSSM range
M_0 (GeV)	200–2000
$M_{1/2}$ (GeV)	100–1000
A_0 (GeV)	−3000–0
$\tan\beta$	1–8
λ	0.4–0.7
κ	0.3–0.6
$\mu_{\rm eff}$ (GeV)	100–300
A_λ (GeV)	−1000–1000
A_κ (GeV)	−1000–1000

(b)

Parameter	Low-λ-NMSSM range
M_0 (GeV)	200–4000
$M_{1/2}$ (GeV)	100–2000
A_0 (GeV)	−7000–0
$\tan\beta$	5–45
λ	0.001–0.4
κ	0.001–0.3
$\mu_{\rm eff}$ (GeV)	100–2000
A_λ (GeV)	−1000–4000
A_κ (GeV)	−4000–1000

Since large radiative corrections from SUSY sectors are not necessary in the natural limit of the NMSSM, the parameters M_0, $M_{1/2}$, and A_0 are not required to take too large values. Note that while A_0 can in principle be both positive and negative, with a slightly different impact on the physical mass of the SM-like Higgs boson for an identical set of other input parameters in each case, we restricted the scans to its negative values only, in order to increase the scanning efficiency.

In the remaining sixth scan, we considered the complementary parameter space of the NMSSM, with λ and κ kept to relatively smaller (and $\tan\beta$ to larger) values, so as to prevent too large singlet-doublet mixing. In fact, for $\lambda, \kappa \to 0$, when the singlet sector gets effectively decoupled, H_1, which is by default identified with $H_{\rm obs}$, has properties very identical to the lightest Higgs boson of the MSSM. Since H_1 in such a case does not obtain a maximal tree-level mass that is possible in the most general model, large radiative corrections are needed from the SUSY sector. Hence we used slightly extended ranges of the remaining parameters, which are given in Table 1(b). This scenario, which we refer to as the low-λ-NMSSM scenario henceforth, has been included in our analysis in order to compare the inferences made for the natural NMSSM with an approximate MSSM limit of the model.

Once the scans had been completed, we filtered the points obtained with each by further imposing $123\ {\rm GeV} \leq m_{H_{\rm obs}} \leq 127\ {\rm GeV}$. Note that, in the $H_{\rm obs} = H_1 + H_2$ and $H_{\rm obs} = H_2 + H_3$ scenarios, this condition was imposed on H_2, since in both these scenarios it is typically the Higgs boson with SM-like couplings. The total number of points, $N_{\rm total}$, remaining after this filter is given in Table 2 for each scenario considered. All these points were then tested for consistency with the LEP and LHC exclusion limits on the other, non-SM-like, Higgs bosons of the model, using the package HiggsBounds v4.2.0 [80–83]. The points passing the HiggsBounds test were retained as the "good points" for further analysis, and their number, denoted by $N_{\rm HB}$, for each scenario is also given in Table 2. We point out for later reference that in each of the two $H_{\rm obs} = H_1$ scenarios and $H_{\rm obs} = H_1 + H_2$ scenario, the number of surviving good points (where they are available) is very identical across all input values of ϕ_κ, implying mutually fairly consistent sample sizes.

Next we carried out fits to $H_{\rm obs}$ data for the good points using the public code HiggsSignals v1.3.2 [73]. For obtaining these fits, HiggsSignals requires, along with the masses and BRs of each Higgs boson, H_i, the square of its normalised effective couplings, $(g_{H_iX}/g_{h_{\rm SM}X})^2$, to a given SM particle pair X, with $h_{\rm SM}$ being the SM Higgs boson with the same mass as H_i. Note that when X is a pair of fermions, there is a scalar as well as a pseudoscalar normalised coupling for each H_i, both of which need to be passed separately to HiggsSignals. All these are then used to calculate the normalised cross sections:

$$\mu^X_{H_i} \equiv \frac{\sigma\left(pp \longrightarrow H_i \longrightarrow X\right)}{\sigma\left(pp \longrightarrow h_{\rm SM} \longrightarrow X\right)}, \tag{10}$$

corresponding to a given decay channel, X, in an approximate way. The NMSSMCALC version we used did not provide the normalised Higgs boson couplings as an output. We therefore modified the code to obtain these couplings for adding them as a dedicated block in the SLHA input file for HiggsSignals.

The program HiggsSignals compares the computed $\mu^X_{H_i}$ for each H_i with the experimentally measured ones, $\mu^X_{\rm exp}$, for wide ranges of input Higgs boson masses in a variety of its production and decay channels at the LHC and the Tevatron. We used only the "peak-centred" method and the "latestresults" observable set in the program, with the assignment range variable Λ set to the default value of 1. It thus performed a fit to a total of 81 Higgs boson peak observables (77 from signal strength and 4 from mass measurements), from the CMS, ATLAS, CDF, and DØ collaborations, for a given model point. We assumed a Gaussian theoretical uncertainty of 2 GeV in the masses of the three lightest neutral Higgs bosons of the model. The default values of the uncertainties in the Higgs boson production cross sections as well as BRs were retained. Further details about the fitting procedure can be found in the manual [73] of the package. The main output of HiggsSignals contains the total χ^2 and the p value from the fit, given the number of statistical degrees of freedom, for each model point. Since the aim of this study is a comparison of various $H_{\rm obs}$ scenarios rather than the overall goodness of fit for each, we will quantify our results only in terms of χ^2 and ignore p value.

As an observable indication of the presence of more than one Higgs boson near 125 GeV, the double ratios

$$D_1 = \frac{R^h_{\rm VBF}\left(\gamma\gamma\right)/R^h_{gg}\left(\gamma\gamma\right)}{R^h_{\rm VBF}\left(bb\right)/R^h_{gg}\left(bb\right)};$$

Table 2: Number of scanned points remaining after imposing the mass constraint on $H_{\rm obs}$ and those passing the HiggsBounds test, for each scenario studied. See text for details.

Scenario	Low-λ	$H_{\rm obs} = H_1$	$H_{\rm obs} = H_2$	$H_{\rm obs} = H_3$	$H_{\rm obs} = H_1 + H_2$	$H_{\rm obs} = H_2 + H_3$
			$\phi_\kappa = 0^\circ$			
$N_{\rm total}$	17786	15675	15072	14431	26045	23736
$N_{\rm HB}$	17722	13691	2904	965	11878	2819
			$\phi_\kappa = 3^\circ$			
$N_{\rm total}$	17829	15775	15026	14806	27199	25684
$N_{\rm HB}$	17782	13885	3235	2391	11863	1659
			$\phi_\kappa = 10^\circ$			
$N_{\rm total}$	17847	15784	15080	14810	26735	28348
$N_{\rm HB}$	17786	13866	2411	2495	12607	3369
			$\phi_\kappa = 30^\circ$			
$N_{\rm total}$	17810	16256	15037	14671	31719	28685
$N_{\rm HB}$	17743	14725	247	276	13503	2012
			$\phi_\kappa = 60^\circ$			
$N_{\rm total}$	17810	0	14996	14438	0	30412
$N_{\rm HB}$	17743	0	247	2	0	242

$$D_2 = \frac{R^h_{\rm VBF}(\gamma\gamma)/R^h_{gg}(\gamma\gamma)}{R^h_{\rm VBF}(WW)/R^h_{gg}(WW)};$$
$$D_3 = \frac{R^h_{\rm VBF}(WW)/R^h_{gg}(WW)}{R^h_{\rm VBF}(bb)/R^h_{gg}(bb)} \tag{11}$$

were proposed in [74]. Each of these ratios should be unity if $H_{\rm obs}$ consists of only a single Higgs boson, while the contribution of two (or more) Higgs bosons to $H_{\rm obs}$ signal could result in a deviation of these ratios from 1. In the above expressions, $R^h_Y(X) = R^{H_i}_Y(X) + R^{H_j}_Y(X)$, where H_i and H_j are the two mass-degenerate Higgs bosons in a given scenario and the subscripts VBF and gg imply the vector boson fusion and the gluon fusion production modes, respectively. $R^{H_i}_Y(X)$ for each H_i is defined as

$$R^{H_i}_Y(X) \equiv \frac{\Gamma(H_i \longrightarrow Y)}{\Gamma(h_{\rm SM} \longrightarrow Y)} \times \frac{{\rm BR}(H_i \longrightarrow X)}{{\rm BR}(h_{\rm SM} \longrightarrow X)} = \frac{C^{H_i}_Y C^{H_i}_X}{\Gamma_{H_i}/\Gamma_{h_{\rm SM}}}, \tag{12}$$

with Y being the given production mode and, in the last equality, $C^{H_i}_{X(Y)} = \Gamma(H_i \to X(Y))/\Gamma(h_{\rm SM} \to X(Y))$, the normalised partial decay width of H_i into $X(Y)$ pair. (Note that (12) assumes that $h_{\rm SM}$-normalised production cross sections for Y = VBF and gg processes can be approximated by the normalised partial decay widths of H_i in VV and gg decay channels, resp.) Γ_{H_i} and $\Gamma_{h_{\rm SM}}$ are the total decay widths of H_i and $h_{\rm SM}$, respectively.

We also evaluated the ratios D_1, D_2, and D_3 for the points which give reasonably good fits to the data (to be defined later) in the scenarios with two mass-degenerate Higgs bosons. For this purpose, $R^{H_i}_Y(X)$ for each H_i was calculated by fixing $\Gamma_{h_{\rm SM}}$ in (12) to 4.105×10^{-3} GeV, which is the value given by the program HDECAY [84] for 125 GeV $h_{\rm SM}$. A change of ± 2 GeV in the mass of $h_{\rm SM}$ has only a marginal effect on this width, which we ignore. For calculating the $\Gamma_{h_{\rm SM}}$ with HDECAY, care was taken that all the partial decay widths of $h_{\rm SM}$ were evaluated at the same perturbative order as that implemented in NMSSMCALC for computing Γ_{H_i}. Moreover, $C^{H_i}_Y$ is simply the squared normalised coupling of H_i to a vector boson, V, pair for the VBF production mode and to a gluon pair for gg mode. Similarly, $C^{H_i}_X$ implies H_iVV and $H_i\gamma\gamma$ normalised couplings squared, respectively, for $X = WW$ and $\gamma\gamma$. All these couplings are thus the same ones obtained from NMSSMCALC for passing to HiggsSignals. In the case of $X = b\bar{b}$, though, there is a scalar and pseudoscalar coupling for each H_i, as noted above. For this reason, $C^{H_i}_{b\bar{b}}$'s were calculated using the actual $\Gamma(H_i \to b\bar{b})$ from the NMSSMCALC output for a given model point and $\Gamma(h_{\rm SM} \to b\bar{b})$ obtained from HDECAY for $m_{h_{\rm SM}} = 125$ GeV.

4. Results and Discussion

In Figure 1 we show the total χ^2 obtained for the points from our scans for the various $H_{\rm obs}$ scenarios considered. The green points in the figure correspond to $\phi_\kappa = 0^\circ$, violet to $\phi_\kappa = 3^\circ$, blue to $\phi_\kappa = 10^\circ$, red to $\phi_\kappa = 30^\circ$, and cyan to $\phi_\kappa = 60^\circ$. For the scenarios in which only one of the three lightest neutral Higgs bosons is assumed to be $H_{\rm obs}$, we have made sure that the difference between the mass of $H_{\rm obs}$ and that of each additional Higgs boson nearest to it is always larger than 2.5 GeV. The lower cut-off in χ^2 in each panel, in this figure and in those that follow, varies depending on the minimum value obtained in the corresponding scenario. The upper cut-off in χ^2 for each scenario is chosen so as to include as many points in the corresponding figures as possible without χ^2 getting more than 10 units larger than the minimum obtained in that scenario (given that there are 9 statistical degrees of freedom).

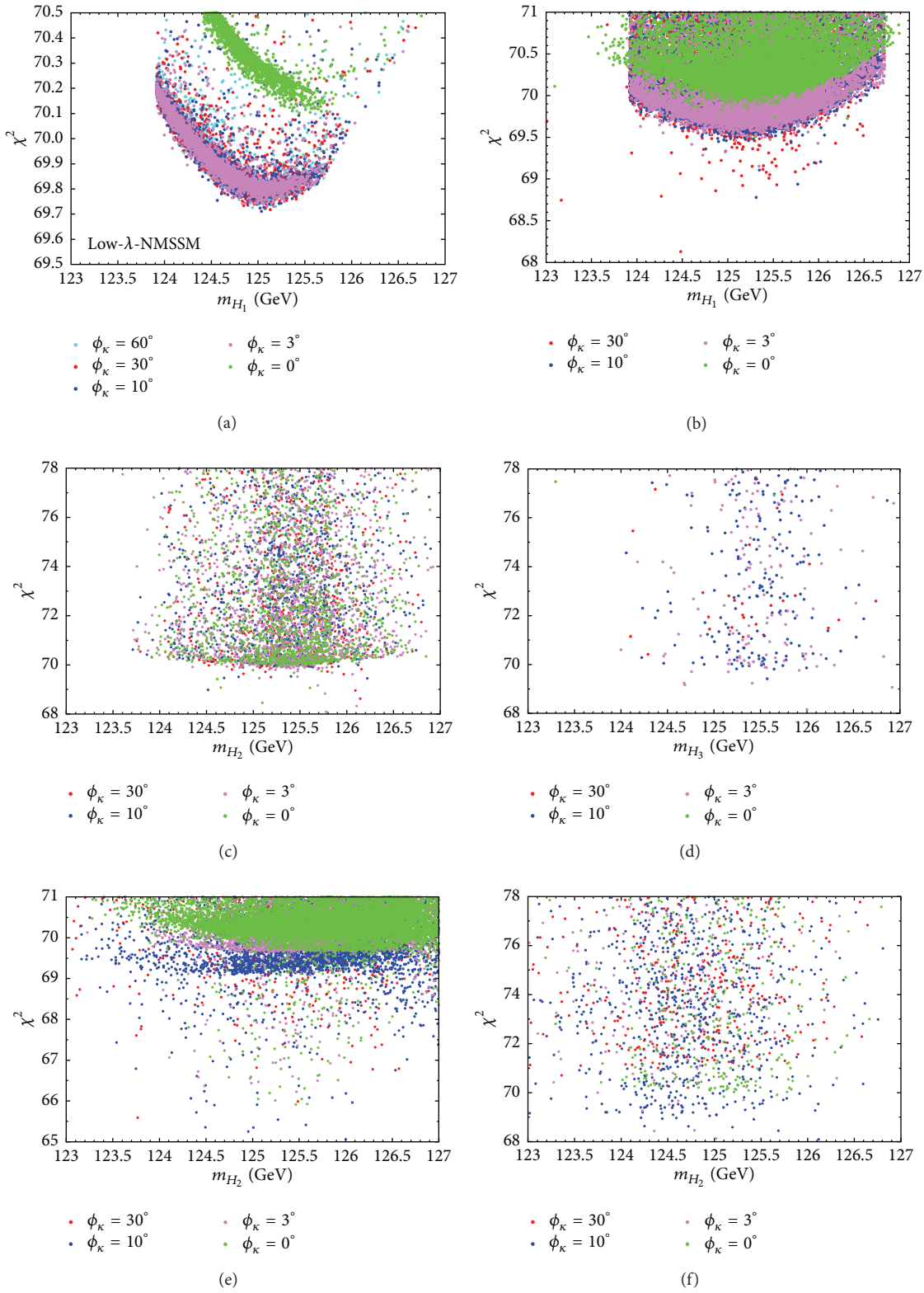

FIGURE 1: Total χ^2 as a function of the following: ((a), (b)) m_{H_1} when only H_1 is assumed to be H_{obs}, for two different sets of scanned ranges of the parameter space (see text for details); (c) m_{H_2} when only H_2 is the H_{obs}; (d) m_{H_3} when only H_3 is H_{obs}; (e) m_{H_2} when both H_1 and H_2 lie near 125 GeV; and (f) m_{H_2} when both H_2 and H_3 lie near 125 GeV.

Figure 1(a) corresponds to the low-λ-NMSSM scenario. One notices in the figure that, for $\phi_\kappa = 0^\circ$, $\chi^2_{\min}$ lies very close to 70 and is thus almost identical to $\chi^2_{\min} = 69.96$ that is given by HiggsSignals for a SM Higgs boson at a mass of 125.1 GeV, with the same settings as those used by us. The input parameters (with the exception of M_0, $M_{1/2}$, and A_0, which can be adjusted with much more freedom) and the masses of the three lightest Higgs bosons are given in Table 3. The negligibly small difference in $\chi^2_{\min}$ value obtained for $h_{\rm SM}$ and for the CP-conserving low-λ-NMSSM results from the fact that λ for the corresponding point in the latter is nonvanishing, as seen in the table, so that the singlet sector is not completely decoupled and an exact MSSM limit is not reached. One can notice in the figure and the table a slightly lower value of $\chi^2_{\min}$ obtained for the sets of points corresponding to nonzero ϕ_κ values. However, λ for all these points is even larger than in the CP-conserving limit. Note also that, for all ϕ_κ, most of the points give $\Delta\chi^2 \leq 1$.

In Figure 1(b), which corresponds to $H_{\rm obs} = H_1$ scenario in the natural NMSSM, we see that there is a large concentration of points above χ^2 value which is very similar to $\chi^2_{\min}$ seen in Figure 1(a), for each corresponding ϕ_κ. For nonzero ϕ_κ though, one also sees a few scattered points with χ^2 lower than that for any of the points in the high concentration region. The overall lowest χ^2 lies very close to 68, for $\phi_\kappa = 30^\circ$, with the mass of $H_{\rm obs}$ for the corresponding point lying at 124.5 GeV. However, according to Table 3, the mass of H_2 for this point is within 3 GeV of that of H_1. It is therefore very likely that the relatively better fit for this particular point is a result of the assignment of H_2 instead of or along with H_1 to some of the observables, especially when their experimental mass resolution is relatively poor. This possibility, which implies that our assumption of two Higgs bosons being individually irresolvable if their masses lie within 2.5 GeV of each other is rather robust, will be discussed further later. For $\phi_\kappa = 60^\circ$ none of the points obtained in the scan for this scenario had H_1 heavier than 123 GeV.

In $H_{\rm obs} = H_2$ scenario, a much smaller number of points were passed by HiggsBounds compared to $H_{\rm obs} = H_1$ scenario, as seen in Figure 1(c), but $\chi^2_{\min}$ is equally low for most ϕ_κ here, including 0°. Only for $\phi_\kappa = 60^\circ$, while plenty of points with $m_{H_2} \approx 125$ GeV were obtained in the scan, χ^2 for them is never low enough to appear in the figure. Once again, in Table 3 one can see that, for the points giving the lowest χ^2 for each ϕ_κ in this scenario, H_1 always lies within 3-4 GeV of H_2. Hence the slightly better fit for this point is again made possible by a contribution of H_1 to some search channels. In Figure 1(d) for $H_{\rm obs} = H_3$ scenario, although very few points with $\Delta\chi^2 < 10$ appear in this scenario compared to the ones above, $\chi^2_{\min}$ is very similar, except for $\phi_\kappa = 0^\circ$ case, when it has a fairly high value of around 77.

In Figure 1(e) is shown the total χ^2 for $H_{\rm obs} = H_1 + H_2$ scenario against H_2 mass. One can observe quite a few similarities between this figure and Figure 1(b) seen above (for $H_{\rm obs} = H_1$ scenario). There are once again a large concentration of points with $\chi^2 \gtrsim 69$ for all ϕ_κ except 60° and also many scattered points below it. Importantly though, there are many points in this scenario which give χ^2 lower than 68, which is the overall lowest value observed for any other scenario here. Most of these points, including the one with the overall lowest χ^2 of ~65, correspond to $\phi_\kappa = 10^\circ$, although some points for other ϕ_κ can also be noticed. In Figure 1(f) one sees $\chi^2_{\min}$ of 68 for $H_{\rm obs} = H_2 + H_3$ scenario also but very few points with $\chi^2 < 71$, in contrast with $H_{\rm obs} = H_1$ and $H_{\rm obs} = H_1 + H_2$ scenarios but similar to $H_{\rm obs} = H_2$ and $H_{\rm obs} = H_3$ scenarios.

From the above discussion, it is clear that certain points, or parameter space configurations, in $H_{\rm obs} = H_1 + H_2$ scenario give the best fit to the current experimental Higgs boson data. A *global* $\chi^2_{\min}$, that is, the lowest χ^2 value across all scenarios examined here, of around 65 has been observed for $\phi_\kappa = 10^\circ$ in this scenario, with some points corresponding to other values of ϕ_κ also lying within 1 unit of χ^2. None of the points obtained for the other scenarios gives χ^2 lying even within 3 units of this global minimum, despite the number of sampled points for the $H_{\rm obs} = H_1$ scenario being typically larger. The reason for a better fit for some points with two nearly degenerate Higgs bosons becomes apparent by looking at the detailed output of HiggsSignals. In the peak-centred method, HiggsSignals assigns to a given observable the Higgs boson with a mass closest to the measured mass provided by the experiment. This mass measurement currently ranges between 124.7 GeV and 126.0 GeV. Thus, when a single Higgs boson is assigned to all the observables, χ^2 contribution is large from the observables for which the measured mass lies away from the mass of the assigned Higgs boson, and the experimental mass resolution is good. On the other hand, when two Higgs bosons lie close to each other, the one assigned to a given observable is the one for which the difference of the predicted mass from the experimental value is the smallest, so that χ^2 contribution from this observable is minimal. This is as long as the mass of the other Higgs boson nearby lies outside the experimental mass resolution; otherwise HiggsSignals automatically assigns both the Higgs bosons to an individual observable if it improves the fit.

Some caveats are in order here though. $\Delta\chi^2 \simeq 3$ is statistically quite insignificant for drawing any concrete inferences about the considered scenarios, since the total number of observables and statistical degrees of freedom is quite large. At the same time, the number of points giving $\Delta\chi^2 \leq 3$ is also fairly small. Moreover, no other experimental constraints have been imposed in our analysis, since the publicly available tools for testing these are so far not compatible with the cNMSSM. It is thus possible that many of the interesting points may have already been ruled out by such constraints. However, the aim of this study is not to disregard one scenario in favour of another, but to simply show that, given the current experimental data, the scenario with two mass-degenerate Higgs bosons in the NMSSM provides as good, if not better, a fit as the scenarios with a single Higgs boson near 125 GeV. This alternative possibility even points towards a source of CP-violation beyond the SM and, therefore, warrants more dedicated analyses as well as experimental probes. In the following we discuss some other interesting aspects of this scenario.

In the left, middle, and right panels of Figure 2 we show the ratios D_1, D_2, and D_3, respectively, as functions of

Table 3: Input parameters and Higgs boson masses corresponding to the points giving the lowest χ^2 for all ϕ_κ cases in each of $H_{\rm obs}$ scenarios considered.

Scenario	Low-λ	$H_{\rm obs} = H_1$	$H_{\rm obs} = H_2$	$H_{\rm obs} = H_3$	$H_{\rm obs} = H_1 + H_2$	$H_{\rm obs} = H_2 + H_3$
			$\phi_\kappa = 0^\circ$			
$\chi^2_{\rm min}$	70.1	69.5	68.5	76.9	65.9	69.8
λ	0.046	0.582	0.653	0.48	0.597	0.597
κ	0.213	0.43	0.511	0.305	0.302	0.327
$\tan\beta$	17.65	1.66	3.6	6.98	2.39	2.07
A_λ	853.6	226.8	609.7	680.7	540.0	179.3
A_κ	−2352	−741.4	−666.0	14.05	−479.3	−3.95
$\mu_{\rm eff}$	130.0	281.5	243.7	102.6	285.2	112.3
m_{H_1}	125.4	125.3	122.1	66.8	123.3	115.1
m_{H_2}	162.8	142.1	125.1	121.0	125.5	125.1
m_{H_3}	1828	510.6	618.5	125.7	730.0	126.6
			$\phi_\kappa = 3^\circ$			
$\chi^2_{\rm min}$	69.7	69.2	68.1	68.2	66.0	68.1
λ	0.184	0.639	0.588	0.662	0.631	0.636
κ	0.291	0.523	0.39	0.349	0.373	0.318
$\tan\beta$	29.6	1.81	2.61	4.24	1.61	6.45
A_λ	2175	162.5	459.6	425.6	222.0	848.6
A_κ	−236.7	−595.1	−597.6	−12.03	345.2	−19.4
$\mu_{\rm eff}$	177.9	218.8	260.5	110.1	196.4	127.4
m_{H_1}	125.1	125.3	122.5	97.2	123.4	105.1
m_{H_2}	444.9	141.7	125.8	122.3	125.2	125.0
m_{H_3}	496.1	405.5	563.6	126.0	366.3	127.2
			$\phi_\kappa = 10^\circ$			
$\chi^2_{\rm min}$	69.7	68.8	69.0	69.4	65.1	68.1
λ	0.138	0.68	056	0.692	0.688	0.585
κ	0.219	0.409	0.345	0.338	0.361	0.306
$\tan\beta$	16.7	1.85	1.91	4.88	1.98	7.55
A_λ	1379	291.6	347.8	557.0	390.8	972.6
A_κ	−623.8	−476.1	−567.8	12.7	−435.1	−30.62
$\mu_{\rm eff}$	133.5	251.0	266.9	124.3	254.0	136.7
m_{H_1}	125.0	125.3	120.3	106.4	123.6	118.7
m_{H_2}	212.2	140.5	124.5	111.6	126.0	126.1
m_{H_3}	631.6	482.5	541.8	125.6	440.1	127.4
			$\phi_\kappa = 30^\circ$			
$\chi^2_{\rm min}$	69.7	68.1	68.6	70.4	65.6	70.2
λ	0.136	0.648	0.679	0.537	0.624	0.481
κ	0.219	0.319	0.586	0.303	0.388	0.311
$\tan\beta$	29.4	2.2	2.13	6.55	2.10	7.67
A_λ	3515	570.1	295.0	702.2	345.7	796.5
A_κ	−781.0	−398.4	−590.7	7.07	330.5	−23.22
$\mu_{\rm eff}$	170.8	288.5	227.8	112.6	209.1	110.0
m_{H_1}	125.1	124.5	123.1	86.5	121.6	107.1
m_{H_2}	234.3	127.4	126.1	116.8	123.8	124.7
m_{H_3}	857.7	462.4	507.8	124.3	405.8	125.8

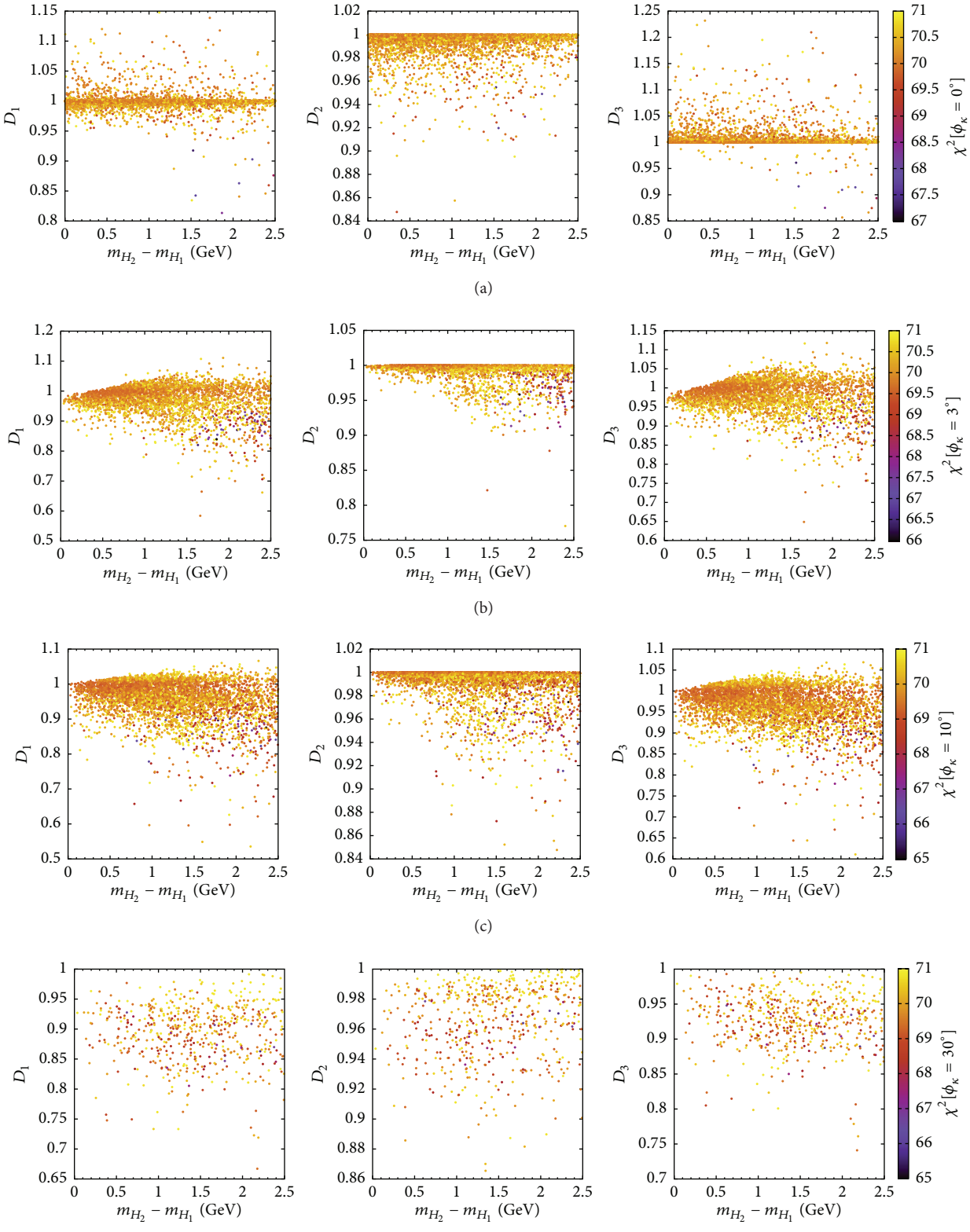

FIGURE 2: The ratios D_1, D_2, and D_3, defined in (11), as functions of the difference between H_2 and H_1 masses, in the scenario when $H_{\text{obs}} = H_1 + H_2$. In (a) ϕ_κ is set to 0°, in (b) to 3°, in (c) to 10°, and in (d) to 30°. The heat map in all the panels corresponds to the total χ^2.

the mass difference, $m_{H_2} - m_{H_1}$, for various ϕ_κ values in $H_{\rm obs} = H_1 + H_2$ scenario. The heat map corresponds to the total χ^2 obtained for the points shown in each panel. χ^2 has a uniform upper cut-off of 71 across all panels, as in Figure 1(e), but its lower cut-off varies according to the minimum obtained for ϕ_κ case that a given panel corresponds to. According to Figure 2(a), for $\phi_\kappa = 0^\circ$ the three ratios remain largely close to unity, but deviations up to 15–20% can be seen for some points. D_2, the ratio dependent on only the bosonic signal strengths, only gets smaller than 1 for some points and its maximum observed deviation is lower than that of D_1 and D_3, each of which can be both above or below unity. Importantly, the points for which a large deviation of each ratio from 1 is seen are also generally the ones giving a relatively good χ^2 fit to the data.

A similar trend is seen also for other values of ϕ_κ. However, deviations of D_1 and D_2 from unity by up to 40–50% are obtained for $\phi_\kappa = 3^\circ$ (Figure 2(b)) and $\phi_\kappa = 10^\circ$ (Figure 2(c)), but there are many more points with significantly large deviations of each of the ratios for the latter phase compared to the former one. For $\phi_\kappa = 30^\circ$ all the points appearing in Figure 2(d) give D_1, D_2, and D_3 smaller than 1 and the overall deviation is generally smaller than for other nonzero phases but larger than for the rNMSSM limit. Thus, for this phase, the measured signal strengths can provide a clear indication whenever two Higgs bosons are present near 125 GeV instead of one. The reason why the deviations of the three ratios are much smaller overall in the case of $\phi_\kappa = 0^\circ$ than for the CPV cases, for points showing the highest consistency with the data, will become clearer below.

As noted earlier, a scenario with two mass-degenerate Higgs bosons in the cNMSSM entails both $H_{\rm obs} = H_1 + H_2$ and $H_{\rm obs} = H_1/H_2 + A_1$ possibilities of the rNMSSM. Thus it is interesting to see which one of these two possibilities is favoured more by the data, for a given ϕ_κ. In the left panels of Figure 3 we thus show the squared normalised coupling $C_{VV}^{H_2}$ against $C_{VV}^{H_1}$, with the heat map corresponding to the total χ^2. Similarly, in the right panels we have plotted $C_{VV}^{H_3}$ versus $C_{VV}^{H_1}$, while the distribution of m_{H_3} is shown by the heat map. For clarity of observation, we have included in this figure points with a total χ^2 reaching up to 80, which is much higher than for the points shown in the earlier figures for this scenario. Also we have imposed an upper cut-off of 300 GeV on the mass of H_3. We expect $C_{VV}^{H_i}$ to either vanish when a given H_i is a pure pseudoscalar (in the rNMSSM limit) or be relatively small when it is pseudoscalar-like (for $\phi_\kappa > 0^\circ$). Note that these couplings satisfy the sum rule [63, 64]

$$\sum_{i=1}^{N} C_{VV}^{H_i} \simeq 1, \tag{13}$$

where N is the total number of neutral Higgs bosons that have a tree-level coupling to the gauge bosons, that is, 5 in the cNMSSM and 3 in the rNMSSM limit. (Note that since $h_{\rm SM}$ is a hypothetical SM Higgs boson with the same mass as a given H_i, at the tree level the ratio $C_X^{H_i}$ in fact corresponds to $(g_{H_iX}/g_{h_{\rm SM}X})^2$ and the equality in (13) is exact. However, since $C_X^{H_i}$ have actually been defined here in terms of the partial decay widths of H_i in X channel, which include higher order effects also, the sum of $C_X^{H_i}$ may deviate slightly from unity.) In the figure we see the above sum rule being satisfied almost completely by the three lightest neutral Higgs bosons under consideration here, implying that the remaining two doublet-like Higgs bosons are nearly decoupled.

In the case of $\phi_\kappa = 0^\circ$ (i.e., in the rNMSSM limit) in the left panel of Figure 3(a), we see two distinct kinds of points. There are some points lying along the diagonal, for which $C_{VV}^{H_1}$ and $C_{VV}^{H_2}$ alone are enough to satisfy the sum rule in (13). It is further evident from the right panel that $C_{VV}^{H_3}$ for these points is exactly 0. H_1 and H_2 in these points should thus be scalars and H_3 should be a pseudoscalar (i.e., A_1). But for the majority of the points, lying along either of the axes, $C_{VV}^{H_1}$ is nearly 1, implying it is an almost pure doublet-like scalar, while $C_{VV}^{H_2}$ is exactly 0, implying it is a pseudoscalar, or vice versa. One can then observe in the right panel that for such points $C_{VV}^{H_3}$, with H_3 being the singlet-like scalar, is responsible for the sum rule being satisfied. Thus when the doublet-like scalar, whether H_1 or H_2, has $C_{VV}^{H_i}$ slightly below 1, $C_{VV}^{H_3}$ is slightly above 0. The mixing of the doublet scalar with H_3 increases as its mass decreases, as is evident from the heat map in the right panel of the figure. As a result, the largest $C_{VV}^{H_3}$, ~0.8, is seen for the lowest m_{H_3} obtained, which lies just above the allowed $H_{\rm obs}$ mass window.

A closer inspection of the heat map in the left panel of Figure 3(a) reveals that the lowest values of χ^2 are obtained for points lying along one of the axes, that is, when the doublet-like scalar is nearly mass-degenerate with the pseudoscalar. For points along the diagonal, χ^2 is in fact always larger than 71. This is the reason for the relatively small deviations of D_1, D_2, and D_3 from 1 seen in Figure 2(a), where only points with χ^2 lower than 71 were shown. For such points, since one of H_1 and H_2 is a pure pseudoscalar as well as singlet-dominated, its contribution to the combined signal strength in WW channel is null and that in $\gamma\gamma$ and $b\bar{b}$ channels is minimal. Therefore, while the presence of H_1 and H_2 of the rNMSSM near 125 GeV may possibly cause D_1, D_2, and D_3 to deviate more significantly from 1, the consistency of this scenario with the LHC data is worse than that of $H_1 + A_1$ scenario.

Figure 3(b) shows that, for $\phi_\kappa = 3^\circ$, H_1 and H_2 are almost always scalar-like while H_3 is highly pseudoscalar-like with a relatively much smaller $C_{VV}^{H_3}$ generally. However, due to CP-mixing, $C_{VV}^{H_3}$ can reach as high as 0.7 or so when the mass of H_3 is close to that of H_1 and H_2, though this happens for only a few points. A very crucial point to note here is that the total χ^2 in the left panel never falls below 68, which is due to the cut-off on the allowed upper value of m_{H_3}. This means that the points which give the overall best fit to the data have a much higher H_3 mass, which leads to a much smaller scalar-pseudoscalar mixing and hence negligible $C_{VV}^{H_3}$.

For $\phi_\kappa = 10^\circ$ case, illustrated in Figure 3(c), while the maximum $C_{VV}^{H_3}$ obtained is relatively small and hence $C_{VV}^{H_1}$ and $C_{VV}^{H_2}$ do not deviate from the diagonal by much in the left panel, there are many more points, compared to $\phi_\kappa = 3^\circ$

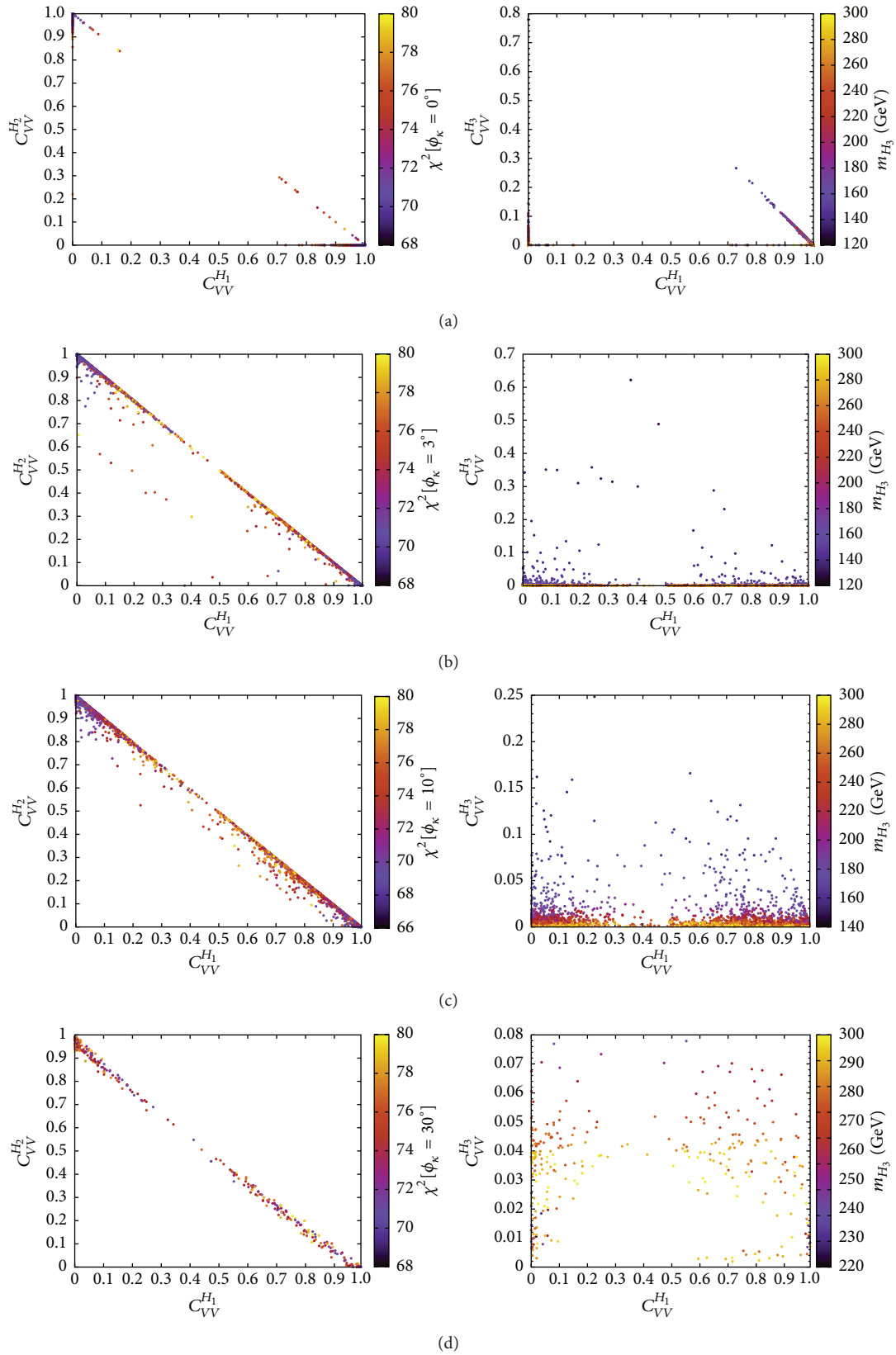

FIGURE 3: Squared normalised coupling of H_1 to the gauge bosons versus that of H_2 (left) and of H_3 (right) in the scenario when $H_{\text{obs}} = H_1 + H_2$, with ϕ_κ set to (a) 0°, (b) 3°, (c) 10°, and (d) 30°. The heat map in the left panels shows the distribution of χ^2 and in the right panels that of m_{H_3}.

case above, for which $C_{VV}^{H_3}$ is significant, according to the right panel. Finally, for $\phi_\kappa = 30^\circ$, although $C_{VV}^{H_3}$ never completely vanishes, it also stays smaller overall than it is for other phases. The reason for this is that the pseudoscalar-like H_3 never achieves a mass below 220 GeV or so, as can be noted from the heat map in the right panel of Figure 3(d). In the left panel one therefore sees that $C_{VV}^{H_1}$ and $C_{VV}^{H_2}$ always remain very close to the diagonal. Hence, for nonzero ϕ_κ the data clearly favours two scalar-like Higgs bosons near 125 GeV, instead of a pair of scalar-like and pseudoscalar-like Higgs bosons.

5. Conclusions

In summary, we have tested the consistency of the real and complex NMSSM with the latest Higgs boson data from the LHC Run I and the Tevatron. In particular, we have focused on scenarios wherein the resonant peak seen by the experiments can be explained in terms of two nearly mass-degenerate Higgs states around 125 GeV. Such scenarios have been verified in the rNMSSM previously and have not been ruled out yet. What we have shown here is that the possibility of such dynamics being available in the NMSSM is somewhat enhanced if some degree of (explicit) CP-violation is allowed in the Higgs sector. This can be done by assuming one or more of the Higgs sector parameters to be complex. By choosing this parameter to be κ, one can evade the fermion EDM measurements, which tightly constrain the other possibly complex parameters in the Higgs and soft SUSY sectors of the NMSSM.

In order to achieve the above we have performed detailed numerical scans of the parameter space of the cNMSSM to obtain various possible configurations with ~125 GeV Higgs boson(s) that also give SM-like signal strengths. In these scans we set the phase of κ to five different values, 0°, 3°, 10°, 30°, and 60°. Through a comprehensive analysis of the points obtained from these scans, we have then established that certain parameter configurations yielding two Higgs bosons near 125 GeV are slightly more favoured by the current data compared to scenarios with a single ~125 GeV Higgs boson. This statement is even stronger when the two Higgs bosons are CP-mixed states. For the case of $\phi_\kappa = 10^\circ$ we thus obtained the following: (i) the point with the global minimum χ^2; (ii) more points with $\Delta\chi^2$ lying within 4 units of the global minimum χ^2 compared to all other scenarios and phases tested; (iii) more points with larger deviations of the ratios D_1, D_2, and D_3 from unity.

While analysing the aforementioned scenario with two Higgs bosons near 125 GeV, we have made sure that their masses are close enough that these two states cannot be distinguished experimentally as separate particles. In doing so we have exploited the fact that the experimental measurements are currently unable to reconstruct Breit-Wigner resonances, given that the experimental resolution in all channels investigated in the Higgs analyses is significantly larger than the intrinsic Higgs boson widths involved (so that LHC data actually reproduce Gaussian shapes). However, (tree-level) interference and (1-loop) mixing effects become crucial and need to be accounted for when the (pole) mass difference between two Higgs states is comparable or smaller that their individual intrinsic width. While we have ignored such effects here for points where they can be relevant, which however make up a very tiny fraction of all the good points from our scans, they are the subject of a dedicated separate study [85].

Finally, in our analysis we have used up-to-date sophisticated computational tools in which state-of-the-art theoretical calculations and/or experimental measurements have been implemented, so that the solidity of our results is assured.

Conflict of Interests

The authors declare that there is no conflict of interests regarding the publication of this paper.

Acknowledgments

Shoaib Munir is thankful to Margarete Mühlleitner for useful discussions regarding the cNMSSM and for help with the NMSSMCALC program. Stefano Moretti is supported in part by the NExT Institute. Shoaib Munir is supported by Korea Ministry of Science, ICT and Future Planning, Gyeongsangbuk-Do, and Pohang City for Independent Junior Research Groups at the Asia Pacific Center for Theoretical Physics.

References

[1] P. Fayet, "Supergauge invariant extension of the Higgs mechanism and a model for the electron and its neutrino," *Nuclear Physics B*, vol. 90, pp. 104–124, 1975.

[2] J. Ellis, J. F. Gunion, H. E. Haber, L. Roszkowski, and F. Zwirner, "Higgs bosons in a nonminimal supersymmetric model," *Physical Review D*, vol. 39, article 844, 1989.

[3] L. Durand and J. L. Lopez, "Upper bounds on Higgs and top quark masses in the flipped SU(5)×U(1) superstring model," *Physics Letters B*, vol. 217, no. 4, pp. 463–466, 1989.

[4] M. Drees, "Supersymmetric models with extended Higgs sector," *International Journal of Modern Physics A*, vol. 4, no. 14, article 3635, 1989.

[5] U. Ellwanger, C. Hugonie, and A. M. Teixeira, "The next-to-minimal supersymmetric standard model," *Physics Reports*, vol. 496, no. 1-2, pp. 1–77, 2010.

[6] M. Maniatis, "The next-to-minimal supersymmetric extension of the standard model reviewed," *International Journal of Modern Physics A*, vol. 25, pp. 3505–3602, 2010.

[7] G. Aad, T. Abajyan, B. Abbott et al., "Observation of a new particle in the search for the Standard Model Higgs boson with the ATLAS detector at the LHC," *Physics Letters B*, vol. 716, no. 1, pp. 1–29, 2012.

[8] S. Chatrchyan, V. Khachatryan, A. M. Sirunyan et al., "Observation of a new boson at a mass of 125 GeV with the CMS experiment at the LHC," *Physics Letters B*, vol. 716, no. 1, pp. 30–61, 2012.

[9] S. Chatrchyan, V. Khachatryan, A. M. Sirunyan et al., "Observation of a new boson with mass near 125 GeV in pp collisions at $\sqrt{s} = 7$ and 8 TeV," *Journal of High Energy Physics*, vol. 2013, no. 6, article 081, 2013.

[10] U. Ellwanger, "A Higgs boson near 125 GeV with enhanced diphoton signal in the NMSSM," *Journal of High Energy Physics*, vol. 2012, no. 3, article 44, 2012.

[11] S. F. King, M. Mühlleitner, and R. Nevzorov, "NMSSM Higgs benchmarks near 125 GeV," *Nuclear Physics B*, vol. 860, no. 2, pp. 207–244, 2012.

[12] J. Cao, Z. Heng, J. M. Yang, Y. Zhang, and J. Zhu, "A SM-like Higgs near 125 GeV in low energy SUSY: a comparative study for MSSM and NMSSM," *Journal of High Energy Physics*, vol. 2012, article 86, 2012.

[13] J. F. Gunion, Y. Jiang, and S. Kraml, "Could two NMSSM Higgs bosons be present near 125 GeV?" *Physical Review D*, vol. 86, no. 7, Article ID 071702, 2012.

[14] S. King, M. Muhlleitner, R. Nevzorov, and K. Walz, "Natural NMSSM Higgs bosons," *Nuclear Physics B*, vol. 870, pp. 323–352, 2013.

[15] T. Gherghetta, B. von Harling, A. D. Medina, and M. A. Schmidt, "The scale-invariant NMSSM and the 126 GeV Higgs boson," *Journal of High Energy Physics*, vol. 2013, no. 2, article 032, 2013.

[16] L. Wu, J. M. Yang, C.-P. Yuan, and M. Zhang, "Higgs self-coupling in the MSSM and NMSSM after the LHC Run 1," *Physics Letters B*, vol. 747, pp. 378–389, 2015.

[17] S. Munir, L. Roszkowski, and S. Trojanowski, "Simultaneous enhancement in gamma.gamma, b.b-bar and tau+.tau− rates in the NMSSM with nearly degenerate scalar and pseudoscalar Higgs bosons," *Physical Review D*, vol. 88, Article ID 055017, 2013.

[18] A. G. Cohen, D. Kaplan, and A. Nelson, "Progress in electroweak baryogenesis," *Annual Review of Nuclear and Particle Science*, vol. 43, pp. 27–70, 1993.

[19] M. Quiros, "Field theory at finite temperature and phase transitions," *Helvetica Physica Acta*, vol. 67, no. 5, pp. 451–583, 1994.

[20] A. Sakharov, "Violation of CP invariance, C asymmetry, and baryonasymmetry of the universe," *Pisma Zh.Eksp.Teor.Fiz*, vol. 5, pp. 32–35, 1967.

[21] T. Ibrahim and P. Nath, "*CP* violation from the standard model to strings," *Reviews of Modern Physics*, vol. 80, article 577, 2008.

[22] T. Cohen, D. E. Morrissey, and A. Pierce, "Electroweak baryogenesis and Higgs signatures," *Physical Review D*, vol. 86, Article ID 013009, 2012.

[23] D. Curtin, P. Jaiswal, and P. Meade, "Excluding electroweak baryogenesis in the MSSM," *Journal of High Energy Physics*, vol. 2012, no. 8, article 005, 2012.

[24] M. Carena, G. Nardini, M. Quiros, and C. E. Wagner, "MSSM electroweak baryogenesis and LHC data," *Journal of High Energy Physics*, vol. 2013, no. 2, article 001, 2013.

[25] A. Pilaftsis, "CP-odd tadpole renormalization of Higgs scalar-pseudoscalar mixing," *Physical Review D*, vol. 58, Article ID 096010, 1998.

[26] A. Pilaftsis, "Higgs scalar—pseudoscalar mixing in the minimal supersymmetric standard model," *Physics Letters B*, vol. 435, pp. 88–100, 1998.

[27] A. Pilaftsis and C. E. M. Wagner, "Higgs bosons in the minimal supersymmetric standard model with explicit CP violation," *Nuclear Physics B*, vol. 553, no. 1-2, pp. 3–42, 1999.

[28] M. S. Carena, J. R. Ellis, A. Pilaftsis, and C. E. M. Wagner, "Renormalization-group-improved effective potential for the MSSM Higgs sector with explicit CP violation," *Nuclear Physics B*, vol. 586, no. 1-2, pp. 92–140, 2000.

[29] S. Y. Choi, M. Drees, and J. S. Lee, "Loop corrections to the neutral Higgs boson sector of the MSSM with explicit CP violation," *Physics Letters B*, vol. 481, no. 1, pp. 57–66, 2000.

[30] M. S. Carena, J. R. Ellis, A. Pilaftsis, and C. Wagner, "Higgs boson pole masses in the MSSM with explicit CP violation," *Nuclear Physics B*, vol. 625, pp. 345–371, 2002.

[31] M. Carena, J. Ellis, S. Mrenna, A. Pilaftsis, and C. E. M. Wagner, "Collider probes of the MSSM Higgs sector with explicit CP violation," *Nuclear Physics B*, vol. 659, no. 1-2, pp. 145–178, 2003.

[32] S. Y. Choi, J. Kalinowski, Y. Liao, and P. M. Zerwas, "*H*/*A* Higgs mixing in *CP*-noninvariant supersymmetric theories," *European Physical Journal C*, vol. 40, no. 4, pp. 555–564, 2005.

[33] C. A. Baker, D. D. Doyle, P. Geltenbort et al., "Improved experimental limit on the electric dipole moment of the neutron," *Physical Review Letters*, vol. 97, no. 13, Article ID 131801, 2006.

[34] E. D. Commins, "Electric dipole moments of elementary particles, nuclei, atoms, and molecules," *Journal of the Physical Society of Japan*, vol. 76, no. 11, Article ID 111010, 2007.

[35] W. C. Griffith, M. D. Swallows, T. H. Loftus, M. V. Romalis, B. R. Heckel, and E. N. Fortson, "Improved limit on the permanent electric dipole moment of Hg-199," *Physical Review Letters*, vol. 102, no. 10, Article ID 101601, 2009.

[36] S. Abel, S. Khalil, and O. Lebedev, "EDM constraints in supersymmetric theories," *Nuclear Physics B*, vol. 606, no. 1-2, pp. 151–182, 2001.

[37] N. Haba, "Explicit *CP* violation in the Higgs sector of the next-to-minimal supersymmetric standard model," *Progress of Theoretical Physics*, vol. 97, no. 2, pp. 301–309, 1997.

[38] T. Ibrahim and P. Nath, "The neutron and the lepton EDMs in MSSM, large CP violating phases, and the cancellation mechanism," *Physical Review D*, vol. 58, Article ID 111301, 1998.

[39] M. Boz, "The Higgs sector and electron electric dipole moment in next-to-minimal supersymmetry with explicit CP violation," *Modern Physics Letters A*, vol. 21, no. 3, pp. 243–264, 2006.

[40] J. R. Ellis, J. S. Lee, and A. Pilaftsis, "Electric dipole moments in the MSSM reloaded," *Journal of High Energy Physics*, vol. 2008, no. 10, article 049, 2008.

[41] Y. Li, S. Profumo, and M. Ramsey-Musolf, "A comprehensive analysis of electric dipole moment constraints on CP-violating phases in the MSSM," *Journal of High Energy Physics*, vol. 2010, article 62, 2010.

[42] S. J. Huber and M. G. Schmidt, "Electroweak baryogenesis: concrete in a SUSY model with a gauge singlet," *Nuclear Physics B*, vol. 606, no. 1-2, pp. 183–230, 2001.

[43] S. J. Huber, T. Konstandin, T. Prokopec, and M. G. Schmidt, "Baryogenesis in the MSSM, nMSSM and NMSSM," *Nuclear Physics A*, vol. 785, no. 1-2, pp. 206–209, 2007.

[44] S. Kanemura, E. Senaha, and T. Shindou, "First-order electroweak phase transition powered by additional F-term loop effects in an extended supersymmetric Higgs sector," *Physics Letters, Section B: Nuclear, Elementary Particle and High-Energy Physics*, vol. 706, no. 1, pp. 40–45, 2011.

[45] K. Cheung, T.-J. Hou, J. S. Lee, and E. Senaha, "Singlino-driven electroweak baryogenesis in the next-to-MSSM," *Physics Letters B*, vol. 710, no. 1, pp. 188–191, 2012.

[46] W. Huang, Z. Kang, J. Shu, P. Wu, and J. M. Yang, "New insights in the electroweak phase transition in the NMSSM," *Physical Review D*, vol. 91, no. 2, Article ID 025006, 2015.

[47] X.-J. Bi, L. Bian, W. Huang, J. Shu, and P.-F. Yin, "Interpretation of the Galactic Center excess and electroweak phase transition in the NMSSM," *Physical Review D*, vol. 92, no. 2, Article ID 023507, 2015.

[48] S. Moretti, S. Munir, and P. Poulose, "125 GeV Higgs boson signal within the complex NMSSM," *Physical Review D*, vol. 89, Article ID 015022, 2014.

[49] D. A. Demir, "Effects of the supersymmetric phases on the neutral Higgs sector," *Physical Review D*, vol. 60, Article ID 055006, 1999.

[50] A. Dedes and S. Moretti, "Effect of large supersymmetric phases on Higgs production," *Physical Review Letters*, vol. 84, no. 1, pp. 22–25, 2000.

[51] A. Dedes and S. Moretti, "Effects of CP violating phases on Higgs boson production at hadron colliders in the minimal supersymmetric standard model," *Nuclear Physics B*, vol. 576, pp. 29–55, 2000.

[52] G. L. Kane and L.-T. Wang, "Implications of supersymmetry phases for Higgs boson signals and limits," *Physics Letters B*, vol. 488, no. 3-4, pp. 383–389, 2000.

[53] A. Arhrib, D. K. Ghosh, and O. C. W. Kong, "Observing CP violating MSSM Higgs bosons at hadron colliders?" *Physics Letters B*, vol. 537, no. 3-4, pp. 217–226, 2002.

[54] S. Y. Choi, K. Hagivvara, and J. S. Lee, "Higgs boson decays in the minimal supersymmetric standard model with radiative Higgs sector CP violation," *Physical Review D*, vol. 64, no. 3, Article ID 032004, 2001.

[55] S. Y. Choi, M. Drees, J. S. Lee, and J. Song, "Supersymmetric Higgs boson decays in the MSSM with explicit CP violation," *European Physical Journal C*, vol. 25, no. 2, pp. 307–313, 2002.

[56] J. R. Ellis, J. S. Lee, and A. Pilaftsis, "CERN LHC signatures of resonant CP violation in a minimal supersymmetric Higgs sector," *Physical Review D*, vol. 70, Article ID 075010, 2004.

[57] S. Hesselbach, S. Moretti, S. Munir, and P. Poulose, "Explicit CP violation in the MSSM through $gg \to H_1 \to \gamma\gamma$," *Physical Review D*, vol. 82, Article ID 074004, 2010.

[58] T. Fritzsche, S. Heinemeyer, H. Rzehak, and C. Schappacher, "Heavy scalar top quark decays in the complex MSSM: a full one-loop analysis," *Physical Review D*, vol. 86, no. 3, Article ID 035014, 2012.

[59] A. Chakraborty, B. Das, J. L. Diaz-Cruz, D. K. Ghosh, S. Moretti, and P. Poulose, "125 GeV Higgs signal at the LHC in the *CP*-violating MSSM," *Physical Review D*, vol. 90, no. 5, Article ID 055005, 2014.

[60] K. Funakubo, S. Tao, and F. Toyoda, "Phase transitions in the NMSSM," *Progress of Theoretical Physics*, vol. 114, no. 2, pp. 369–389, 2005.

[61] S. W. Ham, S. K. Oh, and D. Son, "Neutral Higgs sector of the next-to-minimal supersymmetric standard model with explicit CP violation," *Physical Review D*, vol. 65, Article ID 075004, 2002.

[62] K. Funakubo and S. Tao, "The Higgs sector in the next-to-MSSM," *Progress of Theoretical Physics*, vol. 113, no. 4, pp. 821–842, 2005.

[63] K. Cheung, T.-J. Hou, J. S. Lee, and E. Senaha, "The Higgs boson sector of the Nextto-MSSM with CP violation," *Physical Review D*, vol. 82, Article ID 075007, 2010.

[64] K. Cheung, T.-J. Hou, J. S. Lee, and E. Senaha, "Higgs-mediated electric-dipole moments in the next-to-minimal supersymmetric standard model: an application to electroweak baryogenesis," *Physical Review D*, vol. 84, Article ID 015002, 2011.

[65] S. Munir, "Novel Higgs-to-125 GeV Higgs boson decays in the complex NMSSM," *Physical Review D*, vol. 89, Article ID 095013, 2014.

[66] F. Domingo, "A new tool for the study of the CP-violating NMSSM," *Journal of High Energy Physics*, vol. 2015, no. 6, article 052, 2015.

[67] T. Graf, R. Gröber, M. Mühlleitner, H. Rzehak, and K. Walz, "Higgs boson masses in the complex NMSSM at one-loop level," *Journal of High Energy Physics*, vol. 2012, no. 10, article 122, 2012.

[68] M. Muhlleitner, D. T. Nhung, H. Rzehak, and K. Walz, "Two-loop contributions of the order $\mathcal{O}(\alpha_t\alpha_s)$ to the masses of the Higgs bosons in the CP-violating NMSSM," *Journal of High Energy Physics*, vol. 2015, article 128, 2015.

[69] V. Khachatryan, A. M. Sirunyan, A. Tumasyan et al., "Precise determination of the mass of the Higgs boson and tests of compatibility of its couplings with the standard model predictions using proton collisions at 7 and 8TeV," *The European Physical Journal C*, vol. 75, no. 5, article 212, 2015.

[70] ATLAS Collaboration, "Updated coupling measurements of the Higgs boson with the ATLAS detector using up to 25 fb^{-1} of proton-proton collision data," Tech. Rep. ATLAS-CONF-2014-009, CERN, Geneva, Switzerland, 2014.

[71] J. Baglio, R. Gröber, M. Mühlleitner et al., "NMSSMCALC: a program package for the calculation of loop-corrected Higgs boson masses and decay widths in the (complex) NMSSM," *Computer Physics Communications*, vol. 185, no. 12, pp. 3372–3391, 2014.

[72] G. Aad, B. Abbott, J. Abdallah et al., "Combined measurement of the boson mass in *pp* collisions at $\sqrt{s} = 7$ and 8 TeV with the ATLAS and CMS experiments," *Physical Review Letters*, vol. 114, Article ID 191803, 2015.

[73] P. Bechtle, S. Heinemeyer, O. Stål, T. Stefaniak, and G. Weiglein, "HiggsSignals: confronting arbitrary Higgs sectors with measurements at the Tevatron and the LHC," *The European Physical Journal C*, vol. 74, no. 2, article 2711, 2014.

[74] J. F. Gunion, Y. Jiang, and S. Kraml, "Diagnosing degenerate Higgs bosons at 125 GeV," *Physical Review Letters*, vol. 110, no. 5, Article ID 051801, 2013.

[75] M. D. Goodsell, K. Nickel, and F. Staub, "Two-loop corrections to the Higgs masses in the NMSSM," *Physical Review D*, vol. 91, no. 3, Article ID 035021, 2015.

[76] F. Staub, Privatecommunication.

[77] F. Feroz and M. P. Hobson, "Multimodal nested sampling: an efficient and robust alternative to Markov Chain Monte Carlo methods for astronomical data analyses," *Monthly Notices of the Royal Astronomical Society*, vol. 384, no. 2, pp. 449–463, 2008.

[78] F. Feroz, M. P. Hobson, and M. Bridges, "MultiNest: an efficient and robust Bayesian inference tool for cosmology and particle physics," *Monthly Notices of the Royal Astronomical Society*, vol. 398, no. 4, pp. 1601–1614, 2009.

[79] F. Feroz, M. P. Hobson, E. Cameron, and A. N. Pettitt, "Importance nested sampling and the MultiNest algorithm," http://arxiv.org/abs/1306.2144.

[80] P. Bechtle, O. Brein, S. Heinemeyer, G. Weiglein, and K. E. Williams, "HiggsBounds: confronting arbitrary Higgs sectors with exclusion bounds from LEP and the Tevatron," *Computer Physics Communications*, vol. 181, no. 1, pp. 138–167, 2010.

[81] P. Bechtle, O. Brein, S. Heinemeyer, G. Weiglein, and K. E. Williams, "HiggsBounds 2.0.0: confronting neutral and charged Higgs sector predictions with exclusion bounds from LEP and the Tevatron," *Computer Physics Communications*, vol. 182, no. 12, pp. 2605–2631, 2011.

[82] P. Bechtle, O. Brein, S. Heinemeyer et al., "Recent Developments in HiggsBounds and a Preview of HiggsSignals," PoS CHARGED2012 (2012) 024, http://xxx.lanl.gov/abs/1301.2345.

[83] P. Bechtle, O. Brein, S. Heinemeyer et al., "HiggsBounds-4 : improved tests of extended Higgs sectors against exclusion bounds from LEP, the Tevatron and the LHC," *The European Physical Journal C*, vol. 74, article 2693, 2014.

[84] A. Djouadi, J. Kalinowski, and M. Spira, "HDECAY: a program for Higgs boson decays in the standard model and its supersymmetric extension," *Computer Physics Communications*, vol. 108, no. 1, pp. 56–74, 1998.

[85] B. Das, S. Moretti, S. Munir, and P. Poulose, In preparation.

Hindawi Publishing Corporation
Advances in High Energy Physics
Volume 2015, Article ID 686572, 22 pages
http://dx.doi.org/10.1155/2015/686572

Review Article

Lepton Flavor Violation beyond the MSSM

A. Vicente[1,2]

[1] *Instituto de Física Corpuscular, CSIC, Universitat de València, Apartado 22085, 46071 Valencia, Spain*
[2] *IFPA, AGO Département, Université de Liège, Bat. B5, Sart-Tilman, 4000 Liège 1, Belgium*

Correspondence should be addressed to A. Vicente; avelino.vicente@ulg.ac.be

Received 27 March 2015; Accepted 22 June 2015

Academic Editor: Michal Malinský

Most extensions of the Standard Model lepton sector predict large lepton flavor violating rates. Given the promising experimental perspectives for lepton flavor violation in the next few years, this generic expectation might offer a powerful indirect probe to look for new physics. In this review we will cover several aspects of lepton flavor violation in supersymmetric models beyond the Minimal Supersymmetric Standard Model. In particular, we will concentrate on three different scenarios: high-scale and low-scale seesaw models as well as models with R-parity violation. We will see that in some cases the LFV phenomenology can have characteristic features for specific scenarios, implying that dedicated studies must be performed in order to correctly understand the phenomenology in nonminimal supersymmetric models.

1. Introduction

The Standard Model (SM) particle content has been recently completed with the discovery of the long-awaited Higgs boson at the CERN Large Hadron Collider (LHC) [1, 2]. This constitutes a well deserved reward after decades of intense search, with great efforts from the theory and experimental communities. Furthermore, it also confirms that the SM must be, at least to a good approximation, a precise description of nature up to the energies explored. In fact, and apart from some phenomenological facts that indeed require some unknown new physics (NP), like the existence of dark matter and neutrino masses, the SM explains to a high level of accuracy all the observations made in a wide variety of experiments.

For the last decades, the progress in theoretical particle physics has been driven by naturalness considerations in the form of the famous hierarchy problem. This has led to many extensions of the SM, all of them attempting to explain why the weak scale has not been pushed to much higher energy scales by some hypothetical NP degrees of freedom. Among the many proposals to address this issue, supersymmetry (SUSY) is certainly the most popular one. However, and similarly to other analogous solutions to the hierarchy problem, the predicted new particles at the weak scale have not been observed at the LHC.

This has of course raised some doubts about the existence of supersymmetry close to the weak scale. Since this proximity is to be expected in case supersymmetry has something to do with the hierarchy problem, the whole idea of weak scale supersymmetry is under some pressure at the moment. However, it is worth keeping in mind that most experimental searches for SUSY focus on the Minimal Supersymmetric Standard Model (MSSM). This model, which constitutes the minimal extension of the SM that incorporates SUSY, has some underlying assumptions that lead to very specific signatures. For example, in the MSSM one assumes the conservation of a discrete symmetry, known as R-parity [3, 4], which forbids all renormalizable lepton and baryon number violating operators and leads to the existence of a stable particle, the lightest supersymmetric particle (LSP), which in turn leads to large amounts of missing energy in supersymmetric events at the LHC. There are, however, many known (and well motivated) supersymmetric scenarios with R-parity violation and, in fact, several authors have shown that simply by allowing for nonzero B-violating terms in the superpotential, the current LHC bounds can be clearly relaxed, allowing for the existence of light squarks and gluinos

hidden in the huge QCD background [5, 6]. Similarly, one can extend the MSSM in many other directions, often changing the phenomenology at colliders dramatically. This suggests that it might be too soon to give up on SUSY, a framework with many possibilities yet to be fully explored.

As explained above, there are some well-grounded phenomenological issues that cannot be explained within the SM. One of these open problems is the existence of nonzero neutrino masses and mixings, nowadays firmly established by neutrino oscillation experiments [7–9]. In fact, this issue is not addressed in the MSSM either, since neutrinos remain massless in the same way as in the SM. This calls for an extension of the MSSM that extends the lepton sector and accommodates the observations in neutrino oscillation experiments. This can be done in two different ways: (1) *high-energy extensions*, in which the new degrees of freedom responsible for the generation of neutrino masses live at very high energy scales, and (2) *low-energy extensions*, with new particles and/or interactions at the SUSY scale.

One of the most generic predictions in neutrino mass models is lepton flavor violation (LFV). In fact, neutrino oscillations are the proof that lepton flavor is not a conserved symmetry of nature, since neutrinos produced with a given flavor change it as they propagate. Therefore, all neutrino mass models built to give an explanation to oscillation experiments violate lepton flavor. However, we have never observed LFV processes involving charged leptons although, in principle, there is no symmetry (besides lepton flavor, which we know to be broken) that forbids processes like $\mu^- \to e^-\gamma$, $\tau^- \to e^-\mu^+\mu^-$, or $K_L \to e^-\mu^+$. This fact can be well understood in some minimal frameworks, such as the minimal extension of the SM with Dirac neutrinos. In this case, LFV in the charged lepton sector is strongly suppressed, since neutrino masses are the only source of LFV, leading to unobservable LFV rates, like $\mathrm{BR}(\mu^- \to e^-\gamma) \sim 10^{-55}$ [10]. However, as soon as one extends the SM, this conclusion can be clearly altered [11, 12]. In fact, new sources of LFV can be found in most extensions of the leptonic sector, caused either by new interactions, by new particles, or even by complete new sectors that couple to the SM leptons.

After this discussion on LFV and neutrino masses a clarification is in order. Although neutrino oscillations imply LFV, LFV does not necessarily imply neutrino oscillations. There are models that predict charged lepton LFV without generating a mass for the neutrinos. The simplest example of this class of models is the general Two-Higgs-Doublet of type-III, where neutrinos remain massless but lepton flavor is violated due to the existence of off-diagonal $h - \ell_i - \ell_j$ vertices. Another relevant example is the MSSM itself, where neutrinos are also massless, but the slepton soft masses can induce LFV processes if they contain off-diagonal entries. One can actually estimate the branching ratio for the radiative LFV decay $\ell_i \to \ell_j\gamma$ as [13]

$$\mathrm{BR}\left(\ell_i \longrightarrow \ell_j\gamma\right) \simeq \frac{48\pi^3\alpha}{G_F^2}\frac{\left|\left(m_{\tilde{\ell}}^2\right)_{ij}\right|^2}{M_{\mathrm{SUSY}}^8}\mathrm{BR}\left(\ell_i \longrightarrow \ell_j\nu_i\overline{\nu}_j\right), \quad (1)$$

where G_F is the Fermi constant, α is the fine structure constant, $(m_{\tilde{\ell}}^2)_{ij}$ are the dominant off-diagonal elements of the soft SUSY breaking slepton mass matrices, and M_{SUSY} is the typical mass of the SUSY particles, expected to be in the TeV ballpark. This estimate clearly shows that rather small off-diagonal elements are required to satisfy the experimental bounds [14].

In general, large LFV rates are expected in most models beyond the SM. This observation leads to the so-called *flavor puzzle*: the nonobservation of LFV is a rather surprising fact, since generic new physics would predict LFV rates clearly above the current experimental limits. This suggests that flavor structures in new physics models cannot be generic, but some organizing principle, such as a flavor symmetry, might be at work. Furthermore, it also motivates the study of LFV as an indirect probe of new physics and, in particular, of supersymmetric models beyond the MSSM. This is the subject of this review. The field of lepton flavor violation beyond the MSSM has been intensely explored for many years and contains a vast literature. In this review I present my personal view of the subject and thus I must apologize for those papers which are not cited. In particular, we will concentrate on three different scenarios: high-scale and low-scale seesaw models as well as models with R-parity violation. As we will see, the LFV phenomenology turns out to be very different depending on the exact scenario, implying that lepton flavor violation may be richer than in the MSSM. In some cases the common lore (established in the MSSM) turns out to be wrong, and specific studies must be performed in order to correctly understand the corresponding LFV phenomenology.

Before concluding the introduction, let us clarify the title of this review. As explained above, the MSSM can be made lepton flavor violating by introducing nonzero off-diagonal terms in the soft SUSY breaking terms for the sleptons. These LFV sources will be present in any supersymmetric model that includes the MSSM. In contrast, in this review we will consider a scenario to be *beyond the MSSM* if it contains additional LFV sources besides those in the MSSM. With this definition, the three specific supersymmetric scenarios discussed in this review fall within this category.

This review is organized as follows: in Section 2 we give an overview of the current experimental situation and briefly discuss some projects that will take place in the near future. Then we review the LFV phenomenology of three different types of models beyond the MSSM: high-scale seesaw models (in Section 3), low-scale seesaw models (in Section 4), and models with R-parity violation (in Section 5). Finally, we conclude in Section 6.

2. Current Experimental Situation and Future Projects

The search for LFV is soon going to live a *golden age* given the upcoming experiments devoted to high-intensity physics (see [15–17] for recent reviews). In addition to the LFV searches already taking place in several experiments, new projects will join the effort in the next few years.

In what concerns the radiative decay $\ell_i \to \ell_j \gamma$, the experiment leading to the most stringent constraints is MEG. This experiment, located at the Paul Scherrer Institute in Switzerland, searches for the radiative process $\mu \to e\gamma$. Recently, the MEG collaboration announced a new limit on the rate for this process based on the analysis of a dataset with 3.6×10^{14} stopped muons. The nonobservation of the LFV process led to the limit $\mathrm{BR}(\mu \to e\gamma) < 5.7 \cdot 10^{-13}$ [18], four times more stringent than the previous limit obtained by the same collaboration. Moreover, the MEG collaboration has announced plans for future upgrades. These will allow reaching a sensitivity of about $6 \cdot 10^{-14}$ after 3 years of acquisition time [19]. This is of great importance, as this observable along with the experimental sensitivity currently provides the most stringent limit on LFV parameters in many models.

The most promising improvements in the near future are expected in $\mu \to 3e$ and $\mu - e$ conversion in nuclei. Regarding the former, the decay $\mu \to 3e$ was searched for long ago by the SINDRUM experiment [20], setting the strong limit $\mathrm{BR}(\mu \to 3e) < 1.0 \cdot 10^{-12}$. The future Mu3e experiment announces a sensitivity of $\sim 10^{-16}$ [21], which would imply an impressive improvement by 4 orders of magnitude. As for the latter, several experiments will compete in the next few years, with sensitivities for the conversion rate ranging from 10^{-14} to an impressive 10^{-18}. These include Mu2e [22–24], DeeMe [25], COMET [26, 27], and the future PRISM/PRIME [28]. In all cases, these experiments will definitely improve on previous experimental limits.

The limits for τ observables are less stringent, although significant improvements are expected from B factories like Belle II [29, 30]. Finally, although the most common way to search for LFV is in low-energy experiments, colliders can also play a very relevant role looking for LFV processes at high energies. The LHCb collaboration reported recently the first bounds on $\tau \to 3\mu$ ever obtained in a hadron collider [31]. Furthermore, the CMS collaboration recently found an intriguing 2.4σ excess in the $h \to \tau\mu$ channel which translates into $\mathrm{BR}(h \to \tau\mu) = (0.84^{+0.39}_{-0.37})\%$ [32]. For reference, in Table 1 we collect present bounds and expected near-future sensitivities for the most popular low-energy LFV observables.

The theoretical understanding of all these processes will be crucial in case a discovery is made. With such a large variety of processes, the determination of hierarchies or correlations in specific models will allow us to extract fundamental information on the underlying physics behind LFV. This goal requires detailed analytical and numerical studies of the different contributions to the LFV processes, in order to get a global picture of the LFV *anatomy* of the relevant models and be able to discriminate among them by means of combinations of observables with definite predictions [33].

Table 1: Current experimental bounds and future sensitivities for the most important LFV observables.

LFV process	Present bound	Future sensitivity
$\mu \to e\gamma$	5.7×10^{-13} [18]	6×10^{-14} [19]
$\tau \to e\gamma$	3.3×10^{-8} [34]	$\sim 3 \times 10^{-9}$ [29]
$\tau \to \mu\gamma$	4.4×10^{-8} [34]	$\sim 3 \times 10^{-9}$ [29]
$\mu \to eee$	1.0×10^{-12} [20]	$\sim 10^{-16}$ [21]
$\tau \to \mu\mu\mu$	2.1×10^{-8} [35]	$\sim 10^{-9}$ [29]
$\tau^- \to e^-\mu^+\mu^-$	2.7×10^{-8} [35]	$\sim 10^{-9}$ [29]
$\tau^- \to \mu^- e^+ e^-$	1.8×10^{-8} [35]	$\sim 10^{-9}$ [29]
$\tau \to eee$	2.7×10^{-8} [35]	$\sim 10^{-9}$ [29]
$\mu^-, \mathrm{Ti} \to e^-, \mathrm{Ti}$	4.3×10^{-12} [36]	$\sim 10^{-18}$ [37]
$\mu^-, \mathrm{Au} \to e^-, \mathrm{Au}$	7×10^{-13} [38]	
$\mu^-, \mathrm{Al} \to e^-, \mathrm{Al}$		10^{-15}–10^{-18}
$\mu^-, \mathrm{SiC} \to e^-, \mathrm{SiC}$		10^{-14} [39]

3. High-Scale Seesaw Models

Neutrino mixing is, by itself, a flavor violating effect. Therefore, all neutrino mass models that aim at explaining the observed pattern of neutrino masses and mixings incorporate lepton flavor violation. However, specific predictions can be very different in different models.

Among the huge number of scenarios proposed for neutrino mass generation, the seesaw mechanism is arguably the most popular one. In its conventional form, the seesaw mechanism explains the smallness of neutrino mass by means of a very large energy scale, the *seesaw scale* M_{SS}, which suppresses neutrino masses as

$$m_\nu \sim \frac{v^2}{M_{\mathrm{SS}}}. \tag{2}$$

Here $\langle H^0 \rangle = v/\sqrt{2} = 174\,\mathrm{GeV}$ is the standard Higgs boson vacuum expectation value (VEV) that determines the weak scale. In order to obtain neutrino masses of about $\sim 0.1\,\mathrm{eV}$, one requires $M_{\mathrm{SS}} \sim 10^{14}\,\mathrm{GeV}$. For this reason, this setup is usually called *high-scale seesaw*. The proximity of the high-energy scale M_{SS} to the grand unification (GUT) scale (as predicted in the MSSM) $m_{\mathrm{GUT}} = 2 \cdot 10^{16}\,\mathrm{GeV}$ suggests an intriguing connection with unification physics, making the seesaw a very well-motivated scenario.

Regarding specific realizations of the seesaw mechanism, it is well-known that, with renormalizable interactions only, three tree-level realizations exist [48]. These are usually called type-I [49–54], type-II [53–59], and type-III [60]. They differ from each other by the nature of the seesaw messengers: in the type-I seesaw these are singlet right-handed neutrinos, in the type-II seesaw scalar $\mathrm{SU}(2)_L$ triplets with hypercharge two, and in the type-III seesaw fermionic $\mathrm{SU}(2)_L$ triplets with vanishing hypercharge. In all cases they lead to a neutrino mass of the form of (2), where M_{SS} is proportional to the mass of the heavy mediators, and the induced neutrino masses are of Majorana type, thus breaking lepton number in two units.

Given the large Majorana masses of the seesaw mediators, one may wonder about how to probe the high-scale seesaw. In supersymmetric scenarios this is possible thanks to the sleptons. Even if their soft terms are flavor conserving at some high-energy scale, the renormalization group running down to the SUSY scale will induce nonzero off-diagonal terms due to their interactions with the seesaw mediators [61].

These can be probed since the misalignment of the slepton mass matrices with respect to that of the SM charged leptons induces LFV processes such as $\ell_i \to \ell_j\gamma$, $\ell_i \to 3\ell_j$ and $\mu - e$ conversion in nuclei. This connection between the phenomenology at low-energies and the high-scale mediators is only possible in supersymmetric models and constitutes an excellent opportunity to test the standard seesaw scenario. In the non-SUSY version of the seesaw mechanism this link between high and low energy scales is lost. In this case probing the origin of neutrino masses becomes a quite challenging task, and only very indirect probes such as neutrinoless double beta decay are possible [62]. However, it is worth pointing out that such clean connection is only possible in the absence of additional sources of LFV. This requires a strong theoretical assumption: universal and flavor conserving boundary conditions for the soft terms at the GUT scale.

In case of high-scale seesaw models, the low-energy theory is simply the MSSM. This allows one to establish definite patterns and hierarchies among the LFV observables. For instance, the branching ratios for the $\ell_i \to \ell_j\gamma$ and $\ell_i \to 3\ell_j$ LFV decays follow the approximate relation [63–65],

$$\begin{aligned}&\mathrm{BR}\left(\ell_i \longrightarrow 3\ell_j\right)\\ &\quad\simeq \frac{\alpha}{3\pi}\left(\log\left(\frac{m^2_{\ell_i}}{m^2_{\ell_j}}\right) - \frac{11}{4}\right)\mathrm{BR}\left(\ell_i \longrightarrow \ell_j\gamma\right).\end{aligned} \tag{3}$$

Therefore, in supersymmetric high-scale seesaw models, the most constraining LFV process is $\ell_i \to \ell_j\gamma$. The relation in (3) is caused by the so-called *dipole dominance* in high-scale seesaw models. Among the different contributions to the 3-body decay $\ell_i \to 3\ell_j$, the dipole photon penguins come multiplied by a large logarithmic term, caused by the infrared divergence that would appear in the $m_{\ell_i} \to 0$ limit, thus becoming the dominant ones and leading to the proportionality between the $\ell_i \to \ell_j\gamma$ and $\ell_i \to 3\ell_j$ branching ratios. An exception to this general rule is found for low pseudoscalar masses and large $\tan\beta$ [66]. In this case, Higgs penguins turn out to be dominant in processes involving the second and third generations, like $\tau \to 3\mu$. However, this region of parameter space is nowadays under some tension due to strong flavor constraints derived from the observation of quark flavor violating processes like $B_s \to \mu^+\mu^-$ [67].

3.1. Standard High-Scale Seesaw Scenarios. Implementing a high-scale seesaw mechanism in supersymmetric scenarios involves an additional complication. This is related to one of the most appealing features of the MSSM: gauge coupling unification. In case of the type-I seesaw, the introduction of the seesaw mediator does not spoil this attractive feature, since the right-handed neutrino superfields are gauge singlets and do not affect the running of the gauge couplings. In contrast, in the type-II and type-III seesaws, new contributions to the running of the $\mathrm{SU}(2)_L$ and $U(1)_Y$ gauge couplings are induced by the seesaw mediators. However, a well-known solution to this problem exists. Unification can be easily restored by embedding the seesaw mediators in full SU(5) multiplets, like **15**-plets in the case of type-II [68] or **24**-plets [69] in the case of type-III. The contributions from the other members of the multiplet guarantee that the three gauge couplings will eventually meet at a high energy scale, m_{GUT}, although the common value of the coupling changes, g_{GUT}, might be different from that of the MSSM. In addition, note that the **24**-plet of SU(5) contains, besides the $\mathrm{SU}(2)_L$ triplet, a singlet state which also contributes to neutrino masses. Hence, in this case one actually has a mixture between type-I and type-III seesaws.

The new superfield content, explicitly denoting gauge charges under $\mathrm{SU}(3)_c \times \mathrm{SU}(2)_L \times U(1)_Y$, and superpotential for each seesaw variant are [70] the following.

(i) *Type-I*. Three generations of right-handed neutrino superfields, singlets of SU(5), are introduced, $\widehat{N}^c \sim (1,1,0)$:

$$W_{\mathrm{I}} = W_{\mathrm{MSSM}} + Y_\nu \widehat{N}^c \widehat{L}\widehat{H}_u + \frac{1}{2}M_R \widehat{N}^c\widehat{N}^c. \tag{4}$$

(ii) *Type-II*. In this case one needs to introduce a vector-like pair of **15** and $\overline{\mathbf{15}}$ of SU(5), decomposed as $\widehat{S} \sim (6,1,-2/3)$, $\widehat{T} \sim (1,3,1)$, and $\widehat{Z} \sim (3,2,1/6)$ (as well as the corresponding bar superfields). $\widehat{T}$ and $\widehat{\overline{T}}$ are the $\mathrm{SU}(2)_L$ triplets responsible for neutrino mass generation. Note that in this case only one generation of **15** and $\overline{\mathbf{15}}$ is required, since the type-II seesaw can generate three nonzero masses for the light neutrinos with only one $\mathrm{SU}(2)_L$ scalar triplet:

$$\begin{aligned}W_{\mathrm{II}} = W_{\mathrm{MSSM}} &+ \frac{1}{\sqrt{2}}\left(Y_T\widehat{L}\widehat{T}\widehat{L} + Y_S\widehat{d}^c\widehat{S}\widehat{d}^c\right) + Y_Z\widehat{d}^c\widehat{Z}\widehat{L}\\ &+ \frac{1}{\sqrt{2}}\left(\lambda_1\widehat{H}_d\widehat{T}\widehat{H}_d + \lambda_2\widehat{H}_u\widehat{\overline{T}}\widehat{H}_u\right) + M_T\widehat{T}\widehat{\overline{T}}\\ &+ M_Z\widehat{Z}\widehat{\overline{Z}} + M_S\widehat{S}\widehat{\overline{S}}.\end{aligned} \tag{5}$$

(iii) *Type-III*. Three generations of **24** of SU(5) are added. They can be decomposed as $\widehat{N}^c \sim (1,1,0)$, $\widehat{G} \sim (8,1,0)$, $\widehat{\Sigma} \sim (1,3,0)$, $\widehat{X} \sim (3,2,-5/6)$, and $\widehat{\overline{X}} \sim (\overline{3},2,5/6)$. As explained above, neutrino masses are generated as a combination of a type-I seesaw (mediated by N^c) and a type-III seesaw (mediated by the $\mathrm{SU}(2)_L$ triplet Σ):

$$\begin{aligned}W_{\mathrm{III}} = W_{\mathrm{MSSM}} &+ \widehat{H}_u\left(Y_\Sigma\widehat{\Sigma} - \sqrt{\frac{3}{10}}Y_\nu\widehat{N}^c\right)\widehat{L}\\ &+ Y_X\widehat{H}_u\widehat{\overline{X}}\widehat{d}^c + \frac{1}{2}M_R\widehat{N}^c\widehat{N}^c + \frac{1}{2}M_G\widehat{G}\widehat{G}\\ &+ \frac{1}{2}M_\Sigma\widehat{\Sigma}\widehat{\Sigma} + M_X\widehat{X}\widehat{\overline{X}}.\end{aligned} \tag{6}$$

The following notation is used in (4), (5), and (6): W_{MSSM} is the MSSM superpotential, $\widehat{H}_d$, $\widehat{H}_u$, and $\widehat{L}$ are the down-Higgs, up-Higgs, and lepton $\mathrm{SU}(2)_L$ doublet superfields,

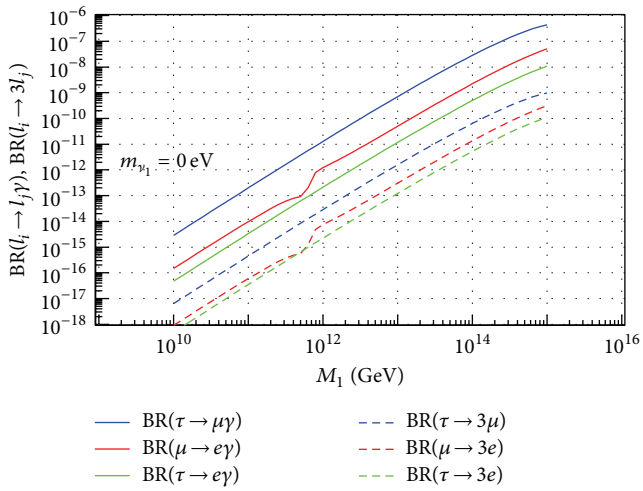

FIGURE 1: Branching ratios for $\ell_i \to \ell_j\gamma$ and $\ell_i \to 3\ell_j$ as a function of the seesaw scale in the SUSY type-I seesaw. This figure was obtained in the standard SPS1a' point, assuming degenerate right-handed neutrinos and fixing the neutrino Yukawas to reproduce tribimaximal mixing. Furthermore, a massless lightest neutrino was also assumed. Figure taken from [40].

respectively, and $\widehat{d}^c$ is the right-handed down-type quark superfield.

The LFV phenomenology of SUSY seesaw models has been studied by many authors. For the type-I seesaw, low-energy LFV decays such as $\ell_i \to \ell_j\gamma$ and $\ell_i \to 3\ell_j$ have been calculated in [40, 64, 65, 71–80]. Similarly, $\mu - e$ conversion in nuclei has been studied in [81, 82]. The other two seesaw variants have received much less attention. The LFV phenomenology of the SUSY type-II seesaw has been considered in [41, 68, 83–87], whereas the SUSY type-III seesaw has been studied in [88–90]. More recently, the interplay between the Higgs mass constraint and LFV was studied in [70] for the three seesaw variants. In the following we comment on some selected results.

Let us first comment on some results for the SUSY type-I seesaw. Figure 1 shows the branching ratios for the $\ell_i \to \ell_j\gamma$ and $\ell_i \to 3\ell_j$ decays as a function of the seesaw scale (the mass of the right-handed neutrino mass). This figure was obtained in [40], using the standard SPS1a' point [42], assuming degenerate right-handed neutrinos and a massless lightest neutrino and fixing the neutrino Yukawas to reproduce tribimaximal mixing. Although this parameter choice is nowadays excluded for several reasons (the SUSY spectrum is too light to pass the constraints from LHC searches and tribimaximal mixing is now excluded after θ_{13} has been measured), it serves to illustrate the dipole dominance discussed above. Indeed, one sees a perfect correlation between the branching ratios of $\ell_i \to \ell_j\gamma$ and $\ell_i \to 3\ell_j$, with $\text{BR}(\ell_i \to 3\ell_j) \ll \text{BR}(\ell_i \to \ell_j\gamma)$. As already discussed, this is due to the fact that the photonic dipole operator $(\overline{\ell}_i F_{\mu\nu}\sigma^{\mu\nu}\ell_j)$ dominates both processes.

We now turn to the SUSY type-II seesaw. In the type-II seesaw, the neutrino mass matrix is proportional to the Y_T Yukawa matrix,

$$m_\nu = \frac{v_u^2}{2}\frac{\lambda_2}{M_T}Y_T. \tag{7}$$

This is derived from the superpotential term $Y_T\widehat{L}\widehat{T}\widehat{L}$ in (5). This direct relation has important consequences for the phenomenology, since it forces the flavor structure of Y_T to be the same as that of m_ν, the latter being *measured* in neutrino oscillation experiments. In contrast, in the type-I and type-III seesaws the analogous relation is quadratic in the Yukawa coupling. This introduces extra freedom in the determination of the seesaw parameters (usually encoded in the so-called R matrix [91]) and makes it impossible to predict the Yukawa flavor structure only from neutrino oscillation data. In other words, if all the neutrino masses, angles, and phases were known, Y_T would be completely fixed (up to an overall constant). Since Y_T determines the LFV phenomenology, this implies correlations between the neutrino oscillation parameters and LFV observables.

A clear illustration of the previous point is shown in Figure 2, borrowed from [41]. By computing the ratios $\text{BR}(\ell_i \to \ell_j\gamma)/\text{BR}(\ell_m \to \ell_n\gamma)$ one gets rid of the unknown overall factor in the Y_T Yukawas, thus obtaining direct predictions in terms of neutrino parameters. In this case, the figure shows the dependence of these ratios on the mixing angle θ_{13} and the Dirac CP violating phase δ. We see that this scenario is extremely predictive. For example, finding experimentally $\text{BR}(\tau \to e\gamma) > \text{BR}(\mu \to e\gamma)$ would immediately rule out the model, at least in its minimal form. One way to spoil these strict predictions is to introduce a second $\text{SU}(2)_L$ triplet T'. In this case m_ν would receive contributions from T and T', $m_\nu = m_\nu^T + m_\nu^{T'}$, and the proportionality in (7) would be lost.

Additional ways to test high-scale SUSY seesaws include slepton mass splittings [92] (directly related to LFV) and the study of the SUSY spectrum, usually *deformed* with respect to the standard spectra in constrained (CMSSM) scenarios. In particular, one can construct certain *invariants* that contain information about the high-energy scale; see, for example, [69, 93, 94]. See also [95] for related ideas.

3.2. Extended High-Scale Seesaw Scenarios. We now turn our attention to extended high-scale SUSY seesaw scenarios beyond the *classical* type-I, type-II, and type-III seesaws. However, before we concentrate on the extended models, let us make a general observation. As already discussed, flavor violating entries in the slepton soft terms $m_{\widetilde{L}}^2$ and $m_{\widetilde{e}}^2$ (the left and right slepton squared soft masses, resp.) are induced due to their interactions with the seesaw mediators. Even if they are flavor diagonal at the unification scale, off-diagonal terms are generated at low energies by renormalization group running, thus inducing all kinds of LFV processes. In the case

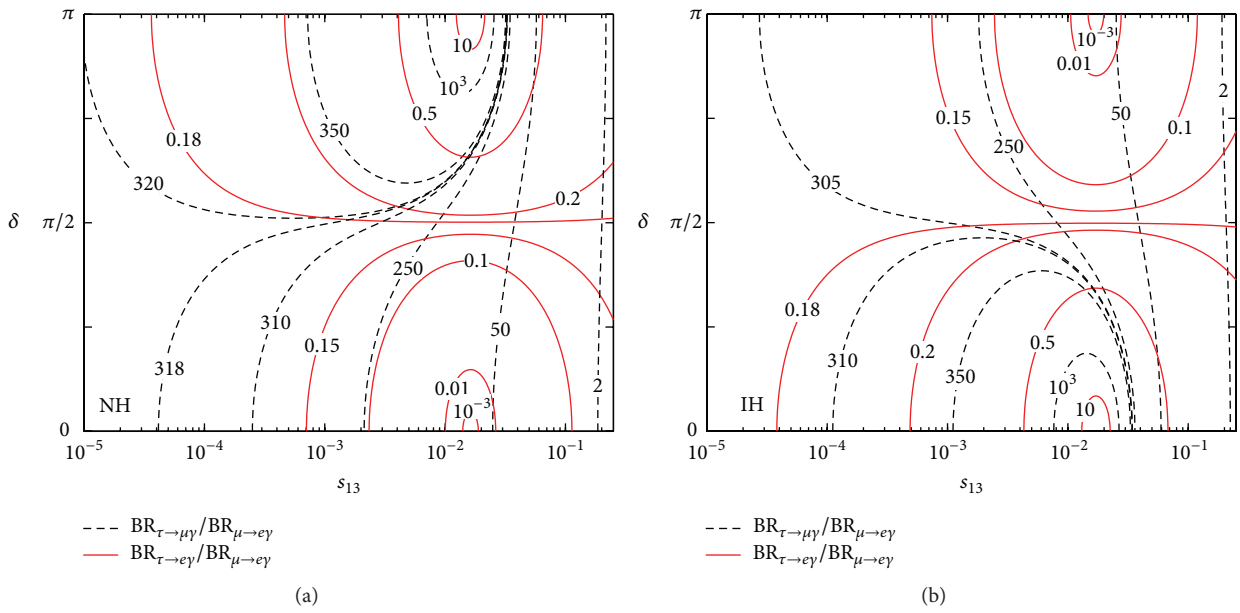

FIGURE 2: Contours of the ratios $\mathrm{BR}(\tau \to \mu\gamma)/\mathrm{BR}(\mu \to e\gamma)$ (black, dashed lines) and $\mathrm{BR}(\tau \to e\gamma)/\mathrm{BR}(\mu \to e\gamma)$ (red, solid lines) in the $(\sin\theta_{13}, \delta)$ plane, for normal hierarchy (a) and inverted hierarchy (b) for the neutrino mass spectrum. Figure taken from [41].

of the radiative $\ell_i \to \ell_j\gamma$, the effective dipole operator that contributes to the decay can be written as

$$\mathscr{L}_{\text{dipole}} = e\frac{m_{\ell_i}}{2}\bar{\ell}_i\sigma_{\mu\nu}F^{\mu\nu}\left(A_L^{ij}P_L + A_R^{ij}P_R\right)\ell_j + \text{h.c.}, \quad (8)$$

where $P_{L,R} = (1/2)(1 \mp \gamma_5)$ are the usual chirality projectors and e is the electric charge. The Wilson coefficients A_L and A_R are generated by loops with left and right sleptons, respectively. One finds

$$A_L^{ij} \sim \frac{\left(m_{\tilde{L}}^2\right)_{ij}}{M_{\text{SUSY}}^4}, \qquad A_R^{ij} \sim \frac{\left(m_{\tilde{e}}^2\right)_{ij}}{M_{\text{SUSY}}^4}, \quad (9)$$

where it has been assumed that A-terms mixing left-right transitions are negligible. $\mathrm{BR}(\ell_i \to \ell_j\gamma)$ can be computed in terms of A_L and A_R as

$$\mathrm{BR}\left(\ell_i \longrightarrow \ell_j\gamma\right) \simeq \frac{48\pi^3\alpha}{G_F^2}\left(\left|A_L^{ij}\right|^2 + \left|A_R^{ij}\right|^2\right)\mathrm{BR}\left(\ell_i \longrightarrow \ell_j\nu_i\bar{\nu}_j\right). \quad (10)$$

The straightforward combination of (9) and (10) leads to (1).

In the minimal SUSY seesaw models discussed above, the seesaw mediators only couple to the left sleptons. For instance, in the type-I case this interaction is given by the superpotential coupling $Y_\nu\widehat{L}\widehat{H}_u\widehat{N}$, whereas in the type-II case it is given by the $Y_T\widehat{L}\widehat{T}\widehat{L}$ term. For this reason, negligible off-diagonal entries in $m_{\tilde{e}}^2$ are induced, implying that minimal SUSY seesaw models predict $A_R \simeq 0$. As we will see below, this has an impact on some low-energy observables that allow, in principle, testing the minimality of the high-scale seesaw mechanism.

3.2.1. Supersymmetric Models with Nonminimal Seesaw Mechanisms. As an example supersymmetric model with nonminimal seesaw mechanisms, we consider the left-right symmetric model of [96, 97] (in the following simply called "the LR model"). The LFV and dark matter phenomenology of this model has been studied in detail in [43, 98].

The model is defined below the GUTscale (the model implicitly assumes the existence of a GUT model at higher energies; at m_{GUT}, the gauge couplings and soft terms unify), where the gauge group is $\mathrm{SU}(3)_c \times \mathrm{SU}(2)_L \times \mathrm{SU}(2)_R \times U(1)_{B-L}$. In addition, we assume that parity is conserved. The matter content of the model is given in Table 2. Here $\widehat{Q}$, $\widehat{Q}^c$, $\widehat{L}$, and $\widehat{L}^c$ are the quark and lepton superfields of the MSSM with the addition of (three) right-handed neutrino superfields to complete the $\widehat{L}^c\mathrm{SU}(2)_R$ doublets.

Two $\widehat{\Phi}$ superfields, bidoublets under $\mathrm{SU}(2)_L \times \mathrm{SU}(2)_R$, are introduced. Among their components, they contain the standard $\widehat{H}_d$ and $\widehat{H}_u$ MSSM Higgs doublets. Finally, the rest of the superfields in Table 2 are introduced to break the LR symmetry.

With the representations in Table 2, the most general superpotential compatible with the gauge symmetry and parity is

$$\begin{aligned} W_{\text{LR}} = {} & Y_Q\widehat{Q}\widehat{\Phi}\widehat{Q}^c + Y_L\widehat{L}\widehat{\Phi}\widehat{L}^c - \frac{\mu}{2}\widehat{\Phi}\widehat{\Phi} + f\widehat{L}\widehat{\Delta}\widehat{L} \\ & + f^*\widehat{L}^c\widehat{\Delta}^c\widehat{L}^c + a\widehat{\Delta}\widehat{\Omega}\widehat{\Delta} + a^*\widehat{\Delta}^c\widehat{\Omega}^c\widehat{\Delta}^c + \alpha\widehat{\Omega}\widehat{\Phi}\widehat{\Phi} \\ & + \alpha^*\widehat{\Omega}^c\widehat{\Phi}\widehat{\Phi} + M_\Delta\widehat{\Delta}\widehat{\Delta} + M_\Delta^*\widehat{\Delta}^c\widehat{\Delta}^c + M_\Omega\widehat{\Omega}\widehat{\Omega} \\ & + M_\Omega^*\widehat{\Omega}^c\widehat{\Omega}^c. \end{aligned} \quad (11)$$

Family and gauge indices have been omitted in (11); more detailed expressions can be found in [96]. Note that this

Table 2: LR model. Matter content between the GUT scale and the $SU(2)_R$ breaking scale. The electric charge operator is defined as $Q = I_{3L} + I_{3R} + (B - L)/2$.

Superfield	Generations	$SU(3)_c$	$SU(2)_L$	$SU(2)_R$	$U(1)_{B-L}$
$\widehat{Q}$	3	3	2	1	$\frac{1}{3}$
$\widehat{Q}^c$	3	$\overline{3}$	1	2	$-\frac{1}{3}$
$\widehat{L}$	3	1	2	1	−1
$\widehat{L}^c$	3	1	1	2	1
$\widehat{\Phi}$	2	1	2	2	0
$\widehat{\Delta}$	1	1	3	1	2
$\widehat{\overline{\Delta}}$	1	1	3	1	−2
$\widehat{\Delta}^c$	1	1	1	3	−2
$\widehat{\overline{\Delta}}^c$	1	1	1	3	2
$\widehat{\Omega}$	1	1	3	1	0
$\widehat{\Omega}^c$	1	1	1	3	0

superpotential is invariant under the parity transformations $\widehat{Q} \leftrightarrow (\widehat{Q}^c)^*$, $\widehat{L} \leftrightarrow (\widehat{L}^c)^*$, $\widehat{\Phi} \leftrightarrow \widehat{\Phi}^\dagger$, $\widehat{\Delta} \leftrightarrow (\widehat{\Delta}^c)^*$, $\widehat{\overline{\Delta}} \leftrightarrow (\widehat{\overline{\Delta}}^c)^*$, and $\widehat{\Omega} \leftrightarrow (\widehat{\Omega}^c)^*$. This discrete symmetry reduces the number of free parameters of the model.

The breaking of the left-right gauge group to the MSSM gauge group takes place in two steps: $\mathrm{SU}(2)_R \times U(1)_{B-L} \to U(1)_R \times U(1)_{B-L} \to U(1)_Y$. In the first step, the neutral component of the triplet Ω takes a VEV,

$$\left\langle \Omega^{c0} \right\rangle = \frac{v_R}{\sqrt{2}}, \tag{12}$$

which breaks $\mathrm{SU}(2)_R$. However, since $I_{3R}(\Omega^{c0}) = 0$ there is a $U(1)_R$ symmetry left over. Next, the group $U(1)_R \times U(1)_{B-L}$ is broken by

$$\begin{aligned} \left\langle \Delta^{c0} \right\rangle &= \frac{v_{BL}}{\sqrt{2}}, \\ \left\langle \overline{\Delta}^{c0} \right\rangle &= \frac{\overline{v}_{BL}}{\sqrt{2}}. \end{aligned} \tag{13}$$

The remaining symmetry is now $U(1)_Y$ with hypercharge defined as $Y = I_{3R} + (B - L)/2$.

Regarding neutrino masses, assuming that the left triplets (Δ and $\overline{\Delta}$) have vanishing VEVs, one induces neutrinos masses from a type-I seesaw only thanks to the presence of the right-handed neutrinos [96].

Before discussing how to test this scenario with lepton flavor violation, let us mention some other nonminimal SUSY seesaw models. The phenomenological study in [99] is based on a model very similar to the discussed here, without $\widehat{\Omega}$ superfields. See also [100] for a comprehensive study of supersymmetric models with extended gauge groups at intermediate steps. Finally, the seesaw mechanism can also be embedded in SUSY GUTs, usually leading to very predictive scenarios [101–106].

3.2.2. Probing Nonminimal Seesaw Mechanisms. As already discussed, a pure seesaw model predicts $A_R \simeq 0$ simply because the right sleptons do not couple to the seesaw mediators. However, in models with nonminimal seesaw mechanisms, new interactions between the right sleptons and the members of the extended particle content at high energies might exist. When this is the case, nonzero A_R coefficients can be induced.

Let us consider an example. In the LR model, the left-right symmetry implies that, above the parity breaking scale, the flavor violating entries generated in $m_{\tilde{e}}^2$ are exactly as large as the ones in $m_{\tilde{L}}^2$. As a consequence of this, $A_R \neq 0$ is obtained at low energies. In fact, one can even get a handle on the symmetry breaking pattern at high energies. Below the $\mathrm{SU}(2)_R$ breaking scale, parity is broken and left and right slepton soft masses evolve differently. The left ones keep running from the $\mathrm{SU}(2)_R$ breaking scale to the $U(1)_{B-L}$ scale due to the left slepton couplings with the right-handed neutrinos. One thus expects larger flavor violating effects in the left slepton sector, and the difference between left and right must correlate with the ratio v_{BL}/v_R, which measures the hierarchy between the two breaking scales.

The question is how to measure this difference. For this purpose one can use the positron polarization asymmetry, defined as

$$\mathscr{A}\left(\mu^+ \longrightarrow e^+\gamma\right) = \frac{\left|A_L\right|^2 - \left|A_R\right|^2}{\left|A_L\right|^2 + \left|A_R\right|^2}. \tag{14}$$

If MEG observes $\mu^+ \to e^+\gamma$ events, the angular distribution of the outgoing positrons can be used to discriminate between left- and right-handed polarized states and measure $\mathscr{A}$ [107, 108]. And this can in turn be used to get information on A_L and A_R.

In a pure SUSY seesaw model one expects $\mathscr{A} \simeq +1$ to a very good accuracy. However, in models with nonminimal seesaw mechanisms $\mathscr{A}$ can significantly depart from +1. For example, the LR model typically leads to significant departures from this expectation, giving an interesting signature of the high-energy restoration of parity. This is shown in Figure 3, extracted from [43]. First of all, it is clear that the polarization asymmetry $\mathscr{A}(\mu^+ \to e^+\gamma)$ is well correlated with the quantity $\log(v_R/m_{\mathrm{GUT}})/\log(v_{BL}/m_{\mathrm{GUT}})$. One finds that as v_{BL} and v_R become very different, $\mathscr{A}$ approaches +1. In contrast, when the two breaking scales are close, $v_{BL}/v_R \sim 1$, this effect disappears and the positron polarization asymmetry approaches $\mathscr{A} = 0$. Note that a negative value for $\mathscr{A}$ is not possible in this model, since the LFV terms in the right slepton sector never run more than the corresponding terms in the left one.

There are alternative ways to test nonminimal high-scale SUSY seesaw scenarios. These include the study of the SUSY spectrum and, in particular, of the *invariants* pointed out for minimal seesaw models. In this case, they contain information about the high-energy intermediate scales [100, 109].

4. Low-Scale Seesaw Models

The high-scale seesaw has an important drawback: the heaviness of the seesaw mediators precludes any chance of direct

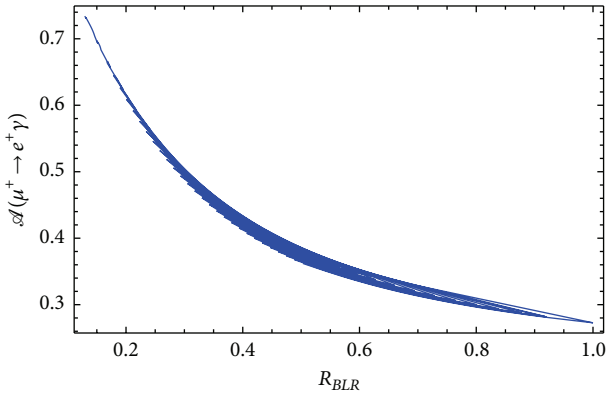

FIGURE 3: Positron polarization asymmetry $\mathscr{A}(\mu^+ \to e^+\gamma)$ as a function of the ratio $R_{BLR} = \log(v_R/m_{\text{GUT}})/\log(v_{BL}/m_{\text{GUT}})$. The seesaw scale M_{SS} has been fixed to 10^{13} GeV, whereas v_{BL} and v_R take values in the ranges $v_{BL} \in [10^{14}, 10^{15}]$ GeV and $v_R \in [10^{15}, 10^{16}]$ GeV. Lighter colours indicate larger v_{BL}. The CMSSM-like parameters have been taken as in the SPS3 benchmark point [42]. Figure taken from [43].

tests. Only indirect tests, based on low-energy processes which may have an imprint of the high seesaw scale M_{SS}, are possible, as explained in Section 3. In contrast to high-scale models, *low-scale seesaw models* [110] offer a richer phenomenological perspective since the seesaw mediators are allowed to be light. In this type of neutrino mass models, instead of (2), neutrino masses are given by

$$m_\nu \sim \mu_\nu \frac{v^2}{M_{\text{SS}}^2}, \tag{15}$$

where M_{SS} is again given by the mass scale of the seesaw mediators and μ_ν (not to be confused with the μ parameter of the MSSM) is a small dimensionful parameter, $\mu_\nu \ll v, M_{\text{SS}}$. In this case, the smallness of neutrino masses is not obtained with a large M_{SS} scale, but with a tiny μ_ν parameter. Indeed, if $M_{\text{SS}} \sim$ TeV, (15) implies a μ_ν parameter of the order of the eV in order to get m_ν in the ~0.1 eV ballpark. Therefore, one can simultaneously obtain the correct size of neutrino masses while having seesaw mediators at the TeV scale. This leads to a plethora of new effects, not present in high-scale seesaw models, induced by the *light* seesaw mediators. In particular, novel (and sizable) contributions to LFV processes are possible, sometimes breaking the relation in (3).

The μ_ν parameter is intimately related to the breaking of lepton number. In fact, in the $\mu_\nu \to 0$ limit, lepton number is restored and the Majorana neutrino masses in (15) vanish. This makes the smallness of the μ_ν parameter natural, in the sense of 't Hooft [111], since the symmetry of the Lagrangian gets increased when the parameter is set to zero. For this reason, low-scale seesaw models are also said to have *almost conserved* or *slightly broken* lepton number.

The collider phenomenology of low-scale seesaw models is much richer than that of high-scale ones. The seesaw mediators can in principle be produced and, through their decays, one may be able to test the mechanism behind neutrino masses. At the LHC, one typically expects multilepton final states, often including missing energy carried away by undetected neutrinos. In addition, the LFV signatures can be as frequent as the flavor conserving ones. For an incomplete list of references on the phenomenology of low-scale seesaw models see [112–135]. This list includes phenomenological studies on the production of right-handed neutrinos [112, 113, 117, 122–125, 128, 130, 133, 135] and related processes at colliders [120, 121, 124, 125, 129], works where other low-scale seesaw mediators are considered [112, 126, 132], sneutrino dark matter studies in low-scale seesaw scenarios [118, 119, 123, 129], papers that explore the impact of light right-handed neutrinos on the unitarity of the leptonic mixing matrix [114], some works on the way the supersymmetric spectrum is altered in the presence of light right-handed neutrino superfields [115, 116, 120], and papers discussing other phenomenological issues in extended frameworks [115, 131]. The phenomenology of light right-handed neutrinos is also reviewed in detail in [127, 134]. In the case of a type-I seesaw, the seesaw mediator is a fermionic gauge singlet. This usually suppresses its production in hadronic colliders. However, sizable right-handed neutrino production cross sections are possible in some type-I seesaw realizations due to the mixing with the left-handed neutrinos, which serves as a portal to the gauge sector. Furthermore, when the type-I seesaw is embedded in a left-right symmetric scenario [136–138] new production mechanisms are possible thanks to the new charged currents mediated by the $W_R^\pm$ gauge bosons. This allows for further collider tests or the model, including searches for lepton number violation; see, for example, [139–145].

We now present the most popular representative of the low-scale seesaw models: the inverse seesaw. For other low-scale seesaw models and their LFV phenomenology see [146–151].

4.1. The Supersymmetric Inverse Seesaw. In the supersymmetric inverse seesaw (ISS) [152–154], the MSSM particle content is extended with 3 generations of right-handed neutrino superfields $\widehat{N}^c$ and 3 generations of singlet superfields $\widehat{X}$. More minimal realizations of the ISS are possible [155–159]. However, for simplicity, we will stick to the most common version with 3+3 singlet superfields. The superpotential takes the form

$$W = W_{\text{MSSM}} + Y_\nu \widehat{N}^c \widehat{L} \widehat{H}_u + M_R \widehat{N}^c \widehat{X} + \frac{1}{2}\mu_\nu \widehat{X}\widehat{X}, \tag{16}$$

where we have omitted family indices. Y_ν and M_R are general 3×3 complex mass matrices and μ_ν is a complex symmetric 3×3 matrix. One can easily check that the superpotential in (16) violates lepton number by two units. In this case, all lepton number assignments are arbitrary. However, they serve to illustrate the violation of lepton number. For example, it is common practice to assign lepton numbers −1 and +1 to the $\widehat{N}^c$ and $\widehat{X}$ superfields, respectively. With this lepton number assignment, while M_R generates a lepton number conserving Dirac mass term for the fermion singlets, μ_ν violates lepton number by two units. This Majorana mass term also leads to a small mass splitting in the heavy neutrino sector,

which is then composed by three quasi-Dirac neutrinos. The corresponding soft SUSY breaking Lagrangian is given by

$$\begin{aligned} -\mathscr{L}^{\text{soft}} &= -\mathscr{L}^{\text{soft}}_{\text{MSSM}} + \widetilde{N}^c m^2_{\widetilde{N}} \widetilde{N}^{c*} + \widetilde{X}^* m^2_{\widetilde{X}} \widetilde{X} \\ &+ \left(T_\nu \widetilde{N}^c \widetilde{L} H_u + B_{M_R} \widetilde{N}^c \widetilde{X} + \frac{1}{2} B_{\mu_\nu} \widetilde{X} \widetilde{X} \right. \\ &\left. + \widetilde{X}^* m^2_{\widetilde{X}\widetilde{N}} \widetilde{N}^c + \text{h.c.} \right), \end{aligned} \tag{17}$$

where B_{M_R} and B_{μ_ν} are the new parameters involving the scalar superpartners of the singlet neutrino states. Notice that, with the previous lepton number assignment, while the former conserves lepton number, the latter violates lepton number by two units. Finally, $\mathscr{L}^{\text{soft}}_{\text{MSSM}}$ contains the soft SUSY breaking terms of the MSSM.

The scalar potential of the model is such that the neutral components of the Higgs superfields get nonzero VEVs,

$$\begin{aligned} \left\langle H_d^0 \right\rangle &= \frac{v_d}{\sqrt{2}}, \\ \left\langle H_u^0 \right\rangle &= \frac{v_u}{\sqrt{2}}, \end{aligned} \tag{18}$$

triggering electroweak symmetry breaking (EWSB). This induces mixings in the neutrino sector. In the basis $\nu = (\nu_L, N^c, X)$, the 9×9 neutrino mass matrix is given by

$$\mathscr{M}_{\text{ISS}} = \begin{pmatrix} 0 & m_D^T & 0 \\ m_D & 0 & M_R \\ 0 & M_R^T & \mu_\nu \end{pmatrix}, \tag{19}$$

where $m_D = (1/\sqrt{2}) Y_\nu v_u$. Assuming the hierarchy $\mu_\nu \ll m_D \ll M_R$, the mass matrix $\mathscr{M}_{\text{ISS}}$ can be approximately block-diagonalized to give the effective mass matrix for the light neutrinos [160]

$$m_{\text{light}} \simeq m_D^T M_R^{T^{-1}} \mu_\nu M_R^{-1} m_D. \tag{20}$$

On the other hand, the other neutrino states form three heavy quasi-Dirac pairs, with masses corresponding approximately to the entries of M_R.

Equation (20) has the same form as (15), with $M_{\text{SS}} \sim M_R$. Therefore, by taking a small μ_ν parameter, the model allows for small neutrino masses, sizable Y_ν Yukawa couplings, and singlet neutrinos at the TeV scale (or below).

4.2. LFV in the Supersymmetric Inverse Seesaw. The presence of light singlet neutrinos induces all sorts of effects. Here we will concentrate on their contributions to LFV processes. For some recent works on phenomenological aspects of light singlet neutrinos see [124, 127, 130, 134, 135, 161–169].

There is a vast literature on LFV in models with light singlet neutrinos. Potentially large enhancements, with respect to the usual high-scale models, were already pointed out in early studies [63, 77, 82, 154]. More recently, several works have explored in detail the LFV anatomy of these models, highlighting the relevance of (non-SUSY) box diagrams induced by singlet neutrinos [149, 170–172], computing Higgs penguin contributions [173], and showing enhancements in the usual photon penguin contributions [163]. Regarding purely supersymmetric contributions, the relevance of Z penguins with right sneutrinos was recently readdressed in [174], solving an inconsistency in the analytical results of [65] and [175]. Finally, [44] constitutes the first complete analysis of LFV in the supersymmetric inverse seesaw, taking into account all possible contributions, supersymmetric as well as nonsupersymmetric.

We will now present the main results in [44]. These were obtained using `FlavorKit` [176], a tool that combines the analytical power of `SARAH` [177–181] with the numerical routines of `SPheno` [182, 183] to obtain predictions in a wide range of models, based on the automatic computation of the lepton flavor violating observables. See [184] for a comprehensive and pedagogical review of this set of tools.

In the following, we will discuss numerical results obtained using universal boundary conditions at the gauge coupling unification scale, $m_{\text{GUT}} \simeq 2 \cdot 10^{16}$ GeV, setting $M_{\text{SUSY}} = m_0 = M_{1/2} = -A_0$. In addition, we fixed $\tan\beta = 10$, $\mu > 0$ and considered a degenerate singlet spectrum ($M_R^i \equiv M_R$ with $i = 1, 2, 3$). We also fixed the B_{μ_ν} and B_{M_R} bilinear parameters to $B_{\mu_\nu} = 100\mu_\nu$ and $B_{M_R} = 100 M_R$, although we explicitly checked that they have small impact on the LFV phenomenology. Furthermore, we fixed the Y_ν Yukawa couplings using a modified Casas-Ibarra parameterization [91], adapted for the inverse seesaw [161, 185]. With the help of this parameterization, we were able to reproduce the best-fit values for the neutrino squared mass differences and mixing angles determined in the global fit [186] (see also [7] for an update). For simplicity, we considered a Casas-Ibarra matrix R equal to the unit matrix, normal hierarchy for the light neutrinos and a lightest neutrino mass $m_{\nu_1} = 10^{-4}$ eV.

A general conclusion one can draw from [44] is that the LFV phenomenology strongly depends on M_R and M_{SUSY}. The first scale determines the mass of the singlet neutrinos, whereas the second one sets the superparticle masses and their relative size determines the phenomenology. This can be seen in Figure 4, where $\text{BR}(\mu \to e\gamma)$ is shown as a function of M_{SUSY} and M_R. The results are displayed in three curves: the full observable, the SUSY contributions, and the non-SUSY ones. The latter consist of contributions from ν-$W^\pm$ and ν-$H^\pm$ loop diagrams, thus involving the singlet neutrinos in combination with the W boson or a charged Higgs. One finds that the relative weight of SUSY and non-SUSY contributions is given by the hierarchy between these two mass scales. For $M_{\text{SUSY}} \gg M_R$, non-SUSY contributions induced by the singlet neutrinos dominate the $\mu \to e\gamma$ amplitude, whereas for $M_{\text{SUSY}} \ll M_R$, the usual MSSM contributions generated by chargino/sneutrino and neutralino/slepton loops turn out to be dominant. Moreover, we find that non-SUSY contributions can have strong cancellations.

A similar behavior is found in case of the 3-body decays $\ell_i \to 3\ell_j$. In Figure 5 we display numerical results for $\text{BR}(\mu \to 3e)$ as well as for various contributions to this observable. The anatomy of this decay is more involved,

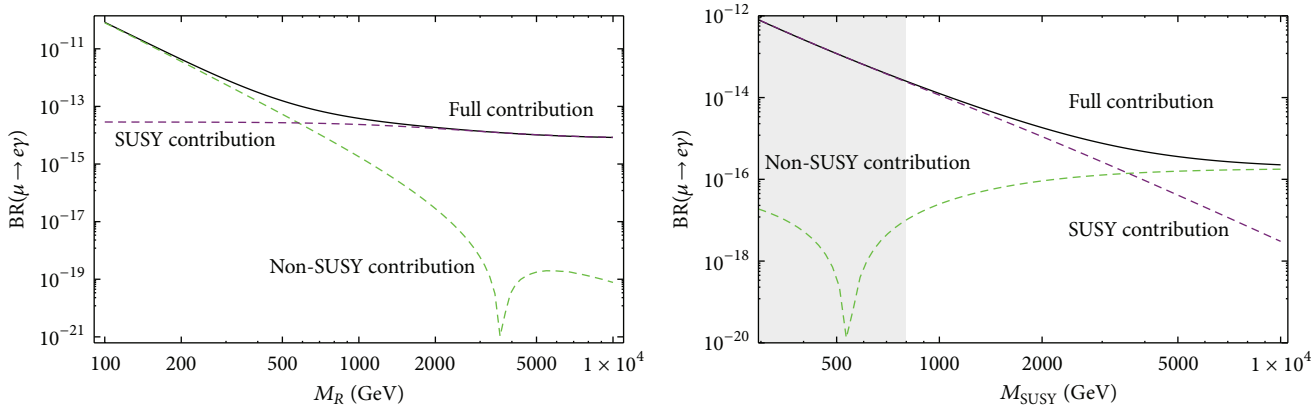

FIGURE 4: BR($\mu \to e\gamma$) as a function of M_{SUSY} and M_R. In (a) $M_{\text{SUSY}} = 1$ TeV is fixed, whereas in (b) we set $M_R = 2$ TeV. The other parameters are given in the text. The gray area roughly corresponds to the parameter space excluded by the LHC SUSY searches. Figure taken from [44].

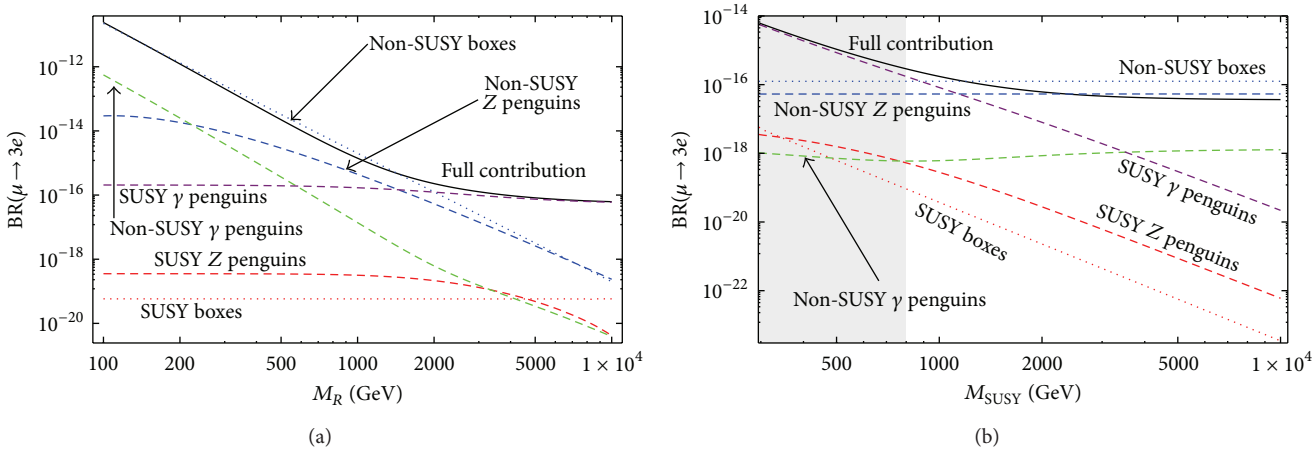

FIGURE 5: As Figure 4, but with BR($\mu \to 3e$) as a function of M_{SUSY} and M_R. Figure taken from [44].

since more types of Feynman diagrams contribute to the amplitude: SUSY and non-SUSY photon, Z and Higgs penguins, and box diagrams. As for $\ell_i \to \ell_j\gamma$, we observe that non-SUSY contributions dominate for low M_R ($<M_{\text{SUSY}}$). In particular, we see on the left-hand side of Figure 5 that non-SUSY boxes become completely dominant as soon as one goes to M_R values below ~2 TeV. This generic feature was already noted in [149, 170–172]. For higher values of M_R SUSY contributions, and in particular the standard photon dipole penguin, dominate. On the right-hand side we find complementary information, with the different contributions as a function of M_{SUSY} for a fixed M_R. It is worth noticing that supersymmetric Z penguins never dominate.

Analogous results are obtained for the $\mu - e$ conversion in nuclei rates. Interestingly, the large non-SUSY boxes found at low M_R break the dipole dominance, leading to a clear departure from (3). This is illustrated in Figure 6, where BR($\mu \to e\gamma$), BR($\mu \to 3e$), and the $\mu - e$ conversion rates in Ti and Al are shown as a function of M_R. Indeed, for $M_R \lesssim 500$ GeV, the rates for all LFV processes have similar sizes. In this scenario, experiments looking for $\mu \to 3e$ and $\mu - e$ conversion in nuclei will soon provide the most stringent constraints in this model.

Finally, although we have assumed a degenerate right-handed neutrino spectrum in all the results presented in this section, we note that the qualitative picture would be exactly the same in scenarios with nondegenerate right-handed neutrinos. Furthermore, we emphasize once more that low-scale seesaw models have a rich collider phenomenology, complementary to LFV searches. We refer to the beginning of this section for a discussion and references.

5. R-Parity Violating Models

The particle content and symmetries of the MSSM allow for the following superpotential terms

$$W^{\not R_p} = \frac{1}{2}\lambda_{ijk}\widehat{L}_i\widehat{L}_j\widehat{e}^c_k + \lambda'_{ijk}\widehat{L}_i\widehat{Q}_j\widehat{d}^c_k + \epsilon_i\widehat{L}_i\widehat{H}_u + \frac{1}{2}\lambda''_{ijk}\widehat{u}^c_i\widehat{d}^c_j\widehat{d}^c_k, \tag{21}$$

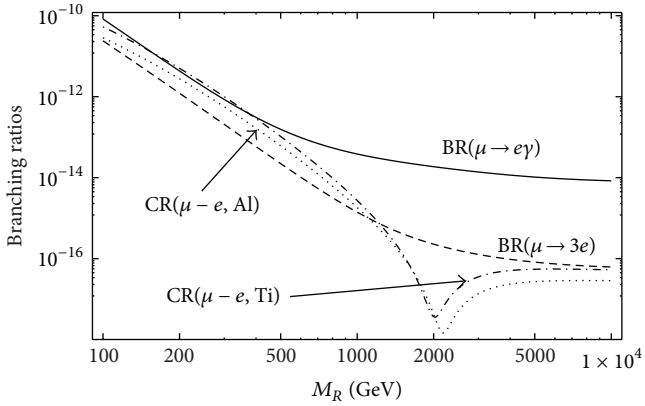

FIGURE 6: BR($\mu \to e\gamma$), BR($\mu \to 3e$) and $\mu - e$ conversion rates in Ti and Al as a function of M_R. M_{SUSY} is fixed to 1 TeV. The other parameters are given in the text. Figure taken from [44].

where we have explicitly introduced family indices. Here $\widehat{u}^c$ and $\widehat{e}^c$ are the right-handed up-quark and charged lepton superfields, respectively, and the rest of the superfields have been already defined. The first three terms in $W^{\not{R}_p}$ break lepton number (L) whereas the last one breaks baryon number (B). In principle, these couplings are not welcome, since they give rise to many lepton and baryon number violating processes, never observed in nature. For example, the simultaneous presence of the λ' and λ'' couplings would lead to proton decay [187, 188]. This phenomenological problem is solved in the MSSM by introducing *by hand* a new discrete symmetry that forbids all terms in $W^{\not{R}_p}$. This symmetry is known as R-parity [3, 4] and is defined as

$$R_p = (-1)^{3(B-L)+2s}. \tag{22}$$

Here s is the spin of the particle. It is straightforward to verify that all terms in (21) break R-parity and thus they are forbidden once this symmetry is imposed. The MSSM is defined as R-parity conserving.

However, several arguments can be raised against R-parity:

(i) *R-parity is imposed by hand.* Unlike the SM, where L and B conservation is automatic, in the MSSM this has to be forced by introducing a new symmetry, not derived from first principles. This is clearly a step back from the SM. However, it is worth pointing out that in the absence of R-parity some mechanism must be introduced in order to suppress the dangerous $\not{R}_p$ parameters.

(ii) *R-parity does not solve fast proton decay.* It is well known that R-parity does not forbid some dangerous dimension-5 operators that lead to proton decay [189–191]. For example, the operator $\mathcal{O}_5 = (f/M)\widehat{Q}\widehat{Q}\widehat{Q}\widehat{L}$ has $R_p(\mathcal{O}_5) = +1$ and thus conserves R-parity. The bounds obtained from the nonobservation of proton decay imply that, even for $M = M_{\text{Planck}}$, f must be smaller than 10^{-7} [192]. In order to forbid $\mathcal{O}_5$ and other similar dimension-5 operators, one may resort to additional flavor symmetries [193].

(iii) *There is no reason to forbid all the L and B violating operators.* Proton decay requires the simultaneous presence of L and B violating couplings. Therefore, it is sufficient to impose the conservation of just one of these two symmetries in order to forbid proton decay. This has led to the consideration of alternative discrete symmetries which allow for either L or B violation while protecting the proton. An example of such symmetries is baryon triality (Z_3^B) [189, 194].

Furthermore, there are several good motivations to consider R-parity violating ($\not{R}_p$) scenarios. The violation of lepton number by any of the first three couplings in (21) automatically leads to nonzero neutrino masses [195–197]. Moreover, the presence of $\not{R}_p$ couplings leads to a rich collider phenomenology due to the decay of the LSP. This can be translated into longer decay chains, changing the expected signatures at the LHC [198, 199]. In fact, $\not{R}_p$ has also been considered as a way to relax the stringent bounds on the squark and gluino masses; see, for example, [5, 6, 200, 201].

Finally, in $\not{R}_p$ the standard neutralino LSP is lost as a dark matter candidate. Therefore, alternative candidates must be considered. Examples in the literature include (i) gravitinos [202–204], (ii) the axion [205, 206], or (iii) its superpartner, the axino [207, 208]. For general reviews on R-parity violation and collections on bounds on the $\not{R}_p$ couplings see [209–212].

We will now discuss separately the LFV phenomenology of two very different supersymmetric scenarios with R-parity violation: explicit R-parity violation (e-$\not{R}_p$) and spontaneous R-parity violation (s-$\not{R}_p$).

5.1. Explicit R-Parity Violation. The most characteristic signatures of R-parity violating models are, of course, processes with L or B violation. Nevertheless, processes that violate lepton flavor can provide interesting signatures as well and, in fact, they can be more attractive due to the large number of upcoming LFV experiments.

5.1.1. Higgs LFV Decays. After the historical discovery of the Higgs boson [1, 2], a lot of effort has been put into the determination of its properties. In particular, the Higgs boson decays may contain a lot of valuable information, with potential indications of new physics. Recently, the CMS collaboration reported on an intriguing 2.4σ excess in the $h \to \tau\mu$ channel [32]. This hint, which translates into $\text{BR}(h \to \tau\mu) = (0.84^{+0.39}_{-0.37})$, is based on the analysis of the 2012 dataset, taken at $\sqrt{s} = 8$ TeV and an integrated luminosity of 19.7 fb^{-1}. This large Higgs LFV (For pioneer works on Higgs LFV decays see [213, 214].) branching ratio is quite challenging and most NP models cannot accommodate it [215]. In fact, the flavor conserving Higgs decay $h \to \tau\tau$ has a branching ratio of *only* ~6%, not much higher than the LFV one found by CMS. Although independent confirmation by ATLAS, as well as additional statistics in CMS, would be required in order to confirm that this hint is not just a

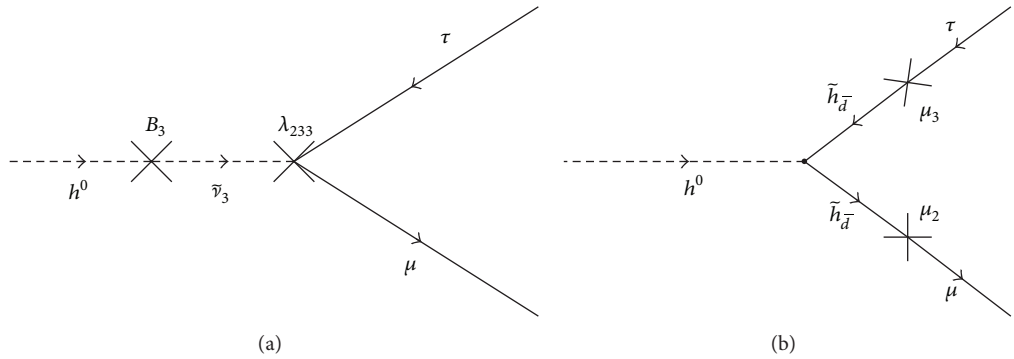

FIGURE 7: Tree-level $\not{R}_p$ contributions to $h \to \tau\mu$. (a) A $B\lambda$ contribution. (b) A ϵ_i^2 (denoted as μ_i^2 in [45]) contribution. Figure borrowed from [45].

fluctuation but an evidence of new physics, it is interesting to explore different models in order to determine what type of frameworks can accommodate this signal.

Regarding supersymmetric models, several scenarios have been recently explored, some of them even before the CMS hint was announced. In particular, the authors of [45, 216] considered an extension of the MSSM including all L violating couplings in (21). The particles-sparticles mixing due to the $\not{R}_p$ couplings induce Higgs LFV decays at tree-level, thus potentially being able to reach branching ratios as high as the one found by the CMS collaboration. Two specific examples are shown in Figure 7. However, the existing experimental bounds on the relevant combinations of $\not{R}_p$ couplings contributing to $h \to \tau\mu$ forbid such large LFV branching ratios. For example, in the $B\lambda$ contribution both $\not{R}_p$ parameters are strongly constrained. In case of B_i, the $\not{R}_p$ mixings between the Higgs boson and the sneutrinos ($\mathscr{L} \supset B_i \tilde{L}_i H_u$), they have strong bounds since they induce nonzero neutrino masses [217–219]. Moreover, the λ couplings are constrained by charged current experiments [209]. Once these constraints are taken into account, the maximum BR($h \to \tau\mu$) one can get is not very impressive. This is illustrated in Figure 8, where BR($h \to \tau\mu$) contours are drawn on the $B_2 - \lambda_{232}$ plane. From this figure one concludes that BR($h \to \tau\mu$) can reach, at most, a few $\times 10^{-5}$, clearly below the CMS hint. Similar conclusions are obtained when other combinations of $\not{R}_p$ parameters are considered.

The supersymmetric inverse seesaw has also been considered as a possible setup to reproduce a Higgs LFV branching ratio into $\tau\mu$ at the 1% level [220]. In this case, $h \to \tau\mu$ takes place at 1-loop, naturally suppressing the branching ratio. As a result of this, as well as due to the constraints from other LFV processes such as $\ell_i \to \ell_j\gamma$, one finds that the maximum allowed BR($h \to \tau\mu$) is about $\sim 10^{-5}$. Therefore, this model cannot account for a branching ratio as obtained by CMS either. In order to conclude this discussion on $h \to \tau\mu$ with a positive note, let us mention that known models that can account for BR($h \to \tau\mu$) $\sim$ 1% exist in the literature. They all involve extended Higgs sectors. In particular, it has been shown that Two-Higgs-Doublet models of type-III, in

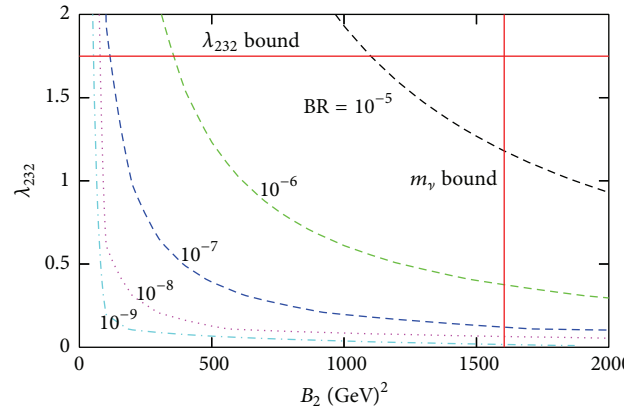

FIGURE 8: BR($h \to \mu\tau$) contours on the $B_2 - \lambda_{232}$ plane. The continuous horizontal and vertical lines show approximate limits due to neutrino masses (in case of B_2) and charged current experiments (in case of λ_{232}). Figure borrowed from [45].

which both Higgs doublets can couple to up- and down-type fermions, can easily accommodate the CMS signal [215, 221–225]. The MSSM, being Two-Higgs-Doublet models of type-II in which one Higgs doublet couples to up- and the other to down-type fermions, cannot. In fact, several studies have shown that one cannot accommodate BR($h \to \tau\mu$) $\sim$ 1% when the low-energy theory is the MSSM [226, 227]. The same conclusion applies to heavy Higgs LFV decays [228].

5.1.2. Trilinear R-Parity Violation and LFV. In principle, the usual LFV processes studied in R-parity conserving models can be studied in the R-parity violating ones and, in some cases, they get additional $\not{R}_p$ contributions. This is the case of $\ell_i \to 3\ell_j$, $M \to \ell_i\ell_j$ and $\tau \to M\ell_i$, where M is a neutral meson, which, in the presence of trilinear $\not{R}_p$ couplings, can be induced at tree-level [229]. This is represented in Figure 9, where two examples are shown: $\ell_i \to 3\ell_j$ induced by λ couplings and sneutrino exchange and $\tau \to M\mu$ induced by λ' couplings and squark exchange. This allows one to derive a large collection of bounds on the size of the trilinear

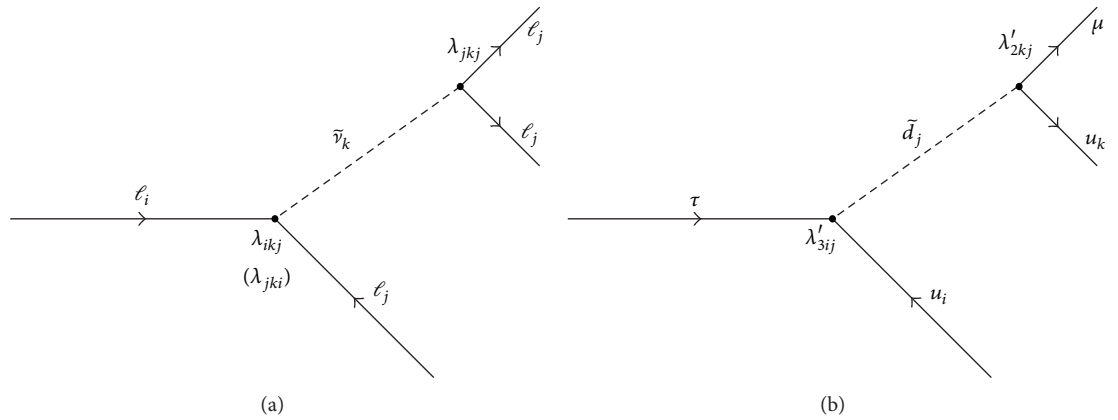

FIGURE 9: (a) $\ell_i \to 3\ell_j$ induced by trilinear λ couplings and sneutrino exchange. (b) $\tau \to M\mu$ induced by λ' couplings and squark exchange.

couplings and the masses of the superparticles mediating the LFV decays [230, 231].

Let us consider the right-hand side of Figure 9. After dressing the quarks in the final state, this Feynman diagram induces $\tau \to M\mu$ at tree-level. Since the exchanged particle, a down-type squark in this case, is much heavier than the rest of particles, this process can be well described by the 4-fermion effective Lagrangian

$$\mathscr{L}_{\text{eff}} = -\frac{\lambda'_{3ij}\lambda'^{*}_{2kj}}{m^2_{\tilde{d}_j}}\left(\overline{\tau^c}P_L u_i\right)\left(\overline{u}_k P_R \mu^c\right), \tag{23}$$

obtained after integrating out the heavy squark. One can now use this Lagrangian and, together with the relevant hadronic form factors, compute rates for processes such as $\tau \to \mu\pi^+\pi^-$. The authors of [231] followed this method and used Belle results on searches for τ LFV decays [232–234] to obtain the limit

$$\lambda'_{31j}\lambda'^{*}_{21j} < 2.1 \cdot 10^{-4}\left(\frac{m_{\tilde{d}_j}}{100\,\text{GeV}}\right)^2. \tag{24}$$

One can exploit this idea using other LFV observables involving mesons. We refer to [230, 231] for a more complete list of constraints.

Similarly, trilinear $\not{R}_p$ couplings can also trigger $\mu - e$ conversion in nuclei, induced by diagrams very similar to the one on the right-hand side of Figure 9. Interestingly, in this case $\mu - e$ conversion in nuclei would take place at tree-level, while the more popular $\mu \to e\gamma$ would take place at 1-loop. This has been recently pointed out by the authors of [235], who argue that experiments looking for μ–e conversion in nuclei might be the first (and perhaps the only ones) to observe a nonzero signal in the next round of experiments.

5.1.3. Other Results on LFV in $\not{R}_p$ Scenarios. Before concluding, let us briefly comment on other aspects of LFV in $\not{R}_p$ models. An interesting feature of $\not{R}_p$ models is that some lepton number violating processes at colliders might look like lepton flavor violating ones. This is, for example, the case of sneutrino decay in bilinear R-parity violation [46], as shown in Figure 10. This process is possible thanks to the mixing between the MSSM charginos and the standard charged leptons and, being lepton number violating, it also violates lepton flavor. However, at the LHC, if the sneutrinos are directly produced, the process would look simply like a LFV one.

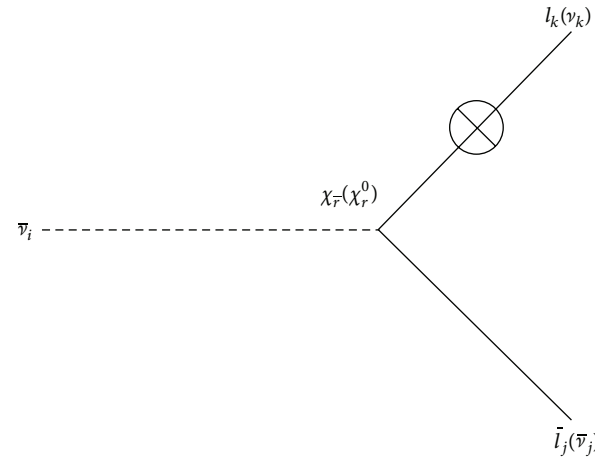

FIGURE 10: Sneutrino decay to $\ell_k\overline{\ell}_j$ in bilinear R-parity violation. The open circle with a cross indicates the $\not{R}_p$ induced mixing between charginos and charged leptons. Figure taken from [46].

Finally, for other recent works on LFV in $\not{R}_p$ models see [236–238].

5.2. Spontaneous R-Parity Violation. A very attractive scenario for LFV is that of spontaneous R-parity violation. When a scalar field oddly charged under R-parity gets a VEV in a theory with R-parity conserving Lagrangian, R-parity gets spontaneously broken. Here we will concentrate on spontaneous L and R_p violation. Although R-parity is a discrete symmetry, its breaking comes along with the breaking of the continuous global symmetry $U(1)_L$. This implies the existence of a massless Goldstone boson, usually called the majoron (J) [239, 240].

The nature of the majoron is crucial for the phenomenological success of the model. In fact, in the first model with s-$\not{R}_p$ [241], the breaking of R-parity was triggered by the VEV of a left-handed sneutrino. This simple setup was eventually excluded since the doublet nature of the majoron leads to conflict with LEP bounds on the Z boson invisible decay width and astrophysical data [206, 242]. However, more refined models where the violation of lepton number is induced by a gauge singlet are perfectly valid possibilities. As a benchmark example of this family we will consider here the model introduced in [243]. For alternative models with gauged lepton number see, for example, [244–246].

In the model of [243], the particle content is extended with three additional singlet superfields, namely, $\widehat{\nu}^c$, $\widehat{S}$, and $\widehat{\Phi}$, with lepton number assignments of $L = -1, 1, 0$, respectively. By assumption, the Lagrangian of the theory conserves lepton number. Therefore, the superpotential can be written as

$$W_{\text{SRPV}} = W_{\text{MSSM}} + Y_\nu \widehat{L}\widehat{N}^c \widehat{H}_u - h_0 \widehat{H}_d \widehat{H}_u \widehat{\Phi} + h\widehat{\Phi}\widehat{N}^c\widehat{S} + \frac{\lambda}{3!}\widehat{\Phi}^3. \tag{25}$$

For simplicity, one can simply consider one generation of $\widehat{N}^c$ and $\widehat{S}$ superfields. Several scalar fields acquire VEVs after electroweak symmetry breaking. In addition to the usual MSSM Higgs boson VEVs, v_d and v_u, these are $\langle\Phi\rangle = v_\Phi/\sqrt{2}$, $\langle\widetilde{N}^c\rangle = v_R/\sqrt{2}$, $\langle\widetilde{S}\rangle = v_S/\sqrt{2}$, and $\langle\widetilde{\nu_{Li}}\rangle = v_i/\sqrt{2}$. This vacuum configuration breaks lepton number and R-parity. In fact, we notice that $v_R \neq 0$ generates the effective bilinear $\not{R}_p$ terms $\epsilon_i = Y_\nu^i v_R/\sqrt{2}$. Furthermore, neglecting $v_i \ll v_R, v_S$, one finds the resulting majoron profile

$$J \simeq \text{Im}\left(\frac{v_S}{V}\widetilde{S} - \frac{v_R}{V}\widetilde{N}^c\right), \tag{26}$$

where $V = \sqrt{v_R^2 + v_S^2}$. Equation (26) shows that the majoron inherits the singlet nature of the scalar fields that break lepton number with their VEVs, thus suppressing the couplings to the Z boson and evading the stringent LEP bound.

Here we are interested in novel LFV features due to the presence of the majoron. Another interesting signature present in majoron models is the invisible decay of the Higgs boson, $h \to JJ$ [247, 248]. This new massless state dramatically changes the phenomenology both at collider and low-energy experiments [47, 249]. In particular, it leads to new LFV processes, such as $\mu \to eJ$ or $\mu \to eJ\gamma$. The exotic muon decay $\mu \to eJ$ was first studied in [250] and later revisited in [47], where the decay with an additional photon was also considered. Furthermore, the impact of the majoron on $\mu - e$ conversion in nuclei was discussed in [251] (see also [252] for similar LFV processes in the context of invisible axions).

The rate of the $\mu \to eJ$ decay is determined by the $e-\mu-J$ coupling, $O_{e\mu J}$, which, in the model under consideration, is of the form $O_{e\mu J} \sim 1/v_R \times$ RPV parameters. This makes us conclude that, in general, one expects large partial muon decay widths to majorons for low v_R. However, currently there are no experiments looking for $\mu \to eJ$ and the current best limit on the branching ratio, $\text{BR}(\mu \to eJ) \lesssim 10^{-5}$, dates back to 1986 [253]. Regarding the decay including a photon, $\mu \to eJ\gamma$, one can profit from the MEG experiment and its search for the more popular channel $\mu \to e\gamma$.

The two branching ratios are related by

$$\text{BR}\left(\mu \longrightarrow eJ\gamma\right) = \frac{\alpha}{2\pi}\mathcal{J}\left(x_{\min}, y_{\min}\right)\text{BR}\left(\mu \longrightarrow eJ\right). \tag{27}$$

Here $\mathcal{J}(x_{\min}, y_{\min})$ is a 3-body phase space integral defined as

$$\mathcal{J}\left(x_{\min}, y_{\min}\right) = \int dx\, dy \frac{(x-1)(2-xy-y)}{y^2(1-x-y)}, \tag{28}$$

the dimensionless parameters x, y are defined as

$$x = \frac{2E_e}{m_\mu}, \qquad y = \frac{2E_\gamma}{m_\mu}, \tag{29}$$

and $x_{\min}$ and $y_{\min}$ are the minimal electron and photon energies that a given experiment can measure. Indeed, the integral in (28), which would contain infrared and collinear divergences, is regularized by the specific choices made by an experiment.

As explained above, the main advantage of $\mu \to eJ\gamma$ is the existence of the MEG experiment. However, the question is whether it is sensitive to this exotic LFV process or not. Figure 11 shows the value of the phase space integral $\mathcal{J}(x_{\min}, y_{\min})$ as a function of $x_{\min}$ for three different values of $y_{\min}$ and for two choices of $\cos\theta_{e\gamma}$ (the relative angle between the electron and photon directions). Unfortunately, the MEG experiment is specifically designed for a single search. In fact, the cuts used in the search for $\mu \to e\gamma$ are very restrictive: $x_{\min} \geq 0.995$, $y_{\min} \geq 0.99$, and $|\pi - \theta_{e\gamma}| \leq 8.4$ mrad. For these exact values one finds a tiny phase space integral, $\mathcal{J} \simeq 6 \cdot 10^{-10}$. As a consequence of this, a limit for $\text{BR}(\mu \to e\gamma)$ of the order of $\leq 10^{-13}$ would translate into the useless limit $\text{BR}(\mu \to eJ) < 0.14$. To improve upon this bound, it is necessary to relax the cuts. For example, by relaxing the cut on the opening angle to $\cos\theta_{e\gamma} = -0.99$. However, this is prone to induce additional unwanted background events, in particular, accidental background from muon annihilation in flight. Therefore, although one could in principle increase the value of the phase space integral $\mathcal{J}(x_{\min}, y_{\min})$, the background in that case would make the search for a positive signal impossible. This discussion suggests that a better timing resolution of the experiment would be welcome in order to reduce the background and be sensitive to final states including majorons.

6. Summary and Conclusions

In summary, we have reviewed the lepton flavor violating phenomenology of several nonminimal supersymmetric models: high-scale and low-scale seesaw models as well as models with explicit or spontaneous R-parity violation.

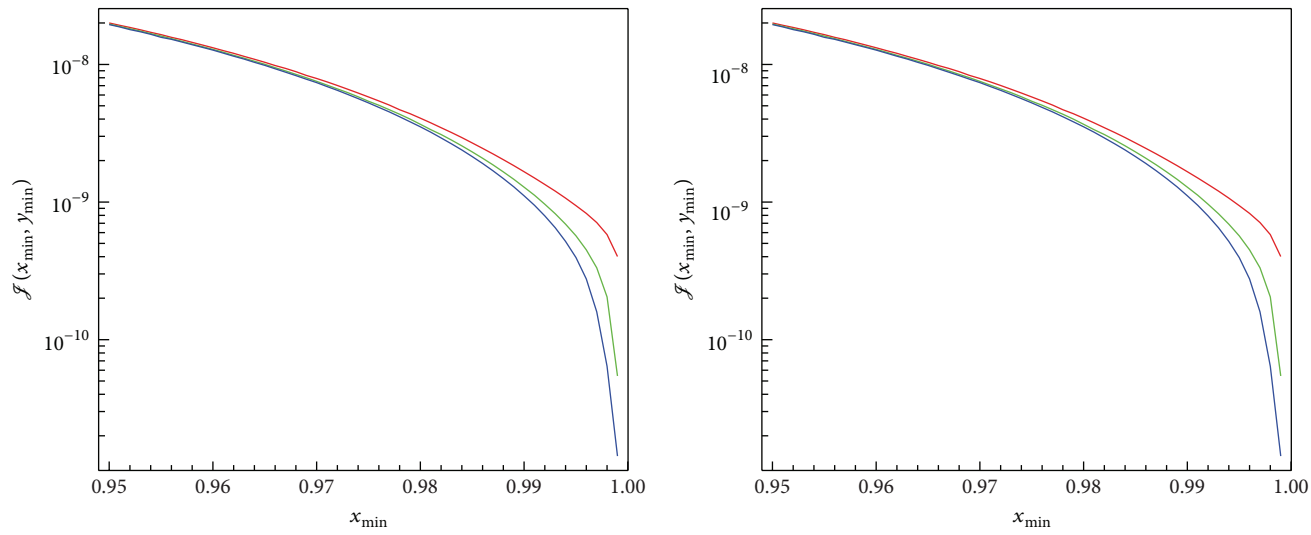

FIGURE 11: The phase space integral for the decay $\mu \to eJ\gamma$ as a function of $x_{\min}$ for three different values of $y_{\min} = 0.95, 0.99, 0.995$ from top to bottom and for two different values of $\cos\theta_{e\gamma}$. (a) $\cos\theta_{e\gamma} = -0.99$, whereas (b) $\cos\theta_{e\gamma} = -0.99997$. Figure taken from [47].

The main conclusion from this overview is that the lepton flavor violating signatures can be very different from those found in the MSSM. This translates into two important messages:

(i) *For the Theorists*. Lepton flavor violation might be much more intricate than what minimal models predict. Therefore, we should be careful when extrapolating our expectations (derived from the MSSM) to extended frameworks.

(ii) *For the Experimentalists*. Although minimal models are of course well motivated, lepton flavor violation might show up in nonstandard channels. We must be ready to avoid missing a relevant signal.

The comparison between SUSY and non-SUSY LFV is not straightforward. In general, one can use LFV to distinguish between two models, but it is often impossible to tell whether the underlying physics is supersymmetric or not. There are two main reasons for this. First, nonminimal SUSY models typically contain non-SUSY contributions to LFV observables, making hard a clear distinction. The discussion in Section 4 is a clear example of this interplay. And second, there are many non-SUSY models with LFV phenomenologies that resemble the standard phenomenology in SUSY models (for instance, due to the dominance of dipole operators). Perhaps, the only scenario where a clear distinction can be made is that of high-scale seesaw models: if they are nonsupersymmetric no sizable LFV is induced at low energies, whereas sizable LFV rates at low energies are in principle expected if they are supersymmetric.

The connection between neutrino masses and lepton flavor is one of the main motivations to search for LFV processes. As we have seen in this review, different neutrino mass models typically lead to different LFV phenomenologies. This can in principle be used to unravel the origin of neutrino masses by exploring this link with LFV once one or several positive discoveries are made in the next round of LFV experiments. Although precise numerical predictions are impossible due to the existence of many free parameters in most neutrino mass models, correlations and patterns can favor specific scenarios. For example, the discovery of a clear departure from a dipole dominated scenario could point towards the existence of light singlet neutrinos.

Nevertheless, it has been already emphasized in this review that LFV can take place even in the absence of neutrino masses. Similarly, although all neutrino mass models discussed in this review include Majorana neutrinos and lepton number violation, this aspect is not particularly relevant for our discussion on LFV. Indeed, Majorana neutrino masses are related to the breaking of lepton number, which is conceptually different to the breaking of lepton flavor.

To conclude, let us emphasize once more that properly identifying the underlying physics will be crucial in case a positive observation in one or several LFV experiments is made. This problem might soon have to be addressed, given the exciting projects that are currently going on or soon starting their search for LFV. Hopefully, this review, as well as the many phenomenological studies in the bibliography, will help shedding some light on this matter.

Conflict of Interests

The author declares that there is no conflict of interests regarding the publication of this paper.

Acknowledgments

The author is extremely grateful to the collaborators in the subjects discussed in this review. The author also acknowledges partial support from the EXPL/FIS-NUC/0460/2013 project financed by the Portuguese FCT.

References

[1] G. Aad, T. Abajyan, B. Abbott et al., "Observation of a new particle in the search for the standard model Higgs boson with the ATLAS detector at the LHC," *Physics Letters B*, vol. 716, no. 1, pp. 1–29, 2012.

[2] S. Chatrchyan, V. Khachatryan, A. M. Sirunyan et al., "Observation of a new boson at a mass of 125 GeV with the CMS experiment at the LHC," *Physics Letters B*, vol. 716, no. 1, pp. 30–61, 2012.

[3] P. Fayet, "Supergauge invariant extension of the Higgs mechanism and a model for the electron and its neutrino," *Nuclear Physics Section B*, vol. 90, pp. 104–124, 1975.

[4] G. R. Farrar and P. Fayet, "Phenomenology of the production, decay, and detection of new hadronic states associated with supersymmetry," *Physics Letters B*, vol. 76, no. 5, pp. 575–579, 1978.

[5] J. A. Evans and Y. Kats, "LHC coverage of RPV MSSM with light stops," *Journal of High Energy Physics*, vol. 2013, no. 4, article 028, 2013.

[6] B. Bhattacherjee, J. L. Evans, M. Ibe, S. Matsumoto, and T. T. Yanagida, "Natural supersymmetry's last hope: R-parity violation via UDD operators," *Physical Review D*, vol. 87, no. 11, Article ID 115002, 2013.

[7] D. Forero, M. Tortola, and J. Valle, "Neutrino oscillations refitted," *Physical Review D*, vol. 90, no. 9, Article ID 093006, 10 pages, 2014.

[8] M. C. Gonzalez-Garcia, M. Maltoni, and T. Schwetz, "Updated fit to three neutrino mixing: status of leptonic CP violation," *Journal of High Energy Physics*, vol. 2014, no. 11, article 052, 2014.

[9] F. Capozzi, G. L. Fogli, E. Lisi, A. Marrone, D. Montanino, and A. Palazzo, "Status of three-neutrino oscillation parameters, circa 2013," *Physical Review D*, vol. 89, no. 9, Article ID 093018, 2014.

[10] S. Petcov, "The processes $\mu \to e\gamma \to ee\bar{e}$, $\nu' \to \nu\gamma$ in the Weinberg Salam model with neutrino mixing," *Soviet Journal of Nuclear Physics*, vol. 25, p. 340, 1977.

[11] T. P. Cheng and L.-F. Li, "Nonconservation of separate μ- and e-lepton numbers in gauge theories with $V + A$ currents," *Physical Review Letters*, vol. 38, no. 8, pp. 381–384, 1977.

[12] S. M. Bilenky, S. T. Petcov, and B. Pontecorvo, "Lepton mixing, $\mu \to e + \gamma$ decay and neutrino oscillations," *Physics Letters B*, vol. 67, no. 3, pp. 309–312, 1977.

[13] Y. Kuno and Y. Okada, "Muon decay and physics beyond the standard model," *Reviews of Modern Physics*, vol. 73, pp. 151–202, 2001.

[14] K. A. Olive, K. Agashe, C. Amsler et al., "Review of particle physics," *Chinese Physics C*, vol. 38, no. 9, Article ID 090001, 2014.

[15] R. H. Bernstein and P. S. Cooper, "Charged lepton flavor violation: an experimenter's guide," *Physics Reports*, vol. 532, no. 2, pp. 27–64, 2013.

[16] S. Mihara, J. P. Miller, P. Paradisi, and G. Piredda, "Charged lepton flavor-violation experiments," *Annual Review of Nuclear and Particle Science*, vol. 63, pp. 531–552, 2013.

[17] G. Signorelli, "Charged Lepton flavor violation experiments," http://arxiv.org/abs/1307.8346.

[18] J. Adam, X. Bai, A. M. Baldini et al., "New constraint on the existence of the $\mu^+ \to e^+\gamma$ decay," *Physical Review Letters*, vol. 110, Article ID 201801, 2013.

[19] A. Baldini, F. Cei, C. Cerri et al., "MEG upgrade proposal," http://arxiv.org/abs/1301.7225.

[20] U. Bellgardt, G. Otter, R. Eichler et al., "Search for the decay $\mu^+ \to e^+e^+e^-$," *Nuclear Physics B*, vol. 299, no. 1, pp. 1–6, 1988.

[21] A. Blondel, A. Bravar, M. Pohl et al., "Research proposal for an experiment to search for the decay $\mu \to eee$," http://arxiv.org/abs/1301.6113.

[22] R. M. Carey, K. R. Lynch, J. P. Miller et al., "Proposal to search for $\mu^- N \to e^- N$ with a single event sensitivity below 10^{-16}," Tech. Rep., Fermi National Accelerator Laboratory, Batavia, Ill, USA, 2008.

[23] D. Glenzinski, "The Mu2e experiment at fermilab," *AIP Conference Proceedings*, vol. 1222, pp. 383–386, 2010.

[24] R. J. Abrams, D. Alezander, G. Ambrosio et al., "Mu2e conceptual sesign report," http://arxiv.org/abs/1211.7019.

[25] M. Aoki, "A new idea for an experimental search for μ-e conversion," in *Proceedings of the 35th International Conference of High Energy Physics (ICHEP '10)*, p. 279, 2010.

[26] Y. Cui, Y. Arimoto, Y. Igarashi et al., "Conceptual design report for experimental search for lepton flavor violating mu- - e-conversion at sensitivity of 10^{**}(-16) with a slow-extracted bunched proton beam (COMET)," in *Proceedings of the KEK*, 2009.

[27] Y. Kuno and COMET Collaboration, "A search for muon-to-electron conversion at J-PARC: the COMET experiment," *Progress of Theoretical and Experimental Physics*, vol. 2013, no. 2, Article ID 022C01, 2013.

[28] R. J. Barlow, "The PRISM/PRIME project," *Nuclear Physics B—Proceedings Supplements*, vol. 218, no. 1, pp. 44–49, 2011.

[29] T. Aushev, W. Bartel, A. Bondar et al., "Physics at super B factory," http://arxiv.org/abs/1002.5012.

[30] A. Bevan, B. Golob, S. Prell et al., "The physics of the B factories," *The European Physical Journal C*, vol. 74, article 3026, 2014.

[31] R. Aaij, C. Abellan Beteta, B. Adeva et al., "Searches for violation of lepton flavour and baryon number in tau lepton decays at LHCb," *Physics Letters B*, vol. 724, no. 1–3, pp. 36–45, 2013.

[32] V. Khachatryan and CMS Collaboration, "Search for lepton-flavour-violating decays of the Higgs boson," http://arxiv.org/abs/1502.07400.

[33] A. J. Buras, B. Duling, T. Feldmann, T. Heidsieck, and C. Promberger, "Lepton flavour violation in the presence of a fourth generation of quarks and leptons," *Journal of High Energy Physics*, vol. 2010, no. 9, article 104, 2010.

[34] BaBar Collaboration Collaboration, "Searches for lepton flavor violation in the decays $\tau^\pm \to e^\pm\gamma$ and $\tau^\pm \to \mu^\pm\gamma$," *Physical Review Letters*, vol. 104, Article ID 021802, 2010.

[35] K. Hayasaka, K. Inami, Y. Miyazaki et al., "Search for lepton flavor violating Tau decays into three leptons with 719 million produced Tau^+Tau^- Pairs," *Physics Letters B*, vol. 687, no. 2-3, pp. 139–143, 2010.

[36] C. Dohmen, K.-D. Groth, B. Heer et al., "Test of lepton flavor-conservation in $\mu \to e$ conversion on titanium," *Physics Letters B*, vol. 317, no. 4, pp. 631–636, 1993.

[37] The PRIME Working Group Collaboration, "Search for the $\mu \to e$ conversion process at an ultimate sensitivity of the order of 10^{-18} with prism," loi to j-parc 50-gev ps, loi-25, http://www-ps.kek.jp/jhf-np/LOIlist/pdf/L25.pdf.

[38] W. H. Bertl, F. Rosenbaum, N. M. Ryskulov et al., "A search for muon to electron conversion in muonic gold," *The European Physical Journal C*, vol. 47, no. 2, pp. 337–346, 2006.

[39] H. Natori, "DeeMe experiment—an experimental search for a mu-e conversion reaction at J-PARC MLF," *Nuclear Physics B—Proceedings Supplements*, vol. 248–250, pp. 52–57, 2014.

[40] M. Hirsch, J. W. F. Valle, W. Porod, J. C. Romao, and A. V. Del Moral, "Probing minimal supergravity in the type-I seesaw mechanism with lepton flavor violation at the CERN LHC," *Physical Review D*, vol. 78, no. 1, Article ID 013006, 2008.

[41] F. R. Joaquim and A. Rossi, "Phenomenology of the triplet seesaw mechanism with Gauge and Yukawa mediation of SUSY breaking," *Nuclear Physics B*, vol. 765, no. 1-2, pp. 71–117, 2007.

[42] B. C. Allanach, M. Battaglia, G. A. Blair et al., "The Snowmass points and slopes: benchmarks for SUSY searches," *The European Physical Journal C—Particles and Fields*, vol. 25, no. 1, pp. 113–123, 2002.

[43] J. N. Esteves, J. C. Romao, M. Hirsch, A. Vicente, W. Porod, and F. Staub, "LHC and lepton flavour violation phenomenology of a left-right extension of the MSSM," *Journal of High Energy Physics*, vol. 2010, no. 12, article 077, 2010.

[44] A. Abada, M. E. Krauss, W. Porod, F. Staub, A. Vicente, and C. Weiland, "Lepton flavor violation in low-scale seesaw models: SUSY and non-SUSY contributions," *Food Security*, vol. 2014, no. 11, article 048, 2014.

[45] A. Arhrib, Y. Cheng, and O. C. Kong, "Higgs to $\mu^{\mp}\tau^{\pm}$ decay in supersymmetry without R-parity," *Europhysics Letters*, vol. 101, no. 3, Article ID 31003, 2013.

[46] D. A. Sierra, D. Restrepo, and S. Spinner, "LSP sneutrino novel decays," *Journal of High Energy Physics*, vol. 2013, no. 5, article 046, 2013.

[47] M. Hirsch, A. Vicente, J. Meyer, and W. Porod, "Majoron emission in muon and tau decays revisited," *Physical Review D*, vol. 79, no. 5, Article ID 055023, 2009.

[48] E. Ma, "Pathways to naturally small neutrino masses," *Physical Review Letters*, vol. 81, pp. 1171–1174, 1998.

[49] P. Minkowski, "$\mu \to e\gamma$ at a rate of one out of 10^9 muon decays?" *Physics Letters B*, vol. 67, no. 4, pp. 421–428, 1977.

[50] T. Yanagida, "Horizontal symmetry and masses of neutrinos," in *Proceedings of the Workshop on Unified Theories and Baryon Number in the Universe*, O. Sawada and A. Sugamoto, Eds., KEK Lectures, KEK, 1979.

[51] M. Gell-Mann, P. Ramond, and R. Slansky, "Complex spinors and unified theories," Conference Proceedings C 790927, pp. 315–321, http://arxiv.org/abs/1306.4669.

[52] R. N. Mohapatra and G. Senjanovic, "Neutrino mass and spontaneous parity violation," *Physical Review Letters*, vol. 44, article 912, 1980.

[53] J. Schechter and J. W. F. Valle, "Neutrino masses in SU(2) × U(1) theories," *Physical Review D*, vol. 22, no. 9, pp. 2227–2235, 1980.

[54] J. Schechter and J. W. F. Valle, "Neutrino decay and spontaneous violation of lepton number," *Physical Review D*, vol. 25, no. 3, pp. 774–783, 1982.

[55] W. Konetschny and W. Kummer, "Nonconservation of total lepton number with scalar bosons," *Physics Letters B*, vol. 70, no. 4, pp. 433–435, 1977.

[56] R. E. Marshak and R. N. Mohapatra, "Selection rules for baryon number nonconservation in Gauge models," in *Recent Developments in High-Energy Physics*, pp. 277–287, Springer, New York, NY, USA, 1980.

[57] G. Lazarides, Q. Shafi, and C. Wetterich, "Proton lifetime and fermion masses in an SO(10) model," *Nuclear Physics Section B*, vol. 181, no. 2, pp. 287–300, 1981.

[58] R. N. Mohapatra and G. Senjanović, "Neutrino masses and mixings in gauge models with spontaneous parity violation," *Physical Review D*, vol. 23, no. 1, pp. 165–180, 1981.

[59] T. Cheng and L.-F. Li, "Neutrino masses, mixings, and oscillations in SU(2) × U(1) models of electroweak interactions," *Physical Review D*, vol. 22, no. 11, pp. 2860–2868, 1980.

[60] R. Foot, H. Lew, X.-G. He, and G. C. Joshi, "See-saw neutrino masses induced by a triplet of leptons," *Zeitschrift für Physik C Particles and Fields*, vol. 44, no. 3, pp. 441–444, 1989.

[61] F. Borzumati and A. Masiero, "Large muon- and electron-number nonconservation in supergravity theories," *Physical Review Letters*, vol. 57, no. 8, pp. 961–964, 1986.

[62] F. F. Deppisch, M. Hirsch, and H. Pas, "Neutrinoless double beta decay and physics beyond the standard model," *Journal of Physics G*, vol. 39, no. 12, Article ID 124007, 2012.

[63] A. Ilakovac and A. Pilaftsis, "Flavour-violating charged lepton decays in seesaw-type models," *Nuclear Physics B*, vol. 437, no. 3, pp. 491–519, 1995.

[64] J. Hisano, T. Moroi, K. Tobe, and M. Yamaguchi, "Lepton-flavor violation via right-handed neutrino Yukawa couplings in the supersymmetric standard model," *Physical Review D: Particles, Fields, Gravitation and Cosmology*, vol. 53, no. 5, pp. 2442–2459, 1996.

[65] E. Arganda and M. J. Herrero, "Testing supersymmetry with lepton flavor violating τ and μ decays," *Physical Review D*, vol. 73, no. 5, Article ID 055003, 2006.

[66] K. Babu and C. Kolda, "Higgs mediated $\tau \to 3\mu$ in the supersymmetric seesaw model," *Physical Review Letters*, vol. 89, no. 24, Article ID 241802, 4 pages, 2002.

[67] R. Aaij, C. Abellan Beteta, C. Adametz et al., "First evidence for the decay $B_s^0 \to \mu^+\mu^-$," *Physical Review Letters*, vol. 110, no. 2, Article ID 021801, 2013.

[68] A. Rossi, "Supersymmetric seesaw mechanism without singlet neutrinos: neutrino masses and lepton-flavor violation," *Physical Review D—Particles, Fields, Gravitation and Cosmology*, vol. 66, no. 7, Article ID 075003, 2002.

[69] M. R. Buckley and H. Murayama, "How can we test seesaw experimentally?" *Physical Review Letters*, vol. 97, Article ID 231801, 2006.

[70] M. Hirsch, F. R. Joaquim, and A. Vicente, "Constrained SUSY seesaws with a 125 GeV Higgs," *Journal of High Energy Physics*, vol. 2012, no. 11, article 105, 2012.

[71] J. Hisano, T. Moroi, K. Tobe, M. Yamaguchi, and T. Yanagida, "Lepton-flavor violation in the supersymmetric standard model with seesaw-induced neutrino masses," *Physics Letters B*, vol. 357, no. 4, pp. 579–587, 1995.

[72] J. R. Ellis, J. Hisano, M. Raidal, and Y. Shimizu, "A new parametrization of the seesaw mechanism and applications in supersymmetric models," *Physical Review D*, vol. 66, Article ID 115013, 2002.

[73] F. Deppisch, H. Päs, A. Redelbach, R. Rückl, and Y. Shimizu, "Probing the Majorana mass scale of right-handed neutrinos in mSUGRA," *European Physical Journal C*, vol. 28, no. 3, pp. 365–374, 2003.

[74] S. T. Petcov, S. Profumo, Y. Takanishi, and C. E. Yaguna, "Charged lepton flavor violating decays: leading logarithmic approximation versus full RG results," *Nuclear Physics B*, vol. 676, no. 1-2, pp. 453–480, 2004.

[75] S. T. Petcov, T. Shindou, and Y. Takanishi, "Majorana CP-violating phases, RG running of neutrino mixing parameters and charged lepton flavour violating decays," *Nuclear Physics B*, vol. 738, no. 1-2, pp. 219–242, 2006.

[76] S. Antusch, E. Arganda, M. J. Herrero, and A. M. Teixeira, "Impact of θ_{13} on lepton flavour violating processes within SUSY seesaw," *Journal of High Energy Physics*, vol. 2006, no. 11, article 90, 2006.

[77] F. Deppisch and J. W. F. Valle, "Enhanced lepton flavor violation in the supersymmetric inverse seesaw model," *Physical Review D*, vol. 72, Article ID 036001, 2005.

[78] A. Abada, A. J. R. Figueiredo, J. C. Romão, and A. M. Teixeira, "Interplay of LFV and slepton mass splittings at the LHC as a probe of the SUSY seesaw," *Journal of High Energy Physics*, vol. 2010, no. 10, Article ID 000658, 2010.

[79] A. Abada, A. J. R. Figueiredo, J. C. Romão, and A. M. Teixeira, "Lepton flavour violation: physics potential of a Linear Collider," *Journal of High Energy Physics*, vol. 2012, no. 8, article 138, 2012.

[80] A. J. R. Figueiredo and A. M. Teixeira, "Slepton mass splittings and cLFV in the SUSY seesaw in the light of recent experimental results," *Journal of High Energy Physics*, vol. 2014, no. 1, article 15, 2014.

[81] E. Arganda, M. J. Herrero, and A. M. Teixeira, "μ-e conversion in nuclei within the CMSSM seesaw: universality versus non-universality," *Journal of High Energy Physics*, vol. 2007, no. 10, article 104, 2007.

[82] F. Deppisch, T. S. Kosmas, and J. W. F. Valle, "Enhanced $\mu^- - e^-$ conversion in nuclei in the inverse seesaw model," *Nuclear Physics B*, vol. 752, no. 1-2, pp. 80–92, 2006.

[83] F. R. Joaquim and A. Rossi, "Gauge and Yukawa mediated supersymmetry breaking in the triplet seesaw scenario," *Physical Review Letters*, vol. 97, no. 18, Article ID 181801, 2006.

[84] M. Hirsch, S. Kaneko, and W. Porod, "Supersymmetric type-II seesaw mechanism: CERN LHC and lepton flavor violating phenomenology," *Physical Review D*, vol. 78, no. 9, Article ID 093004, 2008.

[85] J. N. Esteves, S. Kaneko, J. C. Romao, M. Hirsch, and W. Porod, "Dark matter in minimal supergravity with type-II seesaw mechanism," *Physical Review D: Particles, Fields, Gravitation and Cosmology*, vol. 80, no. 9, Article ID 095003, 2009.

[86] F. Joaquim, "Running effects on neutrino parameters and $\ell_i \to \ell_j \gamma$ predictions in the triplet-extended MSSM," *Journal of High Energy Physics*, vol. 2010, no. 6, article 79, 2010.

[87] A. Brignole, F. R. Joaquim, and A. Rossi, "Beyond the standard seesaw: neutrino masses from Kähler operators and broken supersymmetry," *Journal of High Energy Physics*, vol. 2010, no. 8, article 133, 2010.

[88] J. N. Esteves, J. C. Romao, M. Hirsch, F. Staub, and W. Porod, "Supersymmetric type-III seesaw mechanism: lepton flavor violating decays and dark matter," *Physical Review D*, vol. 83, no. 1, Article ID 013003, 2011.

[89] A. Abada, A. Figueiredo, J. Romao, and A. Teixeira, "Probing the supersymmetric type III seesaw: LFV at low-energies and at the LHC," *Journal of High Energy Physics*, vol. 2011, no. 8, article 099, 2011.

[90] M. Hirsch, W. Porod, C. Weiß, and F. Staub, "Supersymmetric type-III seesaw mechanism: lepton flavor violation and LHC phenomenology," *Physical Review D*, vol. 87, no. 1, Article ID 013010, 2013.

[91] J. Casas and A. Ibarra, "Oscillating neutrinos and $\mu \to e\gamma$," *Nuclear Physics B*, vol. 618, pp. 171–204, 2001.

[92] A. J. Buras, L. Calibbi, and P. Paradisi, "Slepton mass-splittings as a signal of LFV at the LHC," *Journal of High Energy Physics*, vol. 2010, no. 6, article 42, 2010.

[93] M. Hirsch, L. Reichert, and W. Porod, "Supersymmetric mass spectra and the seesaw scale," *Journal of High Energy Physics*, vol. 2011, no. 5, article 086, 2011.

[94] C. Arbeláez, M. Hirsch, and L. Reichert, "Supersymmetric mass spectra and the seesaw type-I scale," *Journal of High Energy Physics*, vol. 2012, no. 2, article 112, 2012.

[95] C. Biggio, L. Calibbi, A. Masiero, and S. K. Vempati, "Postcards from oases in the desert: phenomenology of SUSY with intermediate scales," *Journal of High Energy Physics*, vol. 2012, no. 8, article 150, 2012.

[96] C. S. Aulakh, K. Benakli, and G. Senjanović, "Reconciling high-scale left-right symmetry with supersymmetry," *Physical Review Letters*, vol. 79, no. 12, pp. 2188–2191, 1997.

[97] C. S. Aulakh, A. Melfo, A. Rašin, and G. Senjanović, "Supersymmetry and large scale left-right symmetry," *Physical Review D*, vol. 58, Article ID 115007, 1998.

[98] J. N. Esteves, J. C. Romao, M. Hirsch, W. Porod, F. Staub, and A. Vicente, "Dark matter and LHC phenomenology in a left-right supersymmetric model," *Journal of High Energy Physics*, vol. 2012, article 95, 2012.

[99] W. Chao, "Neutrino masses and lepton-flavor-violating τ decays in the supersymmetric left-right model," *Chinese Physics C*, vol. 35, no. 3, pp. 214–222, 2011.

[100] C. Arbelaez, R. M. Fonseca, M. Hirsch, and J. C. Romao, "Supersymmetric $SO(10)$-inspired GUTs with sliding scales," *Physical Review D*, vol. 87, no. 7, Article ID 075010, 2013.

[101] L. Calibbi, A. Faccia, A. Masiero, and S. K. Vempati, "Lepton flavor violation from supersymmetric grand unified theories: where do we stand for MEG, PRISM/PRIME, and a super flavor factory," *Physical Review D—Particles, Fields, Gravitation and Cosmology*, vol. 74, no. 11, Article ID 116002, 2006.

[102] L. Calibbi, A. Faccia, A. Masiero, and S. Vempati, "Running U_{e3} and BR ($\mu \to e + \gamma$) in SUSY-GUTs," *Journal of High Energy Physics*, vol. 2007, no. 7, article 012, 2007.

[103] L. Calibbi, M. Frigerio, S. Lavignac, and A. Romanino, "Flavour violation in supersymmetric SO(10) unification with a type II seesaw mechanism," *Journal of High Energy Physics*, vol. 2009, no. 12, article 057, 2009.

[104] A. J. Buras, M. Nagai, and P. Paradisi, "Footprints of SUSY GUTs in flavour physics," *Journal of High Energy Physics*, vol. 2011, no. 5, article 5, 2011.

[105] C. Biggio and L. Calibbi, "Phenomenology of SUSY SU(5) with type I+III seesaw," *Journal of High Energy Physics*, vol. 2010, no. 10, article 37, 2010.

[106] L. Calibbi, D. Chowdhury, A. Masiero, K. M. Patel, and S. K. Vempati, "Status of supersymmetric type-I seesaw in SO(10) inspired models," *Journal of High Energy Physics*, vol. 2012, no. 11, article 40, 2012.

[107] Y. Okada, K.-I. Okumura, and Y. Shimizu, "$\overline{\mu}e\gamma$ and $\overline{\mu}3e$ processes with polarized muons and supersymmetric grand unified theories," *Physical Review D*, vol. 61, Article ID 094001, 2000.

[108] J. Hisano, M. Nagai, P. Paradisi, and Y. Shimizu, "Waiting for $\mu \to e\gamma$ from the MEG experiment," *Journal of High Energy Physics*, vol. 2009, no. 12, article 030, 2009.

[109] V. De Romeri, M. Hirsch, and M. Malinsky, "Soft masses in supersymmetric SO(10) GUTs with low intermediate scales," *Physical Review D*, vol. 84, Article ID 053012, 2011.

[110] S. M. Boucenna, S. Morisi, and J. W. F. Valle, "The low-scale approach to neutrino masses," *Advances in High Energy Physics*, vol. 2014, Article ID 831598, 15 pages, 2014.

[111] G. 't Hooft, "Naturalness, chiral symmetry, and spontaneous chiral symmetry breaking," *Nato Science Series B*, vol. 59, article 135, 1980.

[112] F. del Aguila and J. A. Aguilar-Saavedra, "Distinguishing seesaw models at LHC with multi-lepton signals," *Nuclear Physics B*, vol. 813, no. 1-2, pp. 22–90, 2009.

[113] A. Atre, T. Han, S. Pascoli, and B. Zhang, "The search for heavy Majorana neutrinos," *Journal of High Energy Physics*, vol. 2009, no. 5, article 030, 2009.

[114] P. S. B. Dev and R. N. Mohapatra, "TeV scale inverse seesaw model in $SO(10)$ and leptonic nonunitarity effects," *Physical Review D*, vol. 81, Article ID 013001, 2010.

[115] P. S. B. Dev and R. N. Mohapatra, "Electroweak symmetry breaking and proton decay in SO(10) supersymmetric GUT with TeV W_R," *Physical Review D*, vol. 82, no. 3, Article ID 035014, 2010.

[116] M. Hirsch, M. Malinský, W. Porod, L. Reichert, and F. Staub, "Hefty MSSM-like light Higgs in extended gauge models," *Journal of High Energy Physics*, vol. 2012, no. 2, article 84, 2012.

[117] C.-Y. Chen and P. B. Dev, "Multilepton collider signatures of heavy Dirac and Majorana neutrinos," *Physical Review D*, vol. 85, no. 9, Article ID 093018, 8 pages, 2012.

[118] H. An, P. S. B. Dev, Y. Cai, and R. N. Mohapatra, "Sneutrino dark matter in gauged inverse seesaw models for neutrinos," *Physical Review Letters*, vol. 108, no. 8, Article ID 081806, 2012.

[119] V. De Romeri and M. Hirsch, "Sneutrino dark matter in low-scale seesaw scenarios," *Journal of High Energy Physics*, vol. 2012, article 106, 2012.

[120] M. Hirsch, W. Porod, L. Reichert, and F. Staub, "Phenomenology of the minimal supersymmetric $U(1)_{B-L} \times U(1)_R$ extension of the standard model," *Physical Review D*, vol. 86, Article ID 093018, 2012.

[121] S. Mondal, S. Biswas, P. Ghosh, and S. Roy, "Exploring novel correlations in trilepton channels at the LHC for the minimal supersymmetric inverse seesaw model," *Journal of High Energy Physics*, vol. 2012, no. 5, article 134, 2012.

[122] A. Das and N. Okada, "Inverse seesaw neutrino signatures at the LHC and ILC," *Physical Review D*, vol. 88, no. 11, Article ID 113001, 2013.

[123] P. S. B. Dev, S. Mondal, B. Mukhopadhyaya, and S. Roy, "Phenomenology of light sneutrino dark matter in cMSSM/mSUGRA with inverse seesaw," *Journal of High Energy Physics*, vol. 2012, no. 9, article 110, 2012.

[124] P. S. B. Dev, R. Franceschini, and R. N. Mohapatra, "Bounds on TeV seesaw models from LHC Higgs data," *Physical Review D: Particles, Fields, Gravitation and Cosmology*, vol. 86, no. 9, Article ID 093010, 2012.

[125] P. Bandyopadhyay, E. J. Chun, H. Okada, and J.-C. Park, "Higgs signatures in inverse seesaw model at the LHC," *Journal of High Energy Physics*, vol. 2013, no. 10, article 079, 2013.

[126] P. Bhupal Dev, D. K. Ghosh, N. Okada, and I. Saha, "125 GeV Higgs boson and the type-II seesaw model," *Journal of High Energy Physics*, vol. 2013, no. 3, article 150, 2013.

[127] M. Drewes, "The phenomenology of right handed neutrinos," *International Journal of Modern Physics E*, vol. 22, no. 8, Article ID 1330019, 2013.

[128] J. C. Helo, M. Hirsch, and S. Kovalenko, "Heavy neutrino searches at the LHC with displaced vertices," *Physical Review D*, vol. 89, no. 7, Article ID 073005, 7 pages, 2014.

[129] S. Banerjee, P. S. B. Dev, S. Mondal, B. Mukhopadhyaya, and S. Roy, "Invisible higgs decay in a supersymmetric inverse seesaw model with light sneutrino dark matter," *Journal of High Energy Physics*, vol. 2013, article 221, 2013.

[130] P. B. Dev, A. Pilaftsis, and U.-k. Yang, "Production Mechanism for Heavy Neutrinos at the LHC," *Phys.Rev.Lett*, vol. 112 no. 8, 2014, arXiv:1308.2209.

[131] F. F. Deppisch, N. Desai, and J. W. F. Valle, "Is charged lepton flavor violation a high energy phenomenon?" *Physical Review D—Particles, Fields, Gravitation and Cosmology*, vol. 89, no. 5, Article ID 051302, 2014.

[132] J. Aguilar-Saavedra, P. Boavida, and F. Joaquim, "Flavored searches for type-III seesaw mechanism at the LHC," *Physical Review D*, vol. 88, Article ID 113008, 2013.

[133] A. Das, P. Bhupal Dev, and N. Okada, "Direct bounds on electroweak scale pseudo-Dirac neutrinos from $\sqrt{s} = 8$ TeV LHC data," *Physics Letters B*, vol. 735, pp. 364–370, 2014.

[134] F. F. Deppisch, P. S. B. Dev, and A. Pilaftsis, "Neutrinos and collider physics," http://arxiv.org/abs/1502.06541.

[135] S. Banerjee, P. S. B. Dev, A. Ibarra, T. Mandal, and M. Mitra, "Prospects of heavy neutrino searches at future lepton colliders," http://arxiv.org/abs/1503.05491.

[136] J. C. Pati and A. Salam, "Lepton number as the fourth 'color'," *Physical Review D*, vol. 10, no. 1, pp. 275–289, 1974.

[137] R. N. Mohapatra and J. C. Pati, "'Natural' left-right symmetry," *Physical Review D*, vol. 11, no. 9, pp. 2558–2561, 1975.

[138] G. Senjanovic and R. N. Mohapatra, "Exact left-right symmetry and spontaneous violation of parity," *Physical Review D*, vol. 12, no. 5, pp. 1502–1505, 1975.

[139] W.-Y. Keung and G. Senjanović, "Majorana neutrinos and the production of the right-handed charged gauge boson," *Physical Review Letters*, vol. 50, no. 19, pp. 1427–1430, 1983.

[140] J. A. Aguilar-Saavedra, F. Deppisch, O. Kittel, and J. W. F. Valle, "Flavour in heavy neutrino searches at the LHC," *Physical Review D*, vol. 85, Article ID 091301, 2012.

[141] S. P. Das, F. F. Deppisch, O. Kittel, and J. W. F. Valle, "Heavy neutrinos and lepton flavor violation in left-right symmetric models at the LHC," *Physical Review D—Particles, Fields, Gravitation and Cosmology*, vol. 86, no. 5, Article ID 055006, 2012.

[142] C.-Y. Chen, P. S. B. Dev, and R. Mohapatra, "Probing heavy-light neutrino mixing in left-right seesaw models at the LHC," *Physical Review D*, vol. 88, no. 3, Article ID 033014, 7 pages, 2013.

[143] A. Maiezza and M. Nemevšek, "Strong P invariance, neutron electric dipole moment, and minimal left-right parity at LHC," *Physical Review D—Particles, Fields, Gravitation and Cosmology*, vol. 90, no. 9, Article ID 095002, 2014.

[144] S. Bertolini, A. Maiezza, and F. Nesti, "Present and future K and B meson mixing constraints on TeV scale left-right symmetry," *Physical Review D: Particles, Fields, Gravitation and Cosmology*, vol. 89, no. 9, Article ID 095028, 2014.

[145] A. Maiezza, M. Nemevsek, and F. Nesti, "Lepton number violation in Higgs decay," http://arxiv.org/abs/1503.06834.

[146] A. Abada, C. Biggio, F. Bonnet, M. B. Gavela, and T. Hambye, "Low energy effects of neutrino masses," *Journal of High Energy Physics*, vol. 2007, no. 12, article 061, 2007.

[147] A. Abada, C. Biggio, F. Bonnet, M. Gavela, and T. Hambye, "$\mu \to e\gamma$ and $\tau \to l\gamma$ decays in the fermion triplet seesaw model," *Physical Review D*, vol. 78, Article ID 033007, 2008.

[148] A. Ibarra, E. Molinaro, and S. T. Petcov, "Low energy signatures of the TeV scale seesaw mechanism," *Physical Review D*, vol. 84, Article ID 013005, 2011.

[149] D. N. Dinh, A. Ibarra, E. Molinaro, and S. T. Petcov, "The $\mu - e$ conversion in nuclei, $\mu \to e\gamma, \mu \to 3e$ decays and TeV scale see-saw scenarios of neutrino mass generation," *Journal of High Energy Physics*, vol. 2012, article 125, 2012.

[150] C. G. Cely, A. Ibarra, E. Molinaro, and S. T. Petcov, "Higgs decays in the low scale type I see-saw model," *Physics Letters, Section B: Nuclear, Elementary Particle and High-Energy Physics*, vol. 718, no. 3, pp. 957–964, 2013.

[151] D. N. Dinh and S. T. Petcov, "Lepton flavor violating τ decays in TeV scale type i see-saw and Higgs triplet models," *Journal of High Energy Physics*, vol. 2013, no. 9, article 86, 2013.

[152] R. N. Mohapatra, "Mechanism for understanding small neutrino mass in superstring theories," *Physical Review Letters*, vol. 56, no. 6, pp. 561–563, 1986.

[153] R. N. Mohapatra and J. W. F. Valle, "Neutrino mass and baryon-number nonconservation in superstring models," *Physical Review D*, vol. 34, no. 5, pp. 1642–1645, 1986.

[154] J. Bernabéu, A. Santamaria, J. Vidal, A. Mendez, and J. W. F. Valle, "Lepton flavour non-conservation at high energies in a superstring inspired standard model," *Physics Letters B*, vol. 187, no. 3-4, pp. 303–308, 1987.

[155] M. Hirsch, T. Kernreiter, J. Romao, and A. Villanova del Moral, "Minimal supersymmetric inverse seesaw: neutrino masses, lepton flavour violation and LHC phenomenology," *Journal of High Energy Physics*, vol. 2010, no. 10, article 103, 2010.

[156] M. Malinský, T. Ohlsson, Z.-Z. Xing, and H. Zhang, "Non-unitary neutrino mixing and CP violation in the minimal inverse seesaw model," *Physics Letters B*, vol. 679, no. 3, pp. 242–248, 2009.

[157] M. B. Gavela, T. Hambye, D. Hernández, and P. Hernández, "Minimal flavour seesaw models," *Journal of High Energy Physics*, vol. 2009, no. 9, article 038, 2009.

[158] P. S. B. Dev and A. Pilaftsis, "Minimal radiative neutrino mass mechanism for inverse seesaw models," *Physical Review D*, vol. 86, Article ID 113001, 2012.

[159] A. Abada and M. Lucente, "Looking for the minimal inverse seesaw realisation," *Nuclear Physics B*, vol. 885, pp. 651–678, 2014.

[160] M. C. Gonzalez-Garcia and J. W. F. Valle, "Fast decaying neutrinos and observable flavour violation in a new class of majoron models," *Physics Letters B*, vol. 216, no. 3-4, pp. 360–366, 1989.

[161] A. Abada, D. Das, A. Teixeira, A. Vicente, and C. Weiland, "Tree-level lepton universality violation in the presence of sterile neutrinos: impact for R_K and R_π," *Journal of High Energy Physics*, vol. 2013, no. 2, article 048, 2013.

[162] E. Akhmedov, A. Kartavtsev, M. Lindner, L. Michaels, and J. Smirnov, "Improving electro-weak fits with TeV-scale sterile neutrinos," *Journal of High Energy Physics*, vol. 2013, no. 5, article 081, 2013.

[163] C.-H. Lee, P. S. B. Dev, and R. N. Mohapatra, "Natural TeV-scale left-right seesaw mechanism for neutrinos and experimental tests," *Physical Review D: Particles, Fields, Gravitation and Cosmology*, vol. 88, no. 9, Article ID 093010, 2013.

[164] A. Abada, A. M. Teixeira, A. Vicente, and C. Weiland, "Sterile neutrinos in leptonic and semileptonic decays," *Journal of High Energy Physics*, vol. 2014, no. 2, article 091, 2014.

[165] A. Abada, V. De Romeri, and A. M. Teixeira, "Effect of steriles states on lepton magnetic moments and neutrinoless double beta decay," *Journal of High Energy Physics*, vol. 2014, no. 9, article 074, 2014.

[166] S. Antusch and O. Fischer, "Non-unitarity of the leptonic mixing matrix: present bounds and future sensitivities," *Journal of High Energy Physics*, vol. 2014, no. 10, article 94, 2014.

[167] A. Abada, V. De Romeri, S. Monteil, J. Orloff, and A. M. Teixeira, "Indirect searches for sterile neutrinos at a high-luminosity Z-factory," *Journal of High Energy Physics*, vol. 2015, article 51, 2015.

[168] S. Antusch and O. Fischer, "Testing sterile neutrino extensions of the standard model at future lepton colliders," *Journal of High Energy Physics*, vol. 2015, no. 5, article 053, 2015.

[169] M. Drewes and B. Garbrecht, "Experimental and cosmological constraints on heavy neutrinos," http://arxiv.org/abs/1502.00477.

[170] A. Ilakovac and A. Pilaftsis, "Supersymmetric lepton flavor violation in low-scale seesaw models," *Physical Review D*, vol. 80, Article ID 091902, 2009.

[171] R. Alonso, M. Dhen, M. Gavela, and T. Hambye, "Muon conversion to electron in nuclei in type-I seesaw models," *Journal of High Energy Physics*, vol. 2013, no. 1, article 118, 2013.

[172] A. Ilakovac, A. Pilaftsis, and L. Popov, "Charged lepton flavor violation in supersymmetric low-scale seesaw models," *Physical Review D*, vol. 87, no. 5, Article ID 053014, 2013.

[173] A. Abada, D. Das, and C. Weiland, "Enhanced Higgs mediated lepton flavour violating processes in the supersymmetric inverse seesaw model," *Journal of High Energy Physics*, vol. 2012, no. 3, article 100, 2012.

[174] M. E. Krauss, W. Porod, F. Staub, A. Abada, A. Vicente, and C. Weiland, "Decoupling of heavy sneutrinos in low-scale seesaw models," *Physical Review D: Particles, Fields, Gravitation and Cosmology*, vol. 90, no. 1, Article ID 013008, 2014.

[175] M. Hirsch, F. Staub, and A. Vicente, "Enhancing $l_i \to 3l_j$ with the Z^0-penguin," *Physical Review D*, vol. 85, no. 5, Article ID 113013, 2012.

[176] W. Porod, F. Staub, and A. Vicente, "A flavor kit for BSM models," *The European Physical Journal C*, vol. 74, no. 8, article 2992, 2014.

[177] F. Staub, "Sarah," http://arxiv.org/abs/0806.0538.

[178] F. Staub, "From superpotential to model files for FeynArts and CalcHep/CompHep," *Computer Physics Communications*, vol. 181, no. 6, pp. 1077–1086, 2010.

[179] F. Staub, "Automatic calculation of supersymmetric renormalization group equations and self energies," *Computer Physics Communications*, vol. 182, pp. 808–833, 2011.

[180] F. Staub, "SARAH 3.2: dirac gauginos, UFO output, and more," *Computer Physics Communications*, vol. 184, no. 7, pp. 1792–1809, 2013.

[181] F. Staub, "SARAH 4: a tool for (not only SUSY) model builders," *Computer Physics Communications*, vol. 185, no. 6, pp. 1773–1790, 2014.

[182] W. Porod, "SPheno, a program for calculating supersymmetric spectra, SUSY particle decays and SUSY particle production at e^+e^- colliders," *Computer Physics Communications*, vol. 153, no. 2, pp. 275–315, 2003.

[183] W. Porod and F. Staub, "SPheno 3.1: extensions including flavour, CP-phases and models beyond the MSSM," *Computer Physics Communications*, vol. 183, no. 11, pp. 2458–2469, 2012.

[184] F. Staub, "Exploring new models in all detail with SARAH," http://arxiv.org/abs/1503.04200.

[185] L. Basso, A. Belyaev, D. Chowdhury et al., "Proposal for generalised Supersymmetry Les Houches Accord for see-saw models and PDG numbering scheme," *Computer Physics Communications*, vol. 184, no. 3, pp. 698–719, 2013.

[186] D. V. Forero, M. Tórtola, and J. W. F. Valle, "Global status of neutrino oscillation parameters after Neutrino-2012," *Physical Review D*, vol. 86, Article ID 073012, 2012.

[187] I. Hinchliffe and T. Kaeding, "*B*- and *L*-violating couplings in the minimal supersymmetric standard model," *Physical Review D*, vol. 47, no. 1, pp. 279–284, 1993.

[188] P. Nath and P. Fileviez Perez, "Proton stability in grand unified theories, in strings and in branes," *Physics Reports*, vol. 441, no. 5-6, pp. 191–317, 2007.

[189] L. E. Ibáñez and G. G. Ross, "Discrete gauge symmetries and the origin of baryon and lepton number conservation in supersymmetric versions of the standard model," *Nuclear Physics. B*, vol. 368, no. 1, pp. 3–37, 1992.

[190] N. Sakai and T. Yanagida, "Proton decay in a class of supersymmetric grand unified models," *Nuclear Physics, Section B*, vol. 197, no. 3, pp. 533–542, 1982.

[191] S. Weinberg, "Supersymmetry at ordinary energies. Masses and conservation laws," *Physical Review D*, vol. 26, no. 1, pp. 287–302, 1982.

[192] J. R. Ellis, J. S. Hagelin, D. V. Nanopoulos, and K. Tamvakis, "Observable gravitationally induced baryon decay," *Physics Letters B*, vol. 124, no. 6, pp. 484–490, 1983.

[193] S. Morisi, E. Peinado, and A. Vicente, "Flavor origin of R-parity," *Journal of Physics G*, vol. 40, Article ID 085004, 2013.

[194] H. K. Dreiner, C. Luhn, and M. Thormeier, "What is the discrete gauge symmetry of the minimal supersymmetric standard model," *Physical Review D*, vol. 73, no. 7, Article ID 075007, 16 pages, 2006.

[195] L. J. Hall and M. Suzuki, "Explicit R-parity breaking in supersymmetric models," *Nuclear Physics, Section B*, vol. 231, no. 3, pp. 419–444, 1984.

[196] G. G. Ross and J. W. F. Valle, "Supersymmetric models without R-parity," *Physics Letters B*, vol. 151, no. 5-6, pp. 375–381, 1985.

[197] M. Hirsch and J. W. F. Valle, "Supersymmetric origin of neutrino mass," *New Journal of Physics*, vol. 6, article 76, 2004.

[198] H. K. Dreiner, F. Staub, A. Vicente, and W. Porod, "General MSSM signatures at the LHC with and without R-parity," *Physical Review D*, vol. 86, no. 3, Article ID 035021, 2012.

[199] H. Dreiner, F. Staub, and A. Vicente, "General NMSSM signatures at the LHC," *Physical Review D*, vol. 87, no. 3, Article ID 035009, 2013.

[200] P. W. Graham, D. E. Kaplan, S. Rajendran, and P. Saraswat, "Displaced supersymmetry," *Journal of High Energy Physics*, vol. 2012, no. 7, article 149, 2012.

[201] M. Hanussek and J. S. Kim, "Testing neutrino masses in the R-parity violating minimal supersymmetric standard model with LHC results," *Physical Review D*, vol. 85, no. 11, Article ID 115021, 2012.

[202] S. Borgani, A. Masiero, and M. Yamaguchi, "Light gravitinos as mixed dark matter," *Physics Letters B*, vol. 386, pp. 189–197, 1996.

[203] F. Takayama and M. Yamaguchi, "Gravitino dark matter without R-parity," *Physics Letters B*, vol. 485, no. 4, pp. 388–392, 2000.

[204] M. Hirsch, W. Porod, and D. Restrepo, "Collider signals of gravitino dark matter in bilinearly broken R-parity," *Journal of High Energy Physics*, vol. 2005, no. 3, article 062, 2005.

[205] J. E. Kim, "Light pseudoscalars, particle physics and cosmology," *Physics Reports*, vol. 150, no. 1-2, pp. 1–177, 1987.

[206] G. Raffelt, *Stars as Laboratories for Fundamental Physics*, University of Chicago Press, 1996.

[207] E. J. Chun and H. B. Kim, "Nonthermal axino as cool dark matter in the supersymmetric standard model without *R* parity," *Physical Review D*, vol. 60, Article ID 095006, 1999.

[208] E. J. Chun and H. B. Kim, "Axino light dark matter and neutrino masses with R-parity violation," *Journal of High Energy Physics*, vol. 2006, no. 10, article 082, 2006.

[209] R. Barbier, C. Bérat, M. Besançon et al., "*R*-Parity-violating supersymmetry," *Physics Reports*, vol. 420, no. 1–6, pp. 1–195, 2005.

[210] M. Chemtob, "Phenomenological constraints on broken R parity symmetry in supersymmetry models," *Progress in Particle and Nuclear Physics*, vol. 54, no. 1, pp. 71–191, 2005.

[211] Y. Kao and T. Takeuchi, "Single-coupling bounds on R-parity violating supersymmetry, an update," http://arxiv.org/abs/0910.4980.

[212] R. N. Mohapatra, "Supersymmetry and *R*-parity: an overview," *Physica Scripta*, vol. 90, no. 8, Article ID 088004, 2015.

[213] A. Pilaftsis, "Lepton flavor nonconservation in H^0 decays," *Physics Letters B*, vol. 285, no. 1-2, pp. 68–74, 1992.

[214] J. L. Diaz-Cruz and J. J. Toscano, "Lepton flavor violating decays of Higgs bosons beyond the standard model," *Physical Review D*, vol. 62, Article ID 116005, 2000.

[215] I. Doršner, S. Fajfer, A. Greljo, J. F. Kamenik, N. Košnik, and I. Nišandžić, "New physics models facing lepton flavor violating Higgs decays at the percent level," *Journal of High Energy Physics*, vol. 2015, no. 6, article 108, 2015.

[216] A. Arhrib, Y. Cheng, and O. C. W. Kong, "Comprehensive analysis on lepton flavor violating Higgs boson to $\mu^{\mp}\tau^{\pm}$ decay in supersymmetry without *R* parity," *Physical Review D*, vol. 87, no. 1, Article ID 015025, 2013.

[217] Y. Grossman and H. E. Haber, "(S)neutrino properties in *R*-parity-violating supersymmetry: *CP*-conserving phenomena," *Physical Review D*, vol. 59, no. 9, Article ID 093008, 15 pages, 1999.

[218] E. J. Chun and S. K. Kang, "One-loop corrected neutrino masses and mixing in the supersymmetric standard model without *R* parity," *Physical Review D*, vol. 61, Article ID 075012, 2000.

[219] S. Davidson and M. Losada, "Neutrino masses in the R_p violating MSSM," *Journal of High Energy Physics*, vol. 2000, no. 5, article 021, 2000.

[220] E. Arganda, M. J. Herrero, X. Marcano, and C. Weiland, "Imprints of massive inverse seesaw model neutrinos in lepton flavor violating Higgs boson decays," *Physical Review D*, vol. 91, no. 1, Article ID 015001, 2015.

[221] S. Davidson and G. J. Grenier, "Lepton flavor violating Higgs bosons and $\tau \to \mu\gamma$," *Physical Review D*, vol. 81, Article ID 095016, 2010.

[222] J. Kopp and M. Nardecchia, "Flavor and CP violation in Higgs decays," *Journal of High Energy Physics*, vol. 2014, article 156, 2014.

[223] D. A. Sierra and A. Vicente, "Explaining the CMS Higgs flavor-violating decay excess," *Physical Review D: Particles, Fields, Gravitation and Cosmology*, vol. 90, no. 11, Article ID 115004, 2014.

[224] J. Heeck, M. Holthausen, W. Rodejohann, and Y. Shimizu, "Higgs $\to \mu\tau$ in Abelian and non-Abelian flavor symmetry models," *Nuclear Physics B*, vol. 896, pp. 281–310, 2015.

[225] A. Crivellin, G. D'Ambrosio, and J. Heeck, "Explaining $h \to \mu^{\pm}\tau^{\mp}, B \to K^{*}\mu^{+}\mu^{-}$ and $B \to K\mu^{+}\mu^{-}/B \to Ke^{+}e^{-}$ in a two-Higgs-doublet model with gauged $L_{\mu}-L_{\tau}$," *Physical Review Letters*, vol. 114, Article ID 151801, 2015.

[226] E. Arganda, A. M. Curiel, M. J. Herrero, and D. Temes, "Lepton flavor violating Higgs boson decays from massive seesaw neutrinos," *Physical Review D*, vol. 71, no. 3, Article ID 035011, 2005.

[227] M. Arana-Catania, E. Arganda, and M. J. Herrero, "Non-decoupling SUSY in LFV Higgs decays: a window to new physics at the LHC," *Journal of High Energy Physics*, vol. 2013, article 160, 2013.

[228] J. L. Diaz-Cruz, D. K. Ghosh, and S. Moretti, "Lepton flavour violating heavy Higgs decays within the νMSSM and their detection at the LHC," *Physics Letters B*, vol. 679, no. 4, pp. 376–381, 2009.

[229] A. de Gouvêa, S. Lola, and K. Tobe, "Lepton-flavor violation in supersymmetric models with trilinear R-parity violation," *Physical Review D*, vol. 63, no. 3, Article ID 035004, 2001.

[230] H. Dreiner, M. Kramer, and B. O'Leary, "Bounds on R-parity violating supersymmetric couplings from leptonic and semi-leptonic meson decays," *Physical Review D*, vol. 75, Article ID 114016, 2007.

[231] J. Daub, H. Dreiner, C. Hanhart, B. Kubis, and U. Meißner, "Improving the hadron physics of non-Standard-Model decays: example bounds on R-parity violation," *Journal of High Energy Physics*, vol. 2013, no. 1, article 179, 2013.

[232] Y. Miyazaki, I. Adachi, H. Aihara et al., "Search for lepton-flavor-violating τ decay into a lepton and an $f_0(980)$ meson," *Physics Letters B*, vol. 672, no. 4-5, pp. 317–322, 2009.

[233] Y. Miyazaki, H. Aihara, K. Arinstein et al., "Search for lepton-flavor-violating τ decays into a lepton and a vector meson," *Physics Letters B*, vol. 699, no. 4, pp. 251–257, 2011.

[234] Y. Miyazaki, K. Hayasaka, I. Adachi et al., "Search for lepton-flavor and lepton-number-violating $\tau \to lhh'$ decay modes," *Physics Letters B*, vol. 719, no. 4-5, pp. 346–353, 2013.

[235] J. Sato and M. Yamanaka, "A way to crosscheck $\mu-e$ conversion in the case of no signals of $\mu \to e\gamma$ and $\mu \to 3e$," *Physical Review D*, vol. 91, no. 5, Article ID 055018, 17 pages, 2015.

[236] H.-B. Zhang, T.-F. Feng, S.-M. Zhao, and T.-J. Gao, "Lepton-flavor violation and $(g-2)_\mu$ in the $\mu\nu$SSM," *Nuclear Physics B*, vol. 873, no. 2, pp. 300–324, 2013, Erratum in *Nuclear Physics B*, vol. 879, p. 235, 2014.

[237] H.-B. Zhang, T.-F. Feng, G.-H. Luo, Z.-F. Ge, and S.-M. Zhao, "Muon conversion to electron in nuclei within the $\mu\nu$SSM with a 125 GeV Higgs," *Journal of High Energy Physics*, vol. 2013, no. 7, article 069, 2013.

[238] R.-M. Wang, J.-H. Sheng, J. Zhu, Y.-Y. Fan, Y. Gao, and R.-M. Wang, "Studying the lepton number and lepton flavor violating $D^0 \to e^\pm\mu^\mp$ and $D^+_{d/s} \to \pi(K)^+e^\pm\mu^\mp$ decays," *International Journal of Modern Physics A*, vol. 29, no. 29, Article ID 1450169, 2014.

[239] Y. Chikashige, R. N. Mohapatra, and R. D. Peccei, "Are there real goldstone bosons associated with broken lepton number?" *Physics Letters B*, vol. 98, no. 4, pp. 265–268, 1981.

[240] G. B. Gelmini and M. Roncadelli, "Left-handed neutrino mass scale and spontaneously broken lepton number," *Physics Letters B*, vol. 99, no. 5, pp. 411–415, 1981.

[241] C. S. Aulakh and R. N. Mohapatra, "The neutrino as the supersymmetric partner of the majoron," *Physics Letters B*, vol. 119, no. 1–3, pp. 136–140, 1982.

[242] C. Amsler, M. Doser, M. Antonelli et al., "Review of particle physics," *Physics Letters B*, vol. 667, pp. 1–6, 2008.

[243] A. Masiero and J. W. F. Valle, "A model for spontaneous R parity breaking," *Physics Letters, Section B: Nuclear, Elementary Particle and High-Energy Physics*, vol. 251, no. 2, pp. 273–278, 1990.

[244] M. J. Hayashi and A. Murayama, "Radiative breaking of $SU(2)_R \times U(1)_{B-L}$ gauge symmetry induced by broken $N = 1$ supergravity in a left-right symmetric model," *Physics Letters B*, vol. 153, no. 4-5, pp. 251–256, 1985.

[245] P. Fileviez Perez and S. Spinner, "Spontaneous R-parity breaking and left-right symmetry," *Physics Letters B*, vol. 673, no. 4-5, pp. 251–254, 2009.

[246] V. Barger, P. F. Pérez, and S. Spinner, "Minimal gauged $U(1)_{B-L}$ model with spontaneous R parity violation," *Physical Review Letters*, vol. 102, Article ID 181802, 2009.

[247] A. S. Joshipura and J. W. F. Valle, "Invisible higgs decays and neutrino physics," *Nuclear Physics B*, vol. 397, no. 1-2, pp. 105–122, 1993.

[248] M. Hirsch, J. C. Romao, J. W. F. Valle, and A. Villanova del Moral, "Invisible Higgs boson decays in spontaneously broken R-parity," *Physical Review D—Particles, Fields, Gravitation and Cosmology*, vol. 70, no. 7, Article ID 73012, 2004.

[249] M. Hirsch, A. Vicente, and W. Porod, "Spontaneous R-parity violation: lightest neutralino decays and neutrino mixing angles at future colliders," *Physical Review D*, vol. 77, no. 7, Article ID 075005, 2008.

[250] J. C. Romão, N. Rius, and J. W. F. Valle, "Supersymmetric signals in muon and tau decays," *Nuclear Physics B*, vol. 363, no. 2-3, pp. 369–384, 1991.

[251] X. G. I. Tormo, D. Bryman, A. Czarnecki, and M. Dowling, "Bounds on Majoron emission from muon to electron conversion experiments," *Physical Review D*, vol. 84, no. 11, Article ID 113010, 2011.

[252] A. Celis, J. Fuentes-Martin, and H. Serodio, "An invisible axion model with controlled FCNCs at tree level," *Physics Letters B*, vol. 741, pp. 117–123, 2015.

[253] A. Jodidio, B. Balke, J. Carr et al., "Search for right-handed currents in muon decay," *Physical Review D*, vol. 34, p. 1967, 1986.

Hindawi Publishing Corporation
Advances in High Energy Physics
Volume 2015, Article ID 581038, 16 pages
http://dx.doi.org/10.1155/2015/581038

Review Article

Status of LHC Searches for SUSY without R-Parity

Roberto Franceschini

CERN, Theory Division, Genève 23, 1211 Geneva, Switzerland

Correspondence should be addressed to Roberto Franceschini; franceschini.roberto@gmail.com

Received 26 March 2015; Revised 29 June 2015; Accepted 28 July 2015

Academic Editor: Michal Malinský

In this contribution we briefly review the status of current searches for supersymmetry at the Large Hadron Collider, focusing especially on viable sub-TeV colored superpartners which can appear in nonstandard scenarios. The presented material covers mostly signals that do not crucially rely on the presence of large missing transverse momentum, with special emphasis on R-parity violating supersymmetry. For some scenarios the prospects for the next run of the Large Hadron Collider and future machines are also presented.

1. Missing Transverse Momentum, Missing Supersymmetry

Supersymmetry is the leading candidate for physics beyond the Standard Model of particle physics. It is currently subject to a very long list of experimental searches that try to use the high-energy collisions of the LHC beams to identify the production of new supersymmetric particles. So far the search for SUSY has generated a *statistically* [1] large number of papers in which any evidence of new physics has not been shown. Generically, searches for SUSY give bounds on the mass of colored superpartners [2]. Consider

$$M_{\text{SUSY}} > 1\ \text{TeV}. \tag{1}$$

In this contribution, we review the qualitative aspects of the searches that have been carried out by the experiments and the possible consequences of these results for our picture of supersymmetry as the theory for physics at the TeV scale.

Searches for new physics are usually conducted by searching for final states containing some combination of

$$\text{jets, leptons, photons, and } \mathbf{mET}. \tag{2}$$

Jets, leptons, and photons are, roughly speaking, the measurable objects that are devised to capture the concepts of an energetic quark or gluon, an isolated electron or muon, and a nonvirtual photon that are used to describe high-energy scattering in terms of a Lagrangian. mET is, instead, a nonmeasurable object that is defined "by contrast" as the imbalance of momentum in the plane orthogonal to the colliding beams. Since momentum is known to be conserved to very high accuracy, we think that mET is a consequence of the production of particles that do not interact with the detector materials. One example of a source of mET is indeed the neutrino, which was originally observed as a violation of momentum conservation in radioactive decays. As the neutrino history demonstrates, the presence of mET above the expected level due to detector imperfections is quite noticeable and immediately suggests the production of particles experiencing only weak interactions [3]. In the Standard Model the only noninstrumental source of mET is the production of neutrinos, which is not very abundant when compared to most other processes, especially when involving strong interactions. For this reason a signal with mET is quite easy to spot over backgrounds, which is why mET is in bold typeface in (2). Because of this experimentally striking nature, most experiments looking for SUSY at particle colliders search for large mET signals. Furthermore, these large mET signals are also predicted by most supersymmetric models, especially those that can provide a Dark Matter candidate. Building on these experimental and theoretical arguments, all large mET searches build their strength (and their weakness at the same time) on the fact that in the production of supersymmetric particles one forcedly produces also purely weakly interacting stable particles that give rise to mET. For these reasons we

can (somewhat provocatively) dub the present searches for supersymmetry as "*searches for supersymmetric Dark Matter in the decay of colored superpartners*."

While this summary of the scope of the present searches might be a bit too hasty, it renders well the actual reach of the present results from the LHC. In fact for most searches if one considers signal cross sections lower than those of colored particles the mass reach quickly vanishes. Similarly as one reduces the amount of missing transverse momentum in the signal events the mass reach quickly drops as well. These two axes, reduction of cross section and reduction of missing transverse momentum, are the two main handles that are typically involved when light supersymmetric particles evade present bounds.

2. Sub-TeV Colored Superpartners

The stringent bounds that emerge from the experimental results of the first run of the LHC are certainly a motivation, and a valuable chance, to reconsider our motivation for SUSY at the TeV scale as well as our approach to the search of its signals.

A common element of the vast majority of searches is the fact that in each new physics event containing supersymmetric particles the scattering reaction has to be of the type

$$pp \longrightarrow \text{SUSY} \longrightarrow \chi\chi + \text{SM}, \tag{3}$$

where χ denotes a generic weakly interacting massive particle that gives rise to mET. Of course if the intermediate supersymmetric states that mediate reaction equation (3) have reduced cross section, their search will be more difficult and the constraints from present searches would be looser. In this contribution we do not consider this type of ways out of the current bounds from the LHC. These situations with reduced cross section for the new physics colored states are typical in models with Dirac Gauginos, which are covered elsewhere in this volume. Instead, we want to consider the possibility of different types of SUSY models where the typical signal does not feature sources of mET beyond those of the SM, that is, in reactions of the type

$$pp \longrightarrow \text{SUSY} \longrightarrow \text{SM}. \tag{4}$$

These two scatterings in (3) and (4) differ most importantly in the amount of mET that they generate. In fact in the case of scatterings of type equation (4) no sources of mET beyond the Standard Model are expected. At the level of theoretical description, the difference between SUSY models giving rise to reactions of type equations (3) and (4) is in the amount of discrete symmetries that one imposes on the model. Therefore the exploration of both types of signals is needed as it is very informative about the symmetries of the new physics. The symmetry structure of the two classes of models differs in the aspects outlined in what follows. Taking the Lagrangian of the Standard Model and extending it to respect SUSY one would obtain the following gauge invariant superpotential interactions in addition to the usual MSSM superpotential:

$$W_{\text{RPV}} = \lambda'' u^c d^c d^c + \lambda' LQd^c + \lambda LLe^c + \mu' LH_u. \tag{5}$$

These interactions violate baryon number (λ'') or lepton number (λ, λ', and μ'). Without advocating a specific origin of these couplings one expects that, once R-parity is broken, all the interactions are generated and both baryon number and lepton number are violated, which is very dangerous in view of the stringent bounds on the conservation of these quantities [21]. The extension of the Standard Model to respect supersymmetry ends up altering the accidental symmetries of the Standard Model through these new Yukawa interactions and mass mixings. In the past, these new interactions have mostly been regarded as a source of trouble, as they make it hard for the model to not be in contrast with experiments. For this reason, a symmetry called R-parity has been put by hand in the model that we usually call *Minimal* Supersymmetric Standard Model (MSSM). R-parity, killing the interactions in (5), forbids the lightest superpartner to decay and hence provides a stable particle which, if weakly interacting, might be a Dark Matter candidate. (Although a weakly interacting particle of mass around the Fermi scale is no longer available as a Dark Matter candidate in RPV models, it is worth mentioning that other Dark Matter candidates exist in these models. One example is the decaying gravitino found in bilinear RPV scenarios, where μ' is the only nonzero RPV coupling [22, 23]. One other example is a stable gravitino in models of baryonic RPV, where only λ'' is nonzero. This gravitino would follow the same dynamics of the usual R-parity conserving gravitino [24] and might easily be heavy enough to suppress proton decay below the current limits [25, 26]. Furthermore axions and particles related to it through supersymmetry could be Dark Matter candidates as well.) This particle is χ in the above equation and is the source of mET around which the vast experimental program for SUSY searches has been built.

Taking a step back in the path that leads from SUSY to mET and Dark Matter we can choose to cope with the new interactions in (5) in a different way. In Section 2.2.1, we discuss which theoretical ideas could provide an approximate symmetry that puts these interactions under theoretical control, still not putting them to zero. In Section 2.2 we explore the observable consequences that a nonvanishing coupling in (5) would have at the LHC experiments.

2.1. Stealth and Compressed SUSY. In some cases reactions equations (3) and (4) might be very hard to distinguish, because of the elusive nature of the χ particles. As invisible particles they can only be observed by "contrast" looking at the entire set of particles produced in the reaction and imposing on them some kind of momentum conservation law. This means that every time that χ does not carry large momentum it might be very difficult to observe the effects of its production.

A typical case where χ gives less observable signals than the ones targeted in standard searches is "stealth" supersymmetry. To understand what it is, we look at the kinematics of a two-body decay. Consider

$$A \longrightarrow bc. \tag{6}$$

Conservation of 4-momentum implies that in the rest frame of the parent particle

$$E_b = \frac{m_A^2 - m_c^2 + m_b^2}{2m_A},$$
$$E_c = \frac{m_A^2 + m_c^2 - m_b^2}{2m_A}, \tag{7}$$

which is the usual monochromatic energy of a two-body decay product in the rest frame of the decaying particle. The same conservation of 4-momentum can also be rewritten in the form of two opposite 3-momenta $\vec{p}_b = -\vec{p}_c$ with equal magnitudes. One has

$$p_c = p_b = \frac{M_A}{2}\sqrt{\lambda\left(1, \frac{m_b^2}{m_A^2}, \frac{m_c^2}{m_A^2}\right)}, \tag{8}$$

where $\lambda(x, y, z) = x^2 + y^2 + z^2 - 2xy - 2xz - 2yz$ is a measure of the available phase-space of the decay. As can be seen from these simple kinematical considerations, when the decay happens close to a degeneracy $m_A \simeq m_b + m_c$ the 3-momenta of the particles b and c are suppressed. Consider

$$p_b \simeq (M_b, 0)$$
$$p_c \simeq (M_c, 0). \tag{9}$$

This situation arises when the spectrum is "compressed"; that is, the masses are almost too heavy to close the phase-space of the decay. In general this situation gives rise to small 3-momenta particle A rest frame, but 3-momenta may be large once the decay is observed in a frame with a large enough boost from the A rest frame. This means that if a new physics signal generically gives little mET because of "compression" of the spectrum, one can in principle try to observe events with larger boosts in order to increase the amount of mET observed in the events. However, there are cases in which changing frame does not help. In fact, if one of the two particles is more massive than the other all the energy of the decaying particle A is transferred to the mass of the heavy particle, whereas the momenta of the decay products are comparably smaller. Consider

$$p_{\text{heavy}} = \{M + O(\epsilon), \epsilon\}$$
$$p_{\text{light}} = \{\epsilon, \epsilon\}. \tag{10}$$

In this situation, the emission of the light particle in the decay can be pictured as almost unnoticeable soft emission in the conversion of the decaying particle into the heavy daughter particle. Although we derived the kinematics of this decay in the rest frame of A, the latter statement holds as well in the laboratory frame, as the Lorentz transformation of p_{light} will again give a vector of negligible momentum compared to the Lorentz transformation of p_{heavy}.

The presence of a light invisible particle in the spectrum can be achieved relatively easily [27], for instance, in scenarios of gauge mediated supersymmetry breaking or any scenario with low scale of mediation of supersymmetry breaking where the gravitino can be much lighter than the other superpartners or in scenarios in which the lightest neutralino is nearly massless. In these circumstances, due to its lightness, it is very hard to tell apart events where χ is present from those where it is not. For this reason, it is very difficult to reject Standard Model events and retain new physics ones on the basis of the measured missing transverse momentum. In these cases, it is also difficult to understand whether the new physics reaction belongs to type equations (3) and (4). However, as we discuss in the next section, (4) can be identified thanks to other distinctive features, such as the presence of new directly measurable resonances in the new physics event.

2.2. R-Parity Violation. As explained above, mET is a very powerful discriminator of physics beyond the Standard Model, due to the relatively low rates of events produced by Standard Model physics with large mET. A similarly powerful discriminator of new physics events is electrons and muons that are at the same time relatively infrequent final states in Standard Model physics and are also very clean to measure. This implies that when one or more among the couplings λ, λ', μ' in (5) are nonzero, the lightest superpartner can decay through these interactions. In general, the decay of the lightest superpartner through these interactions will systematically produce charged leptons as these couplings break lepton number. The result is that when the lepton number violating couplings are important for the decay of the lightest superpartner, new physics events give rise to processes of the type

$$pp \longrightarrow \text{SUSY} \longrightarrow \text{many leptons} + X. \tag{11}$$

For these processes we have very stringent bounds [2] and generically the masses of the superpartners end up being constrained to be at the TeV scale or higher. In view of these bounds from leptonic final states, lepton number violating couplings are of no help if one is trying to explain why sub-TeV SUSY has not been observed in experiments at the TeV scale (see, e.g., [28] for possible exceptions).

A more intriguing possibility is given by the baryon number violating coupling

$$\lambda''_{ijk} \cdot u_i^c d_j^c d_k^c, \tag{12}$$

which breaks baryon number but conserves leptons number and *per se* does not mediate proton decay. When this coupling dominates the decay of the lightest superpartner, we expect purely hadronic final states to appear from the production of new supersymmetric states. One has

$$pp \longrightarrow \text{SUSY} \longrightarrow \text{hadrons}. \tag{13}$$

These final states are very frequent in Standard Model scatterings, owing to the hadronic nature of the initial state of the LHC collisions and to the strength of hadronic interactions. Therefore the discovery of new physics in this type of final states is considerably more challenging than in most other final states. This is true even after taking into account that the absence of sources of mET from physics beyond the Standard

Model opens the possibility of searching for new states through resonance searches. A nice example that displays this fact is squark production. Consider

$$\begin{aligned} pp &\longrightarrow \tilde{q}\tilde{q} \longrightarrow qq\chi\chi \quad \text{(R-parity Conserving)} \\ \text{versus } pp &\longrightarrow \tilde{q}\tilde{q} \longrightarrow qqqq \quad \text{(R-parity Violating)}. \end{aligned} \tag{14}$$

Despite the possibility of reconstructing a resonance from the decay $\tilde{q} \rightarrow qq$, the RPV scenario is very loosely bounded, especially for the most interesting mass range $m_{\tilde{q}} \sim 100\,\text{GeV}$ [5, 29]. If one is interested in just heavy flavor squark states, as a naturalness argument would want them to be the lightest squarks, then no bound exists for $m_{\tilde{t}} > 100\,\text{GeV}$. The stop squark example shows very clearly that sub-TeV superpartners are still allowed when R-parity is not imposed on the MSSM. However it must be stressed that baryonic RPV SUSY has some interesting bounds from the LHC. For instance, the searches for objects such as the gluino can exploit the richer and more structured final state that originates from the gluino decay, which produces a multijet resonance. This search has been the subject of several interesting experimental and theoretical developments in the recent times. For instance, the possibility to use jet-substructure techniques to deal with multijet signals that appear in a final state of unknown (and in general not fixed) multiplicity from the gluino decay has been explored in [15]. These techniques might also be useful to reach the very faint signals that would originate from squark decay as in (14) [30]. Another front of recent progress has to do with the use of heavy flavor tagging in multijet searches. In fact, most theories that explain the origin of the RPV couplings predict peculiar dependences of the couplings on the flavor of the quark. These predictions [25, 31–34] (see also [25] for exceptions to the MFV prediction) tend to favor heavy flavor final states and certain searches for RPV SUSY are already covering the space of possible flavor signatures of the different models [11]. In this case the information about the presence of heavy flavor final states in the decay of new physics particles can make the difference between attaining a discovery and a bound on the faint signals of light RPV stops [35].

2.2.1. Origin of the RPV Couplings. When R-parity is not imposed, one needs to find a dynamical mechanism that makes the RPV couplings small enough to avoid excessive baryon or lepton number violation. Barring the option of just assuming that these couplings are small by accident (although this "feature" would be preserved by nonrenormalization of the superpotential), one interesting possibility to control the size of the RPV couplings is to associate them with the breaking of the flavor symmetries of the Standard Model. In fact if one takes the masses of the fermions of the Standard Model and put them to zero, then the Standard Model Lagrangian acquires a large flavor symmetry that redefines, for instance, the flavor up, charm, and top of the right handed up-type quark fields. Similar symmetries exist for all the fermions of the Standard Model and overall there is a

$$\begin{aligned} SU(3)^6 = {} & SU(3)_Q \otimes SU(3)_u \otimes SU(3)_d \otimes SU(3)_L \\ & \otimes SU(3)_e \otimes SU(3)_\nu \end{aligned} \tag{15}$$

symmetry that one can impose on the supersymmetric extensions of the Standard Model and that would make all the interactions of (5) [31, 32] vanish. In this way, the size of the RPV couplings is connected to the breaking of the flavor symmetry and hence to the masses of the fermions that are involved in the interaction. The generic prediction of complete models is

$$\lambda''_{ijk} \sim f_{\text{CKM}} \cdot \left(\frac{m_{u_i} m_{d_j} m_{d_k}}{m_t^3} \right)^{\alpha}, \tag{16}$$

where f_{CKM} is a factor from the CKM matrix that tends to suppress couplings involving different generations of quarks and $\alpha = 1$ in the most simple models but $\alpha < 1$ is attainable as well [25]. The predictions of these models, especially the minimal models where $\alpha = 1$, tend to favor the production of heavy quark jets. In light of these predictions the experimental exploration [11, 35] of flavored final states from the decay of RPV SUSY states is certainly very motivated.

3. Current Searches and Prospects for the LHC 14 TeV Run and Beyond

The presence of a stable invisible particle at the bottom of each decay chain of supersymmetric particles is the very reason for large mET signals expected in supersymmetric models. The large mET is usually a powerful discriminator to reject backgrounds; however, in some occasions other features of the signal can be helpful as well. For instance, in some cases we can derive from first principles an approximate shape of the distribution of some observable. A classic example is the shape of a Breit-Wigner resonance which can be effectively searched over a smoothly falling background. This has been the case, for instance, of the observation of the Higgs boson decay into two photons (up to the fact that due to resolution effects the shape is actually closer to a gaussian than to a Breit-Wigner).

Supersymmetric models with stable invisible particles unfortunately do not usually benefit from this type of searches because the invisible particles carry away momentum and it is not possible to use them in the reconstruction of the Breit-Wigner resonance. In presence of invisible particles, it is still possible to exploit features of multiparticles invariant masses [36–38] or single particle properties [39, 40]. However, such methods are useful only in searches for specific scenarios [41, 42] and are in general more suited to probe the mass spectrum of the model rather than to isolate a signal from the backgrounds. A more systematic use of resonant features in supersymmetric model requires no invisible particles in the final state of the decays.

As discussed above, invisible supersymmetric particle arises only as a consequence of having imposed R-parity in the MSSM. Without this feature of the model, new interactions are present; they are Yukawa couplings of the type in (5) and in general they can mediate the decay of any superpartner into a set of states of the Standard Model; for instance,

$$\begin{aligned} &\tilde{q} \longrightarrow jj \\ &\text{or } \tilde{g} \longrightarrow q\tilde{q} \longrightarrow q\bar{q}q. \end{aligned} \tag{17}$$

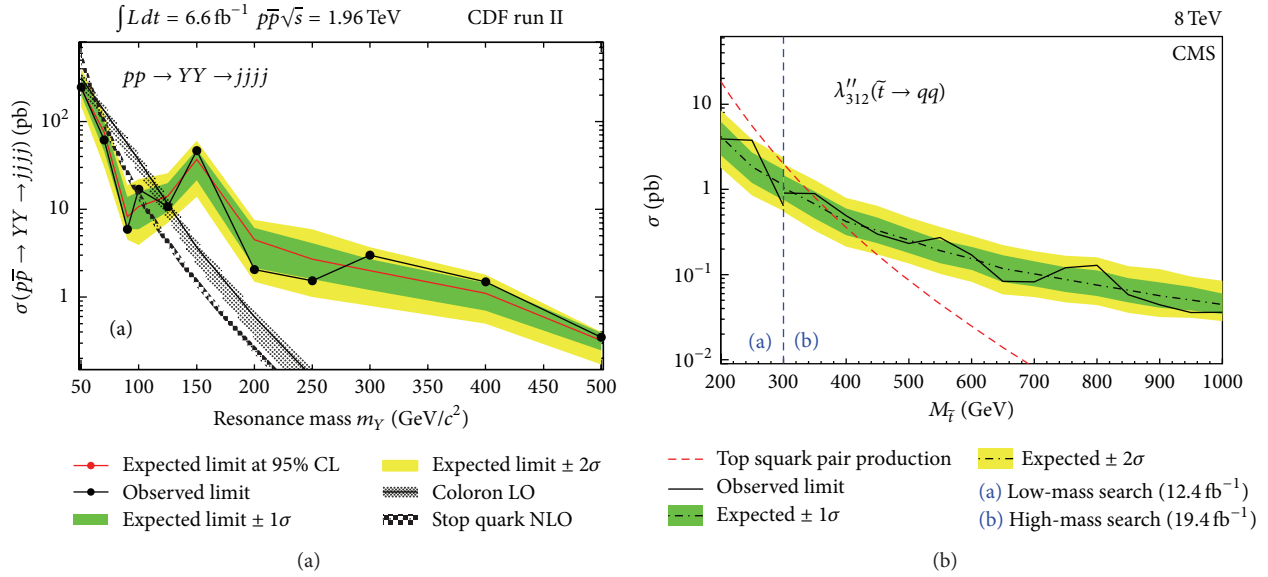

FIGURE 1: Limits on paired dijet production confronted with the production cross section of a single stop quark at the TeVatron [4] (a) and at the LHC [5] (b). As indicated in the legend, the black solid line represents the excluded cross section for the new physics reaction as a function of the mass of the new state. The green and yellow bands are the total 1σ and 2σ uncertainties on the exclusion. The predicted cross section for the new state is indicated by a solid line per each specific new physics model. The model is excluded for each mass choice for which the predicted cross section is above the exclusion.

These couplings in general have to be small because they can mediate baryon number or lepton number violating process such as proton decay or oscillation between neutron and antineutron or mediate flavor changing neutral currents processes. Despite their smallness they are crucial to avoid invisible stable particles in the model. In fact, RPV coupling of order 10^{-5} would still be large enough to give a decay $\chi \to q\bar{q}q$ with average decay path below 10^{-6} meters. In what follows we discuss several simplified models for RPV supersymmetry that give rise to resonances, roughly in the order from lowest multiplicity to higher multiplicity. We concentrate on baryonic RPV signals, as leptonic RPV is usually very tightly bounded by the presence of hard leptons in the final states [43, 44] (scenarios of leptonic RPV where this statement might not be true have been studied in [28]).

3.1. The (Heavy Flavor) RPV Squark Simplified Model. In this simplified model, the only light supersymmetric particle that can be produced via QCD interaction is a squark (see Table 1).

For this simplified model, the signal consists of 4 jets in which one can find a resonance from $\tilde{q} \to jj$. This search is quite challenging as it faces a large QCD background from multijet events. The 2010 run of the LHC at low instantaneous luminosity has been very helpful to probe this type of simplified models as it has provided data with lower trigger thresholds and lower QCD background rates. Together with recent CDF results [4], the ATLAS search [45] provides the best limits of this type of processes at low mass. Recent bounds from high instantaneous luminosity data have been put and constrain squarks from 200 GeV to 350 GeV [5]. The full collection of limits from this search is reported in Figure 1.

TABLE 1

BSM particles	Production	Decay
$\tilde{q}$	$pp \to \tilde{q}\bar{q}^*$	$\tilde{q} \to jj$

For a single squark the limits so far exclude masses up to 100 GeV.

The projection for the exclusion of this simplified model at the LHC Run 2 and High Luminosity LHC have been studied in [6], which finds that masses from 300 GeV to about 1 TeV can be excluded at the end of High Luminosity Run. For a reliable exclusion at low mass, special care is needed as the backgrounds become larger and more uncertain. In [30], the possibility to exploit the lightness of the squarks to search for the production of highly boosted squarks using jet-substructure techniques has been studied. The result is reported in Figure 2 for the expected exclusion if such analysis would be run on 8 TeV LHC data. The estimated exclusion extends up to 150 GeV. Given the nature of this search it is expected to improve as higher energy machines are available, as the production of boosted stops will become more abundant.

If the squark is a heavy flavor, more special signals are expected to arise; for instance,

$$\tilde{t} \longrightarrow bj \quad \text{or } \tilde{b} \longrightarrow tj. \tag{18}$$

The presence of bottom or top quarks in the final state is a powerful handle to discriminate these signals from the background and recently bounds have been obtained [5]

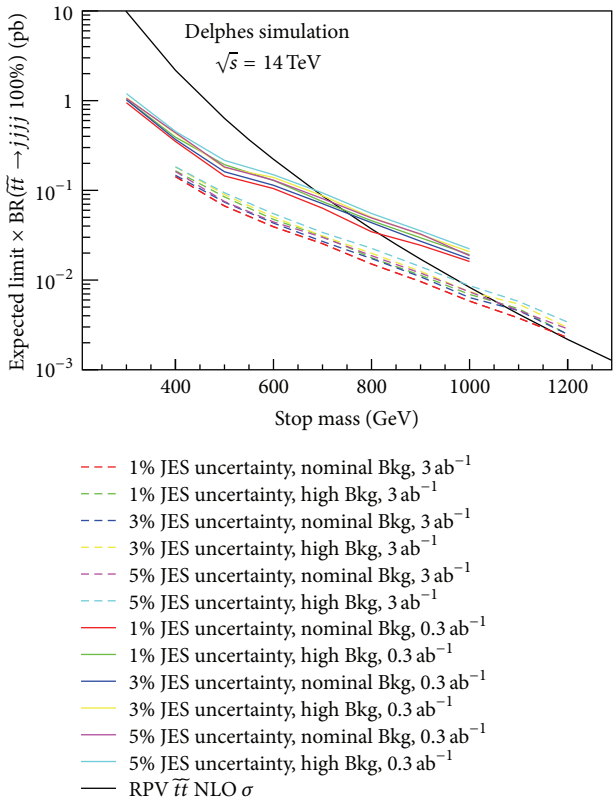

Figure 2: Projected exclusion reach for the LHC Run 2 and beyond [6] for the RPV squark simplified model. In this picture the many colored lines represent the expected exclusion under a given assumption of Jet Energy Scale (JES) uncertainty and background systematics. For more details on this assumption, we refer to the original work [6].

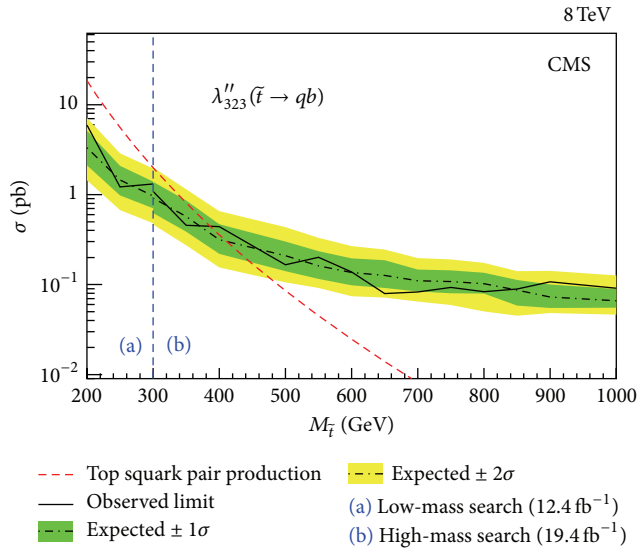

Figure 3: Exclusions on the RPV heavy flavor squark simplified model from the 8 TeV run of the LHC [5]. Color codes are the same as in Figure 1.

Table 2

BSM particles	Production	Decay
$\tilde{g}$	$pp \to \tilde{g}\tilde{g}$	$\tilde{g} \to jjj$

Table 3

BSM particles	Production	Decay
$\tilde{g}$	$pp \to \tilde{g}\tilde{g}$	$\tilde{g} \to J_u J_d J_d$, where $J_u = \{t, c, j\}$ and $J_d = \{b, j\}$

exploiting the presence of heavy flavors in the final state. The bounds are reported in Figure 3 and show an exclusion between 200 GeV and 385 GeV. The region between 100 GeV and 200 GeV is presently not probed by LHC, due to the large thresholds needed for trigger and for QCD background rejection. With an analysis targeted to this region, discovery should be possible from the CDF bound at 100 GeV up to masses around 200 GeV using LHC Run 1 data [30, 35]. Higher energy colliders will be able to extend the discovery reach beyond 200 GeV, as the limitations in this channel arise mainly from the stop production cross section and not from the poor knowledge of the background.

3.2. The (Heavy Flavor) RPV Gluino Simplified Model. In this simplified model, only the gluino is light enough to be produced in pp collisions. The gluino can decay only through a three-body decay into three fermions, mediated by a virtual squark. Depending on the mass of the virtual squark, this might give rise to displaced vertexes, but here we will consider the case of prompt decay, which is usually the case for squarks masses below 1 TeV (see Table 2).

Searches for resonances decaying into 3 light flavor jets have been conducted at both ATLAS and CMS. For the case in which the 3 jets are resolved, limits are reported in Figure 4, which shows a bound up to about 150 GeV [7] and from 200 to about 800 GeV [8–10].

If one of the virtual squarks that mediates the gluino decay has a preference for coupling to a certain flavor of quarks the previous simplified model will not capture this feature, which, as a matter of fact, is rather well justified in concrete models of RPV supersymmetry. To capture this possibility, a slightly different simplified model can be considered with gluino decays to heavy flavors, in suitable flavor combinations $\tilde{g} \to J_u J_d J_d$, where $J_u = \{t, c, j\}$ and $J_d = \{b, j\}$ (see Table 3).

For example, ATLAS puts a bound [46] from 500 GeV to about 1 TeV on the flavor combination $\tilde{g} \to tbj$. A more extensive exploration of the flavor structure of the $J_u J_d J_d$ final state is carried out in [11]. The highest excluded mass varies depending on the flavor combination assumed for the $J_u J_d J_d$ final state. In Figure 5, we report the result for zero charm quarks in the plane of bottom and top branching fraction.

Also for this simplified model, as it was the case for the RPV squark simplified model, it is particularly tough to put bounds on light particles. For instance, in [10], the lowest mass for which it is possible to put a limit is about 400 GeV, because of the trigger thresholds. The limitations arise because the searches try to identify a bump from the jjj resonance over a smooth background from QCD multijet

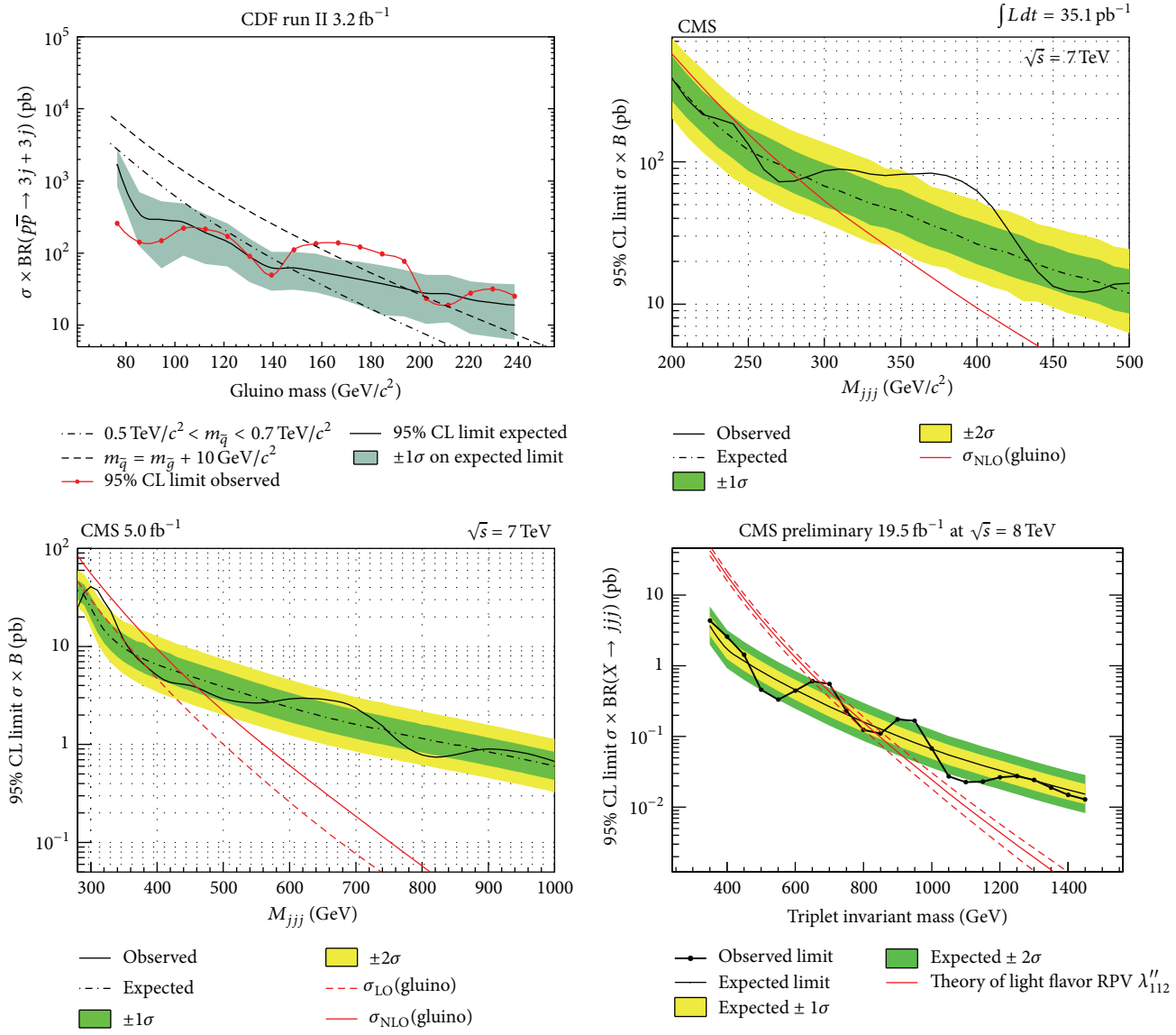

FIGURE 4: Limits on the gluino RPV simplified model for the resolved jet final state [7–10]. Color codes are the same as in Figure 1.

production. To overcome this restriction, searches that compare counted events with theory of Monte Carlo predictions have been performed. These "cut and count" searches are in general not requiring to see a bump or any feature in the spectrum of multijets events. To improve the robustness of the search, they normally use data to normalize the expected number of events in presence of pure background. Nevertheless, they rely more than bump searches on the theoretical prediction of the backgrounds, which makes it more challenging to obtain reliable bounds. Results from this cut and count search [15] are reported in Figure 9, where exclusions from 100 GeV upwards are shown. It is remarkable that light gluinos cross sections are excluded by a large factor, which should guarantee the exclusion even in presence of large uncertainties.

It has been pointed out that for RPV Majorana gluino decaying into heavy flavors it is possible to have a signal with two hard leptons of equal electric charge [47]. Limits from this signal have been obtained from the 8 TeV run of the LHC and exclude masses up to 900 GeV [12]. Estimates for the 14 TeV LHC have been presented in [13] and are reported in Figure 6. From this analysis, the High Luminosity LHC should be able to discover a gluino of mass up to 1.6 TeV.

3.3. High-Multiplicity Resonances Simplified Models. Spectra just slightly richer than those considered above usually give rise to several jets in the final state of the RPV supersymmetric event. A simple and motivated variation of the above models is the addition of a light neutralino in the simplified model. The stop simplified model, for which the search is so difficult at hadronic machines (see Figure 1), now decays via ordinary MSSM couplings into a neutralino, which in turn decays to three jets (see Table 4).

Table 4

BSM particles	Production	Decay
$\tilde{t}, \chi$	$pp \to \tilde{t}\tilde{t}^*$	$\tilde{t} \to t\chi, \chi \to jjj$

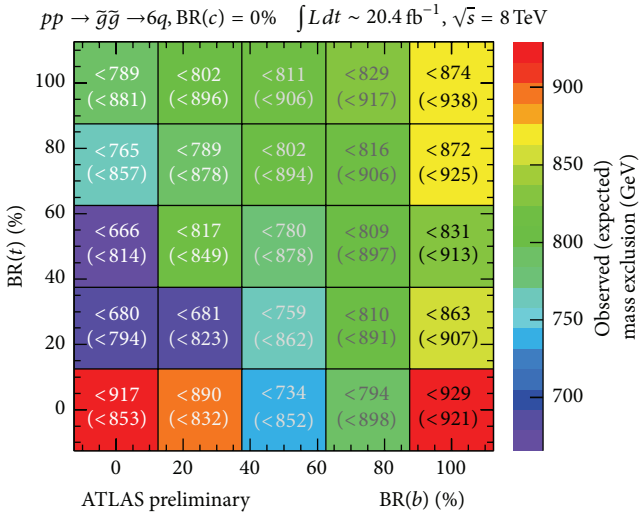

Figure 5: Highest mass excluded at 95% CL in the search for heavy flavor three-body decay of gluino in RPV supersymmetry [11]. Vertical and horizontal axes indicate the branching fraction into b and t quarks and the colored boxes indicate the corresponding highest excluded mass, as indicated by the color coded legend as well.

Considering this high-multiplicity final state, the discovery reach is much improved. We report in Figure 7 the estimated discovery and exclusion reach at the High Luminosity LHC for this simplified model. Masses up to 1.5 TeV will be excluded by the High Luminosity LHC and discovery up to 1 TeV will be possible.

Considering in full generality the possible signals that arise in RPV simplified model one is immediately led to consider a large number of possible final states. Some example of spectra that gives rise to large multiplicity is shown in Figure 8. The spectra in the figure are particularly difficult to discover because of the heaviness of third generation squarks, which gives no top quark final states. Explicit searches have been conducted up 8-jet final state [48] at CMS and up to 7 jets at ATLAS [11]. For higher multiplicities, the typical search for nonperturbative phenomena such as black-hole formation [49] is able to capture signal from complex RPV spectra. The interpretation of these searches in terms of RPV simplified models has been studied in [14]. The result of this recast of ATLAS [11] and CMS [49] analyses gives exclusions of gluino masses up to 1 TeV.

In [6], the reach for these more complex simplified models for pp colliders up to 33 TeV has been explored. The summary of these studies is reported in Table 5.

For these more general final states, it becomes harder to have reliable predictions for many jets backgrounds. Furthermore when a light supersymmetric particle decays into many partons it might be hard to resolve each single parton into a jet. When jets are lost, it also becomes harder to reconstruct resonances as some momentum is not measured. Additionally, if one insists on getting a large number of jets from light particles, then search for a signal in a scarcely populated region of its own phase-space might be needed, that is, in a tail of the signals kinematic distributions. In this case, it is usually harder to have a reliable theoretical prediction of the cross section of the signal in this particular region of phase-space. To overcome these difficulties, the use of jet-substructure techniques has been considered to try to reconstruct resonances in a large radius jet [50–52]. ATLAS has applied this type of ideas to the search of gluinos decaying into three jets $\tilde{g} \to jjj$ and has probed mass as low as 100 GeV both with a "skinny" jet analysis and with a "fat" jet analysis. The results are reported in Figure 9. At the 7 TeV LHC, the performance of the boosted strategy is comparable to the traditional search for low gluino mass. However, this search serves as a first step to validate the fat jet technique, which is expected to become more and more relevant as machines of higher energy become available.

3.4. Displaced RPV Supersymmetry. The RPV couplings are often bounded to be very small to avoid limits on proton decay, neutron-antineutron oscillations, and other limits [21]. For this reason, it is expected that these couplings must be so small that they can result in metastable particles whose decay length can be observed in the detectors, which is usually possible for average decay paths in the range from 0.01 cm to 10 m.

A variety of signals can arise in this scenario [53]. Most of them would easily escape standard searches for new physics, which focus on prompt production and decay of the new particles.

Among the many possible signals explicit bounds from the experiments exist for the squark-neutralino simplified model and for the squark LSP simplified model. In some scenarios, recast bounds [19] are available as well; however, most of them rely on delicate secondary vertex reconstruction, whose efficiency is nontrivial to carry from one model to another. Nevertheless, these recasts fill an important gap in the current searches. Therefore, they are an important element for the current status of searches for displaced signals from RPV supersymmetry.

3.4.1. The Displaced RPV Squark-Neutralino Simplified Model. In the squark-neutralino simplified model, squarks are produced and then decay to a neutralino, whose decay is displaced, and give rise to jets or leptons, or both, depending on the RPV couplings that are assumed (see Table 6).

At present, only bounds for LQD [16, 17] and LLE [18] R-parity violating interactions are given in this simplified model. The bounds are reported in Figure 10 and they usually rule out squarks below about 1 TeV for a large range of detector-size displaced vertexes.

3.4.2. The Displaced RPV Neutralino Simplified Model. This simplified model is obtained from the previous squark-neutralino simplified model when squarks are decoupled (see Table 7).

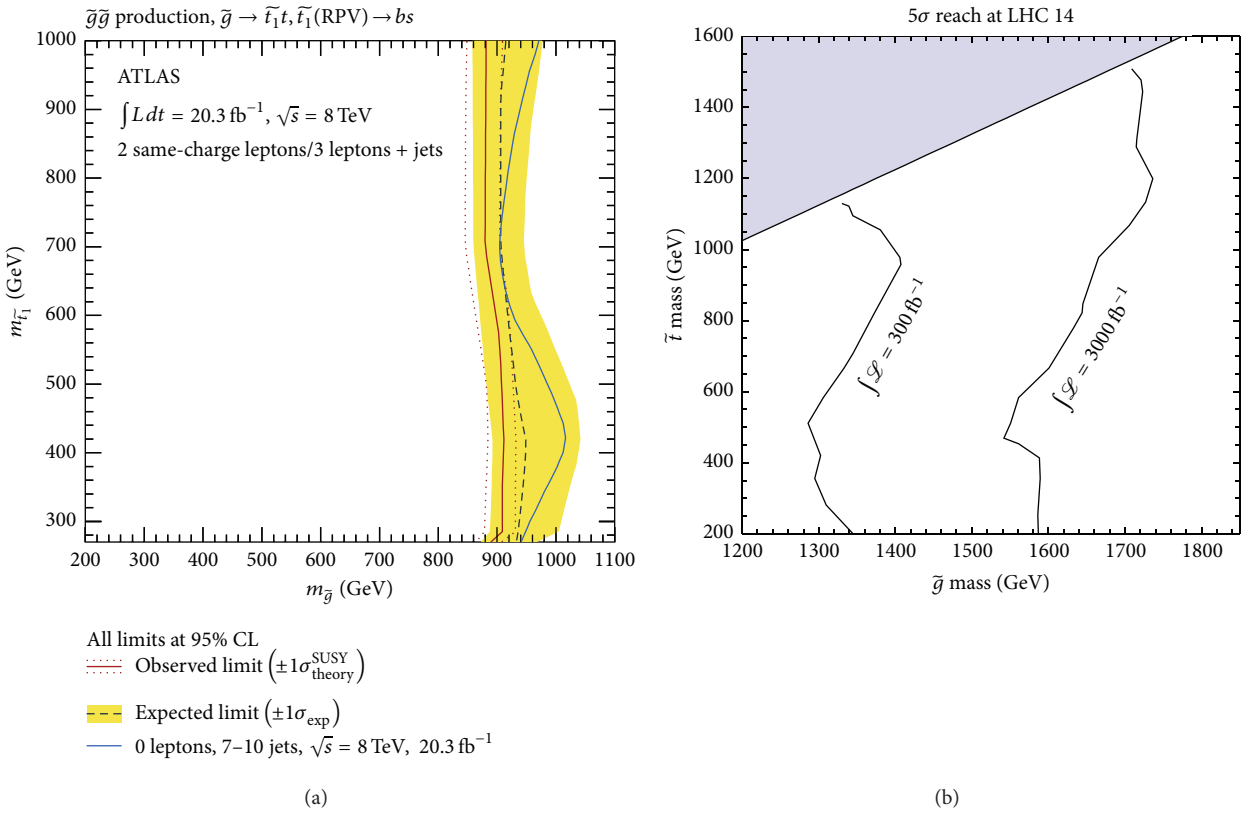

FIGURE 6: Exclusion from the LHC 8 TeV run (a) [12] and expected discovery reach (b) [13] for the RPV gluino simplified model decaying into heavy flavors in the same-sign dilepton channel. Points at the left of the solid lines are excluded under the assumption indicated by the respective labels.

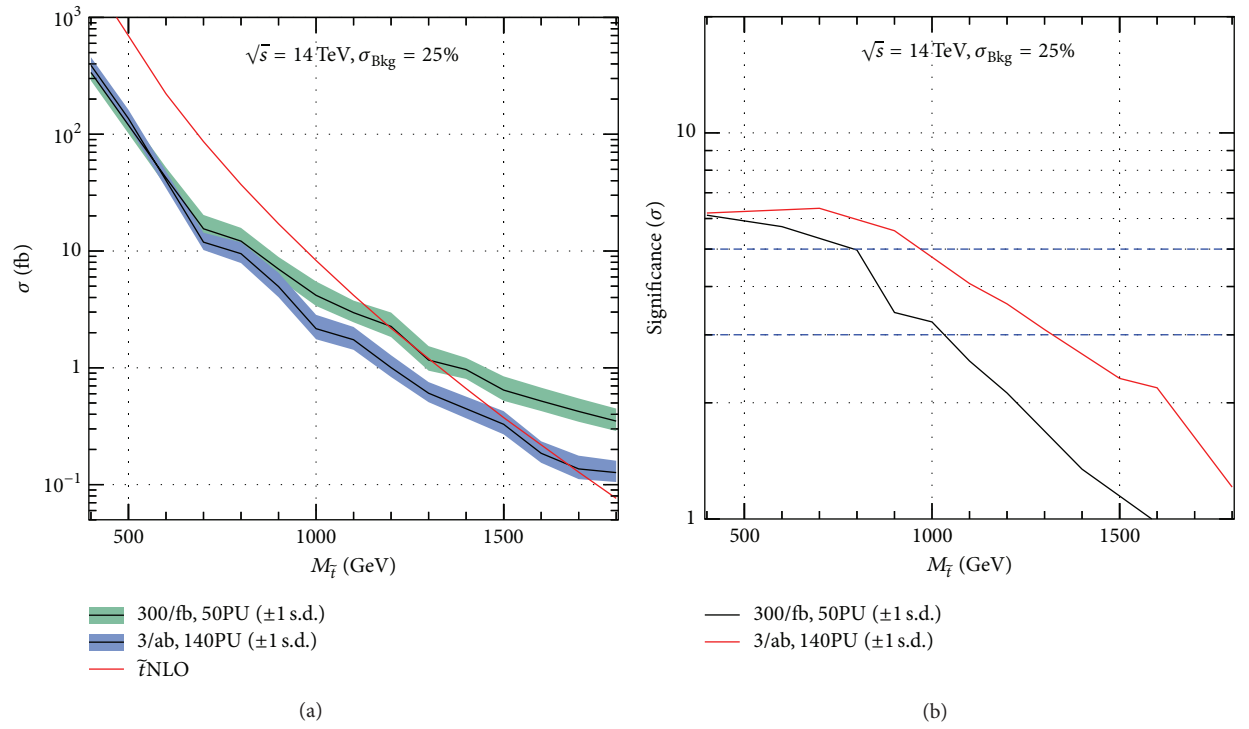

FIGURE 7: Exclusion (a) and discovery reach (b) for the High Luminosity LHC for the $\tilde{t}$-χ RPV simplified model [6]. In the two panels, the two curves correspond to different hypothesis for integrated luminosity and average number of Pile Up (PU) collisions.

Table 5: The exclusion reach of several RPV SUSY simplified models beyond those discussed in the main text [6].

Coupling	Production	Final states	Search	300 fb^{-1}	3 ab^{-1}	33 TeV
LLE122	$\widetilde{g}/\widetilde{q} \to \widetilde{B}$	$jj + \ell^+\ell^-\mu^+\mu^- + \not{E}_T$	Multi-ℓ	3550	4000	8500
	$\widetilde{W}$	$\ell^+\ell^-\mu^+\mu^- + \not{E}_T$	Multi-ℓ	1800	2300	4400
LLE233	$\widetilde{t} \to \widetilde{H}$	$b\bar{b}\tau^+\tau^-\ell^+\ell^- + \not{E}_T$	Multi-ℓ	1650	1950	3750
	$\widetilde{H}$	$\tau^+\tau^-\ell^+\ell^- + \not{E}_T$	Multi-ℓ	950	1300	2900
LQD232	$\widetilde{g} \to \widetilde{t}$	$t\bar{t}\{\mu^+ j\}\{\mu^- j\}$	Multi-ℓ	2500	2800	6300
LQD333	$\widetilde{t}$	$\{\tau^+ b\}\{\tau^- b\}$	3G LQ	1300	1650	—
UDD212	$\widetilde{t} \to \widetilde{B}$	$t\bar{t}\{jjj\}\{jjj\}$	$\ell + n$ jets	1200	1650	—
UDD312	$\widetilde{t}$	$\{jj\}\{jj\}$	Dijet pairs	750	1070	—
LH3	$\widetilde{H}$	$W^+W^-\tau^+\tau^-$	Multi-ℓ	530	610	2800

Table 6

BSM particles	Production	Decay
$\widetilde{q}, \chi$	$pp \to \widetilde{q}\widetilde{q}$	$\widetilde{q} \xrightarrow[\text{prompt}]{} q\chi, \chi \xrightarrow[\text{displaced}]{\text{LQd}^c} \ell jj,$ $\chi \xrightarrow[\text{displaced}]{\text{LLe}^c} \ell\ell\nu, \chi \xrightarrow[\text{displaced}]{u^c d^c d^c} jjj$

Table 7

BSM particles	Production	Decay
χ	$pp \to \chi\chi$	$\chi \xrightarrow[\text{displaced}]{\text{LQd}^c} \ell jj, \chi \xrightarrow[\text{displaced}]{\text{LLe}^c} \ell\ell\nu, \chi \xrightarrow[\text{displaced}]{u^c d^c d^c} jjj$

In this simplified model, there is only pure electroweak production of χ, which gives rise to essentially the same displaced objects as in the case of Section 3.4.1 above. However, the cross sections are usually very small, which prevents obtaining any useful bound.

Despite these difficulties, it has been shown that the analysis [16] might have a sensitivity to this simplified model. The analysis of [16] searches for a pair of jets coming from a common displaced vertex. This signature might be relevant for LQd^c and $u^c d^c d^c$ mediated decays of the neutralino. However an interpretation of the cross section limits on these scenarios is not provided. In Figure 11, we report a recast of [16] done in [19] for models that have a long-lived particle that decays into three partons. The recast crucially depends on an accurate reproduction of the vertexing performances of CMS; therefore an interpretation from the CMS experiment would still be the preferred way to put limits on these scenarios. Nevertheless, the message from [19] is clear, and bounds up to almost 800 GeV for Higgsinos are expected when they give rise to a displaced jet pair. Strikingly, these bounds might be the only bounds from the LHC on RPV Higgsino LSP scenario.

It should be remarked that this search for displaced jets is also sensitive to displaced decays of gluinos, which, despite hadronizing before decaying, should give rise to jets that are very similar to the ones from the electroweak neutralino considered here. Limits for the gluino scenario are reported in Figure 11. The figure also reports recast limits from [19] for large lifetimes, of the order 0.1/m, where the displaced jets search is replaced by a search for Heavy Charged Stable Particles [54, 55], which would be the R-hadron that forms from the long-lived gluinos.

In case of pure electroweak production, the very clean LLe^c decay into leptons might give a signal in the analysis for displaced same-flavor lepton pairs [18], but at present there is no such interpretation.

Table 8

BSM particles	Production	Decay
$\widetilde{t}$	$pp \to \widetilde{t}\widetilde{t}^*$	$\widetilde{t} \xrightarrow[\text{displaced}]{\text{LQd}^c} b\ell, \widetilde{t} \xrightarrow[\text{displaced}]{u^c d^c d^c} jj$

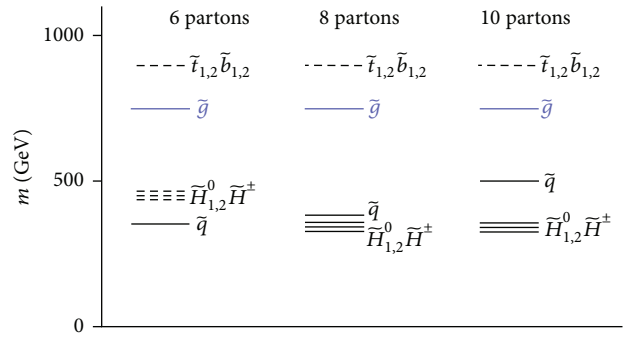

Figure 8: Possible RPV spectra that give rise to large jet multiplicity signals with little or no mET, leptons, or photons [14].

3.4.3. The Displaced RPV Squark Simplified Model. For this simplified model, it is assumed that only squarks are light enough to be produced (see Table 8).

A search by CMS [20] has used this model to put bounds on final states where two different flavors leptons from LQd^c interaction emerge both with large impact parameter. The results are given in Figure 12 and bounds up to about 800 GeV for one stop squark are obtained.

The selection of the analysis [20] is very inclusive, as it targets a final state $e\mu + X$ and no special requirements are imposed on X. For this reason, one could expect that significant bounds can be extracted for light flavor squarks instead of stops decaying to b quarks, $pp \to \widetilde{q}\widetilde{q} \to q\mu qe$, and for more complex signatures such as those from the displaced neutralino studied in previous Sections 3.4.1 and 3.4.2.

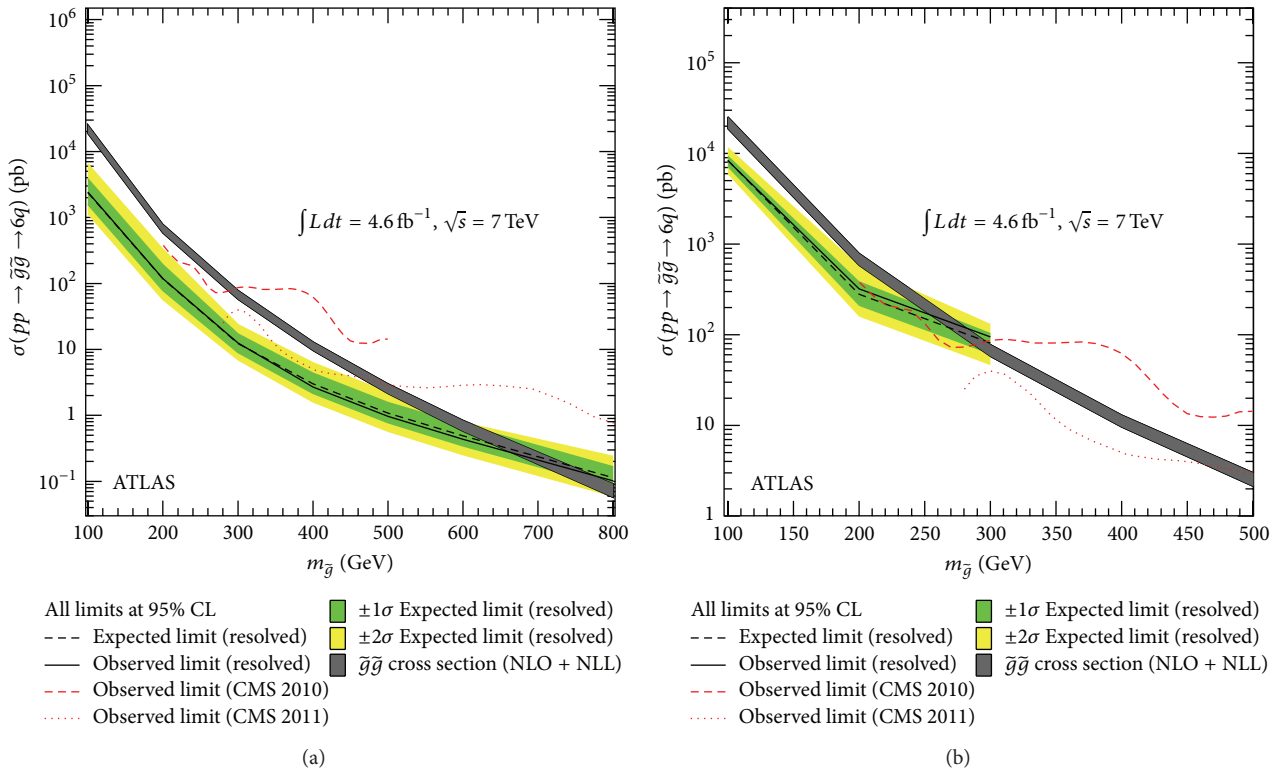

Figure 9: Exclusion of a search in multijet final state (a) and a boosted resonance search with fat jets (b) on the same 7 TeV data set of ATLAS [15]. Color codes as in Figure 1.

For hadronic final states that emerge from squark decay mediated by the $u^c d^c d^c$ interaction, there is no explicit interpretation from the experiments searching for displaced jets; however, as in the cases discussed above, bounds are expected from a displaced jet search such as [16]. The recast of this search proposed by [19] is shown in Figure 13 (together with a typical event display of two largely displaced jets). The results of the recast show clear potential of exclusion for masses up to 1 TeV.

When the RPV couplings are small enough, the squarks will decay only after they have formed hadrons. If the squark is sufficiently long-lived it is best to search for the hadrons produced in its hadronization. In fact, among the hadrons formed, one should be very massive compared to ordinary hadrons and might also be electrically charged. The search for massive stable charged particles has been carried out at the LHC [54, 55] and these limits have also been recast [19] for the scenario of R-hadrons from squark hadronization. The result of this recast is shown in Figure 13, which suggests that squark masses up to 900 GeV should be ruled out by this type of searches.

4. Conclusions

After the first run of the LHC, the most striking signatures of TeV-scale supersymmetric particles have not been observed. The bounds on colored superparticles are particularly stringent and start to seriously challenge the paradigm of minimal models of supersymmetry at the weak scale.

Several mechanisms to avoid LHC bounds have been identified as a reaction to the results of the first run of the experiments. Among the possible ideas to alleviate this tension between supersymmetry and experiments, the possibility of a violation of R-parity emerges as a conceptually very simple and motivated option. Furthermore in recent times a new wave of works on the origin of R-parity breaking couplings [31, 32, 56] has provided new ways to formulate predictive and realistic supersymmetric model without R-parity.

In addition to the results coming from the direct exploration of the TeV scale at particle colliders, the results from Dark Matter searches are also shedding new light on the conservation of R-parity in supersymmetric models. In fact direct searches for weakly interacting massive particles have already excluded large portions of the parameter space of the minimal models with conserved R-parity. This motivates alternative scenarios for Dark Matter, which could easily fit in R-parity violating models, where light and very weakly interacting particles naturally emerge as Dark Matter candidates.

The new directions suggested by the results of the LHC experiments and Dark Matter searches both make supersymmetric models with broken R-parity a very motivated scenario for new physics at the TeV scale.

On top of these motivations from experimental and theoretical considerations, it is remarkable that the breaking of R-parity significantly enlarges the set of experimental signatures of new physics. Therefore one can add a more pragmatic motivation to study R-parity violating models as "signatures

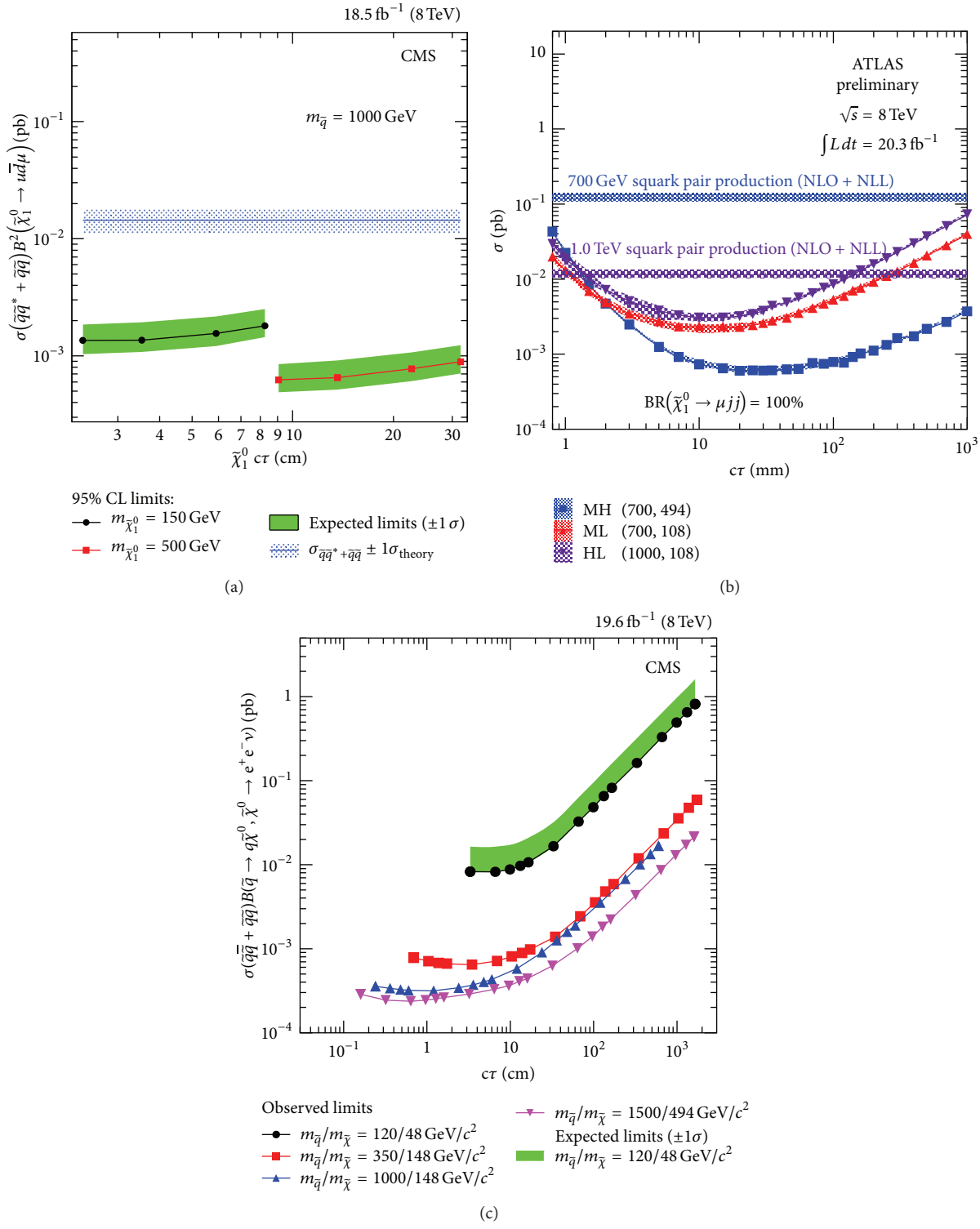

FIGURE 10: Limits on displaced RPV supersymmetry for LQD coupling from displaced jets [16] (a), displaced muon + tracks events [17] (b), and for LLE coupling from displaced same-flavor dileptons [18] (c). In all panels, each colored line represents an example of new physics spectrum for which the cross section indicated in the vertical axis is excluded at 95% Confidence Level under the assumption of the lifetime indicated in the corresponding horizontal axis. The horizontal lines are predictions for the total production cross section in new physics scenarios for new physics particles masses as labeled on each panel.

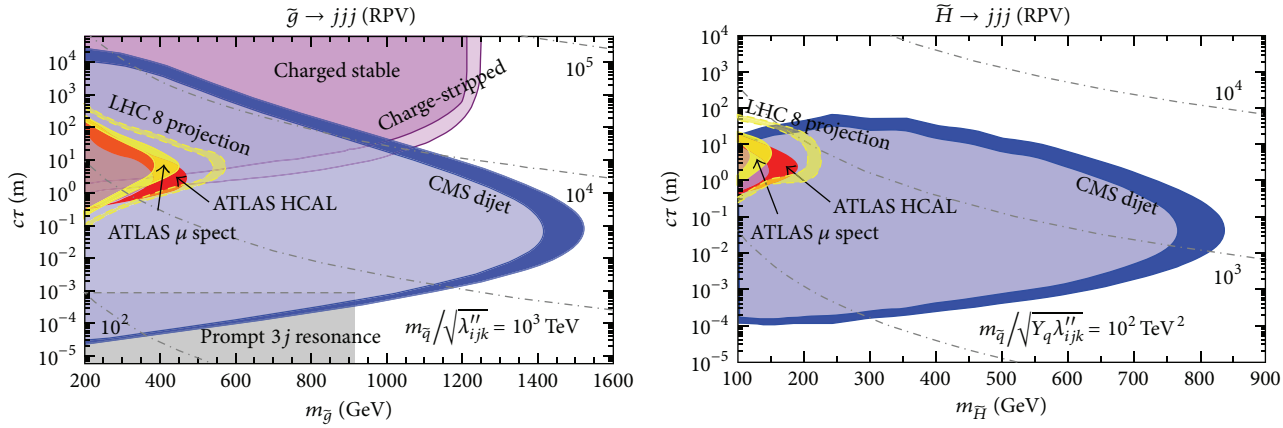

FIGURE 11: Limits on baryonic RPV from displaced jets searches [16] recast in [19]. For each type of search, a colored area indicated the excluded region in the plane lifetime-mass of the metastable new state. The gray area corresponds to the exclusion from searches for prompt (i.e., nondisplaced) new physics, which is substantially weaker than what can be achieved by most displaced searches. For each color, the darker band represents the uncertainty on the excluded area that comes from varying the reconstruction efficiency for displaced objects.

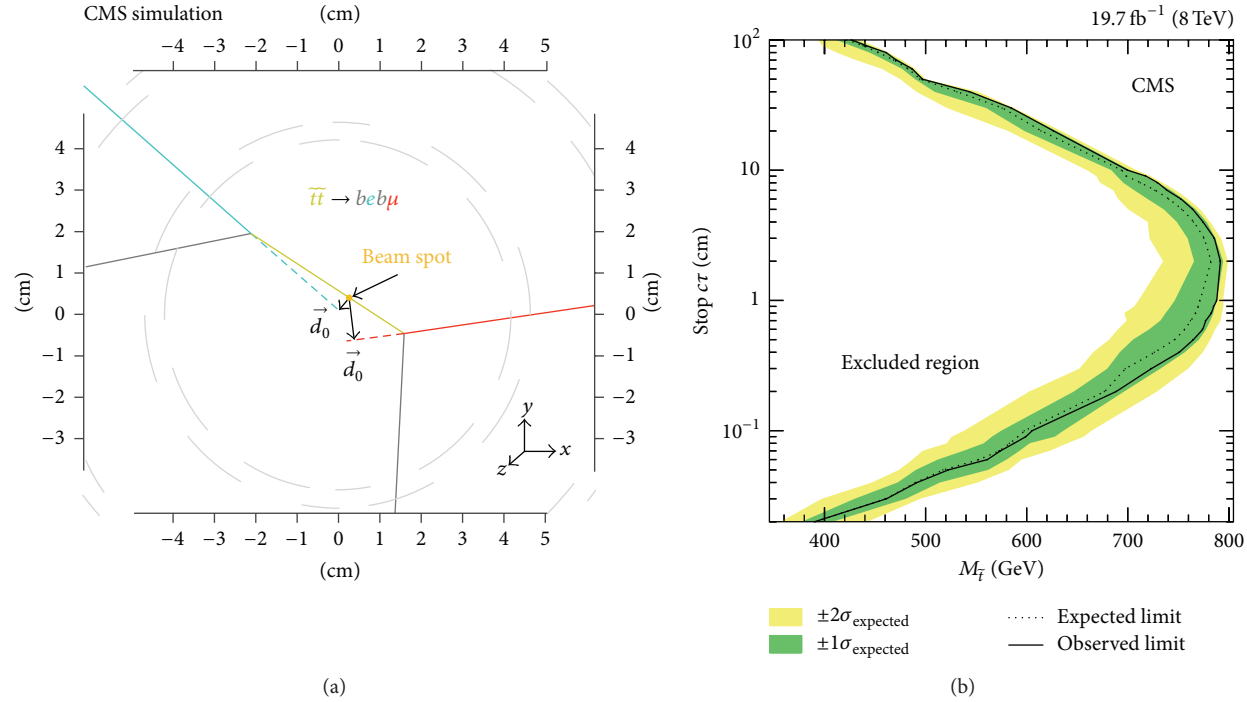

FIGURE 12: Limits on displaced RPV supersymmetry for stops decaying with equal rates into the three leptonic flavors [20]. On panel (a), a sample schematic event display is shown. The panel (b) gives the exclusion in the stop lifetime-mass plane. Points to the left of the solid black curve are excluded. Color codes as in Figure 1.

generators," whose investigation further widens the scope of the search for new physics at the LHC.

In this work, we have presented the large body of results available on the searches for new physics that has been interpreted (or can be relevant) for R-parity violating scenarios. In this large set of results, two examples of the extended coverage for signals of new physics that has been brought to the attention of the experiments by the study of R-parity violating models are multijet resonant signatures and displaced signatures. The latter are a rather interesting example. In fact, the presence of displaced objects (tracks, leptons, jets, etc.) in an event is difficult to deal with at the experimental level. Nevertheless, the experimental difficulties have been overcome and these signatures in many cases provide the most stringent mass bounds on the existence of certain types of new particles. In other cases, such as new particles that decay promptly to many jets, large improvement has been obtained thanks to the input from the phenomenology of R-parity violating models. For instance, the presence of heavy flavor tags has gained importance in resonant multijet

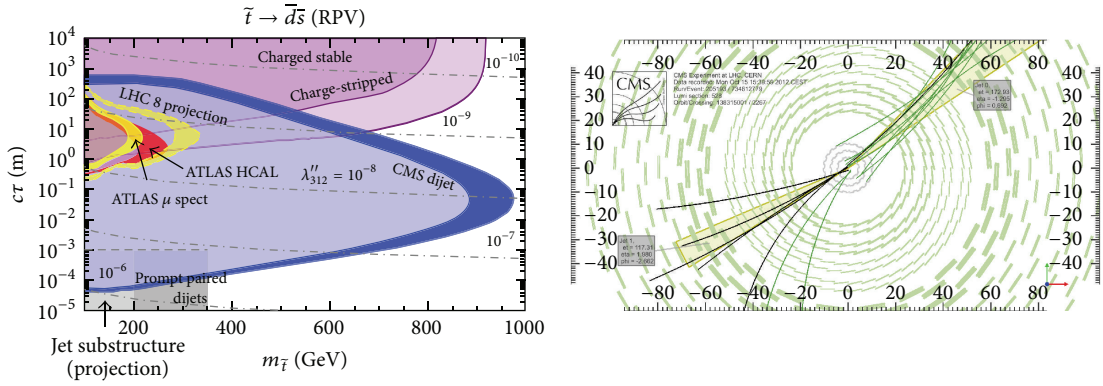

(a) (b)

Figure 13: Results on limits on displaced jets searches [16] recast for baryonic RPV decays of squarks [19] (a). An event display [16] of the tracks that make a jet pair event from a displaced vertex (b). The yellow cones are the two jets making the pair and the black tracks are those fitting to a secondary vertex displaced by 5 cm. Same notation as in Figure 11.

searches. Furthermore, the study of these signals has been useful because it has shown the difficulties that LHC experiments encounter when searching for such signals, thus calling for the development of new strategies to search for new physics.

The large amount of possible hierarchies of RPV couplings and the several motivated spectra of the new particles produce a large set of possible signals, some of which is yet to be captured by the analyses of the LHC experiments, which leaves more work to be done in the future both in including new signatures in LHC searches and in developing more refined ways to highlight new physics signals from the data.

Conflict of Interests

The author declares that there is no conflict of interests regarding the publication of this paper.

Acknowledgments

It is a pleasure to thank Freya Blekman, Dinko Ferenček, Giacomo Polesello, Andrea Romanino, Prashant Saraswat, and Brock Tweedie for stimulating discussions and many inputs on these topics. The author also would like to thank Gabriele Ferretti, Rabindra Mohapatra, Christoffer Petersson, and Riccardo Torre for many discussions and the collaboration for the papers that the author has coauthored. The author would like to thank Andrea Thamm for very useful comments on the paper.

References

[1] B. Nachman and T. Rudelius, "Evidence for conservatism in LHC SUSY searches," *The European Physical Journal Plus*, vol. 127, article 157, 2012.

[2] CMS Collaboration, "SUSY searches summary plots," https://twiki.cern.ch/twiki/bin/view/CMSPublic/PhysicsResultsSUS.

[3] W. Pauli, "Open letter to the group of radioactive people at the Gauverein meeting in Tübingen," http://microboone-docdb.fnal.gov/cgi-bin/RetrieveFile?docid=953;filename=pauli%20letter1930.pdf;version=1.

[4] T. Aaltonen, E. Albin, S. Amerio et al., "Search for pair production of strongly interacting particles decaying to pairs of jets in $p\bar{p}$ collisions at $\sqrt{s} = 1.96$ TeV," *Physical Review Letters*, vol. 111, Article ID 031802, 2013.

[5] CMS Collaboration, "Search for pair-produced resonances decaying to jet pairs in proton-proton collisions at $\sqrt{s} = 8$ TeV," *Physics Letters B*, vol. 747, pp. 98–119, 2015.

[6] D. Duggan, J. A. Evans, J. Hirschauer et al., "Sensitivity of an upgraded LHC to R-parity violating signatures of the MSSM," http://arxiv.org/abs/1308.3903.

[7] T. Aaltonen, B. A. González, S. Amerio et al., "First search for multijet resonances in $\sqrt{s} = 1.96$ TeV $p\bar{p}$ collisions," *Physical Review Letters*, vol. 107, no. 4, Article ID 042001, 2011.

[8] S. Chatrchyan, V. Khachatryan, A. M. Sirunyan et al., "Search for three-jet resonances in pp collisions at $\sqrt{s} = 7$ TeV," *Physical Review Letters*, vol. 107, no. 10, Article ID 101801, 15 pages, 2011.

[9] CMS Collaboration, "Search for three-jet resonances in pp collisions at $\sqrt{s} = 7$ TeV," *Physics Letters B*, vol. 718, pp. 329–347, 2012.

[10] CERN, "Search for light- and heavy-flavor three-jet resonances in multijet final states at 8 tev," Tech. Rep. CMS-PAS-EXO-12-049, CERN, Geneva, Switzerland, 2013, https://twiki.cern.ch/twiki/bin/view/CMSPublic/PhysicsResultsEXO12049.

[11] ATLAS Collaboration, "Search for massive particles in multijet signatures with the ATLAS detector in $\sqrt{s} = 8$ TeV pp collisions at the LHC," Tech. Rep. ATLAS-CONF-2013-091, CERN, Geneva, Switzerland, 2013, https://atlas.web.cern.ch/Atlas/GROUPS/PHYSICS/CONFNOTES/ATLAS-CONF-2013-091/.

[12] ATLAS Collaboration, "Search for supersymmetry at $N\sqrt{s} = 8$ TeV in final states with jets and two same-sign leptons or three leptons with the ATLAS detector," *Journal of High Energy Physics*, vol. 2014, article 35, 2014.

[13] M. Saelim and M. Perelstein, "RPV SUSY with same-sign dileptons at LHC-14," http://arxiv.org/abs/1309.7707.

[14] J. A. Evans, Y. Kats, D. Shih, and M. J. Strassler, "Toward full LHC coverage of natural supersymmetry," *Journal of High Energy Physics*, vol. 2014, no. 7, article 101, 2014.

[15] ATLAS Collaboration, "Search for pair production of massive particles decaying into three quarks with the ATLAS detector in $\sqrt{s} = 7$ TeV pp collisions at the LHC," *Journal of High Energy Physics*, vol. 2012, no. 12, article 86, 2012.

[16] CMS Collaboration, "Search for long-lived neutral particles decaying to quark-antiquark pairs in proton-proton collisions at $\sqrt{s} = 8$ TeV," *Physical Review D*, vol. 91, no. 1, Article ID 012007, 21 pages, 2014.

[17] CERN, "Search for long-lived, heavy particles in final states with a muon and a multi-track displaced vertex in proton-proton collisions at $\sqrt{s} = 8$ TeV with the ATLAS detector," Tech. Rep. ATLAS-CONF-2013-092, CERN, Geneva, Switzerland, 2013, https://atlas.web.cern.ch/Atlas/GROUPS/PHYSICS/CONFNOTES/ATLAS-CONF-2013-092/.

[18] V. Khachatryan, A. M. Sirunyan, A. Tumasyan et al., "Search for long-lived particles that decay into final states containing two electrons or two muons in proton-proton collisions at $\sqrt{s} = 8$ TeV," *Physical Review D*, vol. 91, Article ID 052012, 2015.

[19] Z. Liu and B. Tweedie, "The fate of long-lived superparticles with hadronic decays after LHC Run 1," *Journal of High Energy Physics*, vol. 2015, article 42, 2015.

[20] V. Khachatryan, A. M. Sirunyan, A. Tumasyan et al., "Search for displaced supersymmetry in events with an electron and a muon with large impact parameters," *Physical Review Letters*, vol. 114, Article ID 061801, 2014.

[21] R. Barbier, C. Bérat, M. Besançon et al., "R-Parity-violating supersymmetry," *Physics Reports*, vol. 420, no. 1–6, pp. 1–195, 2005.

[22] W. Buchmüller, L. Covi, K. Hamaguchi, A. Ibarra, and T. T. Yanagida, "Gravitino dark matter in R-parity breaking vacua," *Journal of High Energy Physics*, vol. 3, article 37, 2007.

[23] F. Takayama and M. Yamaguchi, "Gravitino dark matter without R-parity," *Physics Letters B*, vol. 485, no. 4, pp. 388–392, 2000.

[24] F. D. Steffen, "Gravitino dark matter and cosmological constraints," *Journal of Cosmology and Astroparticle Physics*, vol. 2006, no. 9, article 001, 2006.

[25] R. Franceschini and R. N. Mohapatra, "New patterns of natural R-parity violation with supersymmetric gauged flavor," *Journal of High Energy Physics*, vol. 2013, no. 4, article 98, 2013.

[26] C. Csáki, Y. Grossman, and B. Heidenreich, "Minimal flavor violation supersymmetry: a natural theory for R-parity violation," *Physical Review D*, vol. 85, no. 9, Article ID 095009, 2012.

[27] J. Fan, M. Reece, and J. T. Ruderman, "A stealth supersymmetry sampler," *Journal of High Energy Physics*, vol. 2012, no. 7, article 196, 2012.

[28] P. Graham, S. Rajendran, and P. Saraswat, "Supersymmetric crevices: missing signatures of R-parity violation at the LHC," *Physical Review D*, vol. 90, Article ID 075005, 2014.

[29] ATLAS Collaboration, "Search for pair-produced massive coloured scalars in four-jet final states with the ATLAS detector in proton-proton collisions at $\sqrt{s} = 7$ TeV," *The European Physical Journal C*, vol. 73, article 2263, 2013.

[30] Y. Bai, A. Katz, and B. Tweedie, "Pulling out all the stops: searching for RPV SUSY with stop-jets," *Journal of High Energy Physics*, vol. 2014, no. 1, article 040, 2014.

[31] C. Smith, "Minimal flavor violation as an alternative to R-parity," in *Proceedings of the 34th International Conference on High Energy Physics (ICHEP '08)*, Philadelphia, Pa, USA, 2008.

[32] C. Csaki, Y. Grossman, and B. Heidenreich, "MFV SUSY: a natural theory for R-parity violation," *Physical Review D*, vol. 85, no. 9, Article ID 095009, 22 pages, 2012.

[33] G. Krnjaic and D. Stolarski, "Gauging the way to MFV," *Journal of High Energy Physics*, vol. 2013, article 64, 2013.

[34] C. Csáki and B. Heidenreich, "A complete model for R-parity violation," *Physical Review D*, vol. 88, Article ID 055023, 2013.

[35] R. Franceschini and R. Torre, "RPV stops bump off the background," *The European Physical Journal C*, vol. 73, article 2422, 2013.

[36] I. Hinchliffe, F. E. Paige, M. D. Shapiro, J. Söderqvist, and W. Yao, "Precision SUSY measurements at CERN LHC," *Physical Review D*, vol. 55, pp. 5520–5540, 1997.

[37] B. C. Allanach, C. Gorham Lester, M. A. Parker, and B. R. Webber, "Measuring sparticle masses in non-universal string inspired models at the LHC," *Journal of High Energy Physics*, vol. 2000, no. 9, article 004, 2000.

[38] K. Kawagoe, M. M. Nojiri, and G. Polesello, "New supersymmetry mass reconstruction method at the CERN LHC," *Physical Review D—Particles, Fields, Gravitation and Cosmology*, vol. 71, no. 3, Article ID 35008, 2005.

[39] F. W. Stecker, "Cosmic gamma rays," NASA Special Publication 249, 1971.

[40] K. Agashe, R. Franceschini, and D. Kim, "Simple 'invariance' of two-body decay kinematics," *Physical Review D*, vol. 88, no. 5, Article ID 057701, 2013.

[41] J. Eckel, W. Shepherd, and S. Su, "Slepton discovery in electroweak cascade decay," *Journal of High Energy Physics*, vol. 2012, no. 5, article 81, 2012.

[42] I. Low, "Polarized charginos (and tops) in stop decays," *Physical Review D*, vol. 88, Article ID 095018, 2013.

[43] ATLAS Collaboration, "Search for a heavy narrow resonance decaying to $e\mu$, $e\tau$, or $\mu\tau$ with the ATLAS detector in View the MathML sourcepp collisions at the LHC," *Physics Letters B*, vol. 723, no. 1–3, pp. 15–32, 2013.

[44] G. Aad, B. Abbott, J. Abdallah et al., "Search for supersymmetry in events with four or more leptons in $\sqrt{s} = 8$ TeV pp collisions with the ATLAS detector," *Physical Review D*, vol. 90, Article ID 052001, 2014.

[45] ATLAS Collaboration, "Search for massive colored scalars in four-jet final states in $\sqrt{s} = 7$ TeV proton-proton collisions with the ATLAS detector," *The European Physical Journal C*, vol. 71, article 1828, 2011.

[46] ATLAS Collaboration, "Search for new phenomena in final states with large jet multiplicities and missing transverse momentum at $\sqrt{s} = 8$ TeV proton-proton collisions using the ATLAS experiment," *Journal of High Energy Physics*, vol. 2013, no. 10, article 130, 2013.

[47] H. Baer, C.-H. Chen, and X. Tata, "Impact of hadronic decays of the lightest neutralino on the reach of the CERN LHC," *Physical Review D—Particles, Fields, Gravitation and Cosmology*, vol. 55, no. 3, pp. 1466–1470, 1997.

[48] CMS Collaboration, "Search for multijet resonances in the 8-jet final state," Tech. Rep. CMS-PAS-EXO-11-075, 2012, http://cds.cern.ch/record/1482131?ln=en.

[49] S. Chatrchyan, V. Khachatryan, A. M. Sirunyan et al., "Search for microscopic black holes in pp collisions at $\sqrt{s} = 8$ TeV," *Journal of High Energy Physics*, vol. 2013, no. 7, article 178, 2013.

[50] T. Cohen, E. Izaguirre, M. Lisanti, and H. K. Lou, "Jet substructure by accident," *Journal of High Energy Physics*, vol. 2013, article 161, 2013.

[51] T. Cohen, M. Jankowiak, M. Lisanti, H. K. Lou, and J. G. Wacker, "Jet substructure templates: data-driven QCD backgrounds for fat jet searches," *Journal of High Energy Physics*, vol. 2014, no. 5, article 005, 2014.

[52] S. El Hedri, A. Hook, M. Jankowiak, and J. G. Wacker, "Learning how to count: a high multiplicity search for the LHC," *Journal of High Energy Physics*, vol. 2013, no. 8, article 136, 2013.

[53] P. W. Graham, D. E. Kaplan, S. Rajendran, and P. Saraswat, "Displaced supersymmetry," *Journal of High Energy Physics*, vol. 2012, no. 7, article 149, 2012.

[54] CMS Collaboration, "Searches for long-lived charged particles in pp collisions at $\sqrt{s} = 7$ and 8 TeV,," *Journal of High Energy Physics*, vol. 2013, article 122, 2013.

[55] G. Aad, B. Abbott, J. Abdallah et al., "Searches for heavy long-lived charged particles with the ATLAS detector in proton-proton collisions at $\sqrt{s} = 8$ TeV," *Journal of High Energy Physics*, vol. 2015, no. 1, article 068, 2015.

[56] C. Csáki, E. Kuflik, and T. Volansky, "Dynamical R-parity violation," *Physical Review Letters*, vol. 112, no. 13, Article ID 131801, 2014.

Hindawi Publishing Corporation
Advances in High Energy Physics
Volume 2015, Article ID 412487, 9 pages
http://dx.doi.org/10.1155/2015/412487

Research Article

Phenomenological Hints from a Class of String Motivated Model Constructions

Hans Peter Nilles

Bethe Center for Theoretical Physics and Physikalisches Institut der Universität Bonn, Nussallee 12, 53115 Bonn, Germany

Correspondence should be addressed to Hans Peter Nilles; nilles@th.physik.uni-bonn.de

Received 23 April 2015; Accepted 28 July 2015

Academic Editor: Michal Malinský

We use string theory constructions towards the generalisation of the supersymmetric standard model of strong and electroweak interactions. Properties of the models depend crucially on the location of fields in extradimensional compact space. This allows us to extract some generic lessons for the phenomenological properties of the low energy effective action. Within this scheme we present a compelling model based on local grand unification and mirage mediation of supersymmetry breakdown. We analyse the properties of the specific model towards its possible tests at the LHC and the complementarity to direct dark matter searches.

1. Introduction

There are many arguments for physics beyond the $SU(3) \times SU(2) \times U(1)$ standard model (SM) of strong and electroweak interaction. Unfortunately we have not seen any sign of it yet. One could hope that in the near future particle physics experiments at the LHC as well as direct (or indirect) searches for dark matter (DM) might reveal signs of physics beyond the standard model (BSM). We have to rely on theoretical prejudice in the discussion of BSM phenomena. In this paper we want to discuss the possible phenomenology of string motivated models. This is a so-called top-down approach to obtain a unified description of all interactions including gravity. It starts with a universal scheme where many things can come together: supersymmetry, extra dimensions, axions, grand unification additional singlets, additional $U(1)$ gauge bosons, and maybe much more. This is in contrast to bottom-up approaches that start with a very specific idea (e.g., supersymmetry) and work out the consequences within a minimal scheme (e.g., the minimal supersymmetric standard model (MSSM)). In the top-down approach we are not necessarily driven to such minimal schemes; the structure could be much richer.

String theories require $D = 10$ (or $D = 11$) space-time dimensions and supersymmetry for consistency. The connection to our world in $D = 4$ requires the compactification of extra spatial dimensions and this leads to potentially many solutions: sometimes called the "String Landscape." While in $D = 10$ the picture is simple, this is no longer true in $D = 4$. This implies that many of the properties of the low energy effective action depend on details of the compactification scheme. This reduces the predictive power of string theory substantially. "String phenomenology" explores properties of the Landscape and tries to relate low energy phenomena with specific features of the fields in compactified extra dimensions. One looks for possibilities to incorporate particle physics models in a consistent way and tries to identify common properties of such models. A central aspect of string theory is supersymmetry. It is a necessity for the ultraviolet (UV) consistency of the theory. However, supersymmetry has to be partially broken in the process of compactification, but there remains the option of a $N = 1$ supersymmetry down to energies as low as a TeV. This is the assumption we make in the present work. It requires new BSM physics that might be detected experimentally within the near future.

The paper will be structured as follows. In the next section we will discuss the motivation to consider supersymmetric extensions of the standard model from both the bottom-up and the top-down perspective. In Section 3 we will then present string theory constructions and analyse possible lessons for SUSY model building. This will be followed by an analysis of the possible reach of experimental searches at

the LHC given present results of the first LHC run. We will then present a specific string-inspired scenario in Section 5 and analyse its properties and possible signals for LHC as well as dark matter. We will, in particular, discuss the complementarity of collider searches and direct dark matter detection. If dark matter has its origin in supersymmetric particles we might be able to obtain an upper limit on the lightest supersymmetric particle and this might give us important hints for LHC searches. Section 6 will be devoted to conclusions and outlook.

2. The Quest for Supersymmetry

Supersymmetry is a necessary ingredient for any consistent string theory. However, it has to be broken in the process of compactification and a priori we do not know the breakdown scale. In models of particle physics we are confronted with the appearance of mass scales which are widely separated, as, for example, the Planck scale of 10^{18} GeV and the weak scale in the TeV region. In usual quantum field theories these hierarchies of scales might be unstable because of the appearance of quantum corrections. In the standard model this concerns the stability of the mass of the fundamental scalar Higgs boson. A protection of the Higgs mass can be achieved within a supersymmetric scheme; the main motivation for supersymmetry [4, 5] is *the stability of the weak scale*: this mechanism requires new particles at the weak scale, partners of quarks, leptons, and gauge bosons that could be discovered at LHC. These new particles have influence on the evolution of the gauge coupling constants. Remarkably they lead to a situation that (within the MSSM) the gauge couplings of $SU(3)$, $SU(2)$, and $U(1)$ meet at the grand unification scale of order of a few times 10^{16} GeV; a second strong motivation for supersymmetry is *gauge coupling unification*: supersymmetric model requires special care with proton stability. A solution is the postulate of a new (discrete) symmetry, matter parity in the simplest case. Such a symmetry predicts the existence of a new stable particle and this is further motivation for SUSY as it provides *dark matter candidates* that seem to be required by astroparticle and cosmological observations. Good candidates are neutral, weakly interacting particles, known as WIMPs. They could be subject to detection at the LHC as well as dedicated dark matter search experiments.

A further attractive property of supersymmetry from the bottom-up approach is the fact that local (gauged) supersymmetry automatically includes gravitational interactions in the form of *supergravity = gauged supersymmetry*: from the top-down approach this is, of course, obvious as a cornerstone of the unification of all interactions in the framework of string theory. All these arguments make lower energy (TeV) scale supersymmetry a very attractive framework for physics beyond the standard model. In this paper we will therefore assume the presence of low energy supersymmetry.

3. String Model Building

To learn some lessons from string theory we need to proceed to explicit model building towards the MSSM and generalisations thereof. The properties of the low energy effective action depend strongly on the process of compactification. It is not enough to know the nature of the compact manifold but we also need to know the location of the various fields on this manifold. Some of the fields might reside in the full 6-dimensional manifold (called bulk fields) while others are localized on submanifolds (so-called brane fields). We thus need knowledge about the geography of fields in extra dimensions [6]. The localized fields might be subject to different amounts of symmetry both for gauge and supersymmetry. This leads to a scheme known as local grand unification that has enhanced grand unified gauge symmetry for certain brane fields.

While there have been many attempts to construct particle physics models from string theory [7, 8] only few of them are realistic and explicit enough to analyse the questions under consideration. We therefore will concentrate on a set of models based on the so-called MiniLandscape [9–12] and its generalisations [13–23]. These constructions are based on the heterotic $E_8 \times E_8$ string compactified on 6-dimensional orbifolds: the so-called heterotic braneworld [24]. The $SU(3) \times SU(2) \times U(1)$ gauge group of the standard model is a subgroup of one of the E_8 groups with a hidden intermediate $SO(10)$ local GUT structure to admit 16-dimensional spinor representations for the families of quarks and leptons (along the rules of [25]).

These models have the following space-time structure: bulk fields that live in the full 10 space-time dimensions (6 dimensions in compactified space), fixed tori (fields that live in 6-dimensional space-time, i.e., two dimensions in compact space), and fixed points in compact dimensions (fields live in 4-space-time dimensions). In heterotic string theory the gauge fields are bulk fields, while matter or Higgs fields can live either in the bulk, on fixed tori, or on fixed points. Localized fields can experience different amounts of gauge symmetry depending on which point or torus they are localized on (this is the concept of local grand unification (like $SO(10)$ enhancement at some of the fixed points [11])). The relative location of matter and Higgs fields is important for the properties of the low energy effective action as it determines size of couplings and mixings in the Yukawa sector.

With the large number of realistic MSSM and generalized MSSM candidates in the MiniLandscape we can now analyse the properties of the successful models. The models typically contain additional singlets and $U(1)$ gauge symmetries.

3.1. Lessons from the MiniLandscape. There are some amazing universal properties. The first one concerns the Higgs fields: they are bulk fields, and this seems to be a generic property of the successful models. This implies that the Higgs bosons descend from gauge fields in higher dimensions and thus exhibit so-called gauge-Higgs unification. In fact, it is in general nontrivial to keep a massless Higgs pair H, $\overline{H}$ in the low energy theory as this pair is vector-like and could become heavy through a μ-term, $\mu H\overline{H}$ in the superpotential. The MiniLandscape provides a solution to the μ-problem. The μ-term is forbidden by (approximate) discrete R-symmetry

[11, 26], and the supersymmetric vacua are of Minkowski type. This is reminiscent of an earlier suggestion of Casas and Muñoz [27]. A μ-term can be generated with broken supersymmetry and its size is therefore related to soft SUSY breaking parameters. The R-symmetry treats bosons and fermions differently. It descends from the Lorentz groups $SO(6)$ (subgroup of $SO(9,1)$) of compactified space. This is the reason why the light Higgs fields have to live in the bulk. These R-symmetries have to be studied in detail to understand the size of the μ-term also in relation to the gravitino mass [28, 29].

Let us now turn to quarks and leptons. The top-quark is special as it has a mass comparable to the gauge bosons and thus a Yukawa coupling of order of the gauge coupling: so-called gauge-top unification. In the models of the Mini-Landscape the top-quark has (in contrast to most of the other quarks and leptons) a nontrivial trilinear (tree level) coupling to the Higgs field. This gives us the second amazing property of the MiniLandscape. The top-quark is a bulk field as well! It is the large spatial overlap with the Higgs field that provides the large top-quark Yukawa coupling. The location of the other fields of the third family is rather model dependent. In most cases none of the additional fields has trilinear Yukawa couplings.

In contrast to the third family, the first two families live at fixed points. At these special points one typically has enhanced gauge and discrete symmetries. In the models discussed here we find a discrete D_4 family symmetry [11] (a discrete subgroup of an $SU(2)$ flavour symmetry [30]). This alleviates possible problems with flavour changing neutral currents. The first two families are (in models of the Mini-Landscape) subject to an $SO(10)$ local subgroup enhancement (at leading order) at the representative fixed point. We thus see that all the important aspects of particle physics find a convincing geometrical and geographical explanation within the framework of the heterotic MiniLandscape. Basic ingredients are the gauge symmetry structure and the action of discrete symmetries [31], as the R-symmetry in the Higgs sector and the D_4 flavour symmetry. So far our discussion on the structure of supersymmetric models. The models contain possibly additional singlets and $U(1)$ gauge symmetries. The lessons described here are important hints for model building and should therefore be incorporated in bottom-up schemes as well.

3.2. Pattern of Supersymmetry Breakdown. In absence of a convincing alternative one would suggest some kind of gravity (modulus) mediation in the framework of string theory. Analysis of moduli stabilization and SUSY breakdown in type II [32–34] and heterotic theory [35] reveal the important fact that the strength of gravity mediation might even be reduced. Radiative corrections could then become important, leading to contributions that are reminiscent of anomaly mediation. Quite generically this leads to a scheme of so-called mirage mediation, a scheme of mixed modulus (gravity) mediation and anomaly mediation. Contributions of modulus mediation are typically suppressed by a factor $\log(M_{\text{Planck}}/m_{3/2})$ where $m_{3/2}$ denotes the gravitino mass. Radiative contributions become competitive leading to the specific pattern of mirage mediation as explained in detail in [33]. This, in particular, leads to a rather interesting pattern of gaugino masses [36].

Geographical properties of fields in compactified space are important for the discussion of SUSY breakdown as well. In $D = 4$ space-time dimensions we obtain $N = 1$ supersymmetry through the process of compactification. Various subsectors, however, might experience a higher degree of supersymmetry. Bulk fields, for example, live on the six-dimensional torus (underlying the (flat) orbifold). Torus compactification would lead to $N = 4$ extended supersymmetry in $D = 4$. The suppression of the contribution of modulus mediation for bulk fields as described above could be attributed to the presence of this extended supersymmetry (at leading order). Fields on a fixed torus might experience an approximate $N = 2$ supersymmetry while fields at fixed points feel only $N = 1$ at leading order. Therefore the SUSY-protection depends on the location of the fields. We would thus expect a hierarchy of soft mass terms. They would be large for the masses of the first two generations and relatively suppressed for fields of the third generation as well as the gauginos. Less is known concerning the discussion of the μ-term as this is allowed by supersymmetry. Of course, we have a protection with an R-symmetry at the level of the soft SUSY breaking terms [11, 26], but generically we do not know whether this corresponds to the values of the gaugino masses or the (larger) masses of the scalars of the first two generations. As μ determines the mass of the higgsinos (a potential dark matter candidate) it is important to spend more efforts on that issue (see, e.g., [29]). Apart from the μ-term we have, however, a pretty convincing pattern of SUSY breakdown relevant for the phenomenological properties of the models to confront LHC data. It should be stressed that these discussions took place before LHC came into operation and have not been influenced by LHC results. Of course, now we have to analyse whether the scheme is compatible with the experimental results and find out what we can learn from there. We are still in the dark and need some hints from experiment.

4. Experimental Situation after the First LHC Run

Unfortunately there is no sign for either supersymmetry or any physics beyond the standard model. Still we have some results from LHC searches that have to be taken into account. The Higgs boson has been found with a mass of 125 GeV [37, 38]. This is compatible with the MSSM but rather close to the upper limit of, let us say, 130 GeV. A higher Higgs mass would have ruled out SUSY (or the MSSM) and so LHC failed to rule out SUSY. Within the MSSM this large mass of m_{Higgs} requires SUSY partners at a high scale. In this regime the MSSM Higgs is rather similar to the Higgs in the standard model and SUSY partners are heavy. This is not necessarily true for models beyond the MSSM. In models with additional singlets we might have a nontrivial mixing of the Higgs bosons. If we would have known the mass of the Higgs boson before LHC came into operation we would have probably been less optimistic about SUSY searches there.

In that sense, the absence of any sign of SUSY particles at the LHC is not yet incompatible even within the MSSM. The question is as follows: Will the LHC with its energy reach be able to answer the question of any (TeV-scale) physics beyond the standard model? We do not really know. Answers are highly model dependent. So let us go through the basic arguments for SUSY. First there is the stability of the weak scale that requires new states in its vicinity. Typically we could thus look at the question of the amount of fine-tuning needed to explain the absence of light SUSY states. But these fine-tuning arguments have to be taken with care, especially in absence of any other reason for the stability of the weak scale that requires new states in its vicinity.

A second argument is the question of gauge coupling unification present in the MSSM but absent in the SM. This requires new states and we will discuss this issue later in detail. So there remains, as third argument, the solution of the dark matter problem via a SUSY-WIMP. If we consider a WIMP with standard thermal abundance we should be able to get an upper limit on the mass of such a particle. There remains the question of whether the LHC will cover the full range of these possibilities. In that sense there is hope that searches at the next LHC run as well as direct and indirect detection experiments for dark matter might cover the full range of these possibilities (including precision experiments of phenomena like $g-2$, flavour violations, or precision Higgs physics).

Still, the absence of any experimental signal for physics beyond the standard model restricts the parameter space of supersymmetric models considerably. Naive expectations for large missing energy signals have not been seen yet. Simple models are not ruled out at the cost of shifting the SUSY masses (e.g., the gluino mass) to rather high values beyond a TeV. Further restrictions arise when one considers the energy content of the universe. Many models lead to an overabundance of WIMP (e.g., bino) dark matter and need modifications. So we are stuck with our theoretical ideas. We urgently need further impact from experiment. Let us hope that the next run of the LHC provides information of physics beyond the standard model. Still there remains the question of whether LHC has the energy reach to discover supersymmetry. We have to wait and see. Meanwhile we have to work out specific examples in detail that might be testable with the next run.

5. A Representative Scheme

It is impossible to make general predictions based on TeV-scale supersymmetry. Let us therefore discuss a specific example which is motivated from the string-inspired discussion presented earlier. Even there we need to make some more assumptions to narrow down the various possibilities.

We make three explicit assumptions:

(i) We assume a supersymmetric model with new particles connected to the weak scale.

(ii) Dark matter should be given by a supersymmetric WIMP (as, e.g., a neutralino). This might lead to an upper limit on the mass of some of the SUSY particles if we require the correct dark matter abundance.

(iii) We assume (precision) gauge coupling unification. Again this might require new states beyond the standard model within the energy reach of LHC.

We should stress that these are ad hoc assumptions which are not necessarily predicted from the general theoretical perspective, but they seem to be a reasonable starting point to analyse the properties of these string-inspired models.

5.1. The SUSY Mass Scale. The assumption made above can tell us indirectly something about the mass scale of supersymmetric particles [39]. This is pretty obvious for the SUSY-WIMP-interpretation of dark matter which we discuss later in detail. But it is also true for the assumption of grand unification. Within our scheme, SUSY partners of standard model particles (in the TeV range) have to provide the necessary thresholds. Let us parametrize the SUSY scale by a single effective mass scale M_{SUSY}. The threshold for the evolution of the gauge coupling constants is then given by

$$\frac{1}{g_{i,\mathrm{Thr}}^2} = \frac{b_i^{\mathrm{MSSM}} - b_i^{\mathrm{SM}}}{8\pi^2} \ln\left(\frac{M_{\mathrm{SUSY}}}{M_Z}\right), \tag{1}$$

where b_i^{SM} (b_i^{MSSM}) stand for the beta function coefficients of the (supersymmetric) standard model. If all supersymmetric partners have a common mass M, then $M_{\mathrm{SUSY}} = M$. We define M_{GUT} as the scale where the coupling constants g_1 and g_2 meet. The precision of gauge coupling unification can then be parametrized by

$$\epsilon_3 = \frac{g_3^2\left(M_{\mathrm{GUT}}\right) - g_{1,2}^2\left(M_{\mathrm{GUT}}\right)}{g_{1,2}^2\left(M_{\mathrm{GUT}}\right)}. \tag{2}$$

The value of ϵ_3 as a function of M_{SUSY} is shown in Figure 1. It shows that precision unification gives a SUSY scale of 2-3 TeV. This appears to be rather large, given the energy reach of LHC. Of course, there might be other thresholds at higher mass scales that might modify this result to lower values of M_{SUSY}, but there is no a priori reason to assume this. Does this mean that all SUSY partners have to be above this scale? (Un)fortunately not. Different particles affect the evolution of coupling constants differently and we have to compute the effective scale M_{SUSY} explicitly for a given model. Let us assume that squark and slepton masses for a given family are universal (in complete grand unified multiplets). Only "split" multiplets have a nontrivial effect and we obtain for the effective scale [40]

$$M_{\mathrm{SUSY}} = \frac{m_{\widetilde{W}}^{32/19} m_{\widetilde{h}}^{12/19} m_H^{3/19}}{m_{\widetilde{g}}^{28/19}}, \tag{3}$$

with $m_{\widetilde{g}}$, $m_{\widetilde{w}}$, $m_{\widetilde{h}}$, and m_H as the mass for the gluino, wino, higgsino, and heavy Higgs, respectively. From this formula we see that we cannot deduce an upper limit for the mass of the lightest supersymmetric partner. Increasing the mass of the gluino leads to a smaller value of M_{SUSY}. On the other

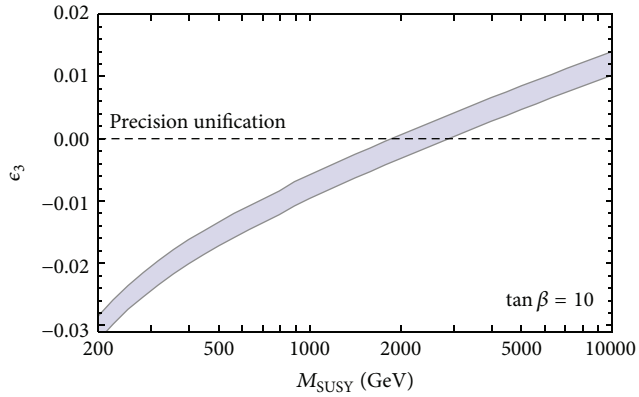

Figure 1: The prediction of grand unification for the effective scale $M_{\rm SUSY}$. The width of the band represents the 1σ experimental error in $\alpha_s(M_Z)$.

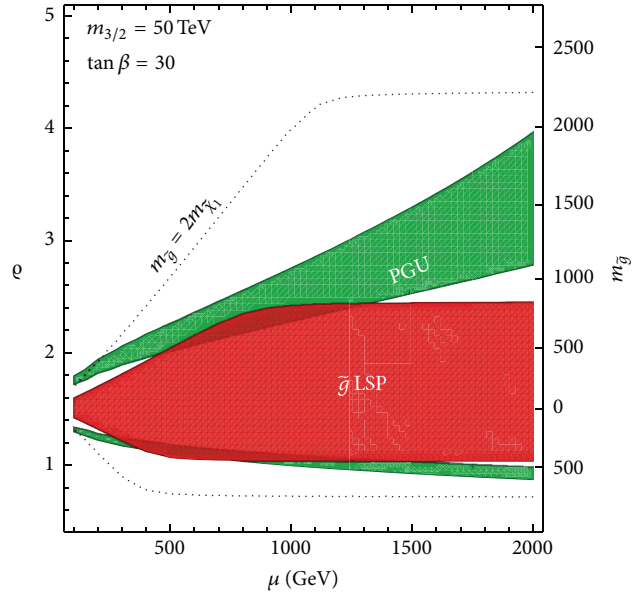

Figure 2: Parameter scan in the (μ, ϱ)-plane for fixed $m_{3/2}$ = 50 TeV. The regions where the gauge couplings unify within the experimental error on the strong coupling are shown in green. In the upper region, the lightest neutralino is predominantly of bino-type, where the lower one corresponds to a wino-like LSP. The red region exhibits a gluino LSP. The dotted contour indicates where the mass ratio between gluino and LSP becomes two.

hand we also see that a large value of $M_{\rm SUSY}$ might still be compatible with rather small masses of some supersymmetric particles in the few-hundred GeV range.

5.2. Mirage Mediation. Explicit discussion of supersymmetry breakdown in type IIB and heterotic string theory have revealed a specific scheme known as mirage mediation [41]. It is a combination of modulus mediation and anomaly mediation. The scheme is explained in detail, for example, in [33, 42]. The contribution of modulus mediation is suppressed by a factor $\log(M_{pl}/m_{3/2}) \sim 4\pi^2$ so that radiative corrections become competitive. One of the specific properties of the scheme is a compressed spectrum of gaugino masses [36]. This has several important consequences:

(i) Gluinos produced at LHC will predominantly decay in neutralinos with a missing energy signal. This signal will be suppressed when the mass splitting of the gauginos is small. LHC search for missing energy will thus be less efficient than previously expected.

(ii) The usual fine-tuning problem of the weak scale is suppressed (compared to other scenarios) because the gluino mass is suppressed with respect to other neutralinos [43].

(iii) It allows the implementation of precision gauge unification in a natural way [39].

(iv) With an ultracompressed spectrum of (nearly degenerate) gauginos potential problems of the thermal relic abundance can be solved via coannihilations [39].

Mirage mediation leads to a specific spectrum: scalar partners of quarks and leptons with masses of order $m_{3/2}$ in the multi-TeV range, A-parameters, gaugino, and Higgsino masses in the TeV range and a compressed gaugino spectrum. These properties and the influence of precision gauge unification (PGU) have been discussed explicitly in [39] where we constructed a large sample of models and compared it to results of LHC search. We recall some of the results here and discuss the question of dark matter candidates in more detail. We define the gaugino masses as

$$M_i = \frac{m_{3/2}}{16\pi^2}\left(\varrho + b_i^{\rm MSSM} g^2\right), \tag{4}$$

such that ϱ parametrizes the contribution from modulus mediation. This leads to

$$M_1 : M_2 : M_3 = (\varrho + 3.3) : 2(\varrho + 0.5) : 6(\varrho - 1.5). \tag{5}$$

Pure modulus mediation would lead to $M_1 : M_2 : M_3 = 1 : 2 : 6$ at a low scale. To reach an effective SUSY scale $M_{\rm SUSY} \approx 2$ TeV would then lead to a higgsino mass

$$m_{\tilde{h}} \simeq 20\ {\rm TeV}\left(\frac{\rm TeV}{m_{1/2}}\right)^{1/3}\left(\frac{\rm TeV}{m_H}\right)^{1/4} \tag{6}$$

and thus a large value for $\mu \sim m_{\tilde{h}}$. This requires a large amount of fine-tuning to obtain a low value of the mass of the Higgs boson. The large value of μ can be directly understood from formula (3). If the mass of the gluino is much larger than the mass of the wino, this discrepancy has to be compensated by a large value of $m_{\tilde{h}}$. In the case of mirage mediation with a compressed spectrum the situation is quite different. The contributions from gluino and wino essentially cancel in formula (3) and gauge unification requires a smaller value of the higgsino mass and thus μ. This is nicely illustrated in Figure 2. The two green regions are consistent with the requirement of (precision) gauge coupling unification. In the upper region (larger ϱ) the bino is the lightest SUSY particle

(LSP), whereas in the lower one we predominantly have a wino WIMP. The red region has a gluino LSP and is therefore disfavoured. We see from Figure 2 that a SUSY scale $M_{\text{SUSY}} \approx 2$ TeV can be obtained with a μ-parameter in the TeV range. Thus the fine-tuning of the weak scale is less severe than in the case of uncompressed gaugino mass spectra.

5.3. Constraints from LHC. To confront the scheme with present LHC results we have generated a large data sample of models within the favoured regions of Figure 2. Details are explained in [39]. As input we have chosen parameters randomly in the intervals

$$\begin{aligned} \mu &= 0.1\text{–}2\ \text{TeV}, \\ \varrho &= 0.5\text{–}30, \\ m_{3/2} &= \frac{40\text{–}200\ \text{TeV}}{\varrho}, \\ \tan\beta &= 10\text{–}50. \end{aligned} \tag{7}$$

The ranges of ϱ and $m_{3/2}$ are correlated and yield a gravity mediated contribution to the gauging masses of 0.25–1.25 TeV. A scatter plot with successful gauge unification models in the gluino and LSP mass plane is shown in Figure 3. The grey dots represent the individual models. To guide the eye we have included representative limits on the gluino mass from LHC searches by ATLAS [1] and CMS [2]. Both limits are not strictly applicable at this point and should be replaced by results of dedicated searches for the models under consideration. More than 90% of the benchmark points fulfil $m_{\tilde{\chi}_1} > 0.5 m_{\tilde{g}}$. The strong compression of gaugino masses makes it more difficult to detect the gluino here than in ordinary SUSY schemes as, for example, the CMSSM. Still with the next run of the LHC it should be possible to cover the full range of small gluino masses up to "kinematic limit," depending on beam energy and collected luminosity [44].

5.4. Constraints from Dark Matter Relic Abundance. More constraints on the models could come from the requirement of the correct thermal relic abundance of the LSP as a candidate for dark matter. Prime contenders are the wino, the bino, and the higgsino. Due to its small annihilation cross section, the bino density from thermal production typically exceeds the observed dark matter density by far. Higgsinos, on the other hand, undergo efficient annihilations into gauge bosons or third-generation quarks, and coannihilations with the charged higgsino further enhance their cross section. Thus, the relic density of the higgsino LSP might typically be below the required dark matter density. In mirage mediation, the gaugino masses, while nonuniversal at the large scale, lead to a highly compressed spectrum at the weak scale as a consequence of the requirement of gauge coupling unification. This nearly degenerate spectrum enhances the possibility for coannihilation favourable to reduce the bino mass density in this mixed scheme. Figure 4 illustrates possible restrictions from the correct relic density. For a given value of the gravitino mass (here 50 TeV) the constraint is fulfilled in the blue region. We can identify two specific

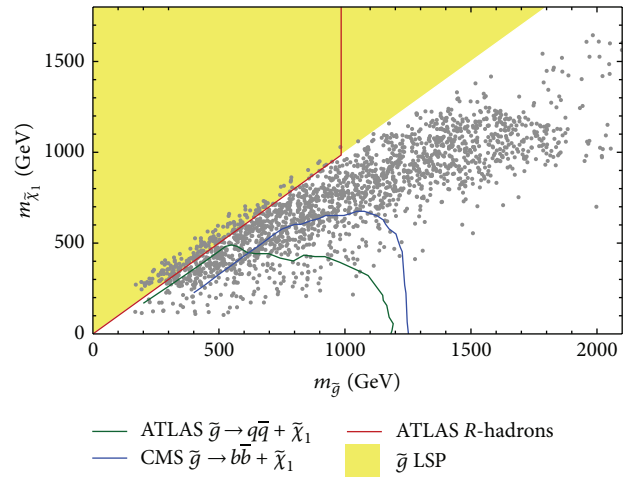

FIGURE 3: Parameter points with successful gauge coupling unification (gray). Also shown are representative constraints on the gluino mass for the decay modes $\tilde{g} \to q\bar{q} + \tilde{\chi}_1$ and $\tilde{g} \to b\bar{b} + \tilde{\chi}_1$ by ATLAS [1] and CMS [2]. The yellow region features a gluino LSP which is constrained by the ATLAS search for stable R-hadrons.

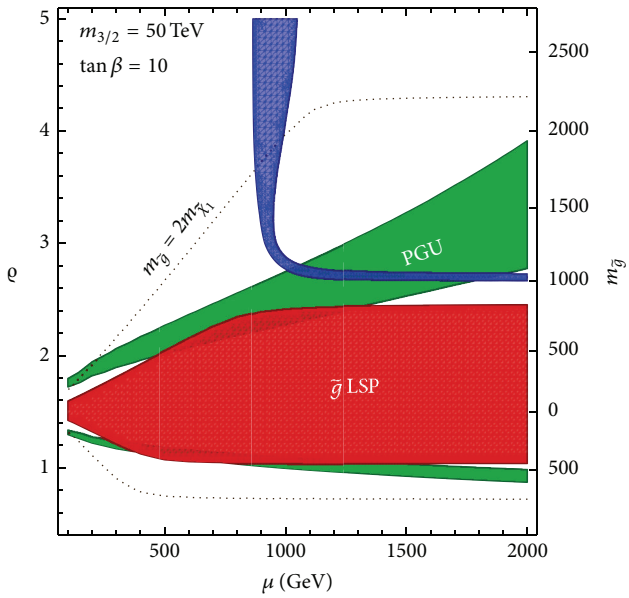

FIGURE 4: Parameter scan in the (μ, ϱ)-plane for fixed $m_{3/2} = 50$ TeV, as described earlier in Figure 2. The blue region identifies the parameters that are compatible with the correct dark matter abundance. The vertical region around $\mu \sim 1$ corresponds to a higgsino LSP, while the horizontal strip corresponds to (mixed) bino LSP, here at a gluino mass around 1 TeV. The gluino mass scales proportional to the gravitino mass.

cases: higgsino dark matter (vertical strip) with $\mu \sim 1$ TeV and a coannihilation strip (horizontal) for a fixed gluino mass (which, however, varies with the gravitino mass). The consequences of this constraint on our model sample are shown in Figure 5. Grey dots do not give the correct relic abundance, black dots refer to the bino coannihilation strip, and the purple ones refer to a higgsino LSP. There are, in

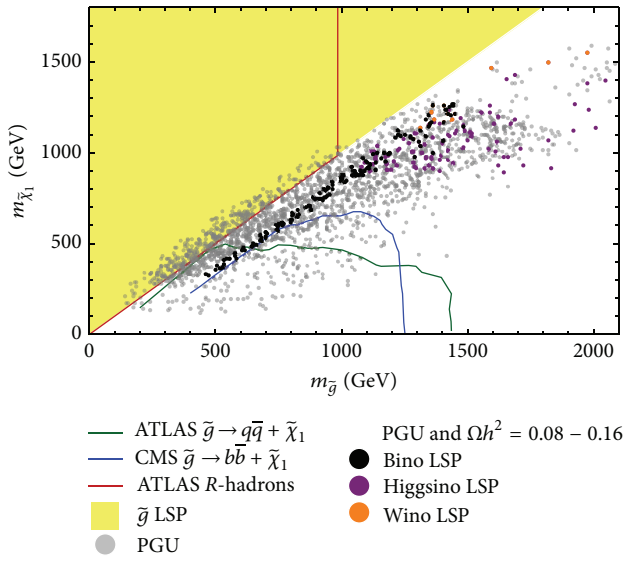

FIGURE 5: This is the same as Figure 3 but with the information on the dark matter candidates and abundance. The grey dots do not provide the correct relic density. Black dots correspond to an LSP that is predominantly bino, while purple (orange) dots correspond to higgsino (wino) LSP. The black dots are approximately aligned in a "coannihilation strip."

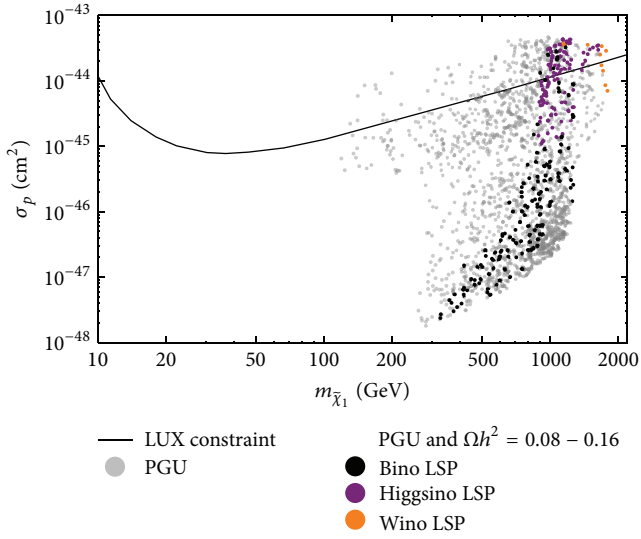

FIGURE 6: Neutralino-proton cross section for the benchmark points with successful gauge coupling unification. The colour coding is the same as in Figure 5. Models denoted by grey dots do not give the correct relic abundance for dark matter. Black, purple, and orange dots correspond to WIMP candidates that are predominantly bino, higgsino, or wino. The current limit from the LUX direct dark matter search [3] is also shown. The latter is valid if the lightest neutralino accounts for all dark matter in the universe.

addition, a few dots (in orange) corresponding to a wino LSP (in case that mirage mediation is dominated by the anomaly contribution corresponding to the lower green region in Figure 2). Most of the favoured models should be within the range of the next LHC run. Particularly the black dots in the coannihilation strip should be testable in the near future, while higgsino and wino LSPs might be out of reach in some of the cases.

5.5. Complementarity of Searches. Fortunately there are other observations that can help in clarifying the situation: experiments for direct dark matter detection. WIMP candidates can be found through their interaction with nucleons. The cross sections of binos, winos, and higgsinos differ quite significantly. In the scheme discussed here, the cross section of the lightest neutralino with nucleons is dominated by the exchange of the light Higgs boson (as the other scalars are in the multi-TeV range). The coupling of the LSP to the Higgs boson is proportional to the gaugino-higgsino mixing angle; it vanishes in the limit of a pure state. The neutralino-proton cross section σ_p for our benchmark points is shown in Figure 6. We find a cross section between 10^{-43} cm^2 and 10^{-48} cm^2. Direct detection experiments as, for example, LUX [3] have just started to probe this regime of cross sections. Experiments of the next generation should be able to test a significant fraction of the benchmark points.

For the specific scheme under consideration we observe a complementarily of direct searches for dark matter with those of the LHC. This is (also in more general cases [45]) a rather fortunate situation. The black dots ((mixed) bino LSP (when we denote the states by wino, bino, and higgsino LSP we identify the dominant component, as the candidates that satisfy the constraints are usually mixed states)) are difficult to detect directly, but according to Figure 5 they might be within the reach of the upcoming run of the LHC. On the other hand, the wino and higgsino WIMP candidates are easier to see in direct detection experiments. If we look at Figure 6, we observe that many of the purple and orange dots are already ruled out. So this region of the parameter space that is possibly beyond the reach of LHC can be tested by direct dark matter detection experiments. In that sense it is likely that our benchmark scheme can be tested within the not so distant future.

6. Conclusions

As we have seen it is a long way from string theory via supersymmetric extensions of the standard model to LHC physics. To test these ideas we need consistent string theory constructions that allow explicit determination of spectrum and interactions to be confronted with the data. At this point only the models of the heterotic MiniLandscape satisfy both criteria. Given these models we can try to extract some generic properties from the successful supersymmetric candidate models. The origin of these lessons comes from the geographic localization of fields in compactified extradimensional space. A coherent picture emerges; Higgs and top multiplets live in the bulk. This provides a solution to the μ-problem with an R-symmetry as well as a large value for the Yukawa coupling of the top-quark (to be consistent with so-called gauge-Yukawa unification). The multiplets of the first

two families are located at fixed points in extradimensional space. They enjoy enhanced gauge and discrete symmetries that alleviate the flavour problem. A slight breakdown of these symmetries provides a small parameter (originated from a Fayet-Iliopoulos term) that could explain the hierarchies of quark and lepton masses as well as the μ-parameter. We expect these properties (derived from the heterotic string theory) to be of more general validity and should also manifest themselves in constructions based on type I, type II, M-, or F-theory.

In the discussion of SUSY breakdown we can identify a rather generic scheme: mirage mediation. It has been found in both type IIB and heterotic theory and is a consequence of the mechanism to obtain a small value of the vacuum energy (compared to the scale of the gravitino mass). The scheme is characterized by two scales for the soft terms separated by a factor $\log(M_{\text{Planck}}/m_{3/2})$. Gaugino masses and A-parameters tend to be at the TeV scale, while gravitino mass and scalar masses are generically at a higher scale. A second characteristic property of the mirage scheme is the possibility of a compressed spectrum of the gaugino masses. It leads to hidden SUSY at the LHC and allows for the correct thermal relic density of the LSP dark matter candidate. Within this scheme we could identify another important result concerning scalar masses, determined by the localization properties of the corresponding fields with a potential protection through extended supersymmetry. Localized fields as, for example, the scalar partners of quarks and leptons of the first two families only feel $N = 1$ SUSY and would be as heavy as the gravitino. Fields at fixed tori or the bulk feel a hidden $N = 2$ or $N = 4$ SUSY and have suppressed masses comparable to those of the gaugino masses. It is this interplay of symmetries that leads to very specific properties of the spectrum of superpartners. The scheme is still consistent with all known experimental data. A large part of the parameter space is within the kinematical reach of the LHC at 13 TeV. This is partially due to the fact that those models that are beyond the reach of the LHC might be ruled out through direct dark matter detection experiments. The next run of the LHC will hopefully be able to test these ideas. Independent of the discussion here, it is obvious that we urgently need new experimental data to clarify the nature of potential physics beyond the standard model. Theoretically we have tried all we could do. There are many well-motivated models that have been analysed, but there are no real predictions. We need help from experimental data.

Conflict of Interests

The author declares that there is no conflict of interests regarding the publication of this paper.

Acknowledgments

The author would like to thank Rolf Kappl and Martin Winkler for very useful discussions as well as the preparation of the figures. This work was partially supported by the SFB-Transregio TR33 "The Dark Universe" (Deutsche Forschungsgemeinschaft).

References

[1] ATLAS Collaboration, "Search for squarks and gluinos with the ATLAS detector using final states with jets and missing transverse momentum and 5.8 fb^{-1} of $\sqrt{s} = 8$ TeV," ATLAS-CONF-2012-109, ATLAS-COM-CONF-2012-140.

[2] CMS Collaboration, Search for Supersymmetry in pp collisions at 8 TeV in events with a single lepton, multiple jets and b-tags, CMS-PAS-SUS-13-007.

[3] D. S. Akerib, H. M. Araújo, X. Bai et al., "First results from the LUX dark matter experiment at the Sanford underground research facility," *Physical Review Letters*, vol. 112, Article ID 091303, 2014.

[4] H. P. Nilles, "Supersymmetry, supergravity and particle physics," *Physics Reports*, vol. 110, no. 1-2, pp. 1–162, 1984.

[5] H. E. Haber and G. L. Kane, "The search for supersymmetry: probing physics beyond the standard model," *Physics Reports*, vol. 117, pp. 75–263, 1985.

[6] H. P. Nilles and P. K. S. Vaudrevange, "Geography of fields in extra dimensions: string theory lessons for particle physics," *Modern Physics Letters A*, vol. 30, no. 10, Article ID 1530008, 2015.

[7] L. E. Ibanez and A. M. Uranga, *String Theory and Particle Physics: An Introduction to String Phenomenology*, Cambridge University Press, Cambridge, UK, 2012.

[8] K.-S. Choi and J. E. Kim, *Quarks and Leptons from Orbifolded Superstring*, vol. 696 of *Lecture Notes in Physics*, Springer, Berlin, Germany, 2006.

[9] O. Lebedev, H. P. Nilles, S. Raby et al., "A mini-landscape of exact MSSM spectra in heterotic orbifolds," *Physics Letters B*, vol. 645, no. 1, pp. 88–94, 2007.

[10] O. Lebedev, H.-P. Nilles, S. Raby et al., "Low energy supersymmetry from the heterotic string landscape," *Physical Review Letters*, vol. 98, Article ID 181602, 2007.

[11] O. Lebedev, H. Nilles, S. Raby et al., "Heterotic road to the MSSM with R parity," *Physical Review D*, vol. 77, Article ID 046013, 2007.

[12] O. Lebedev, H. P. Nilles, S. Ramos-Sánchez, M. Ratz, and P. K. S. Vaudrevange, "Heterotic mini-landscape (II): completing the search for MSSM vacua in a Z_6 orbifold," *Physics Letters B*, vol. 668, no. 4, pp. 331–335, 2008.

[13] T. Kobayashi, S. Raby, and R.-J. Zhang, "Constructing 5d orbifold grand unified theories from heterotic strings," *Physics Letters B*, vol. 593, no. 1–4, pp. 262–270, 2004.

[14] T. Kobayashi, S. Raby, and R. J. Zhang, "Searching for realistic 4d string models with a Pati-Salam symmetry. Orbifold grand unified theories from heterotic string compactification on a Z_6 orbifold," *Nuclear Physics B*, vol. 704, pp. 3–55, 2005.

[15] W. Buchmüller, K. Hamaguchi, O. Lebedev, and M. Ratz, "Supersymmetric standard model from the heterotic string," *Physical Review Letters*, vol. 96, Article ID 121602, 2006.

[16] W. Buchmüller, K. Hamaguchi, O. Lebedev, and M. Ratz, "Supersymmetric standard model from the heterotic string (II)," *Nuclear Physics B*, vol. 785, no. 1-2, pp. 149–209, 2007.

[17] M. Blaszczyk, S. G. Nibbelink, M. Ratz, F. Ruehle, M. Trapletti, and P. K. S. Vaudrevange, "A $Z_2 \times Z_2$ standard model," *Physics Letters B*, vol. 683, pp. 340–348, 2010.

[18] J. E. Kim and B. Kyae, "Flipped $SU(5)$ from Z_{12-I} orbifold with Wilson line," *Nuclear Physics B*, vol. 770, no. 1-2, pp. 47–82, 2007.

[19] J. E. Kim and B. Kyae, "String MSSM through flipped SU(5) from Z_{12} orbifold," http://arxiv.org/abs/hep-th/0608085.

[20] J. E. Kim, J. H. Kim, and B. Kyae, "Superstring standard model from $\mathbb{Z}_{12-I}$ orbifold compactification with and without exotics, and effective R-parity," *Journal of High Energy Physics*, vol. 2007, no. 6, article 034, 2007.

[21] D. K. M. Peña, H. P. Nilles, and P.-K. Oehlmann, "A zip-code for quarks, leptons and Higgs bosons," *Journal of High Energy Physics*, vol. 2012, no. 12, article 024, 2012.

[22] S. G. Nibbelink and O. Loukas, "MSSM-like models on Z_8 toroidal orbifolds," *Journal of High Energy Physics*, vol. 2013, no. 12, article 044, 2013.

[23] H. P. Nilles, S. Ramos-Sanchez, M. Ratz, and P. K. S. Vaudrevange, "From strings to the MSSM," *The European Physical Journal C*, vol. 59, no. 2, pp. 249–267, 2009.

[24] S. Förste, H. P. Nilles, P. Vaudrevange, and A. Wingerter, "Heterotic brane world," *Physical Review D*, vol. 70, Article ID 106008, 2004.

[25] H. P. Nilles, "Five golden rules for superstring phenomenology," in *Proceedings of the 10th International Symposium on Particles, Strings and Cosmology*, August 2004.

[26] R. Kappl, H. P. Nilles, S. Ramos-Sánchez, M. Ratz, K. Schmidt-Hoberg, and P. K. Vaudrevange, "Large hierarchies from approximate *R* symmetries," *Physical Review Letters*, vol. 102, no. 12, Article ID 121602, 2009.

[27] J. A. Casas and C. Muñoz, "A natural solution to the μ problem," *Physics Letters B*, vol. 306, no. 3-4, pp. 288–294, 1993.

[28] H. M. Lee, S. Raby, M. Ratz et al., "A unique $\mathbb{Z}_4^R$ symmetry for the MSSM," *Physics Letters B*, vol. 694, no. 4-5, pp. 491–495, 2011.

[29] M. Ratz and P. K. S. Vaudrevange, "Singlet extensions of the MSSM with Z_{4R} symmetry," http://arxiv.org/abs/1502.07207.

[30] T. Kobayashi, H. P. Nilles, F. Plöger, S. Raby, and M. Ratz, "Stringy origin of non-Abelian discrete flavor symmetries," *Nuclear Physics B*, vol. 768, no. 1-2, pp. 135–156, 2007.

[31] H. P. Nilles, M. Ratz, and P. K. S. Vaudrevange, "Origin of family symmetries," *Fortschritte der Physik*, vol. 61, no. 4-5, pp. 493–506, 2013.

[32] K. Choi, A. Falkowski, H. P. Nilles, M. Olechowski, and S. Pokorski, "Stability of flux compactifications and the pattern of supersymmetry breaking," *Journal of High Energy Physics*, vol. 2004, no. 11, article 076, 2004.

[33] K. Choi, A. Falkowski, H. P. Nilles, and M. Olechowski, "Soft supersymmetry breaking in KKLT flux compactification," *Nuclear Physics B*, vol. 718, no. 1-2, pp. 113–133, 2005.

[34] O. Lebedev, H. P. Nilles, and M. Ratz, "de Sitter vacua from matter superpotentials," *Physics Letters B*, vol. 636, no. 2, pp. 126–131, 2006.

[35] V. Löwen and H. P. Nilles, "Mirage pattern from the heterotic string," *Physical Review D*, vol. 77, Article ID 106007, 2008.

[36] K. Choi and H. P. Nilles, "The gaugino code," *Journal of High Energy Physics*, vol. 2007, no. 4, article 6, 2007.

[37] G. Aad, T. Abajyan, B. Abbott et al., "Observation of a new particle in the search for the Standard Model Higgs boson with the ATLAS detector at the LHC," *Physics Letters B*, vol. 716, no. 1, pp. 1–29, 2012.

[38] S. Chatrchyan, V. Khachatryan, A. M. Sirunyan et al., "Observation of a new boson at a mass of 125 GeV with the CMS experiment at the LHC," *Physics Letters B*, vol. 716, no. 1, pp. 30–61, 2012.

[39] S. Krippendorf, H. P. Nilles, M. Ratz, and M. W. Winkler, "Hidden SUSY from precision gauge unification," *Physical Review D*, vol. 88, Article ID 035022, 2013.

[40] M. Carena, S. Pokorski, and C. E. M. Wagner, "On the unification of couplings in the minimal supersymmetric standard model," *Nuclear Physics B*, vol. 406, no. 1-2, pp. 59–89, 1993.

[41] O. Loaiza–Brito, J. Martin, H. P. Nilles, and M. Ratz, "$\log(M_{Pl}/m_{3/2})$," *AIP Conference Proceedings*, vol. 805, no. 1, pp. 198–204, 2005.

[42] S. Krippendorf, H. P. Nilles, M. Ratz, and M. W. Winkler, "The heterotic string yields natural supersymmetry," *Physics Letters B*, vol. 712, no. 1-2, pp. 87–92, 2012.

[43] O. Lebedev, H. P. Nilles, and M. Ratz, "A note on fine-tuning in mirage mediation," in *Proceedings of the Symposium in Honor of Gustavo C. Branco: CP Violation and the Flavor Puzzle*, Lisbon, Portugal, July 2005.

[44] ATLAS collaboration, "Expected sensitivity studies and quark searches," ATLASNOTE ATL-PHYS-PUB-2015-005, 2015.

[45] G. B. Gelmini, "TASI 2014 lectures: the hunt for dark matter," http://arxiv.org/abs/1502.01320.